

National Aeronautics and Space Administration

NASA History Division

INTRODUCTION TO THE AERODYNAMICS OF FLIGHT [NASA SP-367]

Theodore A. Talay
Langley Research Center

Prepared at Langley Research Center

Scientific and Technical Information Office
National Aeronautics and Space Administration,
Washington, D.C. 1975

FOREWORD

The science of aerodynamics can be traced back thousands of years to its beginnings but, remarkably, only one human life span has separated the first heavier-than-air powered airplane flight at Kitty Hawk from the first manned moon landing. The last few decades have witnessed phenomenal growth in the science and technology of aerodynamics and no letup is in sight. For those who possess an interest, the task of education encompassing all the various aspects of the subject is staggering. Specialization is indicated but a background knowledge is an essential of any education.

This volume is a result of several semesters of the author's teaching of an introductory course in aerodynamics to apprentices and technicians at the NASA Langley Research Center. The problem faced was to provide more than a layman's treatment of the subject but not the detail as taught in many individual courses on the college level. The result is a highly qualitative, illustrated set of notes which, through the teaching process, was modified to fulfill the objectives better.

A thorough revision of these notes with considerable up-to-date material has resulted in the text as presented herein. It is hoped that this volume will stimulate the reader's interest to pursue more specialized education in the many topics of aerodynamics.

//////////

November 2006

Note to the reader: My highest complements to Langley Research Center and Dr. Theodore A. Talay for writing NASA SP-367.

With the permission of NASA's History Office, I've downloaded this terrific publication. I've reformatted the document -- the page numbers in this document will not necessarily match those from the original text. Figure numbers, headings, text, etc. are unchanged.

////////// signed //////////

WAYNE F. HALLGREN, PhD
Colonel, USAF (Retired)
President, Hallgren Associates, Inc

P.O. Box 190
Winter Park, Colorado 80482

(970) 726-6928
HallgrenAssoc@aol.com

CONTENTS

I. A SHORT HISTORY OF FLIGHT

II. BACKGROUND INFORMATION

- The Atmosphere
- Winds and Turbulence
- The Airplane

III. FLUID FLOW

- The Fluid
- The Flow
- Ideal Fluid Flow
- Real Fluid Flow

IV. SUBSONIC FLOW EFFECTS

- Airfoils and Wings
- Aerodynamic Devices
- Total Drag of Airplane
- Propellers and Rotors

V. TRANSONIC FLOW

VI. SUPERSONIC FLOW

- The SST
- Sonic Boom

VII. BEYOND THE SUPERSONIC

- Hypersonic Flight
- Lifting Bodies
- Space Shuttle

VIII. PERFORMANCE.

- Motions of an Airplane
- Class 1 Motion
- Class 2 Motion
- Class 3 Motion-Hovering Flight

IX. STABILITY AND CONTROL

- Stability
- Control

APPENDIX A - AERONAUTICAL NOMENCLATURE

APPENDIX B - DIMENSIONS AND UNITS

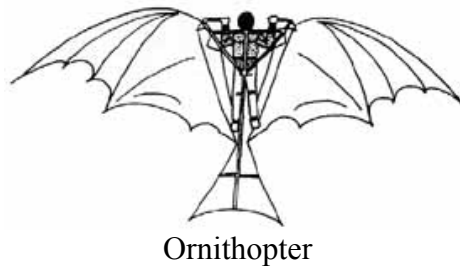
APPENDIX C - COORDINATE SYSTEMS

BIBLIOGRAPHY

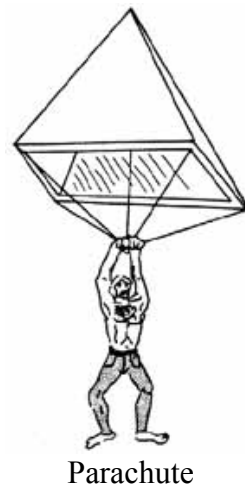
I. A SHORT HISTORY OF FLIGHT

The theory of aerodynamics is the culmination of the works of many individuals. It probably began with prehistoric man's desire to copy the actions of the bird and fly through the air. Early man, being unable to soar into the heavens himself, attributed to his gods the ability to fly. But the serious Greek philosophers began to question: What is this substance called air and can man fly in it? Aristotle conceived the notion that air has weight and Archimedes' law of floating bodies formed a basic principle of lighter-than-air vehicles. Men like Galileo, Roger Bacon, and Pascal proved that air is a gas, is compressible, and its pressure decreases with altitude.

In the years around 1500 one man (Leonardo da Vinci) foresaw the shape of things to come. Through his avid studies of bird flight came the principles and designs that influenced others. Da Vinci correctly concluded that it was the movement of the wing relative to the air and the resulting reaction that produced the lift necessary to fly. As a result of these studies, he designed several ornithopters- machines that were intended to copy the action of a bird's wing-the muscle power being supplied by man. But these designs did not leave the drawing board. His other designs included those for the first helicopter and a parachute. (See [fig 1](#).)



Ornithopter



Parachute



Helicopter

Figure 1.- Designs of Leonardo da Vinci.

The first flying machine to carry man did not imitate the birds. Instead it was based on the lighter-than-air principle and took the form of a large hot-air balloon. (See [fig. 2.](#)) Constructed in 1783 by the two Montgolfier brothers from France, the balloon holds the distinction of initiating the first ascent of man into the atmosphere. Although ballooning thereafter became a popular pastime, man was at the mercy of the winds and could not fly where he willed. Gradually, his balloon designs acquired small engines and steering devices, but they remained lighter-than-air aerostat devices. Heavier-than-air flight was still years away.

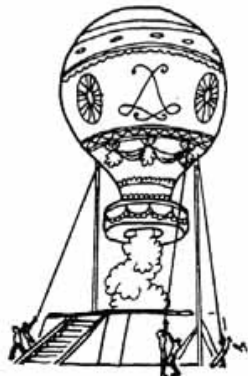


Figure 2.- Montgolfier balloon (1783).

Sir George Cayley of England (1773-1857) is generally recognized as the father of modern aerodynamics. He understood the basic forces acting on a wing and built a glider with a wing and a tail unit which flew successfully. He realized the importance of the wing angle of attack and that curved surfaces would produce more lift force than flat ones. Stability in his designs came with the use of dihedral- an important concept used to this very day. In 1853 it is believed that he built a man-carrying glider which flew once with one of his servants as a passenger. During the late 1800's a number of inventors tried to use a steam engine to power their airplanes and had little success. Meanwhile, toward the end of the nineteenth century, a German named Otto Lilienthal was successfully flying in gliders of his own design. He recorded over 2000 successful flights before crashing to his death in 1896. [Figure 3](#) shows one of his designs. Lilienthal proved the concept of heavier-than-air flight. Today, this form of flying, now called hang-gliding, is enjoying a substantial comeback. Although there are various claims as to who really flew first (the French, the Germans, or the Russians), Americans are generally given the credit.



Figure 3.- Lilienthal glider (1896)

At the Smithsonian Institution in Washington, D.C., Dr. Samuel Pierpont Langley was designing small steam-powered airplanes. His most successful was a 5-meter wing span tandem biplane ([fig. 4](#)), "the Aerodrome," fitted with a steam engine driving two propellers, which flew over 1 kilometer in 1896. Backed by a grant from Congress he built a full-scale version of the same airplane to carry a pilot. Unfortunately, launching gear failure caused it to crash twice during October and December of 1903. On December 17, 1903, the Wright brothers achieved success in a gasoline-engine-powered machine of their own design. Their success lay in continually improving their designs.

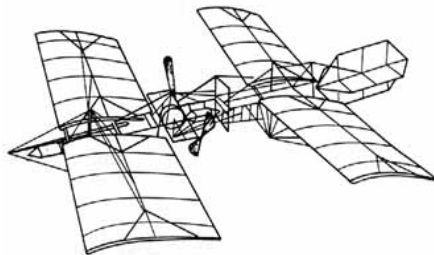


Figure 4.- Samuel Langley's "Aerodrome" (1903).

Aviation and aerodynamics have developed rapidly since 1903. Two world wars and numerous limited wars have spurred advances in the airplane. Aerial combat was commonplace by the end of World War I (1918), and German advanced concepts at the end of World War II (1945) pointed the way to the future. Soon swept wings and jet propulsion dominated both the military and civilian sectors of aviation. (See [fig. 5](#).)

Today at Langley Research Center the research is being pushed forward in the areas of transonic, supersonic, and hypersonic transports, lifting bodies, and the space shuttle. The following material will shed some light on the how and why of an airplane's design.

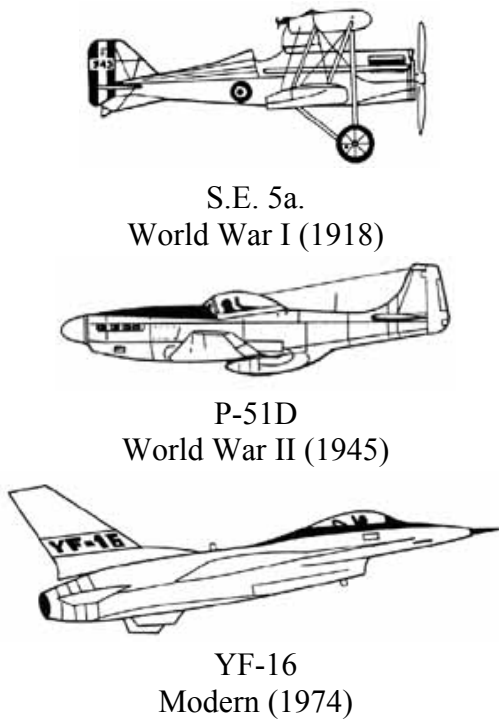


Figure 5.- Design showing advance of aeronautics.

II. BACKGROUND INFORMATION

As a background for the material presented, the reader is urged to examine the material presented in the appendixes. This information is basic and represents required background for the discussions throughout this paper. [Appendix A](#) contains aeronautical nomenclature concerning both general aeronautical definitions and descriptions of aircraft types. [Appendix B](#) discusses dimensions and units as used in this paper. A general discussion of vectors, scalars, and relative motion is also included. [Appendix C](#) describes the various coordinate systems used to define an aircraft's motion above the Earth's surface. The bibliography at the end of the paper will aid the reader in locating further information on the materials presented.

The Atmosphere

Nature of the atmosphere.- The aerodynamicist is concerned about one fluid, namely air. Air makes up the Earth's atmosphere-the gaseous envelope surrounding the Earth-and represents a mixture of several gases. Up to altitudes of approximately 90 km, fluctuating winds and general atmospheric turbulence in all directions keep the air mixed in nearly the same proportions. The normal composition of clean, dry atmospheric air near sea level is given in table I. Not included in the table are water vapor, dust particles, bacteria, etc. Water vapor, although highly variable, is estimated at 0.41-percent total volume. Interestingly, nitrogen and oxygen taken together represent 99 percent of the total volume of all the gases. That the local composition can be made to vary has been brought dramatically to light in recent times by the air pollution problem where in industrialized areas the percentages of carbon monoxide, sulfur dioxide, and numerous other harmful pollutants are markedly higher than in non-industrialized areas.

TABLE I.- NORMAL COMPOSITION OF CLEAN, DRY ATMOSPHERIC AIR NEAR SEA LEVEL

[U.S. Standard atmosphere, 1962]

Constituent gas and formula	Content, percent by volume
Nitrogen (N_2)	78.084
Oxygen (O_2)	20.948
Argon (Ar)	0.934
Carbon Dioxide (CO_2)	0.031
Neon (Ne), helium (He), krypton (Kr), hydrogen (H_2), xenon (Xe), methane (CH_4), nitrogen oxide (N_2O), ozone (O_3), sulfur dioxide (NO_2), ammonia (NH_3), carbon monoxide (CO), and iodine (I_2)	Traces of each gas for a total of 0.003

Above about 90 km, the different gases begin to settle or separate out according to their respective densities. In ascending order one would find high concentrations of oxygen, helium, and then hydrogen which is the lightest of all the gases.

Based on composition, then, there are two atmospheric strata, layers, or "shells." Below 90 km where the composition is essentially constant the shell is the homosphere. Above 90 km where composition varies with altitude, the shell is called the heterosphere. Although composition is one way of distinguishing shells or layers, the most common criterion used is the temperature distribution. In ascending order are the troposphere, stratosphere, mesosphere, thermosphere, and exosphere. [Figure 6](#) shows both the composition- and temperature-defined shells. [Figure 7](#) shows the temperature variation in the various shells.

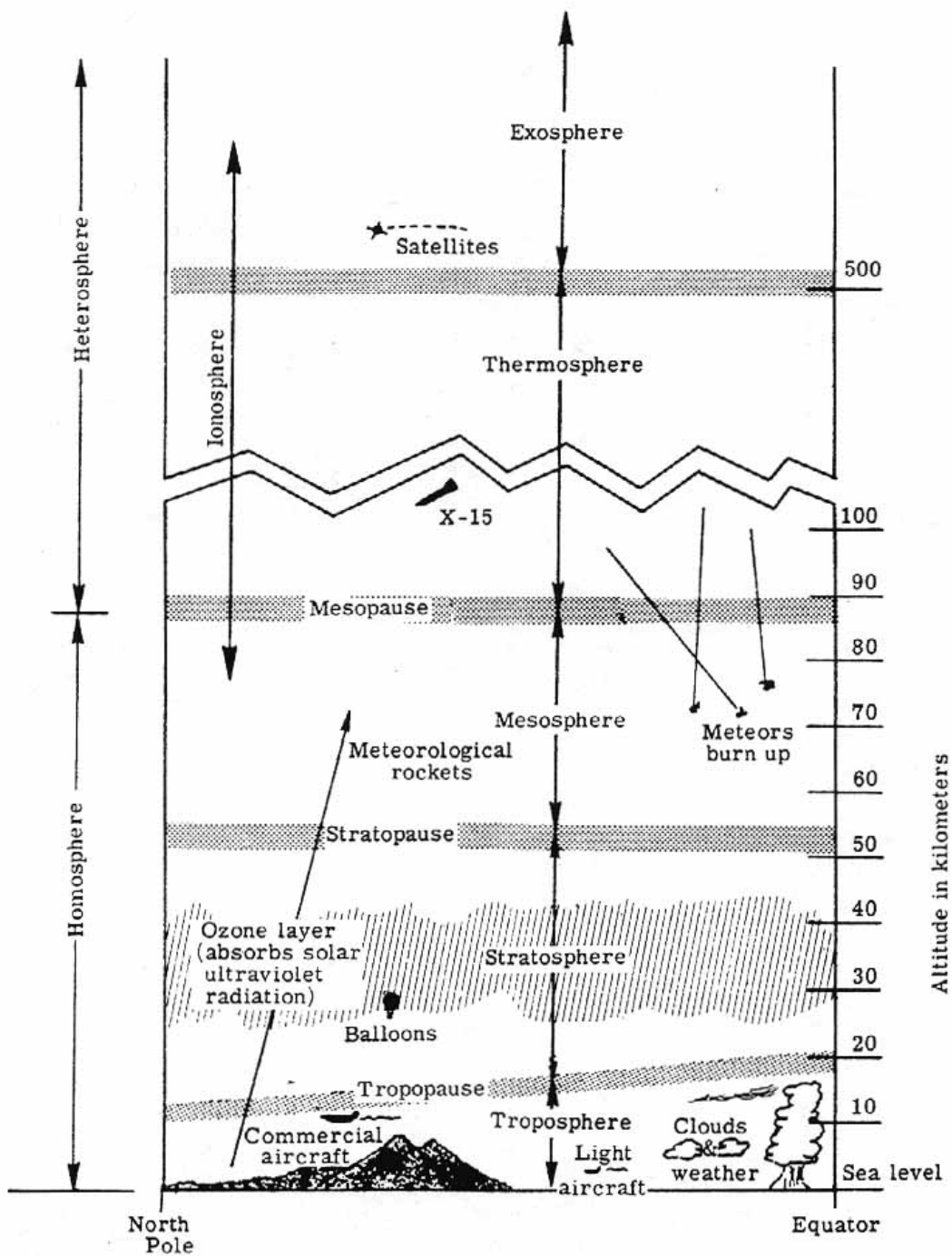


Figure 6.- Atmospheric structure

It is the troposphere which is the most important atmospheric layer to aeronautics since most aircraft fly in this region. Most weather occurs here and, of course, man lives here also. Without the beneficial ozone layer in the stratosphere absorbing harmful solar ultraviolet radiation, life as we know it would not have developed. The ionosphere, a popularly known layer, begins in the mesosphere and extends indefinitely outwards. It represents the region in which ionization of one or more of the atmospheric constituents is significant. The exosphere represents the outer region of the atmosphere where the atmospheric particles can move in free orbits subject only to the Earth's gravitation. It is interesting to note that at these altitudes (greater than 500 km), the solar wind (streams of high-energy particles of plasma from the Sun) becomes a dominant influence so that one has an "atmosphere" which extends all the way to the Sun. The density of the solar wind, however, is negligibly small.

The standard atmosphere - For purposes of pressure altimeter calibrations, aircraft and rocket performance and their design, and so forth, knowledge of the vertical distribution of such quantities as pressure, temperature, density, and speed of sound is required. Since the real atmosphere never remains constant at any particular time or place, a hypothetical model must be employed as an approximation to what may be expected. This model is known as the standard atmosphere. The air in the model is assumed to be devoid of dust, moisture, and water vapor and to be at rest with respect to the Earth (that is, no winds or turbulence).

The first standard atmospheric models were developed in the 1920's in both Europe and the United States. The slight differences between the models were reconciled and an internationally accepted model was introduced in 1952 by the International Civil Aviation Organization (ICAO). This new ICAO Standard Atmosphere was officially accepted by NACA in 1952 and forms the basis of tables in NACA report 1235. The tables extended from 5 km below to 20 km above mean sea level.

With increased knowledge since 1952 because of the large scale use of high-altitude sounding rockets and satellites, extended tables above 20 km were published. Finally in 1962, the U.S. Standard Atmosphere (1962) was published to take into account this new data. For all practical purposes, the U.S. Standard Atmosphere (1962) is in agreement with the ICAO Standard Atmosphere over their common altitude range but extends to 700 km. Uncertainty in values increased with altitude as available data decreased.

With the expansion of this nation's space program requirements, a need was generated for information on the variability of atmospheric structure that would be used in the design of second-generation scientific and military aerospace vehicles.

Systematic variations in the troposphere due to season and latitude had been known to exist and thus a new effort was begun to take those variations into account. The result was the publication of the most up-to-date standard atmospheres-the U.S. Standard Atmosphere Supplements (1966). Essentially there are two sets of tables-one set for altitudes below 120 km and one for altitudes, 120 km to 1000 km. The model atmospheres below 120 km are given for every 15° of latitude for 15° N to 75° N and in most cases for January and July (or winter and summer). Above 120 km, models are presented to take into account varying solar activity. The older 1962 model is classified in the 1966 supplements as an average mid-latitude (30° N to 60° N) spring/fall model.

The 1962 U.S. Standard Atmosphere is the more general model and it is useful to list the standard sea level conditions:

$$\text{Pressure, } p_0 = 101\ 325.0 \text{ N/m}^2$$

$$\text{Density, } \rho_0 = 1.225 \text{ kg/m}^3 [\rho = \text{Greek letter rho}]$$

$$\text{Temperature, } T_0 = 288.15 \text{ K (15° C)}$$

$$\text{Acceleration of gravity, } g_0 = 9.807 \text{ m/sec}^2$$

$$\text{Speed of sound, } a_0 = 340.294 \text{ m/sec}$$

[Figure 7](#) gives a multi-plot of pressure, density, temperature, and speed of sound from sea level to 100 km. It is intended merely to indicate the general variation of these parameters. The temperature-defined atmospheric shells are also included.

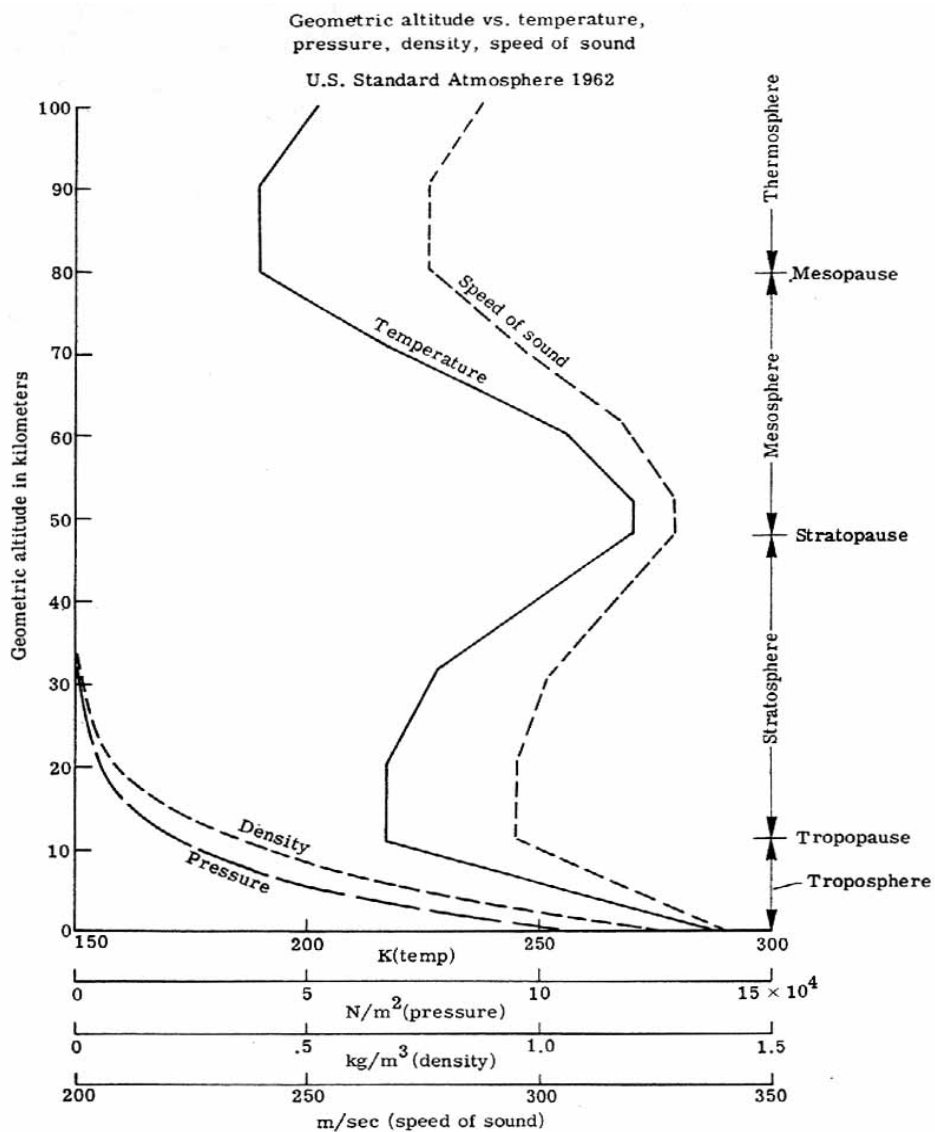


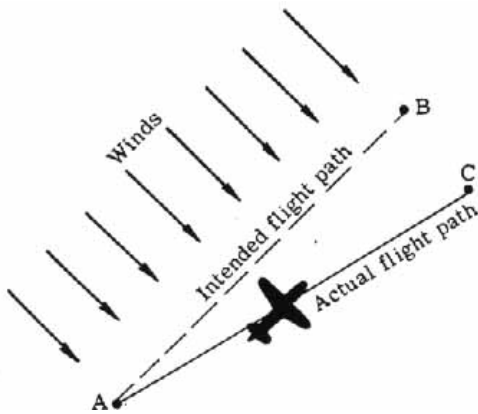
Figure 7.- Atmospheric properties variation. (Based on U.S. Standard Atmosphere, 1962).

In the troposphere (from sea level to 10 to 20 km in the standard atmosphere), it is seen that the temperature decreases linearly with altitude. In the stratosphere it first remains constant at about 217 K before increasing again. The speed of sound shows a similar type of variation. Both the density and pressure are seen to decrease rapidly with altitude. The density curve is of particular importance since, as will be seen, the lift on an airfoil is directly dependent on the density.

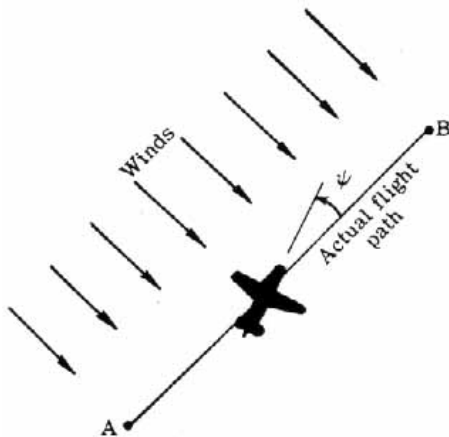
The real atmosphere - It would be fortunate if the Earth's real atmosphere corresponded to a standard atmospheric model but thermal effects of the Sun, the presence of continents and oceans, and the Earth's rotation all combine to stir up the atmosphere into a nonuniform, nonstandard mass of gases in motion. Although a standard atmosphere provides the criteria necessary for design of an aircraft, it is essential that "nonstandard" performance in the real atmosphere be anticipated also. This nonstandard performance shows up in numerous ways, some of which are discussed in this section.

Winds and Turbulence

Unquestionably, the most important real atmospheric effect, and one receiving considerable attention of late, is the relative motion of the atmosphere. Although in the standard atmosphere the air is motionless with respect to the Earth, it is known that the air mass through which an airplane flies is constantly in a state of motion with respect to the surface of the Earth. Its motion is variable both in time and space and is exceedingly complex. The motion may be divided into two classes: (1) large-scale motions and (2) small-scale motions. Large-scale motions of the atmosphere (or winds) affect the navigation and the performance of an aircraft. [Figure 8](#) illustrates one effect.



(a) Aircraft heading parallel to AB. Wind drift causes actual flight path AC.



(b) Aircraft yawed into wind with angle ψ [Greek letter psi] to account for wind drift.
Figure 8.- Effect of winds.

In [figure 8](#) (a) the pilot is attempting to fly his aircraft from point A to point B. He sets his heading and flies directly for point B but winds (representing large-scale motion of the atmosphere relative to the ground) are blowing crosswise to his intended flight path. After the required flight time which would have brought the pilot to point B if there were no winds, the pilot finds himself at point C. The winds, which were not taken into account, had forced him off course. In order to compensate for the winds, the pilot should have pointed the aircraft slightly into the wind as illustrated in [figure 8](#) (b). This change would have canceled out any drifting of the aircraft off course. Compensation for drift requires knowledge of both the aircraft's velocity and the wind velocity with respect to the ground.

Statistical average values of horizontal wind speed as a function of altitude have been calculated and represent more or less a standard curve. [Figure 9](#) represents one such typical statistical curve. Again, in the case of a real atmosphere, the real wind velocity at any particular time and place will vary considerably from the statistical average. In the case of wind drift then, rather than use a statistical curve, the pilot should consult local airports for wind conditions and forecasts along his intended flight path.

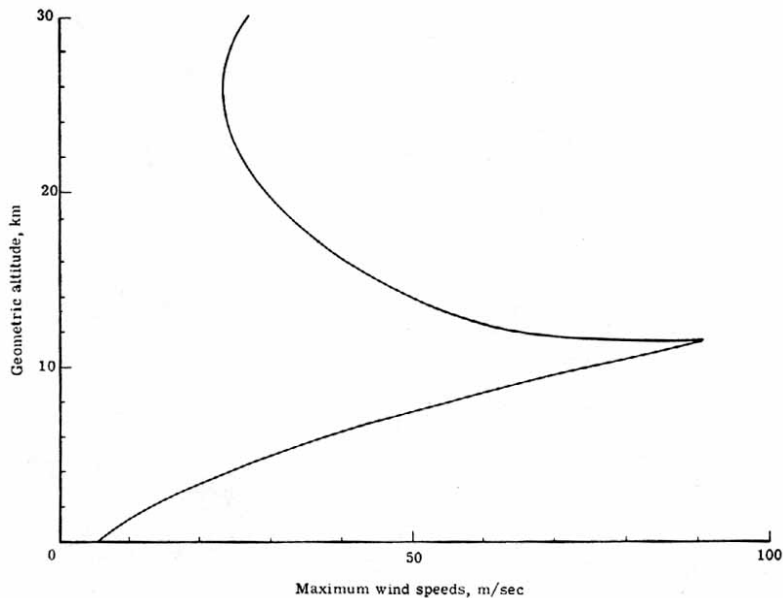


Figure 9.- A typical statistical maximum wind speed curve. USAF Handbook of Geophysics.

The small-scale motion of the atmosphere is called turbulence (or gustiness). The response of an aircraft to turbulence is an important matter. In passenger aircraft, turbulence may cause minor problems such as spilled coffee and in extreme cases injuries if seat belts are not fastened. Excessive shaking or vibration may render the pilot unable to read instruments. In cases of precision flying such as air-to-air refueling, bombing, and gunnery, or aerial photography, turbulence-induced motions of the aircraft are a nuisance. Turbulence-induced stresses and strains over a long period may cause fatigue in the airframe and in extreme cases a particular heavy turbulence may cause the loss of control of an aircraft or even immediate structural failure.

There are several causes of turbulence. The unequal heating of the Earth's surface by the Sun will cause convective currents to rise and make the plane's motion through such unequal currents rough. On a clear day the turbulence is not visible but will be felt; hence, the name "clear air turbulence (CAT)." Turbulence also occurs because of winds blowing over irregular terrain or, by different magnitude or direction, winds blowing side by side and producing a shearing effect.

In the case of the thunderstorm, one has one of the most violent of all turbulences where strong updrafts and downdrafts exist side by side. The severity of the aircraft motion caused by the turbulence will depend upon the magnitude of the updrafts and downdrafts and their directions. Many private aircraft have been lost to thunderstorm turbulence because of structural failure or loss of control. Commercial airliners generally fly around such storms for the comfort and safety of their passengers.

[Figure 10](#) illustrates the flight path of an aircraft through the various turbulences described.

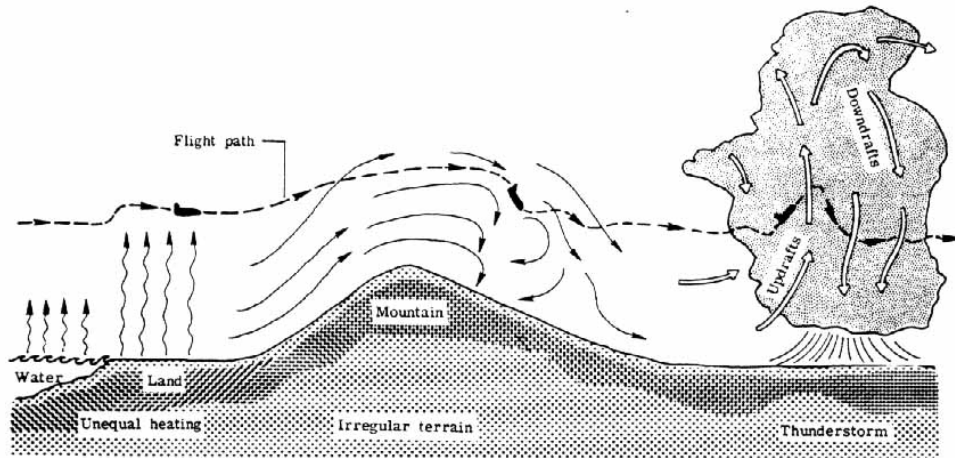


Figure 10.- Flight path of an aircraft through various forms of turbulence.
Relatively stable air exists above thunderstorms.

Another real atmospheric effect is that of moisture. Water in the air, in either its liquid or vapor form, is not accounted for in the pure dry standard atmosphere and will affect an aircraft in varying degrees. Everyone is familiar with the forms of precipitation that can adversely affect aircraft performance such as icing on the wings, zero visibility in fog or snow, and physical damage caused by hail. Water vapor is less dense than dry air and consequently humid air (air containing water vapor) will be less dense than dry air. Because of this, an aircraft requires a longer take-off distance in humid air than in the more dense dry air.

Air density is a very important factor in the lift, drag, and engine power output of an aircraft and depends upon the temperature and pressure locally. Since the standard atmosphere does not indicate true conditions at a particular time and place, it is important for a pilot to contact a local airport for the local atmospheric conditions.

From the local temperature and pressure readings, density may be obtained and, hence, take-off distance and engine power output may be determined.

The local pressure is important in aircraft using pressure altimeters. A pilot must zero his pressure altimeter to local measured sea-level pressure rather than to standard sea-level pressure if he is to obtain accurate altitude readings above sea level.

Although the preceding discussion considers only a few of the many effects of a nonstandard atmosphere on aircraft design and performance, the standard atmosphere still remains as a primary reference in the preliminary design stage of an aircraft.

The Airplane

Basic airplane - Our attention will be centered mainly on that class of aircraft known as airplanes. Before proceeding into any discussion of aerodynamic theory and its application to airplanes, it would be well to consider in some detail the overall physical makeup of a typical airplane.

As [figure 11](#) demonstrates in exploded view form, an airplane may be resolved into several basic components as follows: fuselage, wing, tail assembly and control surfaces, landing gear, and powerplant(s). The aerodynamics of these components is considered later in the discussion.

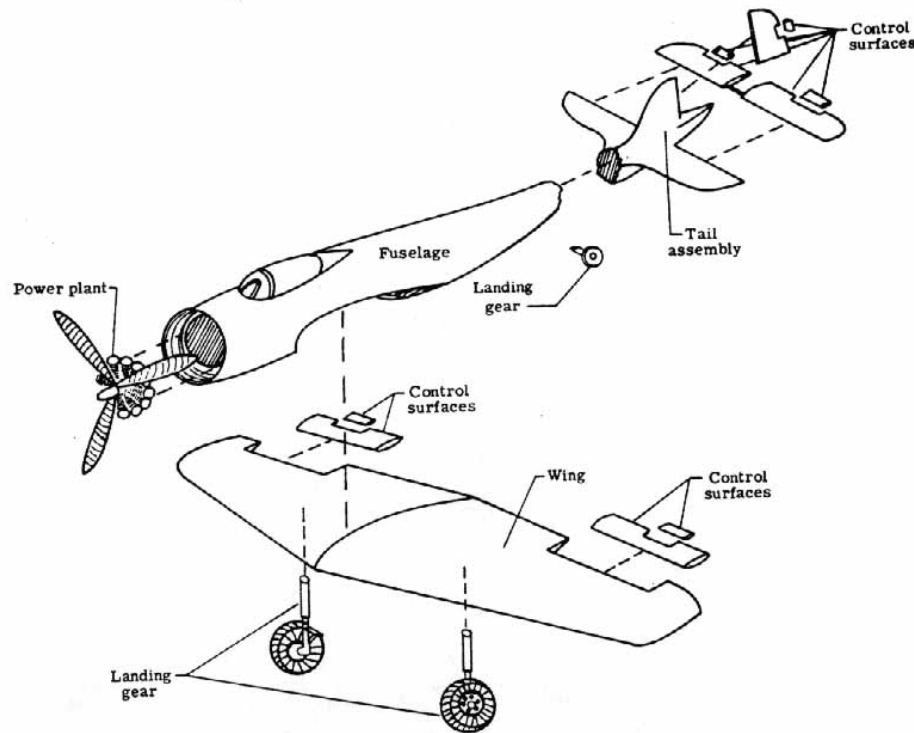


Figure 11.- Basic airplane components.

Fuselage - The body of an airplane is called the fuselage. It houses the crew and the controls necessary for operating and controlling the airplane. It may provide space for cargo and passengers and carry armaments of various sorts. In addition, an engine may be housed in the fuselage. The fuselage is, in one sense, the basic structure of the airplane since many of the other large components are attached to it. It is generally streamlined as much as possible to reduce drag. Designs vary with the mission to be performed and the variations are endless, as illustrated in [figure 12](#).

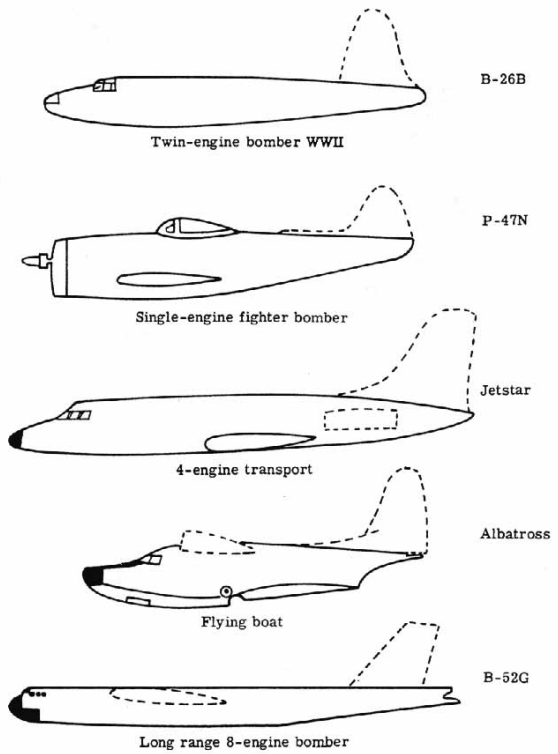


Figure 12.- Various fuselage designs.

Wing - The wing provides the principal lifting force of an airplane. Lift is obtained from the dynamic action of the wing with respect to the air. The cross-sectional shape of the wing is known as the airfoil section. The airfoil section shape, planform shape of the wing, and placement of the wing on the fuselage depend upon the airplane mission and the best compromise necessary in the overall airplane design. [Figure 13](#) illustrates the shapes and placements often used.

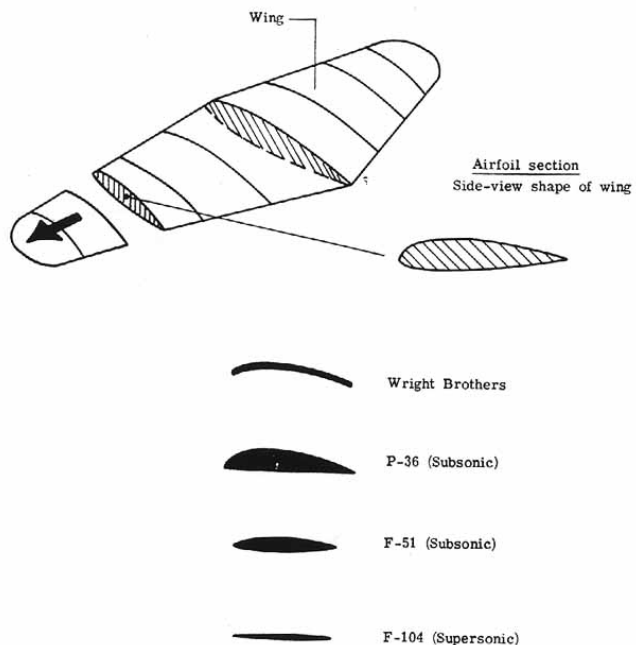
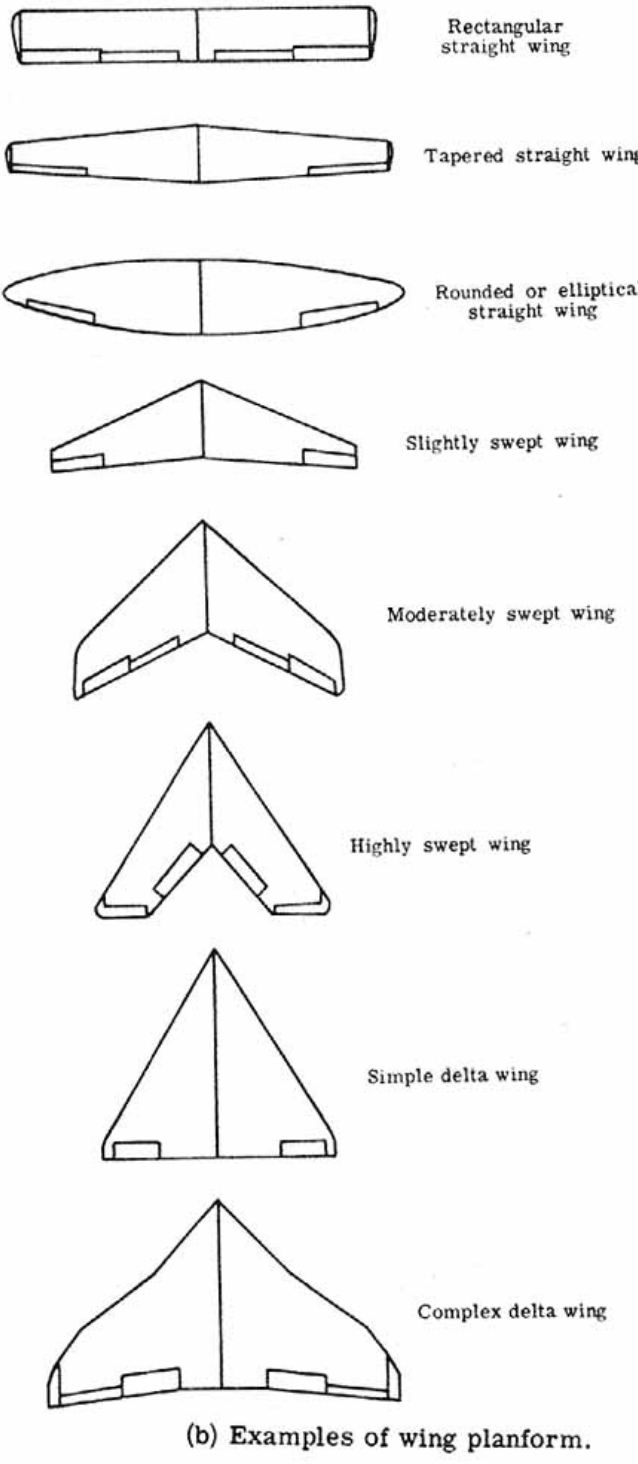


Figure 13 (a) Examples of airfoil shapes.



(b) Examples of wing planform.

Figure 13 (b) Examples of wing planforms

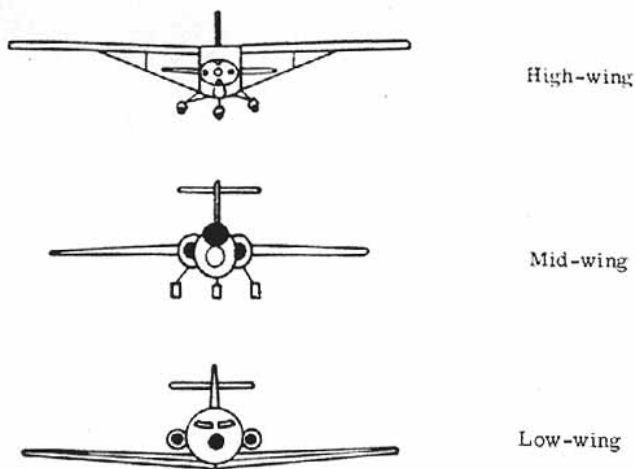


Figure 13 (c) Examples of wing placements

Tail assembly and control surfaces - The tail assembly (appendage) represents the collection of structures at the rear of the airplane. The tail assembly consists of (1) the vertical stabilizer (fin) and rudder which provide directional stability in yaw, and (2) the horizontal stabilizer and elevator which provide longitudinal stability in pitch. [Figure 14](#) illustrates the numerous forms that a tail assembly may take.

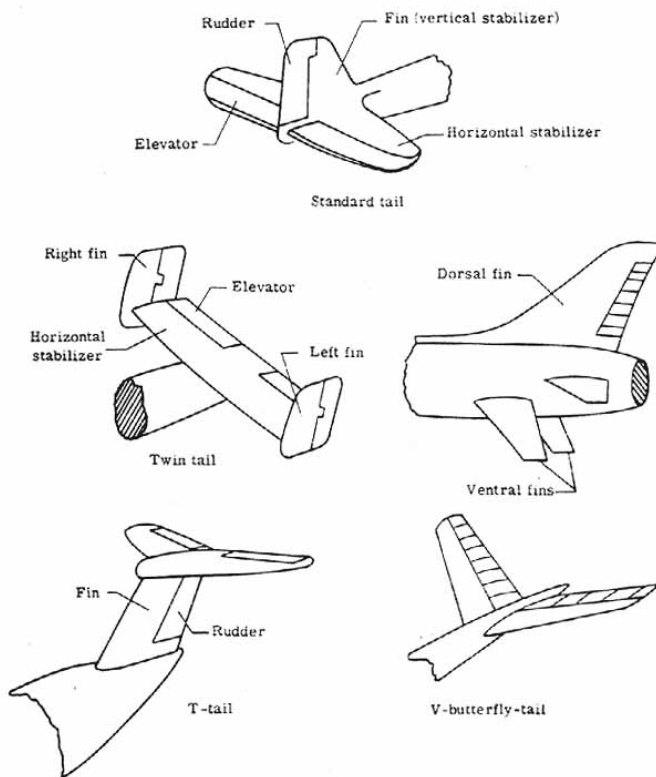
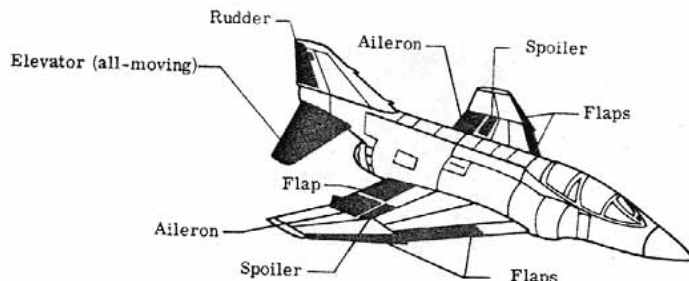
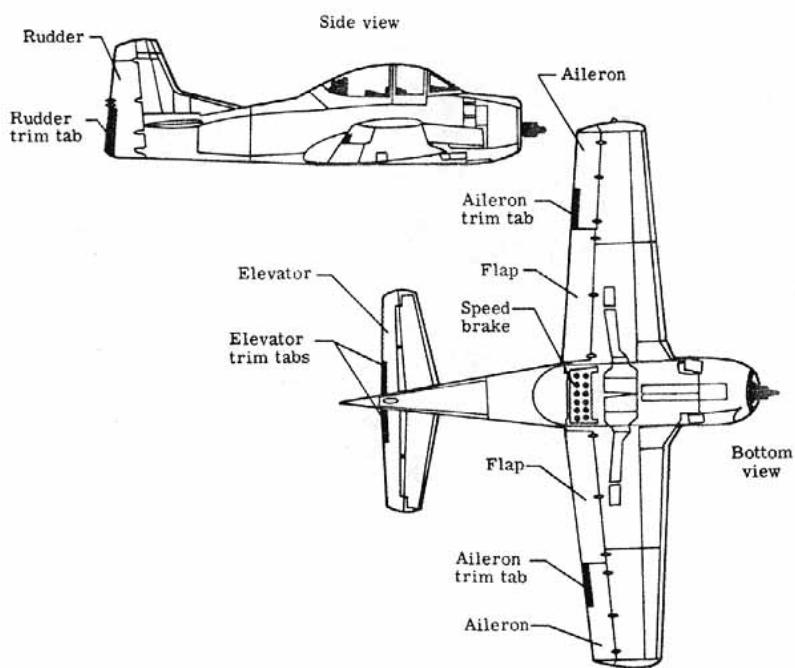


Figure 14.- Tail assembly forms.

Included in the control surfaces are all those moving surfaces of an airplane used for attitude, lift, and drag control. Yaw control (turning the airplane to the left or right) is provided by the rudder which is generally attached to the fin. Pitch control (nosing the airplane up or down) is provided by the elevators which are generally attached to the horizontal stabilizer. Roll control (rolling the wing to the right or left) is provided by the ailerons located generally near the outer trailing edge of the wing. Trim tabs are small auxiliary hinged control surface inserts on the elevator, rudder, and aileron surfaces whose functions are (1) to balance the airplane if it is too nose heavy, tail heavy, or wing heavy to fly in a stable cruise condition, (2) to maintain the elevator, rudder, or ailerons at whatever particular setting the pilot wishes without the pilot maintaining pressures on the controls, (3) to help move the elevators, rudder, and ailerons and thus relieve the pilot of the effort necessary to move the surfaces. Flaps are hinged or pivoted parts of the leading and/or trailing edges of the wing used to increase lift at reduced airspeeds. They are used primarily for landing and takeoff. Spoilers are devices used to reduce the lift on an airplane wing quickly. By operating independently on both sides of the wing, they may provide an alternate form of roll control. [Figure 15](#) illustrates the attitude control surfaces and [figure 16](#) shows a simple aileron and flap installation and a more complicated arrangement used on a large jet airliner.

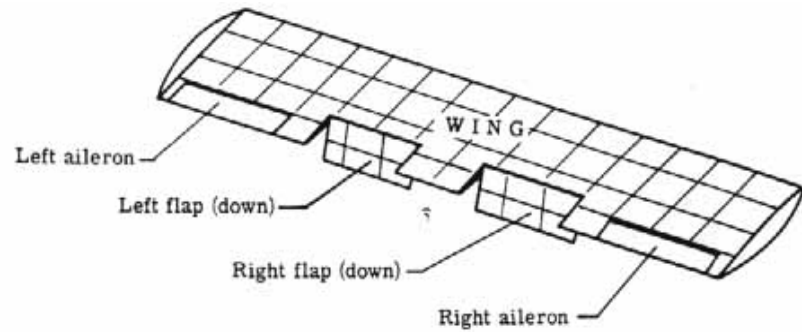


(a) Control surfaces on F-4B Phantom.

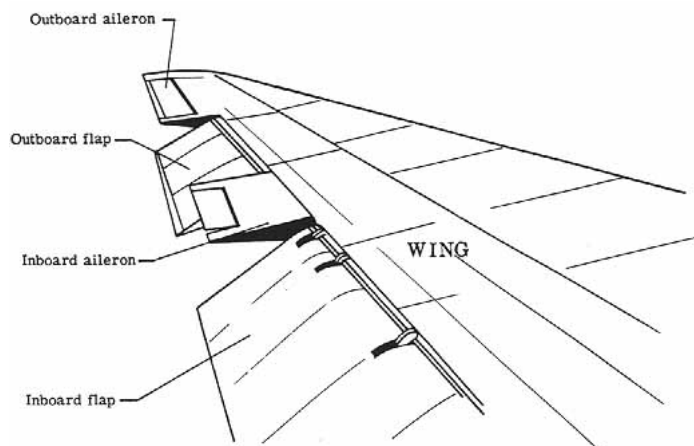


(b) Control surfaces on T-28B.

Figure 15.- Main control surfaces.



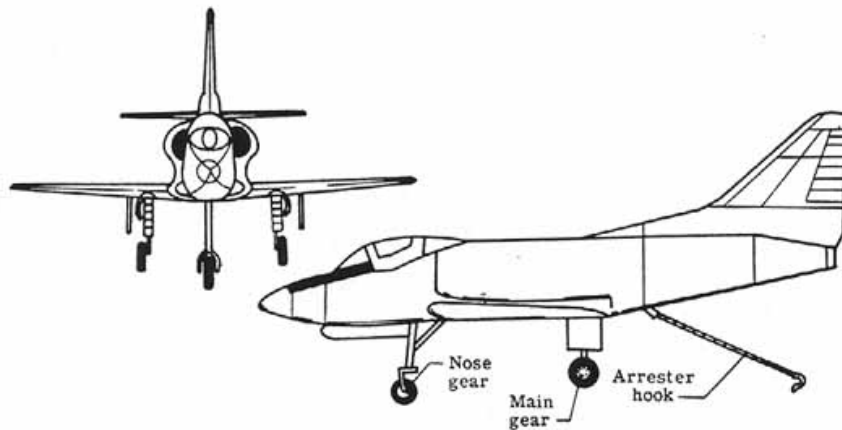
(a) Simple flap arrangement.



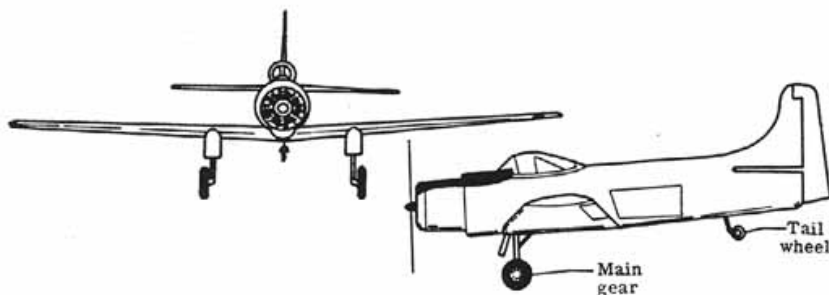
(b) Jet airliner aileron and flap assembly on wing.

Figure 16.- Flaps and ailerons.

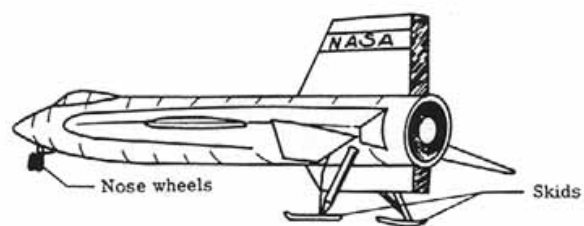
Landing gear - The landing gear, or undercarriage, supports the airplane while it is at rest on the ground or in water, and during the take-off and landing. The gear may be fixed or retractable. The wheels of most airplanes are attached to shock-absorbing struts that use oil or air to cushion the blow of landing. Special types of landing gear include skis for snow and floats for water. For carrier landings, arrester hooks are used. [Figure 17](#) shows several of the gear arrangements found on modern-day airplanes.



(a) Tricycle gear – nose wheel, two main wheels.



(b) Conventional gear – tail wheel, two main wheels.



(c) Unconventional gear – skis, skids, or floats.

Figure 17.- Landing-gear forms.

Power plants - With few exceptions an airplane must possess a thrust-producing device or power plant to sustain flight. The power plant consists of the engine (and propeller, if present), and the related accessories. The main engine types are the reciprocating (or piston type), and the reaction engines such as the ram jet, pulse jet, turbojet, turboprop, and rocket engine. Converting the energy of a reciprocating engine's rotating crankshaft into a thrust force is accomplished by the propeller.

[Figure 18](#) illustrates some of the many varied engine placements possible.

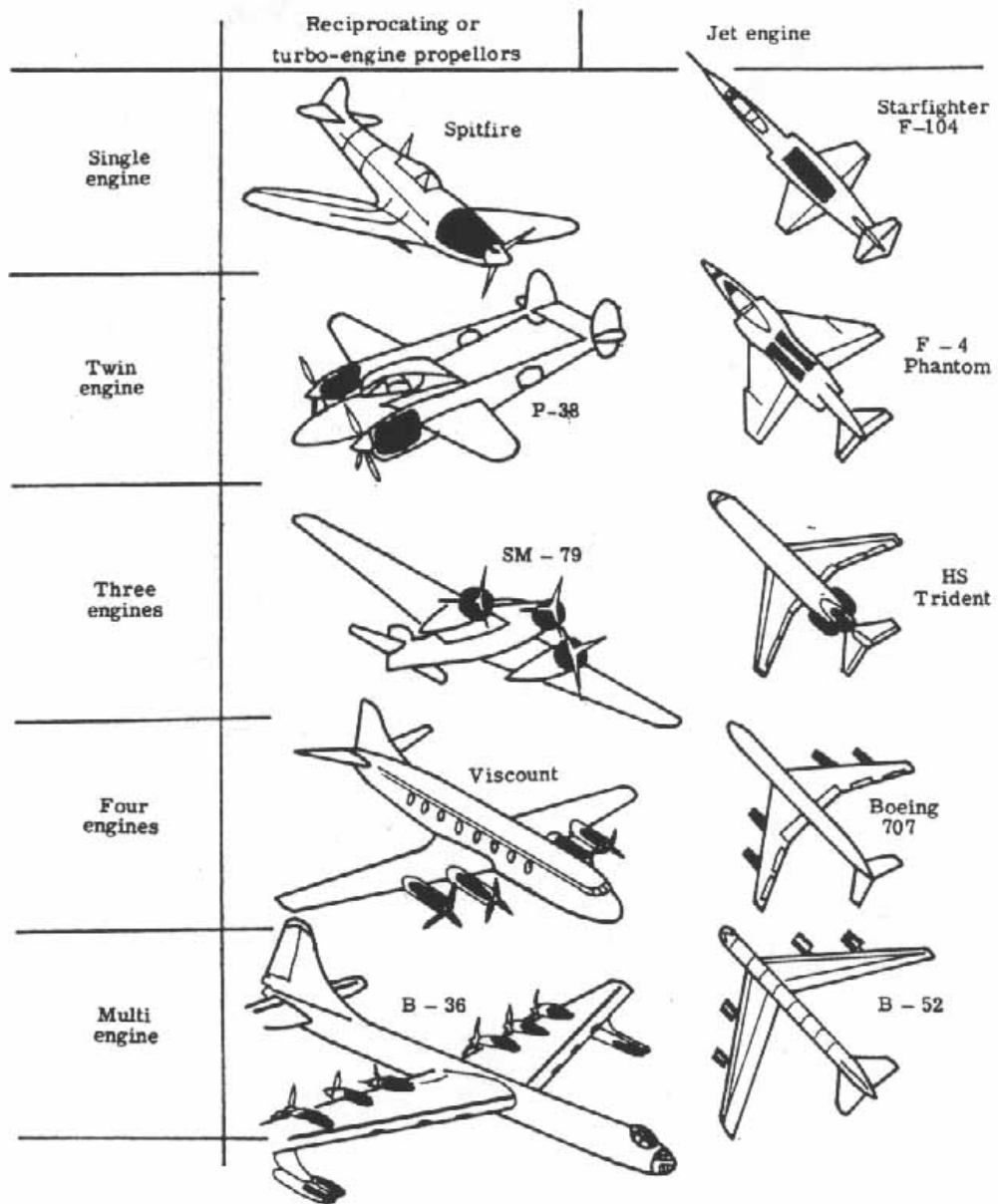


Figure 18.- Power-plant placement.

Forces on an airplane - There are two general types of forces that may act on a body in unaccelerated or steady flight. They may be termed as body forces and surface forces. Body forces act on the body from a distance. For the airplane this is the gravitational force or weight. Surface forces act because of contact between the medium and the body, that is, between the air and the airplane surface. Lift, drag, and thrust, the other three main forces acting on an airplane, are all surface forces. Basically, the forces acting on an airplane are weight, thrust, lift, and drag.

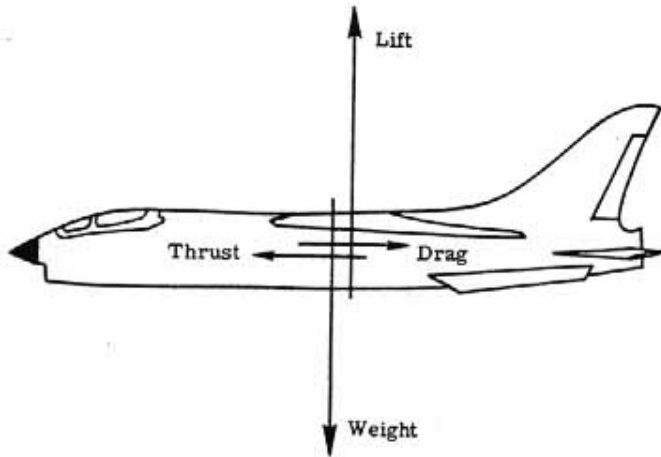


Figure 19.- Forces on an airplane in normal flight.

Weight: The weight includes the airplane itself, the payload, and the fuel. Since fuel is consumed as the airplane flies, the weight decreases. Weight acts in a direction toward the center of the Earth.

Thrust: The driving force of whatever propulsive system is used, engine driven propeller, jet engine, rocket engine, and so forth, is the thrust. It may be taken to act along the longitudinal axis of the airplane (except for vertical take-off airplanes).

Lift: This force is generated by the flow of air around the airplane, the major portion resulting from the wing. It represents the component of the resultant aerodynamic force normal to the line of flight.

Drag: Again, this force arises from the flow of air around the airplane but is the component of the resultant aerodynamic force along the line of flight.

In the simplest flight situation an airplane will travel in straight and level flight at a uniform velocity. [Figure 19](#) shows the disposition of the four forces under these conditions. To maintain this basic flight situation, the lift equals the weight, and the thrust equals the drag. Weight and thrust are physical attributes of an airplane. They generally are known or can be easily determined and controlled. But lift and drag arise because of the dynamic movement of the airplane through the air. The major concern of aerodynamics is the manner in which the lift and drag forces arise. This subject is considered now in some detail.

III. FLUID FLOW

The Fluid

Viscosity - There are basically three states of matter - solid, liquid, and gas. H₂O is commonly called "ice" in the solid state, "water" in the liquid state, and "water vapor" in the gaseous state. Assume one has a piece of ice and side forces are applied to it (called shearing forces). Very large forces are needed to deform or break it. The solid has a very high internal friction or resistance to shearing. The word for internal friction is viscosity and for a solid its value is generally very large.

Liquids and gases are considered to be fluids since they behave differently from a solid. Imagine two layers of water or air. If shear forces are applied to these layers, one discovers a substantial and sustained relative motion of the layers with the air layers sliding faster over one another than the water layers. However, the fact that a shear force must be applied to deform the fluids indicates that they also possess internal friction.

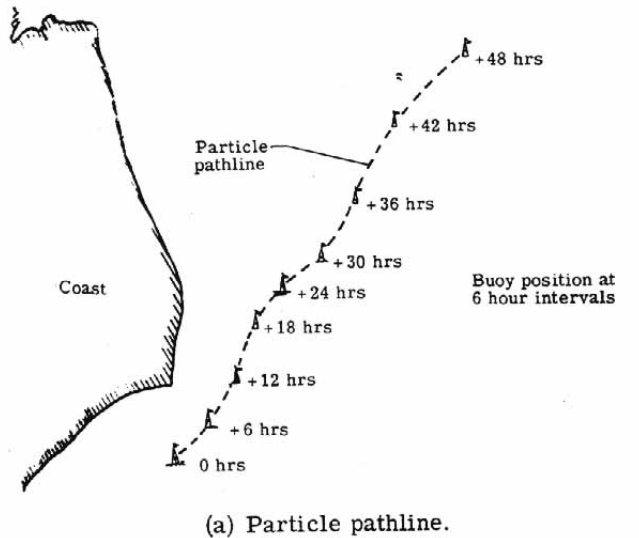
Water, under normal temperatures, is about fifty times more viscous than air. Ice is 5×10^{16} times more viscous than air. One concludes that, in general, solids have extremely high viscosities whereas fluids have low viscosities. Under the category of fluids, liquids generally possess higher viscosities than gases. Air, of primary interest in aerodynamics, has a relatively small viscosity, and in some theories, it is described as a perfect fluid-one that has zero viscosity or is "inviscid." But it will be shown that even this small viscosity of air (or internal friction) has important effects on an airplane in terms of lift and drag.

Compressibility - All fluids are compressible (that is, density increases under increasing pressure) to some extent, but liquids are generally highly incompressible compared with gases. Even gases may be treated as incompressible provided the flow speeds involved are not great. For subsonic flow over an airplane below about 150 m/sec, air may be treated as incompressible (that is, no change in density throughout the flow). At higher speeds the effects of compressibility must be taken into account.

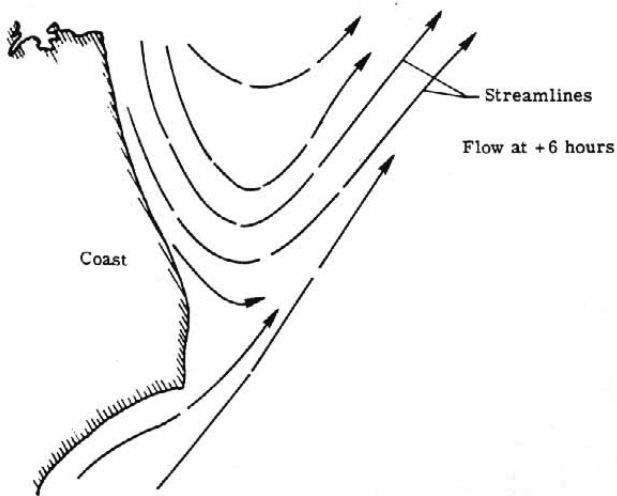
The Flow

Pathlines and streamlines - A fluid flow may be described in two different - the Lagrangian approach and the Eulerian approach. From the Lagrangian standpoint, one particle is chosen and it is followed as it moves through space with time. The line traced out by that one particle is called a particle pathline. An example is a transmitting ocean buoy shown in [figure 20\(a\)](#). Its position has been marked at 6-hour intervals over a period of several days. The path observed is the particle pathline.

In order to obtain a clearer idea of the flow- field at a particular instant, a Eulerian approach is adopted. One is looking at a "photograph" of the flow. [Figure 20\(b\)](#) shows the surface ocean currents at a particular fixed time. The entire flow field is easily visualized. The lines comprising this flow field are called streamlines.



(a) Particle pathline.



(b) Streamlines.

Figure 20.- Particle pathline and streamlines.

It is important to note the differences between a particle pathline and a streamline. A pathline refers to the trace of a single particle in time and space whereas a streamline presents the line of motion of many particles at a fixed time. The question of whether particle pathlines and streamlines are ever the same is considered next.

Steady flow compared with unsteady flow - Of basic importance in understanding fluid movements about an object is the concept of a "steady flow." On a windy day a person calls the wind steady if where he stands it blows constantly from the same direction at a constant speed. If, however, the speed or direction changes, the wind is "gusty" or unsteady. In a similar manner the flow of a fluid about an object is steady if its velocity (speed and direction) at each point in the flow remains constant - this does not necessarily require that the velocity be the same at all points in the fluid.

To consider this further, [figure 21\(a\)](#) presents the fluid flow (of air) about a house on a windy day at one instant of time and [figure 21\(b\)](#) shows the flow an instant of time later. One sees that this flow is unsteady. There are many areas where the flow pattern is different; the streamlines are changing their position and shape with time. Particle pathlines and streamlines for this flow are not equivalent.

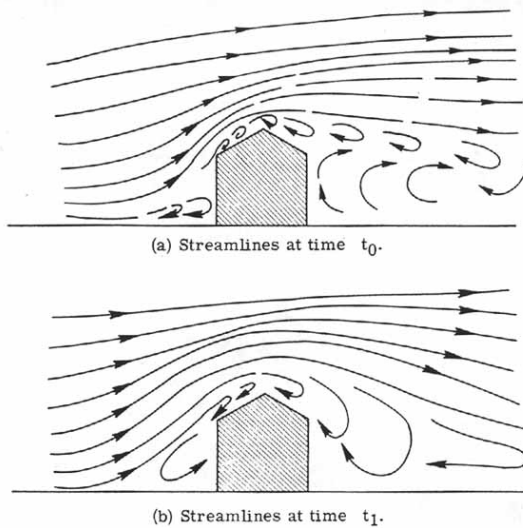


Figure 21.- Unsteady flow of air about a house.

[Figure 22](#) shows a nicely "streamlined" body (as opposed to the bluff-shaped house) in a wind tunnel. At time t_0 the tunnel is not running and no air is flowing. At time t_1 the tunnel is started and air begins flowing about the body; the flow develops further at time t_2 and finally reaches a constant pattern at time t_3 . The flow appears unchanged at time t_4 and time t_5 . When the flow starts, it passes through an unsteady transient state; that is, particle pathlines and streamlines are not the same. From time t_3 onwards a steady flow is established. Streamlines appear fixed in position with respect to the body. A particle P shown on a streamline at time t_3 moves downstream along that streamline as shown at times t_4 and t_5 . The particle pathline coincides with the streamline.

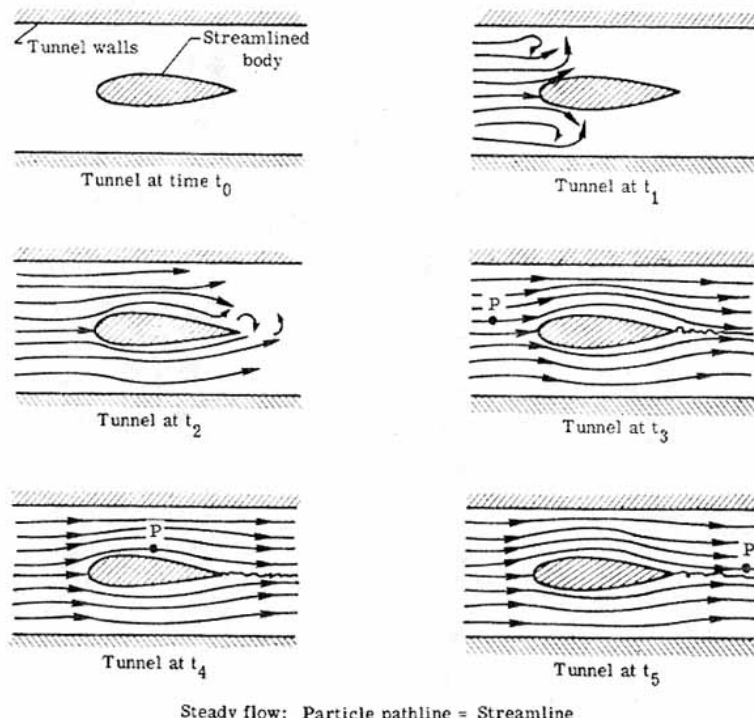
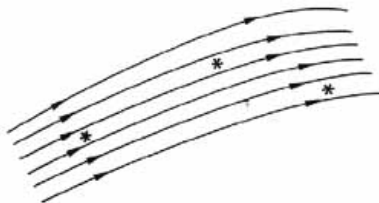


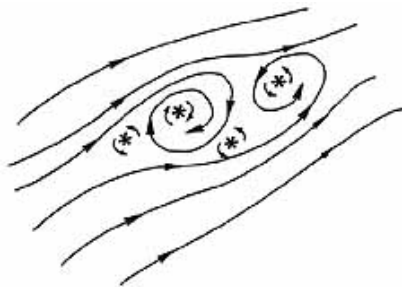
Figure 22.- Unsteady and steady flow

Summarizing, this means that for a steady flow a particle pathline and streamline are equivalent and the Lagrangian point of view is the same as the Eulerian approach for flow visualization.

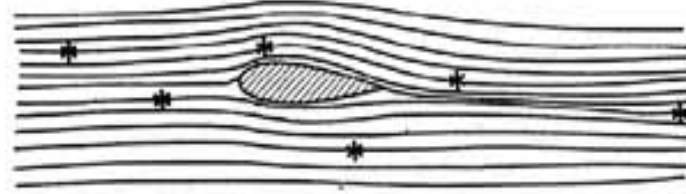
Rotational and irrotational flow - Fluid flow can be rotational or irrotational. If the elements of fluid at each point in the flow have no net angular (spin) velocity about the points, the fluid flow is said to be irrotational. One can imagine a small paddle wheel immersed in a moving fluid as in [figure 23\(a\)](#). If the wheel translates without rotating, the motion is irrotational. If the wheel rotates in a flow, as illustrated in [figure 23\(b\)](#), the flow is rotational.



(a) Irrotational flow.



(b) Rotational flow.



(c) Inviscid, irrotational flow about an airfoil.

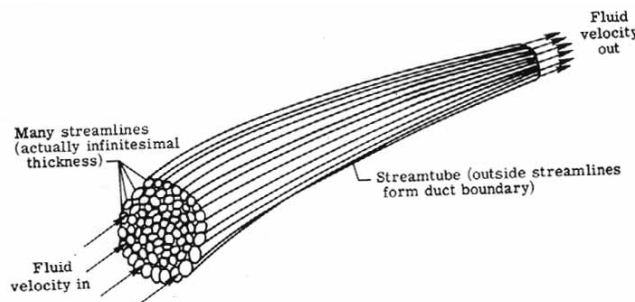
Figure 23.- Rotational and irrotational flow.

According to a theorem of Helmholtz, assuming zero viscosity, if a fluid flow is initially irrotational, it remains irrotational. In [figure 23\(c\)](#), an observer is fixed to the airfoil section shown. The flow far ahead of the airfoil section is uniform and of constant velocity. It is irrotational. As the airflow passes about the airfoil section, it remains irrotational if zero viscosity is assumed. In real life, viscosity effects are limited to a small region near the surface of the airfoil and in its wake. Most of the flow may still be treated as irrotational.

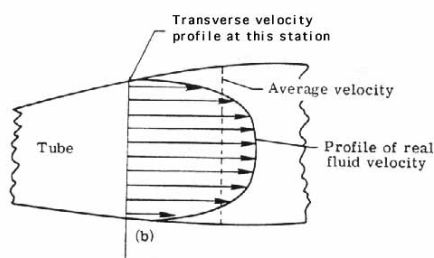
One-dimensional flow - A simplifying argument often employed to aid in understanding basic ideas is that of a one-dimensional flow. [Figure 24\(a\)](#) shows a bundle of streamlines of a simple flow. Each streamline can be thought of as a stream tube since fluid flows along it as if in a tube. In the case of steady flow, the stream tube is permanent. Taken together, the bundle of stream tubes comprise an even larger stream tube. Fluid flows through it as, for example, water flows through a pipe or channel. The velocity varies across the tube, in general, according to the individual streamline velocity variation, as shown in [figure 24\(b\)](#). One can easily imagine an "average" uniform value of velocity at the cross section to represent the actual varying value as indicated in [figure 24\(c\)](#). The velocity then is considered "one dimensional" since it varies only with the particular distance along the tube where observations are made. In addition to velocity, pressure, density, temperature, and other flow properties must also be uniform at each cross section for the flow to be one dimensional.

In order to understand how aerodynamic forces arise, two basic principles must be considered. They are the laws of conservation of mass and conservation of energy. Simply stated, they convey the facts that mass and energy can neither be created nor destroyed.

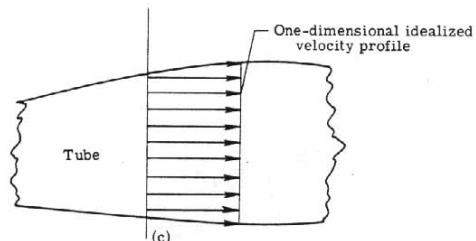
For introductory purposes, simplifying assumptions are made. The fluid is considered to be inviscid and incompressible (and hence, "perfect"). The flow is considered steady and one dimensional.



(a) Stream tubes.



(b) Real velocity flow profile.



(c) One-dimensional flow profile.

Figure 24.- Stream tubes and one-dimensional flow.

Ideal Fluid Flow

The continuity equation - The continuity equation is a statement of the conservation of mass in a system. Consider a pipe which is uniform in diameter at both ends, but has a constriction between the ends as in [figure 25\(a\)](#). This is called a venturi tube. Furthermore, it is assumed that the fluid, under the previously stated assumptions, is flowing in the direction indicated. Stations 1 and 2 have cross-sectional areas A_1 and A_2 , respectively. Let V_1 and V_2 be the average flow speeds at these cross sections (one-dimensional flow). A further assumption is that there are no leaks in the pipe nor is fluid being pumped in through the sides. The continuity equation states that the fluid mass passing station 1 per unit time must equal the fluid mass passing station 2 per unit time. In fact, this "mass flow rate" must be the same value at any cross section examined or there is an accumulation of mass—"mass creation"—and the steady flow assumption is violated. Simply stated,

$$(\text{Mass rate})_1 = (\text{Mass rate})_2 \quad (1)$$

where

$$\text{Mass rate} = \text{Density} \times \text{Area} \times \text{Velocity} \quad (2)$$

This equation reduces to

$$\rho_1 A_1 V_1 = \rho_2 A_2 V_2 \quad (3)$$

Since the fluid is assumed to be incompressible, ρ [Greek letter rho] is a constant and equation (3) reduces to

$$A_1 V_1 = A_2 V_2 \quad (4)$$

This is the simple continuity equation for inviscid, incompressible, steady, one-dimensional flow with no leaks. If the flow were viscous, the statement would still be valid as long as average values of V_1 and V_2 across the cross section are used.

By rearranging equation (4), one obtains

$$V_2 = (A_1/A_2)V_1 \quad (5)$$

Since A_1 is greater than A_2 (see [fig. 25\(a\)](#)), it can be concluded that V_2 is greater than V_1 . This is a most important result. It states, under the assumptions made, that the flow speed increases where the area decreases and the flow speed decreases where the area increases. [Figure 25\(b\)](#) shows this with the longer arrow at the constriction indicating a larger flow speed than at the ends. In fact, by the continuity equation, the highest speed is reached at the station of smallest area. This is at the narrowest part of the constriction commonly called the throat of the venturi tube.

The fact that the product AV remains a constant along a tube of flow allows an interpretation of the streamline picture. [Figure 25\(c\)](#) shows the streamline pattern in the venturi tube. In the area of the throat, the streamlines must crowd closer together than in the wide part. Hence, the distance between streamlines decreases and the fluid speed increases. The conclusion is that, relatively speaking,

widely spaced streamlines indicate regions of low-speed flow and closely spaced streamlines indicate regions of high-speed flow.

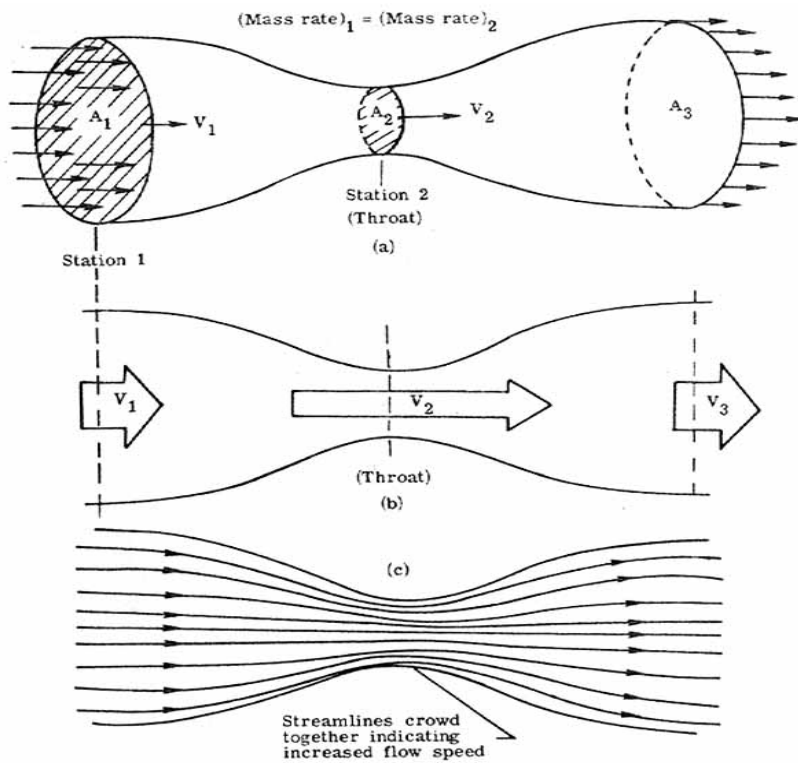


Figure 25.- Venturi tube and continuity principle.

Bernoulli's theorem-the conservation of energy - Assume a fluid flow which, as before, is inviscid, incompressible, steady, and one dimensional. The energy in the flow is composed of several energies. The kinetic energy arises because of the directed motion of the fluid; the pressure energy is due to the random motion within the fluid; and the potential energy is due to the position of the fluid above some reference level. Bernoulli's theorem is an expression of the conservation of the total energy; that is, the sum total of these energies in a fluid flow remains a constant along a streamline. Expressed concisely, the sum of the kinetic energy, pressure energy, and potential energy remains a constant.

If it is further assumed that the fluid flow is horizontal (as, for example, airflow approaching an aircraft in level flight), then the potential energy of the flow is a constant. Bernoulli's theorem reduces to

$$\text{Kinetic energy} + \text{Pressure energy} = \text{Constant} \quad (6)$$

where the constant includes the constant value of potential energy. If one considers the energy per unit volume, one obtains the dimensions of pressure and Bernoulli's theorem may be expressed in terms of pressure.

The kinetic energy per unit volume is called dynamic pressure q and is determined by $q = 1/2\rho V^2$ where ρ and V are, respectively, the fluid flow density and speed at the point in question.

The pressure energy per unit volume (due to random motion within the fluid) is the static pressure of the fluid and is given the symbol p .

The constant energy per unit volume is called the total pressure p_t .

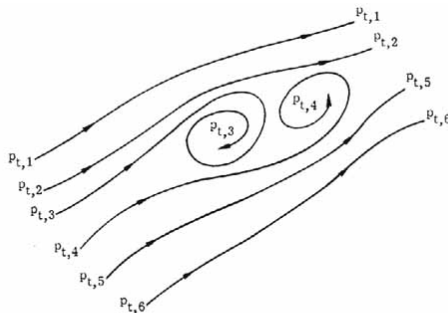
Bernoulli's equation reduces to

$$\text{Dynamic pressure} + \text{Static pressure} = \text{Total pressure} \quad (7)$$

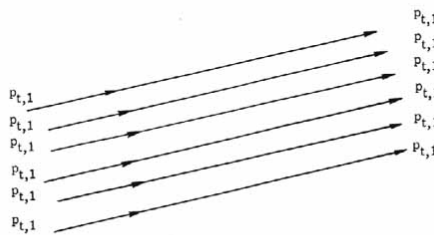
or

$$1/2\rho V^2 + p = p_t \quad (8)$$

For rotational flow the total pressure p_t is constant along a streamline but may vary from streamline to streamline as shown in [figure 26\(a\)](#). In an irrotational flow, the usual case considered for airflow approaching an aircraft, the total pressure is the same constant value everywhere as shown in [figure 26\(b\)](#).



(a) Rotational flow. Total pressure varies from streamline to streamline.



(b) Irrotational flow. Total pressure same constant value $p_{t,1}$ everywhere in flow.

Figure 26.- Total-pressure variation.

Bernoulli's equation states that in a streamline fluid flow, the greater the speed of the flow, the less the static pressure; and the less the speed of the flow, the greater the static pressure. There exists a simple exchange between the dynamic and static pressures such that their total remains the same. As one increases, the other must decrease.

Pressure measurement - Let us now examine how total, static, and dynamic pressures in a flow are measured. [Figure 27\(a\)](#) shows the fluid flow about a simple hollow bent tube, called a pitot tube after its inventor, which is connected to a pressure measurement readout instrument. The fluid dams up immediately at the tube entrance and comes to rest at the "stagnation point" while the rest of the fluid

divides up to flow around the tube. By Bernoulli's equation the static pressure at the stagnation point is the total pressure since the dynamic pressure reduces to zero when the flow stagnates. The pitot tube is, therefore, a total-pressure measuring device.

Figure 27(b) shows the fluid flow about another hollow tube except now the end facing the flow is closed and a number of holes have been drilled into the tube's side. This tube is called a static tube and may be connected to a pressure measuring readout instrument as before. Except at the stagnation point, the fluid is parallel to the tube everywhere. The static pressure of the fluid acts normal to the tube's surface. Since pressure must be continuous, the static pressure normal to the holes is communicated into the interior of the tube. The static tube, therefore, with the holes parallel to the flow direction, is a static-pressure measuring device.

Figure 27(c) shows a combined pilot-static tube. When properly connected to opposite ends of a pressure measuring readout instrument, the difference between total pressure and static pressure is measured. By Bernoulli's equation this difference is the dynamic pressure, defined as $1/2\rho V^2$. If the fluid density ρ is known, the fluid flow speed can be calculated. In actual use on aircraft, the pilot-static tube is connected directly to an airspeed indicator which, by proper gearing, will automatically display the aircraft airspeed to the pilot. The device is sometimes mounted forward on a boom extending from the airplane nose to insure its measuring, as closely as possible, the undisturbed approaching flow (also called the free-stream condition).

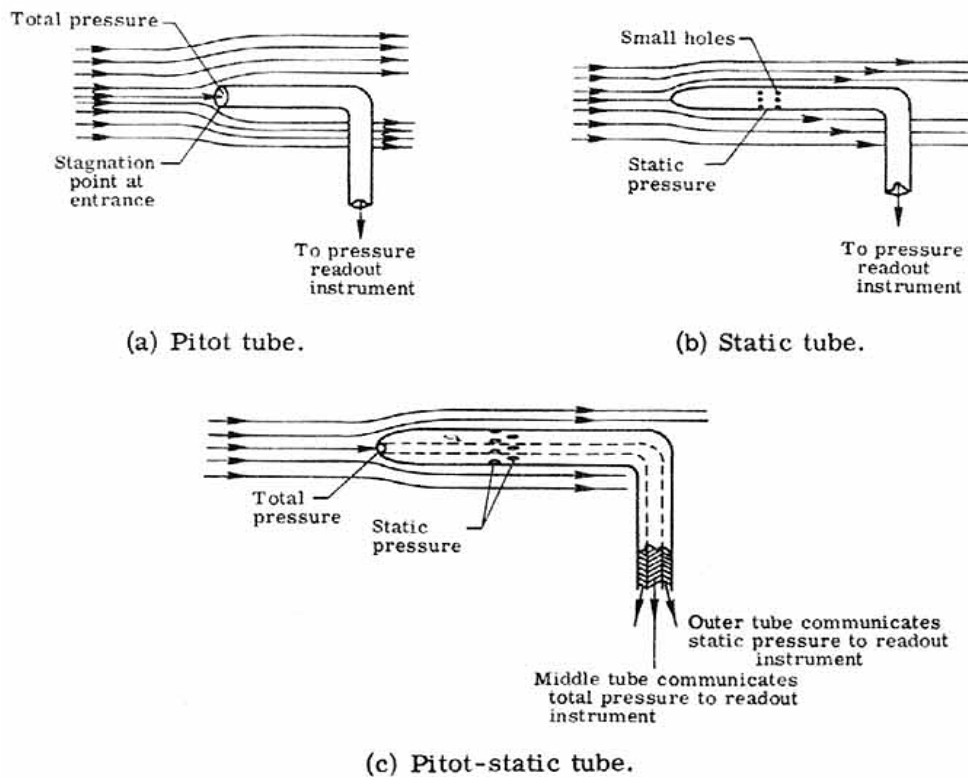
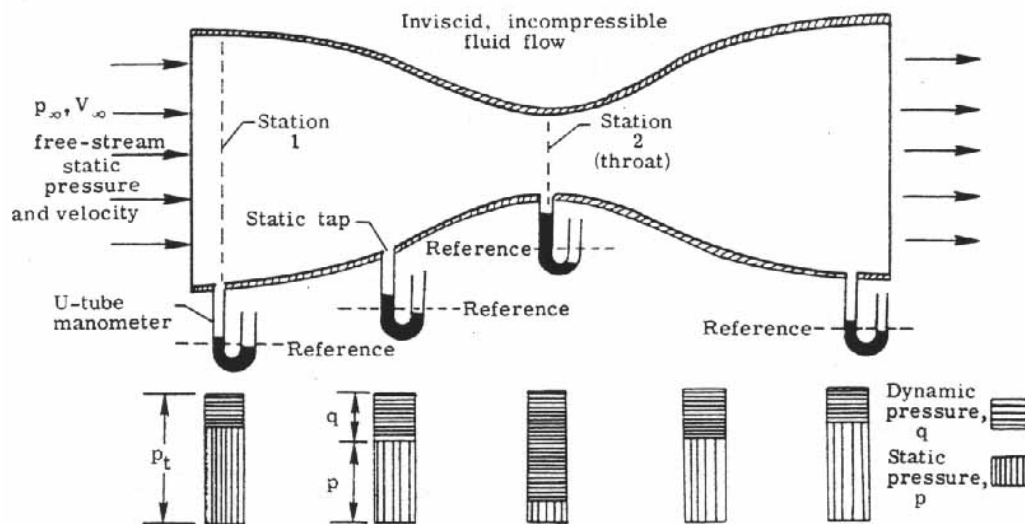


Figure 27.- Pressure measuring devices.

Returning to the discussion of the venturi tube introduced earlier, the continuity and Bernoulli equations may be used to describe the static-pressure distribution along the venturi tube. The static pressure of the undisturbed free-stream fluid flow entering the tube may be used as a reference value. Any variation of static pressure in the tube then is a greater or lesser value than the free-stream static

pressure. In [figure 28](#) holes have been drilled into the walls of the venturi tube similar to the static tube of [figure 27\(b\)](#) to measure the static pressure. These holes are commonly called "static taps" and are connected to a "U-tube manometer" - a tube having a U-shape within which is a liquid such as colored alcohol. When the static pressure measured at the static tap equals the free-stream static pressure, the fluid levels in the tube are at some equal reference level. But static pressures above or below the free-stream pressure are indicated by a decrease or increase in the level of fluid in the tube.



[Figure 28](#).- Venturi tube flow.

[Figure 28](#) shows the complete setup of a venturi tube and a set of manometers and static taps to measure static pressure. By the continuity equation the speed at station 2 V_2 is greater than that at station 1 V_1 as seen previously-the speed at the throat also is the highest speed achieved in the venturi tube. By Bernoulli's equation the total pressure p_t is constant everywhere in the flow (assuming irrotational flow). Therefore, one can express the total pressure p_t in terms of the static and dynamic pressures at stations 1 and 2 using equation (8), namely,

$$\frac{1}{2}\rho V_1^2 + p_1 = \frac{1}{2}\rho V_2^2 + p_2 = p_t \quad (9)$$

Since V_2 is greater than V_1 and $\rho_2 = \rho_1$ (fluid is incompressible) it follows that p_2 is less than p_1 , for as the dynamic pressure, hence speed, increases, the static pressure must decrease to maintain a constant value of total pressure p_t . The block diagrams below the venturi tube show this interchange of dynamic and static pressures all along the venturi tube. The conclusion drawn from this is that the static pressure decreases in the region of high-speed flow and increases in the region of low-speed flow. This is also demonstrated by the liquid levels of the manometers where as one reaches the throat the liquid level has risen above the reference level and indicates lower than free- stream static pressure. At the throat this is the minimum static pressure since the flow speed is the highest.

The airfoil in an ideal fluid - To supply a point of reference in the discussions to follow of a real fluid, the following section expands the previous discussion of venturi flow to the ideal fluid flow past an airfoil. [Figure 29\(a\)](#) shows a "symmetric" (upper and lower surfaces the same) airfoil

operating so that a line drawn through the nose and tail of the airfoil is parallel to the free-stream direction. The free-stream velocity is denoted by V_∞ and the free-stream static pressure by p_∞ . Following the particle pathline (indicated by the dotted line and equal to a streamline in this steady flow) which follows the airfoil contour, the velocity decreases from the free-stream value as one approaches the airfoil nose (points 1 to 2). At the airfoil nose, point 2, the flow comes to rest (stagnates). From Bernoulli's equation the static pressure at the nose, point 2, is equal to the total pressure. Moving from the nose up along the front surface of the airfoil (points 2 to 3), the velocity increases and the static pressure decreases. By the continuity equation, as one reaches the thickest point on the airfoil, point 3, the velocity has acquired its highest value and the static pressure its lowest value.

Beyond this point as one moves along the rear surface of the airfoil, points 3 to 4, the velocity decreases and the static pressure increases until at the trailing edge, point 4, the flow comes to rest with the static pressure equal to the total pressure. Beyond the trailing edge the flow speed increases until the free-stream value is reached and the static pressure returns to free-stream static pressure. These velocity and static-pressure distributions for the center-line streamline are shown in [figures 29\(b\)](#) and [29\(c\)](#).

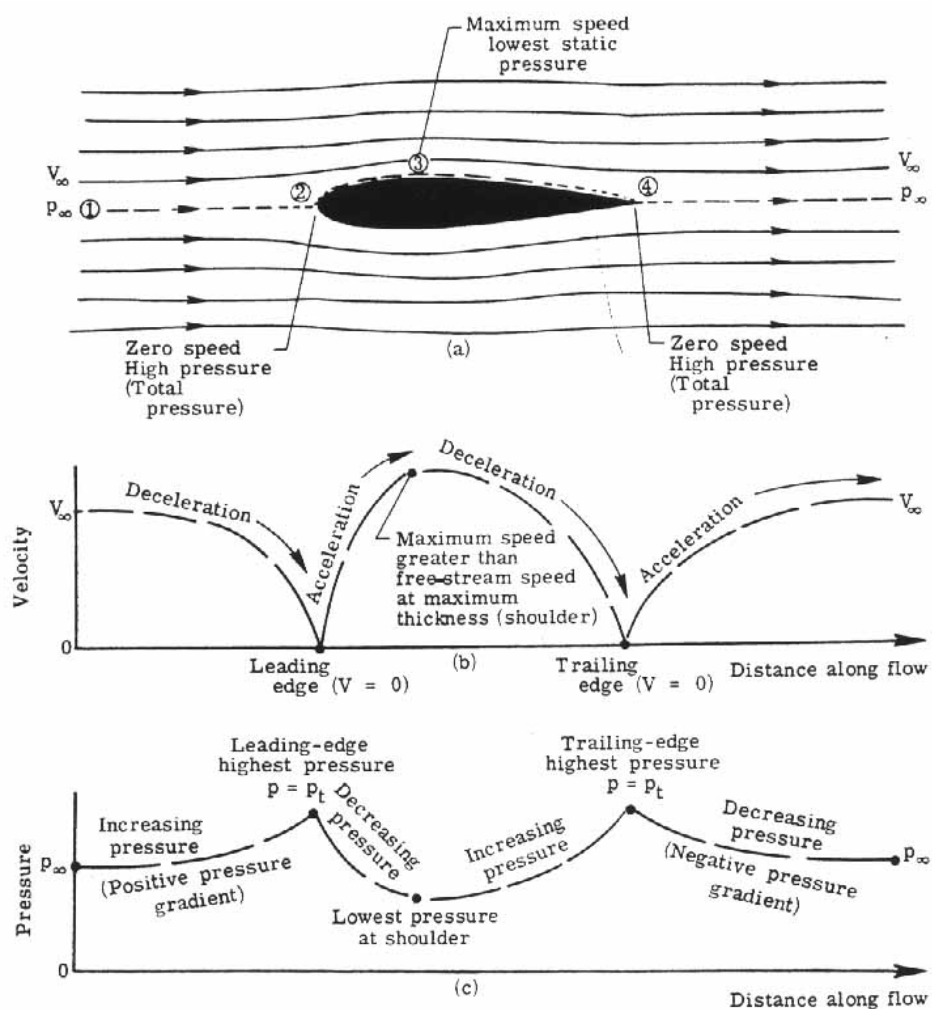


Figure 29.- Ideal fluid flow about an airfoil.

Note particularly that on the front surfaces of the airfoil (up to the station of maximum thickness), one has decreasing pressures (a negative pressure gradient) whereas on the rear surfaces one has increasing pressures (a positive pressure gradient). This relationship will be of importance in the real fluid case.

The lift is defined as the force normal to the free-stream direction and the drag parallel to the free-stream direction. For a planar airfoil section operating in a perfect fluid, the drag is always zero no matter what the orientation of the airfoil is. This seemingly defies physical intuition and is known as D'Alembert's paradox. It is the result of assuming a fluid of zero viscosity. The components of the static-pressure forces parallel to the free-stream direction on the front surface of the airfoil always exactly balance the components of the pressure forces on the rear surface of the airfoil. The lift is determined by the static-pressure difference between the upper and lower surfaces and is zero for this particular case since the pressure distribution is symmetrical. If, however, the airfoil is tilted at an angle to the free stream, the pressure distribution symmetry between the upper and lower surfaces no longer exists and a lift force results. This is very desirable and the main function of the airfoil section.

Air is not a perfect fluid. It possesses viscosity. With slight modification, the continuity and Bernoulli principles still apply in the real world. The airflow over an airfoil will appear to be slightly different with an accompanying reduction in lift and the existence of drag in several forms. The discussions of the past few pages represent basic principles. From this point on, the inviscid assumption is dropped and a real, viscous flow of air is allowed to exist.

Real Fluid Flow

Laminar and turbulent flow - There are two different types of real fluid flow: laminar and turbulent. In laminar flow the fluid moves in layers called laminas. [Figure 30\(a\)](#) shows a laminar flow, the uniform rectilinear flow, consisting of air moving in straight-line layers (laminas) from left to right. The laminas may be considered the adjacent streamtubes and then the streamlines indicate the direction of movement of these fluid layers. Laminar flow need not be in a straight line. [Figure 30\(b\)](#) shows a small segment of the surface of a curved airfoil. For an ideal fluid the flow follows the curved surface smoothly, in laminas. [Figure 30\(c\)](#) shows the more complex flow case for a real fluid to be discussed later. The closer the fluid layers are to the airfoil surface, the slower they move. However, here also, as indicated by the streamlines, the fluid layers slide over one another without fluid being exchanged between layers.

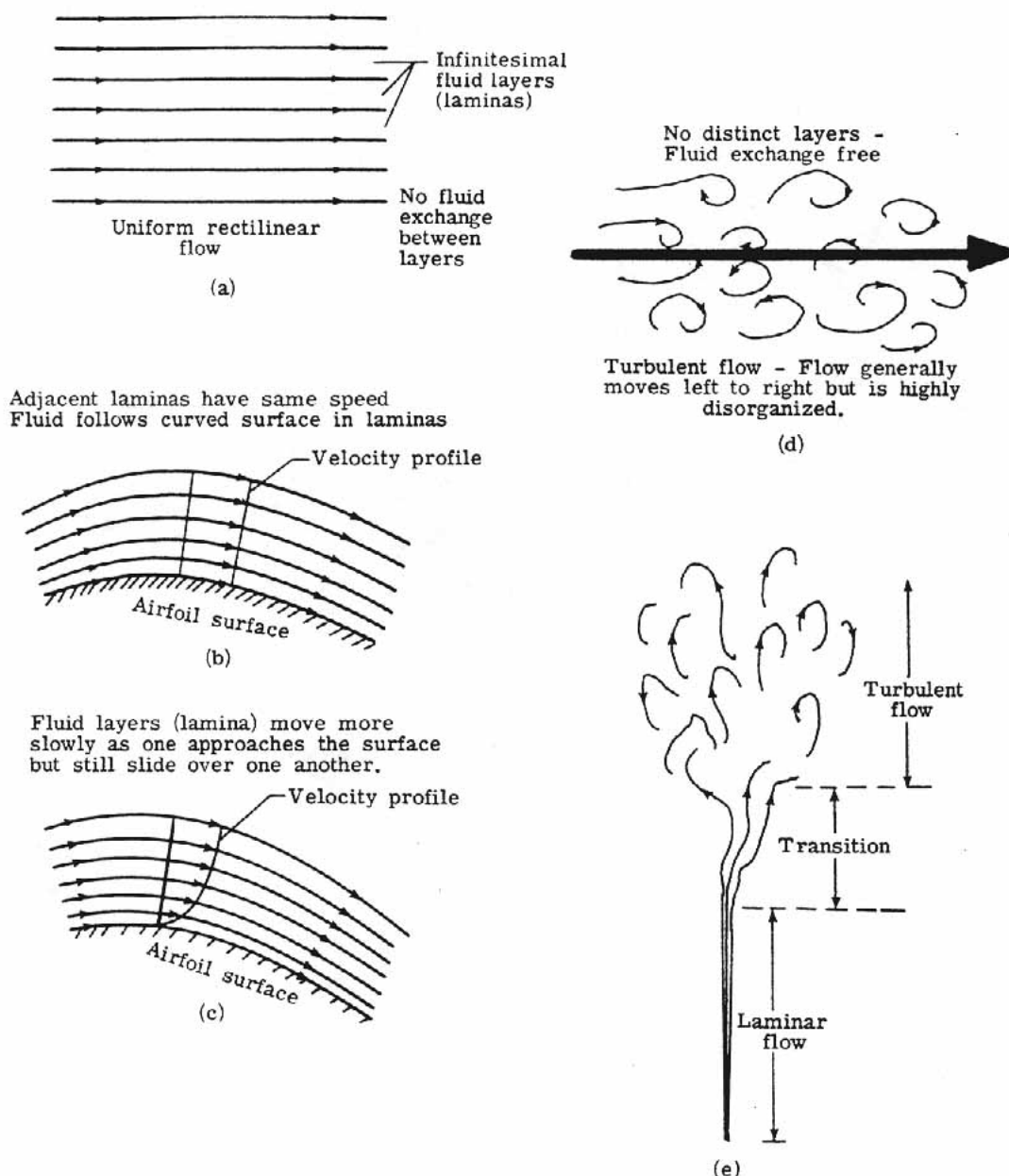


Figure 30.- Laminar and turbulent flow.

In turbulent flow, secondary random motions are superimposed on the principal flow. [Figure 30\(d\)](#) shows a disorganized number of streamlines. They are evidently not fluid layers and there is an exchange of fluid from one adjacent sector to another. More importantly, there is an exchange of momentum such that slow moving fluid particles speed up and fast moving particles give up their momentum to the slower moving particles and slow down themselves. Consider [figure 30\(e\)](#) which shows the smoke rising from a cigarette. For some distance the smoke rises in smooth filaments which may wave around but do not lose their identity; this flow is laminar. The filaments (or streamtubes) suddenly break up into a confused eddying motion some distance above the cigarette; this flow is turbulent. The transition between laminar and turbulent flow moves closer to the cigarette when the air in the room is disturbed. Another example of a common occurrence of laminar and turbulent flow is the water faucet. Opened slightly, at low speeds the water flows out in a clear column - laminar flow. But open the faucet fully and the flow speeds out in a cloudy turbulent column. In a mountain brook the water may slide over smooth rocks in laminas. In the Colorado River the flow churns downstream in the confused turbulent rapids. It will be seen that the flow over airfoil surfaces may assume both a laminar and turbulent characteristic depending upon a number of factors.

In some cases, turbulent flow will appear "naturally" in a laminar flow as in the smoke rising in the air. In other cases, by causing a disturbance, a laminar flow can be changed to a turbulent flow. The question arises as to how one can tell whether a flow is to be laminar or turbulent. In 1883, Osborne Reynolds introduced a dimensionless parameter which gave a quantitative indication of the laminar to turbulent transition.

Reynolds number effects on the flow field - In his experiments, Reynolds demonstrated the fact that under certain circumstances the flow in a tube changes from laminar to turbulent over a given region of the tube. The experimental setup is illustrated in [figure 31\(a\)](#). A large water tank had a long tube outlet with a stopcock at the end of the tube to control the flow speed. The tube was faired smoothly into the tank. A thin filament of colored fluid was injected into the flow at the mouth.

When the speed of the water flowing through the tube was low, the filament of colored fluid maintained its identity for the entire length of the tube. (See [fig. 31\(b\)](#).) However, when the flow speed was high, the filament broke up into the turbulent flow that existed through the cross section. (See [fig. 31\(c\)](#).)

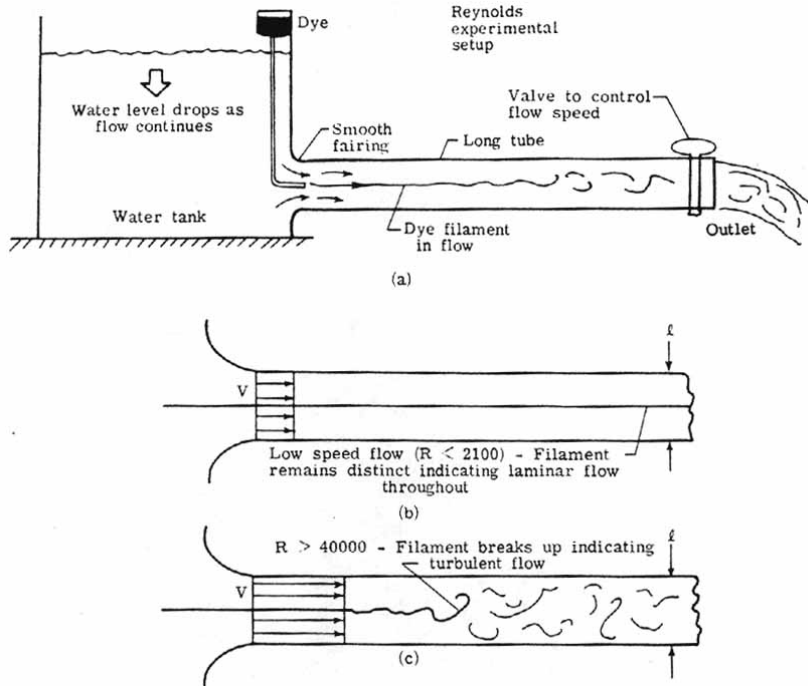


Figure 31.- Dependence of flow on Reynolds number. $R = (\rho V l) / \mu$

Reynolds defined a dimensionless parameter, which has since been known as the Reynolds number, to give a quantitative description of the flow. In equation form the Reynolds number R is

$$R = \rho V l / \mu \quad (10)$$

where

ρ	density of fluid, kg/m^3 [Greek letter rho]
V	mean velocity of fluid, m/sec
l	characteristic length, m
μ	coefficient of viscosity (called simply "viscosity" in the earlier discussion), kg/m-sec

For this setup, Reynolds found, by using water, that below $R = 2100$ the flow in the pipe was laminar as evidenced by the distinct colored filament. This value was true regardless of his varying combinations of values of ρ , V , l , or μ . A transition between laminar and turbulent flow occurred for Reynolds numbers between 2100 and 40 000 depending upon how smooth the tube junction was and how carefully the flow entered the tube. Above $R = 40 000$ the flow was always turbulent, as evidenced by the colored fluid filament breaking up quickly. The fact that the transition Reynolds number (between 2100 and 40 000) was variable indicates the effect that induced turbulence has on the flow.

The numerical values given for the transition are for this particular experiment since the characteristic length chosen l is the diameter of the pipe. For an airfoil, l would be the distance between the leading and trailing edge called the chord length. Additionally, water was used in the Reynolds experiment whereas air flows about an airfoil. Thus, the transition number between laminar

and turbulent flow would be far different for the case of an airfoil. Typically, airfoils operate at Reynolds numbers of several million. The general trends, however, are evident. For a particular body, low Reynolds number flows are laminar and high Reynolds number flows are mostly turbulent.

The Reynolds number may be viewed another way:

$$\text{Reynolds number} \approx \frac{\text{Inertia forces}}{\text{Viscous forces}} \quad (11)$$

The viscous forces arise because of the internal friction of the fluid. The inertia forces represent the fluid's natural resistance to acceleration. In a low Reynolds number flow the inertia forces are negligible compared with the viscous forces whereas in high Reynolds number flows the viscous forces are small relative to the inertia forces. An example of a low Reynolds number flow (called Stoke's flow) is a small steel ball dropped into a container of heavy silicon oil. The ball falls slowly through the liquid; viscous forces are large. Dust particles settling through the air are another case of a low Reynolds number flow. These flows are laminar. In a high Reynolds number flow, such as typically experienced in the flight of aircraft, laminar and turbulent flows are present. Some very interesting contrasts between the results of low Reynolds number flow and high Reynolds number flow will be demonstrated shortly.

Surface roughness effects on the flow field - The effect of surface roughness of a body immersed in a flow field is that it causes the flow near the body to go from laminar to turbulent. As the surface roughness increases, the point of first occurrence of turbulent flow will move upstream along the airfoil. [Figure 32](#) illustrates this point. An airfoil surface is shown. In each succeeding case the degree of surface roughness is increased and the Reynolds number is held fixed. The flow is seen to go turbulent further upstream in each case. The Reynolds number and surface roughness are not independent of each other and both contribute to the determination of the laminar to turbulent transition. A very low Reynolds number flow will be laminar even on a rough surface and a very high Reynolds number flow will be turbulent even though the surface of a body is highly polished.

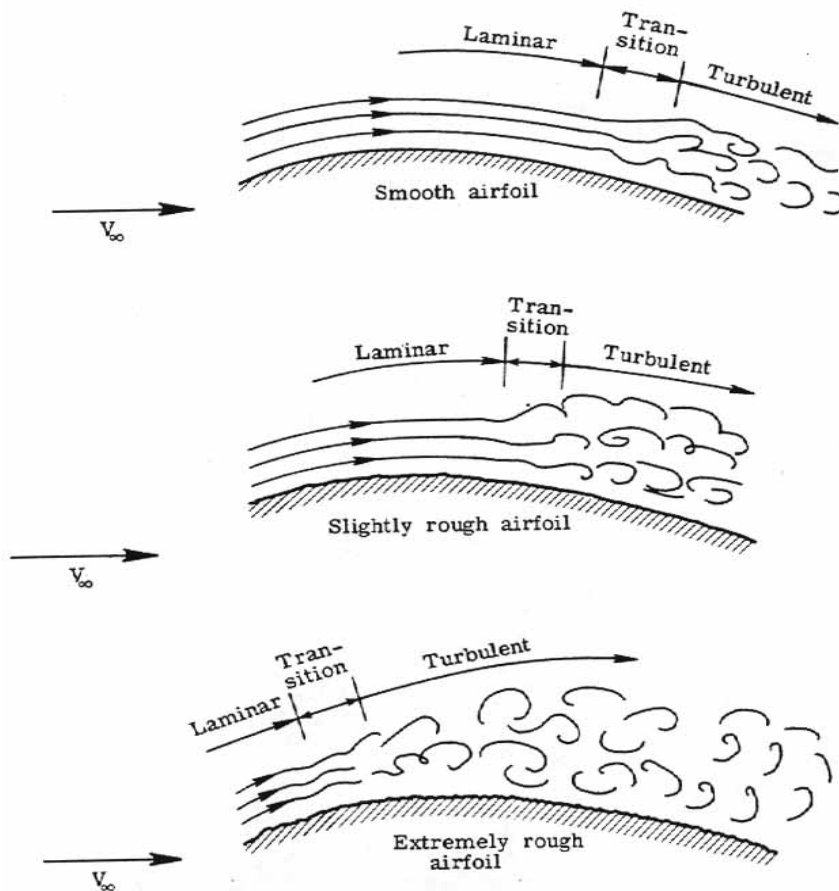


Figure 32.- Surface roughness and flow field. All cases at same Reynolds number.

Pressure gradient effects on the flow field - Another important factor in the transition from laminar to turbulent flow is the pressure gradient in the flow field. If the static pressure increases with downstream distance, disturbances in a laminar flow will be amplified and turbulent flow will result. If the static pressure decreases with downstream distance, disturbances in a laminar flow will damp out and the flow will tend to remain laminar. Recall that over an airfoil the static pressure decreased up to the point of maximum thickness. A laminar flow will be encouraged in this region. Beyond the point of maximum thickness (or shoulder of the airfoil) the static pressure increased. The laminar flow now is hindered and may go turbulent before the trailing edge.

The boundary layer and skin-friction drag - The foregoing discussion has provided the background needed to show how drag is produced on a body immersed in a real fluid flow. An important aerodynamic force during low-speed subsonic flight is the shear force caused by viscous flow over the surfaces of the vehicle. This shear force is referred to as the skin-friction force and is strongly dependent on the factors previously mentioned-Reynolds number, surface roughness, and pressure gradients. [Figure 33](#) shows that in addition to the pressure forces that act everywhere normal to a body immersed in a moving fluid, viscous forces are also present. It is these viscous forces which modify the ideal fluid lift and help create the real fluid drag.

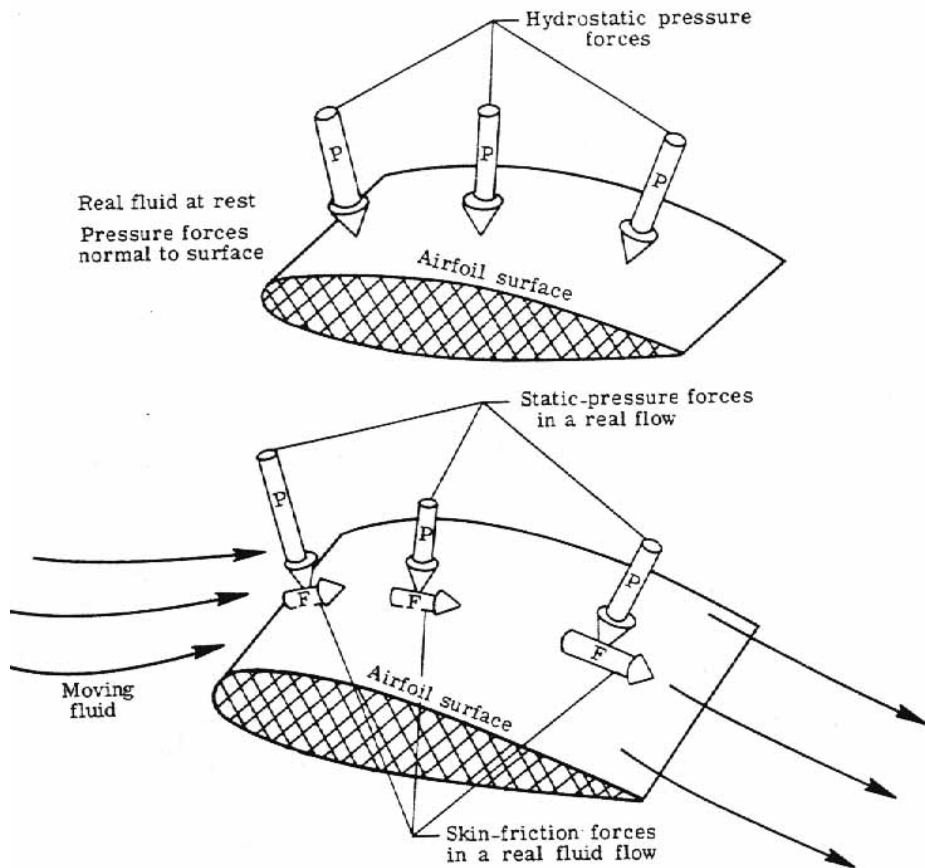
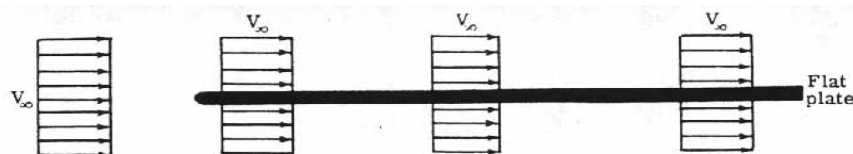
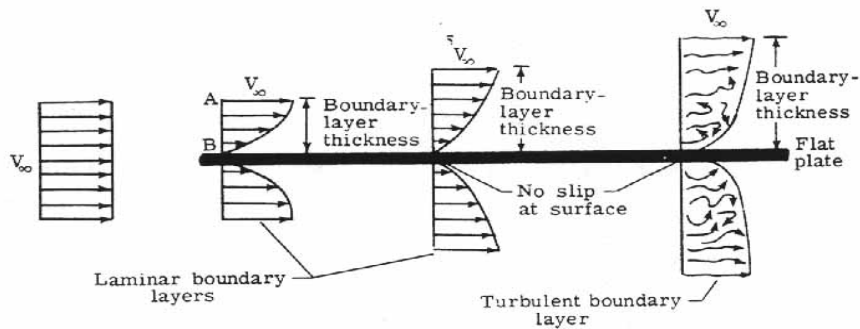


Figure 33.- Pressure and viscous forces.

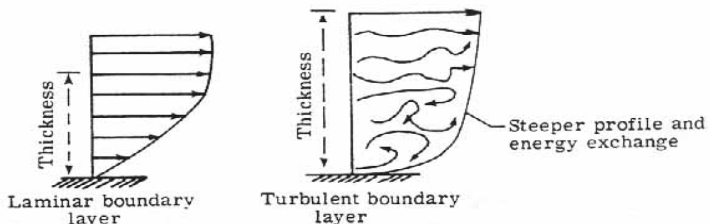
Consider [figure 34](#) which shows a very thin, smooth plate parallel to the approaching flow; the flow ahead of the leading edge of the plate is a uniform free stream.



(a) Inviscid flow along a flat plate.



(b) Viscous flow along a flat plate.



(c) Comparison of laminar and turbulent flow.

Figure 34.- Boundary-layer flow in a real fluid.

If the fluid were ideal, that is, inviscid, the fluid would simply slip over the surface with velocity V_∞ as shown in [figure 34\(a\)](#). At all points along the surface of the plate, the velocity distribution (that is, the variation of velocity as one moves perpendicularly away from the surface) would be a uniform constant value of V_∞ . No drag would result if the fluid were frictionless (inviscid).

In a real fluid, however, a very thin film of fluid adheres to the surface. (See [fig. 34\(b\)](#).) This is the very important no-slip condition. It states that at the surface of a body, point B, the flow velocity is zero. As one moves away from the body the velocity of the fluid gradually increases until at some point A the velocity becomes a constant value; in the case of a flat plate this value is V_∞ . The layer of fluid where the velocity is changing from zero to a constant value is known as the boundary layer. Within the boundary layer there are relative velocities between the particle layers and an internal friction is present. This internal friction extends to the surface of the body. The cumulative effect of all these friction forces is to produce a drag force on the plate. This drag force is referred to as skin-friction drag.

Initially, near the leading edge of the plate, one has a laminar flow and the boundary layer also is steady and layered- hence, a laminar boundary layer. As one moves further downstream, viscosity continues to act and the laminar boundary layer thickens as more and more fluid is slowed down by internal friction. Eventually, a point is reached on the plate where the laminar boundary layer undergoes transition and becomes a turbulent boundary layer. (See [fig. 34\(b\)](#).) As is usual for turbulent flow, there is a random motion in the boundary layer as well as the downstream directed motion. There is no slip at the surface of the plate. Another important difference from the laminar boundary layer is the fact that the velocity builds up more quickly as one moves away from the wall, although the total boundary-layer thickness is greater. This condition can be seen by comparing the two profiles as shown in [figure 34\(c\)](#). This tendency in a turbulent boundary layer of the fluid further away from the wall to reenergize the slower moving fluid near the wall will be shown to produce important consequences.

The Reynolds number has an important effect on the boundary layer. As the Reynolds number increases (caused by increasing the flow speed and/or decreasing the viscosity), the boundary layer thickens more slowly. However, even though the Reynolds number becomes large, the velocity at the surface of the body must be zero. Thus, the boundary layer never disappears.

It is interesting to note that a typical thickness of the boundary layer on an aircraft wing is generally less than a centimeter. Yet, the velocity must vary from zero at the surface of the wing to hundreds of m/sec at the outer edge of the boundary layer. It is clearly evident that tremendous shearing forces (internal friction) must be acting in this region. This gives rise to the skin-friction drag.

[The airfoil in a real fluid - Figure 35](#) illustrates the real fluid flow over the airfoil surface originally considered in [figure 29](#). The same free-stream velocity V_∞ and free-stream static pressure p_∞ apply. The flow field ahead of the airfoil is only slightly modified and for all practical purposes the velocities and static pressures are the same as for the ideal fluid case. Again a stagnation point occurs at the leading edge of the airfoil and the pressure reaches its maximum value of p_t at this point (total or stagnation pressure). From this point on along the airfoil, the picture changes.

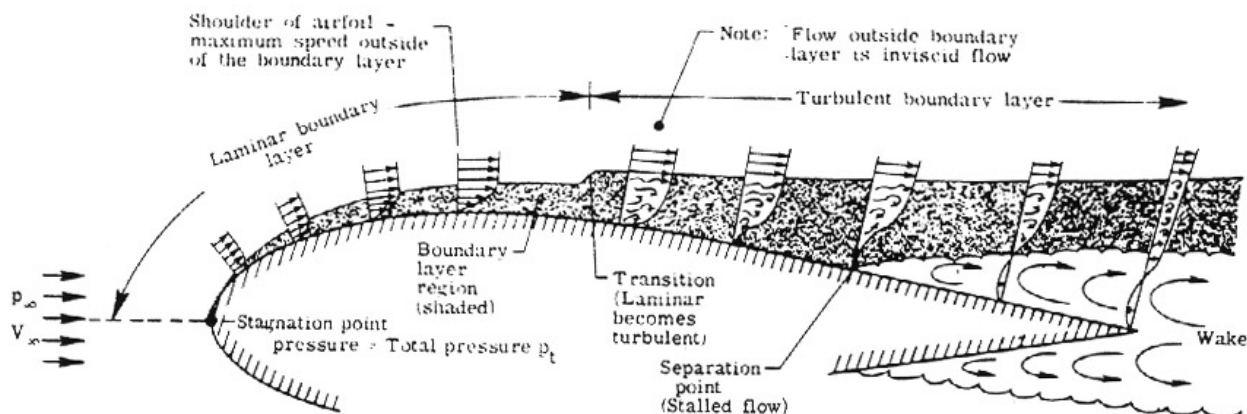


Figure 35.- Real fluid flow about an airfoil. Thickness of boundary layers and wake greatly exaggerated. Bottom flow along lower surface is the same as on the upper surface.

As noted earlier in the example of the flat plate, a boundary layer begins to form because of viscosity. This boundary layer is very thin and outside of it the flow acts very much like that of an ideal fluid. Also, the static pressure acting on the surface of the airfoil is determined by the static pressure outside the boundary layer. This pressure is transmitted through the boundary layer to the surface and thus acts as if the boundary layer were not present at all. But the boundary layer feels this static pressure and will respond to it.

Over the front surface of the airfoil up to the shoulder, an assisting favorable pressure gradient exists (pressure decreasing with distance downstream). The flow speeds up along the airfoil. The flow is laminar and a laminar boundary layer is present. This laminar boundary layer grows in thickness along the airfoil. When the shoulder is reached, however, the fluid particles are moving slower than in the ideal fluid case. This is an unfavorable condition because the previous ideal flow just came to rest at the trailing edge. It would appear now, with viscosity present, that the flow will come to rest at some distance before the trailing edge is reached.

As the flow moves from the shoulder to the rear surface, the static-pressure gradient is unfavorable (increasing pressure with downstream distance). The fluid particles must push against both this unfavorable pressure gradient and the viscous forces. At the transition point, the character of the flow changes and the laminar boundary layer quickly becomes a turbulent boundary layer. This turbulent boundary layer continues to thicken downstream. Pushing against an unfavorable pressure gradient and viscosity is too much for the flow, and at some point, the flow stops completely. The boundary layer has stalled short of reaching the trailing edge. (Remember that the flow reached the trailing edge before stopping in the ideal fluid case.). This stall point is known as the separation point. All along a line starting from this point outward into the flow, the flow is stalling. Beyond this line the flow is actually moving back, upstream toward the nose before turning around. This is a region of eddies and whirlpools and represents "dead," air which is disrupting the flow field away from the airfoil. Thus, flow outside the dead air region is forced to flow away and around it. The region of eddies as shown in [figure 35](#) is called the wake behind the airfoil.

[Figure 36\(a\)](#) compares the ideal fluid case static-pressure distribution at the airfoil surface and center-line streamline with; the real fluid case. Note that up to the separation point, the differences are not very large but once separation occurs the pressure field is greatly modified. In the ideal fluid case the net static-pressure force acting on the front surface of the airfoil (up to the shoulder) parallel to the free stream exactly opposed and canceled that acting on the rear surfaces of the airfoil. (See [fig. 36\(b\)](#).) Now, however, in the real fluid case this symmetry and cancellation of forces is destroyed. The net static-pressure force acting on the front surface parallel to the free-stream direction now exceeds that acting on the rear surface. The net result is a drag force due to the asymmetric pressure distribution called pressure drag. (See [fig. 36\(c\)](#).) This is a drag in addition to the skin-friction drag due to the shearing forces (internal friction) in the boundary layer. Additionally, the modification of the static-pressure distribution causes a decrease in the pressure lift from the ideal fluid case.

[Figure 36\(d\)](#) shows figuratively the lift and drag for an airfoil producing lift in both an ideal and real fluid case. One sees the effects of viscosity - the lift is reduced and a total drag composed of skin-friction drag and pressure drag is present. Both of these are detrimental effects.

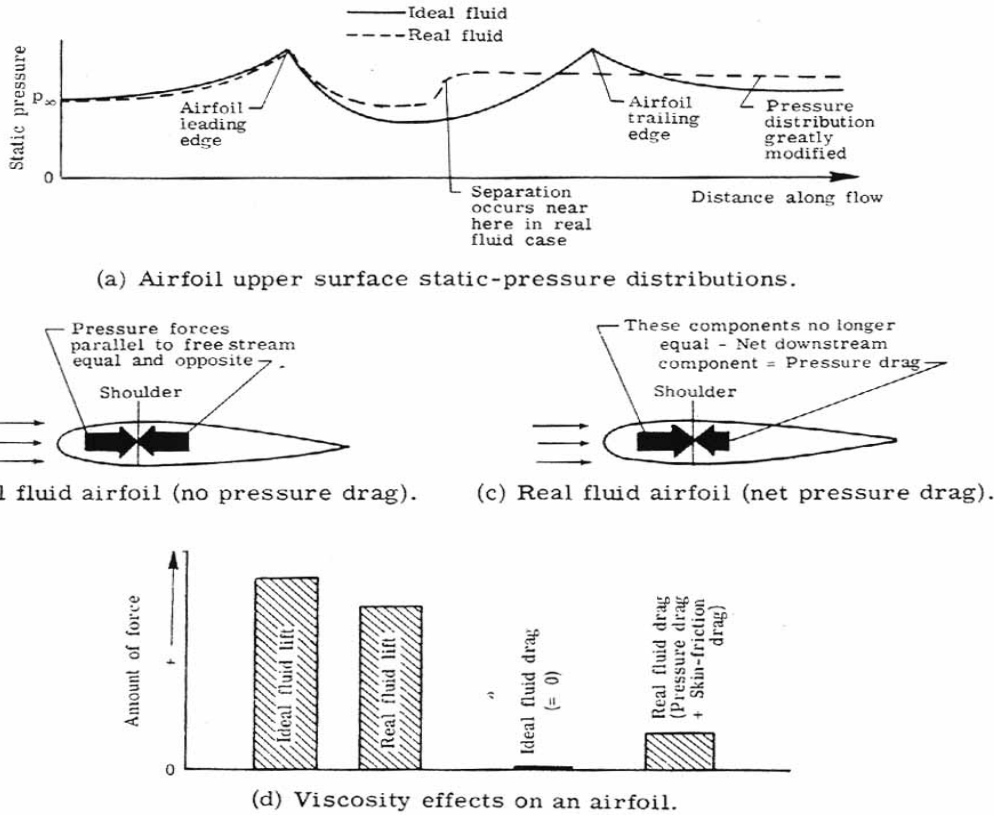


Figure 36. – Real fluid effects on an airfoil

It should be noted, very strongly, that although the previous discussion was limited to an airfoil section, similar processes are occurring on all the other components of the aircraft to one degree or another. It is beyond the scope of this text to treat these in detail but the effects will be noted when the total airplane drag is discussed.

In summarizing this discussion, one observes that the effects of a real fluid flow are the result of the viscosity of the fluid. The viscosity causes a boundary layer and, hence, a skin-friction drag. The flow field is disrupted because of viscosity to the extent that a pressure drag arises. Also, the net pressure lift is reduced. The next section considers the effects of "streamlining."

Effects of streamlining - [Figure 37](#) shows five bodies placed in a real fluid flow of air and the resultant flow field. Four of the bodies are operating at Reynolds numbers normally encountered in the flight of subsonic aircraft ($R = 10^4$ to 10^5). The fifth body is operating at a much higher Reynolds number ($R = 10^7$).

The flat plate placed broadside to the flow has a large wake with separation points at the plate edge. A large pressure drag is the result, the skin-friction drag being a relatively small component. The cylinder, operating at the same Reynolds number, has a smaller wake and the boundary-layer separation occurs, in this case, before the shoulders of the cylinder. The skin-friction drag is a little larger in this case than for the plate, but is still smaller than the pressure drag. Overall, the total drag has been reduced from that of the flat plate; some effects of streamlining are already evident.

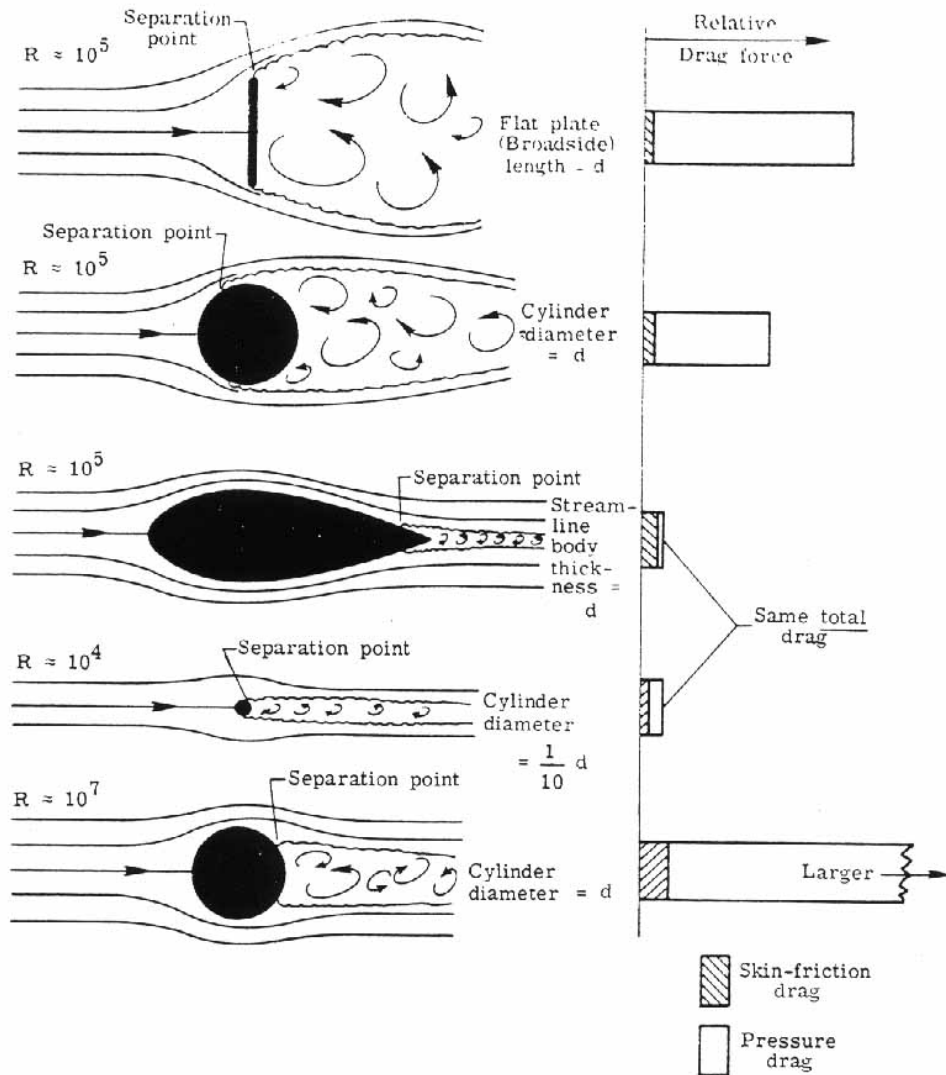


Figure 37.- Effects of streamlining at various Reynolds numbers.

Also, at the same Reynolds number is a streamlined shape. There is almost no boundary-layer separation and the wake is very small. One may assume then that a streamline shape may be defined as the absence of 'boundary-layer separation. Operating in the condition shown, the skin-friction drag now is the dominant component and the pressure drag is very small. Even more noticeable is the very large reduction in overall drag compared with the cylinder or plate. This has been accomplished by eliminating the pressure drag since the skin-friction drag has been increasing only slightly as the bodies became more streamlined. One can explain that the increase in skin-friction drag is due to the simple fact that the streamlined body has more area exposed to the flow and thus has a greater area over which the boundary layer may act.

Finally, in [figure 37](#) at a Reynolds number of 10^4 is a cylinder approximately $1/10$ the diameter of the streamline shape thickness. Surprisingly it has the same drag as the much larger streamlined shape. The pressure drag is large because of the turbulent wake. It is not hard to imagine the reason for the slow speeds of the early biplanes when all the wire bracing used is considered. A considerably

reduced drag could have been realized if the wire were streamlined. However, the introduction of the monoplane and better structures eliminated the need for this wire bracing.

The fifth body shown is a cylinder operating in the flow at a much higher Reynolds number (accomplished by increasing the free-stream velocity). The separation points are downstream of the shoulders of the cylinder and a much smaller wake is evidenced. This result would lead one to expect a smaller pressure drag than for the previously discussed cylinder of the same size. However, the flow speed is higher and the actual drag is much larger. These contradictory facts may be explained by realizing that actual drag values, under different flow speeds, have been compared. A better measure of the performance is needed. This measure is demonstrated in the next section to be the nondimensional drag coefficient.

Aerodynamic coefficients - From everyday experience, consider the factors that determine the aerodynamic resistance on a body. If one places his hand broadside to a flow outside a car window at 20 km/hr, little resistance is felt, but if one speeds along at 100 km/hr, the force felt is considerable. Velocity is one factor that determines the resistance. In fact, considering the flow problems of subsonic flight (high Reynolds number under relatively small viscosities), the resistance depends directly on (velocity) times (velocity) or (velocity)². In the preceding example, although the velocity of 100 km/hr is five times that of 20 km/hr, the aerodynamic resistance is about 25 times as great at the higher velocity.

If one walks along a beach, there is little aerodynamic resistance to doing so. But try to wade in the water at the same speed. It is considerably more difficult, if not impossible. The density of water is much greater than the density of air. Density of the fluid represents another determining factor in the resistance felt by a body.

One more experiment: hold a small piece of cardboard up against a stiff wind. Little resistance is experienced. Now hold a much larger, similarly shaped sheet of cardboard up against the same stiff wind. A considerable resistance is felt. Area (or length times length) exposed to the airflow is another determining factor of resistance.

It is now possible to generalize the discussion by stating that, in the flow of the real fluid, air, about a body, the aerodynamic resistance is dependent on the size, shape, and attitude of the body, the properties of the fluid, and the relative velocity between the body and the fluid (air). To illustrate, consider the lift force defined as the aerodynamic reaction perpendicular to the free-stream velocity direction. From the previous discussion, lift depends on (size shape attitude fluid properties. and velocity). For an ideal fluid, the fluid properties (except for density) did not influence the lift force. For a real fluid, however. viscous, elastic, and turbulent properties are also important. In addition to the shape and attitude of the body the surface roughness has an effect on the force. Based on the introductory discussion of this section, it may be demonstrated that

$$\text{Lift} = \rho_{\infty} \times V_{\infty}^2 \times S \times \text{Factor} \left(\alpha, \frac{\rho_{\infty} V_{\infty} l}{\mu}, \frac{V_{\infty}}{a_{\infty}}, \text{surface roughness, air turbulence} \right) \quad (12)$$

where

ρ_{∞}	free-stream fluid density
V_{∞}	free-stream velocity
S	characteristic body frontal area
l	characteristic body length
α [Greek letter alpha]	attitude of body
μ	coefficient of viscosity
a_{∞}	free-stream speed of sound of fluid

(S is a characteristic body frontal area that is usually chosen to be consistent with a series of comparison experiments. For a cylinder it would be the diameter of the cylinder times its length. For a wing, however, it is usually taken to be the planform area (chord length times wing span for a rectangular wing). Thus, it is necessary to check the particular definition of S used for a body.)

It has previously been shown that the quantity $\frac{\rho_{\infty} V_{\infty} l}{\mu}$ is the Reynolds number or R. Also, $\frac{a_{\infty}}{V_{\infty}}$ is defined to be the Mach number or M. The Reynolds number is the dimensionless quantity associated with the fluid viscosity whereas the Mach number is associated with the fluid compressibility. Surface roughness was shown to have influenced the transition from a laminar to a turbulent flow. Air turbulence represents the degree of the wake formed past the separation points. Furthermore, the effects of attitude and shape of a body are lumped together into the factor. Letting the factor be called K, then,

$$\text{Lift} = \rho_{\infty} \times V_{\infty}^2 \times S \times K \quad (13)$$

The dynamic pressure of a fluid flow was previously defined as $1/2 \rho V^2$ so if a value of $1/2$ is included in equation (13) and the value of K is doubled to keep the equation the same, $2K$ may be replaced by C_L . Finally,

$$\text{Lift} = C_L \times \frac{1}{2} \rho_{\infty} V_{\infty}^2 \times S \quad (14)$$

Equation (14) is the fundamental lift formula for usual aircraft flight. C_L is known as the coefficient of lift. The equation states simply that the aerodynamic lift is determined by a coefficient of lift times the free-stream dynamic pressure times the characteristic body area.

It is very important to realize that the lift coefficient C_L is a number dependent upon the Reynolds number, Mach number, surface roughness, air turbulence, attitude, and body shape. It is not by any means a constant. C_L is generally found by wind-tunnel or flight experiments by measuring lift and the free-stream conditions and having knowledge of the body dimensions. Thus,

$$C_L \equiv \frac{\text{Lift}}{\frac{1}{2} \rho_\infty V_\infty^2 \times S} \quad (15)$$

The aerodynamic drag is the aerodynamic resistance parallel to the free-stream direction. One obtains analogous equations to equations (14) and (15), namely,

$$\text{Drag} = C_D \times \frac{1}{2} \rho_\infty V_\infty^2 \times S \quad (16)$$

or

$$C_D \equiv \frac{\text{Drag}}{\frac{1}{2} \rho_\infty V_\infty^2 \times S} \quad (17)$$

where C_D is the drag coefficient, dependent on the previously enumerated parameters.

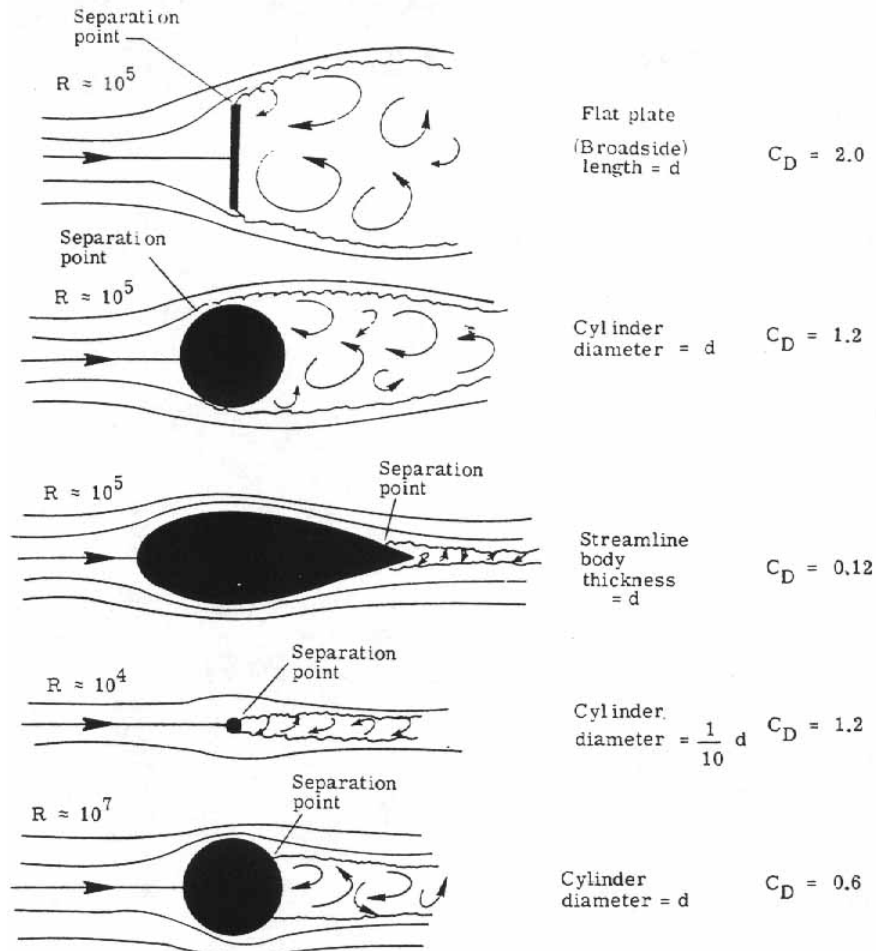


Figure 38.- Drag coefficients of various bodies.

The moment acting on a body is a measure of the body's tendency to turn about its center of gravity. This moment represents the resultant aerodynamic force times a moment distance. Let it be stated that a similar derivation may be applied to the moment equation as used for the lift and drag equations (14) and (16) such that,

$$\text{Moment} = C_m \times \frac{1}{2} \rho_\infty V_\infty^2 \times S \times l \quad (18)$$

or

$$C_m = \frac{\text{Moment}}{\frac{1}{2} \rho_\infty V_\infty^2 S l} \quad (19)$$

C_m is the coefficient of moment and an additional characteristic length l is necessary for it to be dimensionally correct. To reiterate, C_L , C_D , and C_m are dependent on the Reynolds number, Mach number surface roughness, air turbulence, attitude, and body shape.

It is now possible to return to the discussion associated with [figure 37](#) and compare the five bodies by using the force coefficient as a measure of the resistance. The first three bodies demonstrated the effects of progressively more streamlining. All had the same basic body dimension d , the same Reynolds number $R = 10^5$, the same Mach number, and were assumed to be smooth and aligned symmetrically with the flow. The aerodynamic resistance was, therefore, entirely drag and the drag coefficient C_D is a measure of this resistance. By assuming a unit length for the bodies, the frontal area S is the same for all the bodies as is the dynamic pressure. By equation (17), C_D is then directly proportional to the measured drag. [Figure 38](#) repeats the results of [figure 37](#) except that now the relative drag force has been replaced by the drag coefficients C_D . At the Reynolds number of 10^5 , the C_D values for the flat plate, cylinder, and streamline shape are, respectively, 2.0, 1.2, and 0.12. These values include the combined effects of the skin-friction drag and pressure drag.

The small cylinder, operating at a Reynolds number of 10^4 with its diameter reduced to one-tenth the basic dimension of the previous examples, has a C_D of 1.2. From equation (16), the effect of smaller size nullifies the effect of larger C_D and the small cylinder and streamline shape have equivalent aerodynamic drags.

The last cylinder, operating at the higher Reynolds number of 10^7 , has a C_D of 0.6, that is, half as large as the cylinders discussed previously. Its aerodynamic drag in [figure 37](#) is large because V_∞ has been increased to obtain the higher Reynolds number. The smaller drag coefficient indicates the effect of the smaller wake and, hence, smaller pressure drag coefficient component. At high Reynolds numbers, the boundary layer becomes turbulent further upstream along the cylinder. The turbulence in the boundary layer reenergizes the flow close to the surface and the fluid drives further along the cylinder against viscous forces and the unfavorable pressure gradient before stalling. Separation occurs downstream of the shoulders and a smaller wake results. Compare this condition with the separation and wake at the lower Reynolds number.

[Figure 39](#) is a plot of drag coefficient C_D (based on frontal area) against Reynolds number. The values for each body are shown. Also, the solid line is an experimentally determined curve of the C_D of cylinders tested in wind tunnels. At subcritical Reynolds numbers up to about 10^5 , the laminar boundary layer stalls and separates upstream of the shoulders of the cylinder and produces a very

broad wake and high C_D values. At supercritical Reynolds numbers from 10^6 and larger, the laminar boundary layer becomes turbulent and separation is delayed; hence, the smaller C_D values. A rather abrupt transition occurs between Reynolds numbers of 10^5 and 10^6 . These values are the critical Reynolds numbers.

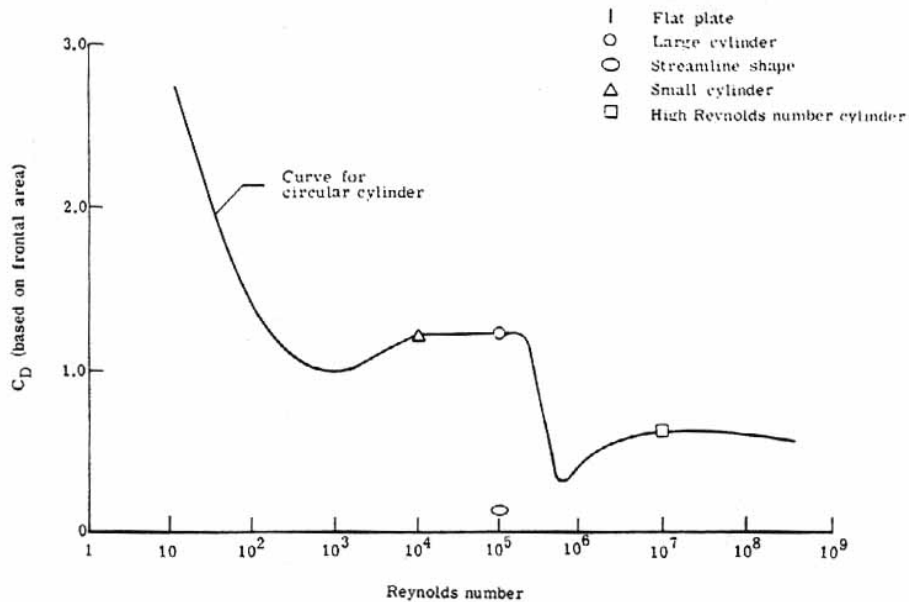


Figure 39.- Drag coefficients as function of Reynolds number.

It is interesting to note that spheres exhibit behavior very similar to that of cylinders. Golf balls of today are dimpled rather than smooth as they once were, to induce a turbulent boundary layer and thus decrease their drag coefficient. Much improved driving distances are the result.

The discussion thus far has been rather general and has introduced many important ideas and principles. Fluid flow behavior has been demonstrated. Numerous references to airfoil or streamline shapes have been made. Viscous flow of the boundary layer and unsteady flow in the turbulent wake have been examined. The flow is two-dimensional since velocity and other flow parameters vary normal to the free-stream direction as well as parallel to it. With these ideas in mind, one may now study aircraft operating in a subsonic flow.

IV. SUBSONIC FLOW EFFECTS

Airfoils and Wings

The airfoil section - [Figure 13](#) showed that by taking a slice out of an airplane wing and viewing it from the side, one has the shape of the airfoil called the airfoil cross section or more simply airfoil section. The question arises as to how this shape is determined.

The ultimate objective of an airfoil is to obtain the lift necessary to keep an airplane in the air. A flat plate at an angle of attack, for example, could be used to create the lift but the drag is excessive. Sir George Cayley and Otto Lilienthal in the 1800's demonstrated that curved surfaces produced more lift and less drag than flat surfaces. [Figure 13](#) shows the airfoil section used by the Wright Brothers in their 1903 airplane.

In those early days of canvas and wood wings, few airfoil shapes evolved from theory. The usual procedure at that time was the "cut and try" method. Improvements came from experimentation. If the modification helped performance, it was adopted. Early tests showed, in addition to a curved surface, the desirability of a rounded leading edge and a sharp trailing edge.

The hit and miss methods of these early days were replaced by much better, systematic methods used at Gottingen, by the Royal Air Force, and finally by the National Advisory Committee for Aeronautics (NACA). The purpose here was to determine as much information as possible about "families" of airfoil shapes. During World War II, NACA investigations produced results that are still in use or influence the design of most of today's airplanes. The discussions that follow are based considerably on these NACA results.

The following six terms are essential in determining the shape of a typical airfoil:

- (1) The leading edge
- (2) The trailing edge
- (3) The chord line
- (4) The camber line (or mean line)
- (5) The upper surface
- (6) The lower surface

[Figure 40](#) illustrates the step-by-step geometric construction of an airfoil section: (1) the desired length of the airfoil section is determined by placing the leading and trailing edges their desired distance apart. The chord line is drawn connecting the two points together, (2) the amount of curvature is determined by the camber line. This curvature greatly aids an airfoil section's lifting abilities, (3) a thickness function is "wrapped" about the camber line, that is, one adds the same amount of thickness above and below the camber line; this thickness determines the upper and lower surfaces, (4) the last step shows the final result- a typical airfoil shape. It has a specific set of aerodynamic characteristics all its own which may be determined from wind-tunnel testing.

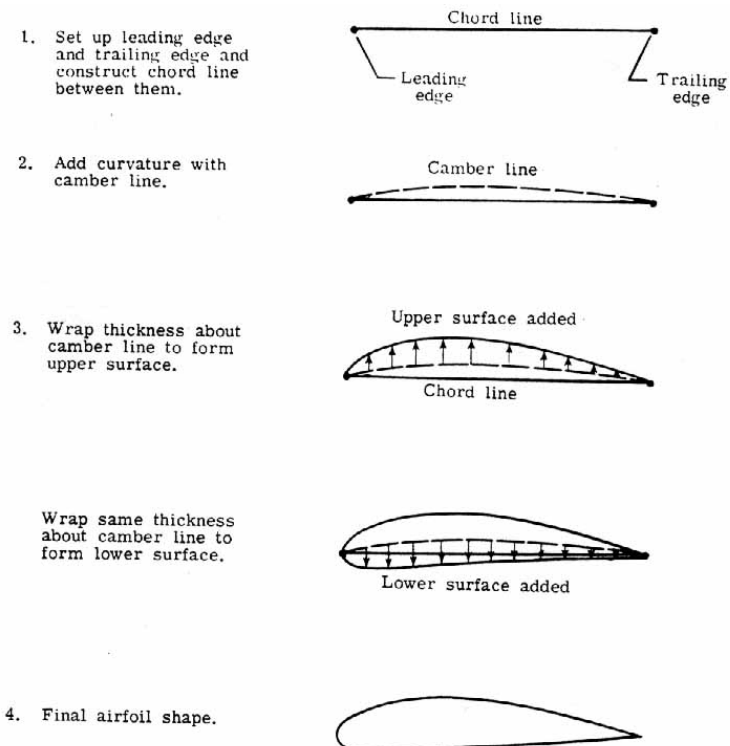


Figure 40.- Geometric construction of an airfoil.

[Figure 41](#) illustrates all the aforementioned terms for several differently shaped airfoil sections.

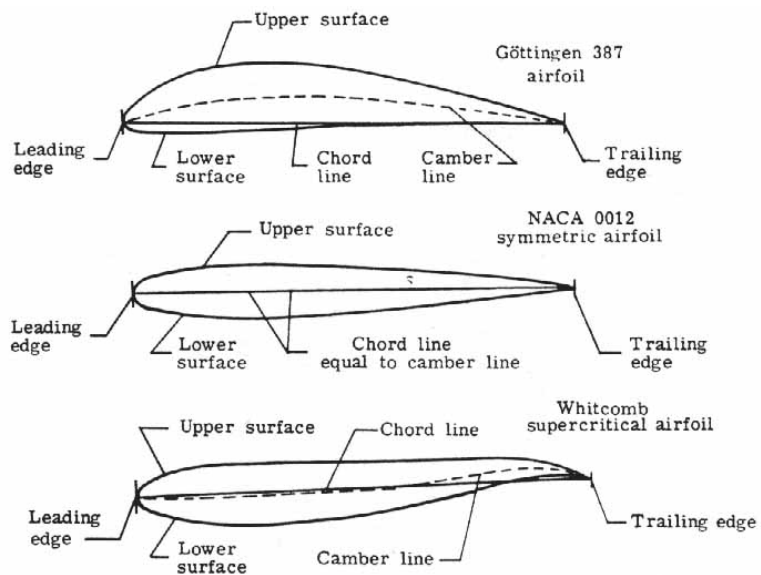


Figure 41.- Airfoil terminology.

[Figure 42](#) illustrates an important aspect of the camber line (or mean line). If the camber line is the same as the chord line, one has a symmetric airfoil (the upper surface is a mirror image of the lower surface about the chord line). When the free-stream velocity of the oncoming airstream is aligned along the chord line, no lift is produced. The angle of attack α [Greek letter alpha] is the angle between the chord line and the free-stream velocity vector. It is zero in this case, that is, $\alpha = 0^\circ$ [α = Greek letter alpha]. Thus, the angle of attack for zero lift is zero, or $\alpha_{L=0} = 0^\circ$.

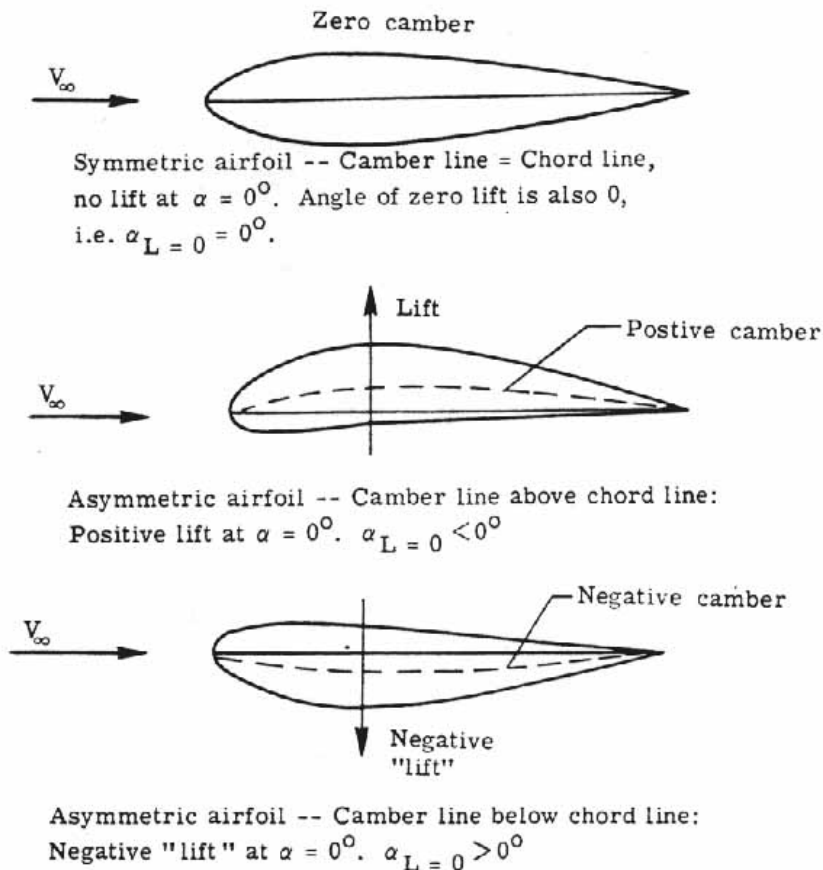


Figure 42. Airfoil camber line variations.

If the camber line lies above the chord line, then an asymmetrical airfoil section results. (Upper surface is not a mirror image of the lower surface.) When the free-stream velocity is aligned along the chord line ($\alpha = 0^\circ$), a positive lift results. The chord line must be negatively inclined with respect to the free stream to obtain zero lift (that is, the angle of zero lift $\alpha_{L=0}$ is less than 0°). In a similar manner negative camber yields an asymmetrical airfoil where the angle of zero lift $\alpha_{L=0}$ is greater than 0° .

The two-dimensional wing - A two-dimensional wing has no variation of aerodynamic characteristics in a spanwise direction. In [figure 43\(a\)](#) the airfoil section at station A is the same as at station B or anywhere along the span, and the wing is limitless in span. The point of this is to prevent air from flowing around the wing tips and causing three-dimensional effects (to be discussed later). One is trying to separate the airfoil's aerodynamic characteristics from the wing's three-dimensional effects.

Of course, no wing is infinite in length but a close simulation may be obtained by insuring that the model of the airfoil section, when placed in the wind tunnel for measurements, spans the wind tunnel from one wall to the other. (See [fig. 43\(b\)](#).) In this case (except for minor tunnel- wall effects that can be corrected for), the wing behaves two dimensionally, that is, there is no spanwise variation of the airfoil section aerodynamic characteristics. A later discussion will show the influence that limiting the wing span has on the aerodynamic characteristics.

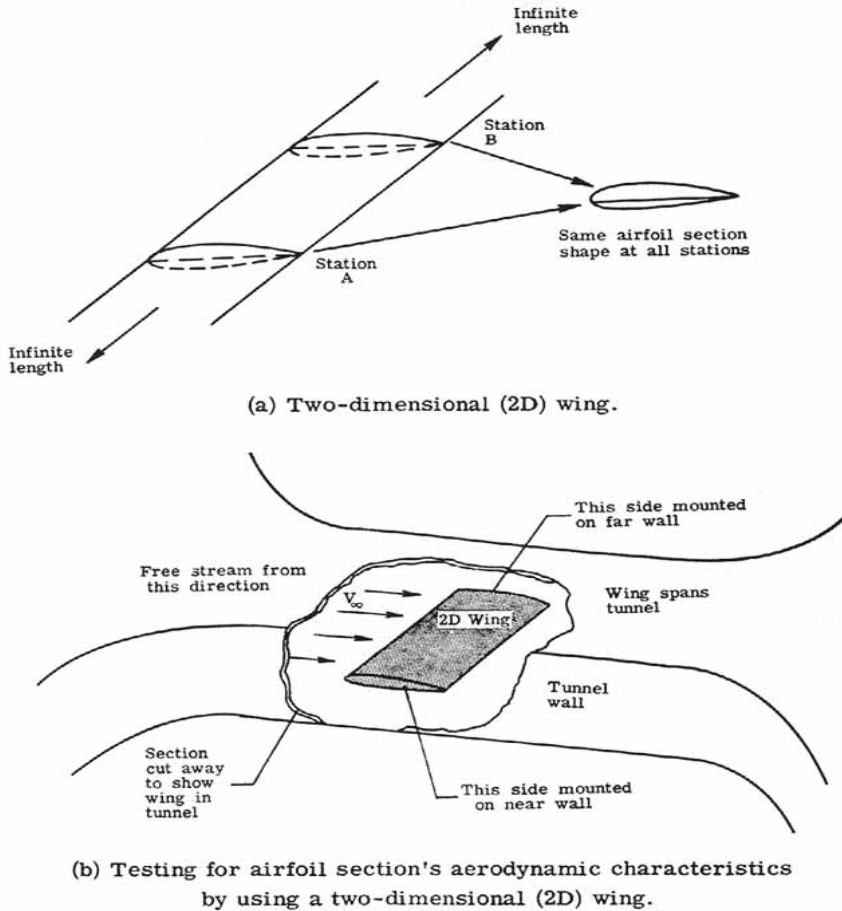
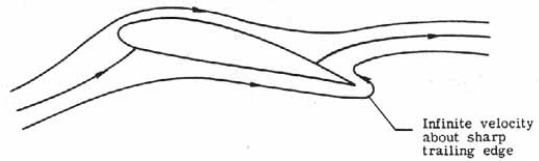
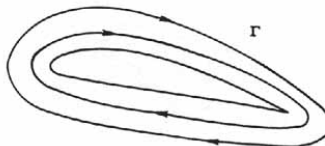


Figure 43. Two dimensional wing testing.

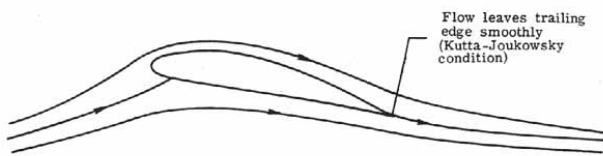
Circulation about a two-dimensional wing - The fluid flow about an airfoil may be viewed as consisting of two superimposed patterns -one is the free-stream motion of the fluid about the airfoil (see [fig. 44\(a\)](#)) and the other is a circulatory flow, or circulation, around the airfoil (see [fig. 44\(b\)](#)). These two flows coexist to give the total flow pattern. The question is, if the free-stream flow is prescribed, can the circulation, represented by Γ (Greek letter capital Gamma] be of any value? A physical condition provides the answer. The flow about the pointed trailing, edge cannot turn a sharp corner without the velocity becoming infinite. As this is not possible with a real fluid. the flow instead leaves the trailing edge tangentially and smoothly ([fig. 44\(c\)](#)). This is the Kutta condition and it sets the required value of Γ such that the rear stagnation point moves to the trailing edge.



(a) Flow with no circulation.



(b) Circulatory flow only.



(c) Flow with circulation.

Figure 44.- Circulation about a 2D wing.

Figure 44. Circulation about 2D wing.

The Kutta- Joukowsky theorem relates the circulation to the section lift by

$$l = \rho_{\infty} V_{\infty} \Gamma \quad (20)$$

where

l	lift/unit span of two-dimensional wing.
ρ_{∞}	free-stream air density. [Greek letter rho]
V_{∞}	free-stream velocity.
Γ	circulation strength. [Greek letter Capital Gamma]

Thus, the circulation strength Γ is set by a necessary physical condition, and the lift l is uniquely determined. For a perfect fluid, the drag per unit length is zero. However, in a viscous fluid flow one must include a skin-friction drag and a pressure drag along with a resulting loss of lift. Later, the changes that occur when a finite wing is considered will be shown.

The two-dimensional coefficients - [Figure 45\(a\)](#) shows the resultant aerodynamic force acting on an airfoil. The point of intersection of the chord line and the line of action of this resultant force is the center of pressure. The resultant aerodynamic force may be resolved into lift and drag components as shown in [figure 45\(b\)](#). The lift, drag, and center of pressure are for the cambered airfoil shown to vary as the angle of attack is changed. No aerodynamic moments are present at the center of pressure because the line of action of the aerodynamic force passes through this point. If one has the airfoil mounted at some fixed point along the chord, for example, a quarter of a chord length behind the leading edge, the moment is not zero unless the resultant aerodynamic force is zero or the point corresponds to the center of pressure.

The moment about the quarter-chord point is generally a function of angle of attack. [Figure 45\(c\)](#) shows a system of reporting a lift, drag, and moment about the quarter-chord point- all are functions of angle of attack.

There is a point, the aerodynamic center, where the moment is independent of the angle of attack. [Figure 45\(d\)](#) shows the lift, drag, and moment about the aerodynamic center. This system of reporting is convenient for a number of aerodynamic calculations.

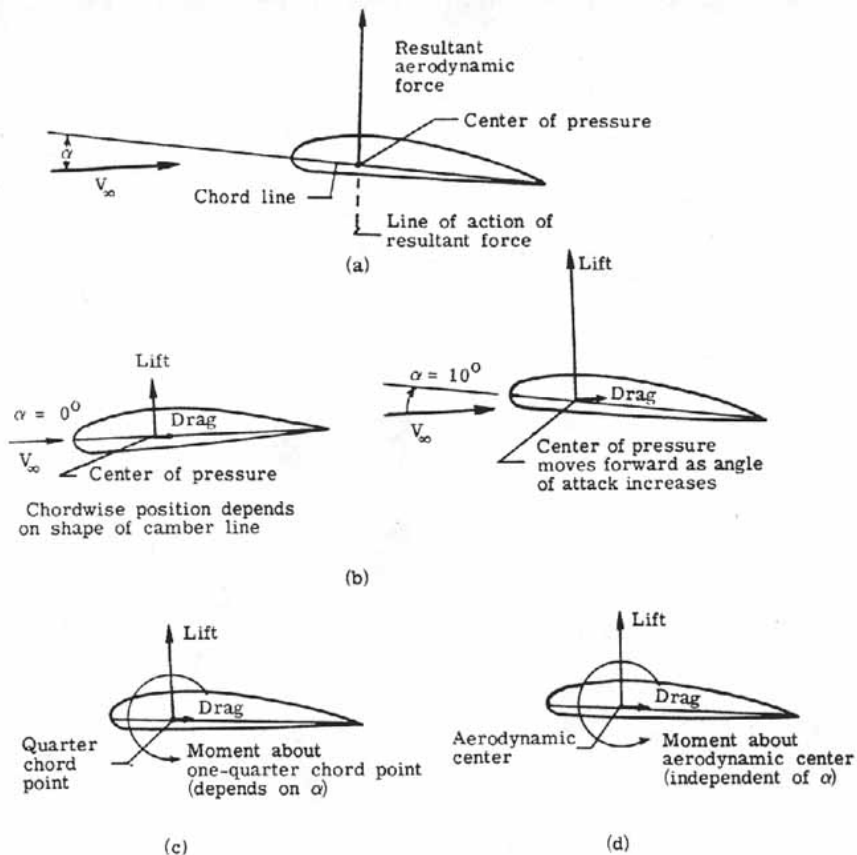


Figure 45.- Airfoil aerodynamic characteristics.

The data obtained by wind-tunnel testing of NACA families of airfoil sections are two-dimensional data. Aerodynamic characteristics recorded include the lift coefficient c_l , the drag coefficient c_d , the moment coefficient about the quarter-chord point (c_m)_{0.25c}, and the moment

coefficient about the aerodynamic center (c_m)_{ac}. These coefficients are obtained by measuring, in wind-tunnel tests, the forces and moments per unit length of the airfoil wing and nondimensionalizing as follows:

$$c_l = l/qc \quad (21)$$

where l is the measured lift per unit length of the airfoil wing, q is the testing dynamic pressure or $1/2 \rho V^2$, and c is the chord length of the airfoil section. Similarly,

$$c_d = d/qc \quad (22)$$

where d is the measured drag per unit length of the airfoil wing and,

$$c_m = m/qc^2 \quad (23)$$

where m is the measured moment per unit length acting on the airfoil (whether at the quarter-chord point or the aerodynamic center or any other point desired).

It has previously been shown that the aerodynamic coefficients are dependent on body shape (airfoil section chosen), attitude (angle of attack α [Greek letter alpha]), Reynolds number, Mach number, surface roughness, and air turbulence. For low subsonic flow, Mach number effects are negligible and air turbulence is dependent on the Reynolds number and surface roughness and need not be indicated as a separate dependency. [Figure 46](#) shows data reported for a particular airfoil shape, namely, an NACA 2415 airfoil. The main point of this figure is to show the dependence of the aerodynamic coefficients on angle of attack, Reynolds number, and surface roughness.

This indicates the dependence of c_L , c_d , and c_m on airfoil shape, angle of attack, Reynolds number, and surface roughness. Air turbulence is included in the Reynolds number and roughness dependency. Mach number effects not included.

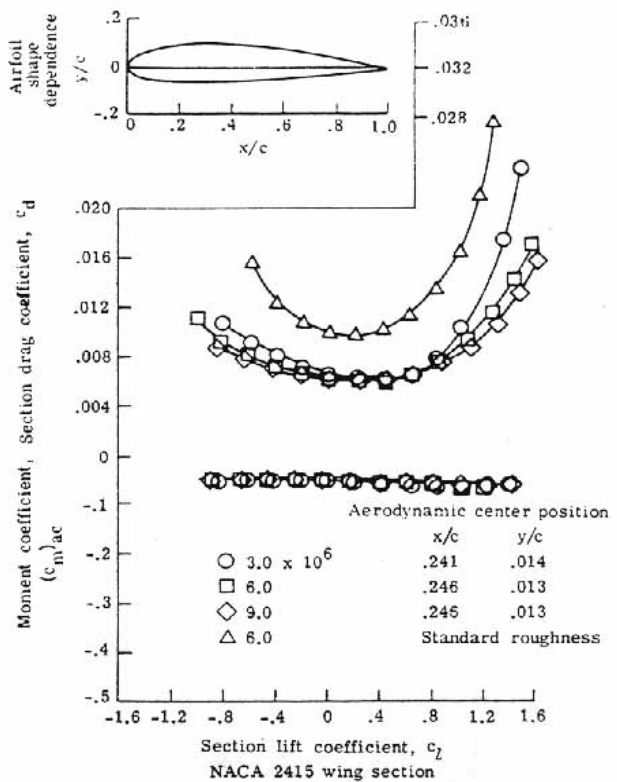
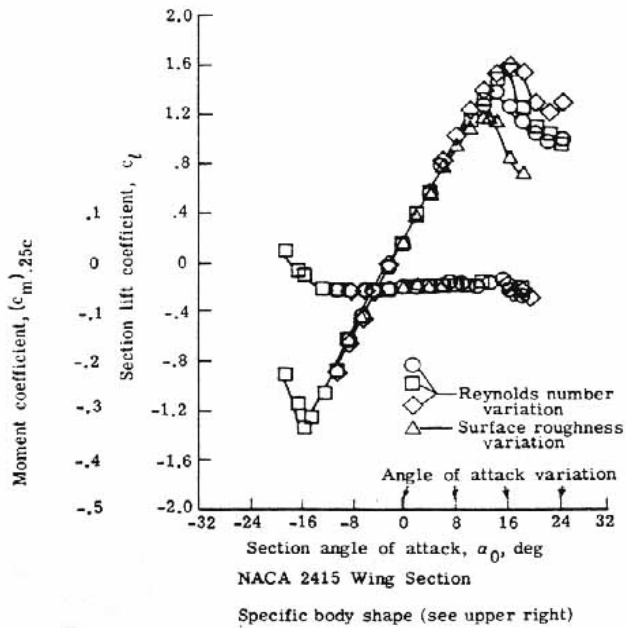


Figure 46.- Aerodynamic coefficient dependencies. c denotes chord length, x and y denote distances along X and Y axes, respectively.

It is best at this point to examine, in a general manner, the variation of the coefficients with angle of attack and to discuss some typical features often found in the informative graphs of these results.

[Figure 47](#) is a typical graph of coefficient of lift c_L against the angle of attack α [Greek letter alpha] of the airfoil section. One of the first things noticed is the fact that at an angle of attack of 0° , there is a positive coefficient of lift, and, hence, positive lift. This is the case of most cambered airfoils and was discussed earlier. One must move to a negative angle of attack to obtain zero lift coefficient (hence zero lift). It will be remembered that this angle is called the angle of zero lift. A symmetric airfoil was shown to have an angle of zero lift equal to 0° as might be expected.

Notice next that from 0° up to about 10° or 12° the "lift curve" is almost a straight line. There is a linear increase in the coefficient of lift with angle of attack. Above this angle, however, the lift coefficient reaches a peak and then declines. The angle at which the lift coefficient (or lift) reaches a maximum is called the stall angle.

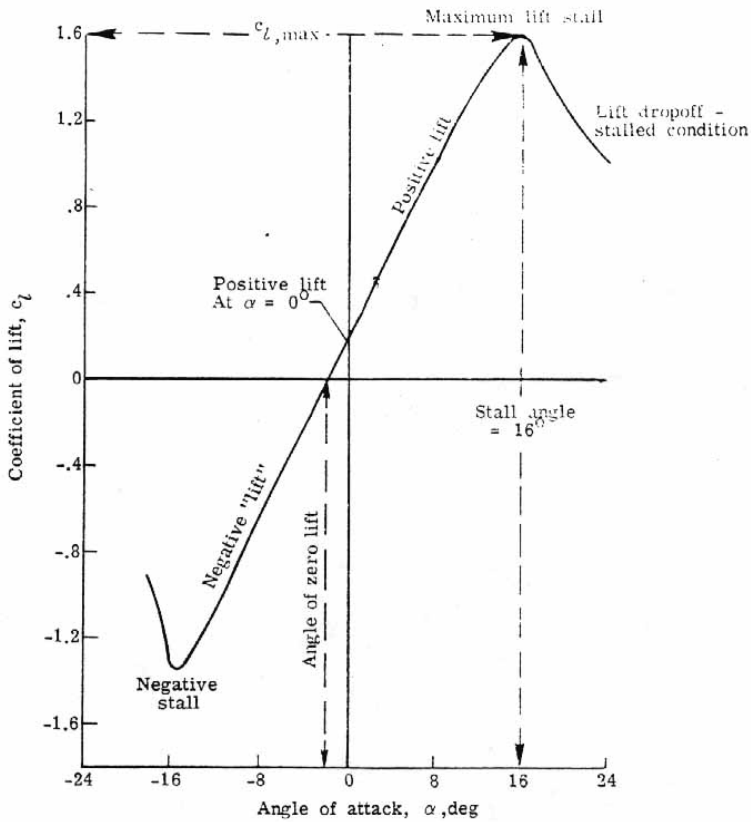


Figure 47.- Coefficient of lift as a function of angle of attack.

The coefficient of lift at the stall angle is the maximum lift coefficient $c_{l,\max}$. Beyond the stall angle, one may state that the airfoil is stalled and a remarkable change in the flow pattern has occurred. [Figure 48](#) shows an airfoil whose angle of attack is being raised from 0° to past the stall angle of attack. Note that below the stall angle, the separation points on the airfoil move forward slowly but remain relatively close to the trailing edge. Near the stall angle the separation points move rapidly forward and the pressure drag rises abruptly. Past the stall angle, the effects of the greatly increased separated flow is to decrease the lift.

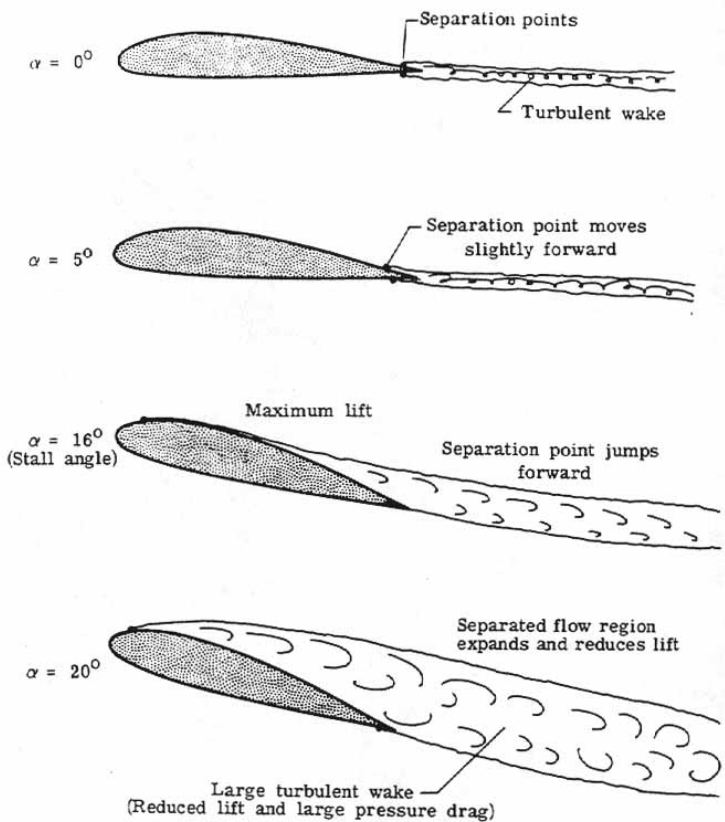


Figure 48.- Stall formation.

It is interesting to note ([fig. 47](#)) that the "lift curve" continues through negative angles of attack and that a negative stall angle occurs also. In general, however, an aircraft will be operating at a positive angle of attack to obtain the lift necessary for flight.

[Figure 49](#) is a typical graph of the coefficient of drag c_d as a function of angle of attack of the airfoil section. Usually, the minimum drag coefficient occurs at a small positive angle of attack corresponding to a positive lift coefficient and builds only gradually at the lower angles. As one nears the stall angle, however, the increase in c_d is rapid because of the greater amount of turbulent and separated flow occurring.

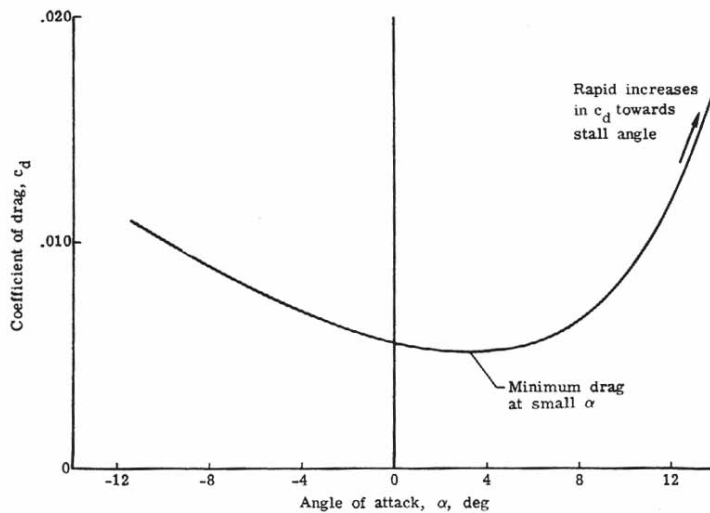


Figure 49.- Coefficient of drag as a function of angle of attack of airfoil section.

The drag coefficient curve may also be plotted as a function of the lift coefficient as shown in [figure 46](#). Since the lift coefficient up to the stall angle is a near-linear function of angle of attack, the c_d curve appears much the same as before and the same comments apply.

The coefficient of moment is an important parameter in the stability and control of an aircraft and will be discussed when that subject is introduced.

Two-dimensional wing compared with three-dimensional wing - The wing shown in [figure 50](#) is a finite-span three-dimensional (3D) version of the infinite-span two-dimensional (2D) wing tested in the wind tunnel ([fig. 43](#)).

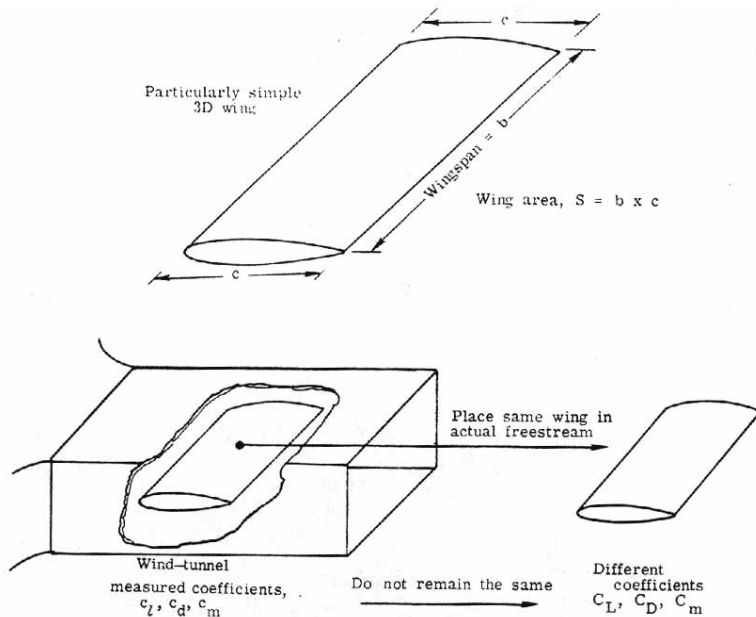


Figure 50.- Two-dimensional compared with three-dimensional conditions.

The wing area is S and is the chord length c times the wing span b . Thus

$$S = bc \quad (24)$$

This is also known as the planform area. If one measures the lift, drag, and moment on this 3D wing and nondimensionalizes by using the wing area, free-stream dynamic pressure, and chord length, one obtains the 3D aerodynamic characteristics of the wing; C_L , C_D , and C_m where

$$C_L = L/qS \quad (L = \text{Total lift on wing}) \quad (25)$$

$$C_D = D/qS \quad (D = \text{Total drag on wing}) \quad (26)$$

$$C_m = M/qSc \quad (M = \text{Total moment acting on wing}) \quad (27)$$

Notice that the coefficients for 3D flow are capitalized whereas the coefficients for 2D flow are lower case letters. This is the notation used to distinguish the finite-span coefficients from the infinite-span coefficients.

The important question now arises: How can one use experimental NACA 2D airfoil characteristics data to obtain the lift, drag, and moments on a real, finite 3D wing? Or to put it another way, how are c_l , c_d , and c_m related to C_L , C_D , and C_m . In [figure 50](#) the wing has simply been moved out in the free stream so that the wing tips are freely exposed. At first glance one might conclude that $c_l = C_L$, $c_d = C_D$, and $c_m = C_m$. But this is wrong! Why? Where does the problem lie? The answer is that the 2D wing tested in the wind tunnel spanned the tunnel walls and did not allow for the possibility of airflow about the wing tips, that is, spanwise flow of air. But the 3D wing is freely exposed in the free stream and spanwise flow may occur. The two-dimensional results must be modified to account for the effects of three dimensional flow.

Circulation and the vortex system of a finite wing - As was shown earlier in the discussion of a two-dimensional wing the airfoil could be represented by a free-stream flow and a circulation of strength Γ determined by the Kutta- Joukowsky condition. For an infinite, two-dimensional wing, at subsonic speeds, the upflow in front of the wing exactly balances the downflow at the rear of the wing, so that there exists no net downward movement of air past wing caused by the circulation Γ . This is not the case for a finite three-dimensional wing.

By a theorem of Helmholtz, a line of circulation or vortex line cannot end in midair. For an infinite wing, the vortex extends to infinity which is permissible but for a finite wing, the vortex line cannot simply end at the wingtips. Instead, the vortex continues outside the wing tips where the free-stream flow forces them to trail back from the wing tips, hence, the names "trailing vortices" or "wing-tip vortices." These tip vortices have the same circulation strength Γ . Physically, the formation of these trailing vortices can be explained as follows.

The static pressure on the upper surface of a wing is for the most part lower than that on the lower surface of the wing operating at a normally positive lift. As shown in [figure 51\(a\)](#), the pressures must become equal at the wing tips since pressure is a continuous function. A pressure gradient exists between the upper and lower surfaces. The tendency of the air is to equalize any pressure differences so that particles of air tend to move from the lower wing surface around the wing tip to the upper surface (from the region of high pressure to the region of low pressure).

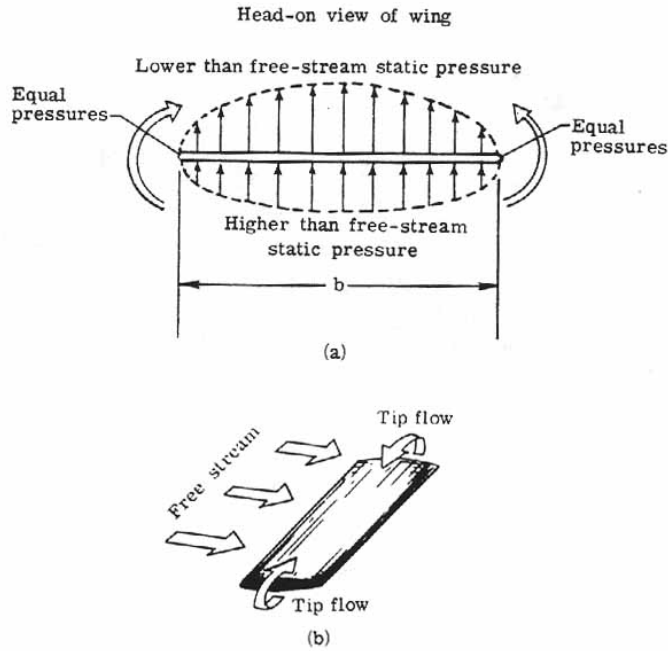


Figure 51.- Finite-wing flow tendencies.

In addition, there exists the oncoming free-stream flow approaching the wing. (See [fig. 51\(b\)](#).) If these two movements of air are combined (superimpose the spanwise flow about the wing on the oncoming free stream), one has an inclined inward flow of air on the upper wing surface and an inclined outward flow of air on the lower wing surface. The spanwise flow is strongest at the wing tips and decreases to zero at the mid-span point as evidenced by the flow direction there being parallel the free-stream direction ([fig. 52\(a\)](#)).

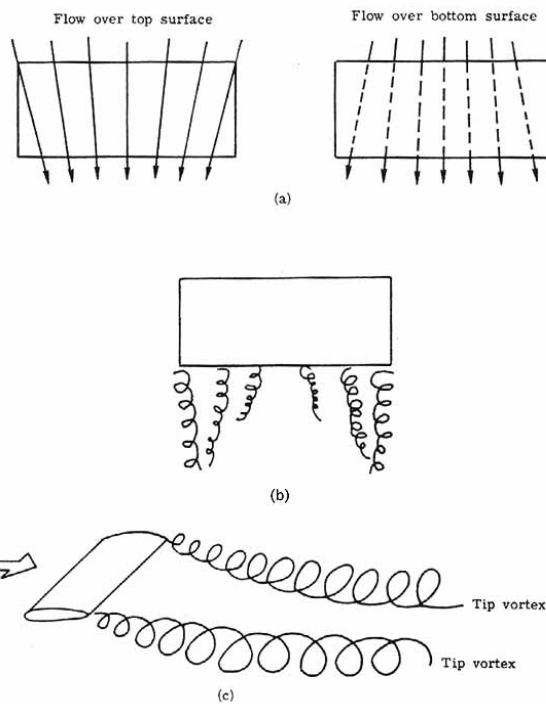


Figure 52.- Formation of wing-tip vortices.

When the air leaves the trailing edge of the wing, the air from the upper surface is inclined to that from the lower surface and helical paths or vortices result. A whole line of vortices trail back from the wing, the vortex "strength" being strongest at the tips and decreasing rapidly to zero at midspan. (See [fig. 52\(b\)](#).) A short distance downstream the vortices roll up and combine into two distinct cylindrical vortices which constitute the so-called "tip vortices." [Figure 52\(c\)](#) shows the simplified picture of the tip vortex system replacing the vortex distribution just discussed.

An account of the tip-vortex effects constitutes the modifications of the 2D airfoil aerodynamic coefficients into their 3D counterparts.

The vortex in the wing (which is equivalent to the lift of the wing ([fig. 53\(a\)](#)) is called the bound vortex. [Figure 53\(b\)](#) shows the bound vortex and the tip vortices for a finite wing (sometimes known as the horseshoe vortex system). Also, the vortex system must be closed in some manner and is accomplished by the so-called starting vortex which is left behind the wing when the wing starts from rest in the case of constant vorticity ([fig. 53\(c\)](#)). If the lift of the wing is being continually changed, new starting vortices are shed. Generally, the starting vortices are soon dissipated because of the air's viscosity. Also, their influence on the flow behind a wing decays rapidly the further back they are left.

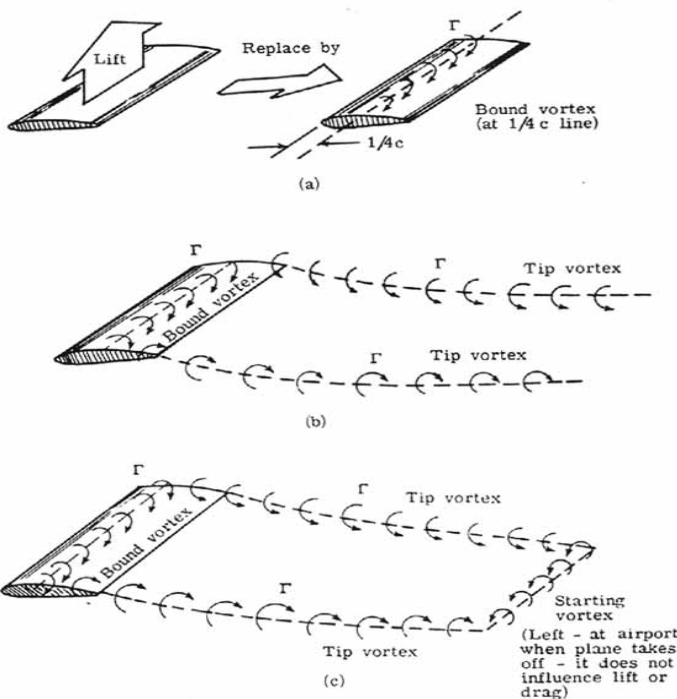


Figure 53.- Complete-wing vortex system.

The tip vortices trail back from the wing tips and they have a tendency to sink and roll toward each other downstream of the wing. Again, eventually the tip vortices dissipate, their energy being transformed by viscosity. As will be discussed later, this change may take some time and may prove to be dangerous to other aircraft.

The important effects of the vortex system are shown in [figure 54](#). Indicated are the directions of air movement due to the vortex system. The left-tip vortex rotates clockwise, the right-tip vortex

rotates counterclockwise (when viewed from behind), and the bound vortex rotates clockwise (when viewed from the left side).

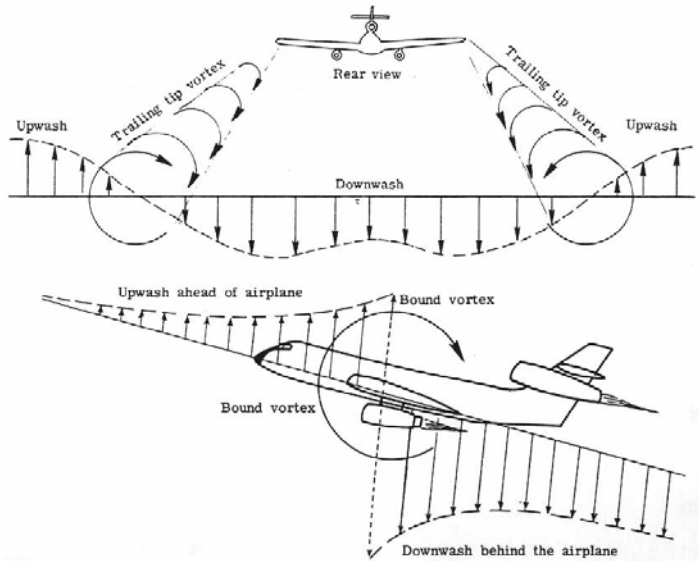


Figure 54.- Vortex flow effects. Note that upwash and downwash are due to both the bound vortex and the tip vortices.

The bound vortex is directly related to the lift on the wing as in the dimensional case. For a finite wing the relation becomes

$$L = \rho_{\infty} V_{\infty} b \Gamma \quad (28)$$

where

L	lift on three-dimensional wing
ρ_{∞}	free-stream air density [Greek letter rho]
V_{∞}	free-stream velocity
b	wing span
Γ	circulation (spin strength) [Greek letter Capital Gamma]

In both the 2D and 3D cases the upflow (or upwash) in front of the wing balanced the downflow (or downwash) in back of the wing caused by the bound vortex. But, in the finite-wing case one must also take into account the Tip vortices (assuming that the influence of the starting vortex is negligible). The tip vortices cause additional down wash behind the wing within the wing span. One can see that, for an observer fixed in the air ([fig. 55](#)) all the air within the vortex system is moving downwards (this is called downwash) whereas all the air outside the vortex system is moving upwards (this is called upwash). Note that an aircraft flying perpendicular to the flight path of the airplane creating the vortex pattern will encounter upwash, downwash, and upwash in that order. The gradient, or change of downwash to upwash, can become very large at the tip vortices and cause extreme motions in the airplane flying through it. Also shown is an airplane flying into a tip vortex.

Note that there is a large tendency for the airplane to roll over. If the control surfaces of the airplane are not effective enough to counteract the airplane roll tendency, the pilot may lose control or in a violent case experience structural failure.

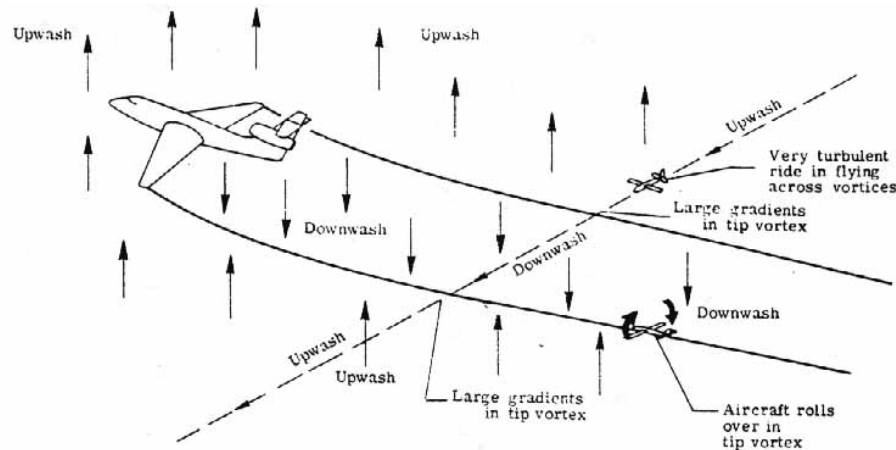


Figure 55.- Upwash and downwash fields around an airplane.

The problems of severe tip vortices are compounded by the take-off and landings of the new generation of jumbo jets. During these times the speed of the airplane is low and the airplane is operating at high lift coefficients to maintain lift. The Federal Aviation Agency has shown that for a 0.27 MN (600 000 lb) plane, the tip vortices may extend back strongly for 5 miles from the airplane and the downwash may approach 160 meters per minute (500 ft/min). Tests also show that a small light aircraft flying into a vortex could be rolled over at rates exceeding 90°/sec. Between 1964 and 1969 at least 100 airplane accidents and countless other incidents could be traced to this vortex phenomenon. Realizing this, the FAA is requesting much greater separation times and distances between the large jets and small aircraft especially during take-offs and landings.

The tip vortices contribute to the downwash field at and behind the wing. To create downwash due to finite-wing contribution requires the expenditure of energy per unit time or power. The power required to induce this component of downwash may be associated with an additional drag force known as induced drag. Additionally, the net lift on the wing is decreased by the tip vortex effects.

It may be noted at this point that induced drag is an ideal fluid effect not in any way associated with a fluid's viscosity. A finite wing operating in an ideal fluid will not possess a skin-friction or pressure drag (taken together often called parasitic drag) but will still possess an induced drag if generating lift and thus a circulation Γ .

The aspect ratio may be defined as

$$\text{Aspect ratio} = (\text{Wing span})^2 / \text{Wing area} \quad (29a)$$

or

$$AR \equiv \frac{b^2}{S} \quad (29b)$$

for any wing.

For the special case of a rectangular wing: $S = b \times c$ so that

$$AR = b/c = \text{Wing span} / \text{Chord length} \quad (30)$$

for a rectangular wing. Aspect ratio is a measure of the slenderness of a wing; a long thin wing has a high aspect ratio compared with a short stubby wing of low aspect ratio.

With this in mind, return to the case of the 2D and 3D wings shown in [figure 50](#). The 2D wing is the equivalent of an infinite span wing and, as such, one can say it has an infinite aspect ratio. The 3D wing has a finite aspect ratio whose value is determined by equation (30). [Figure 56](#) shows the coefficient of lift curves ("lift curves") obtained for both wings by experiment. Readily evident is the effect that the tip vortices have in creating the additional downwash w at the wing; the lift curve is flattened out so that at the same angle of attack less lift is obtained for the smaller aspect ratio wing. This is not a beneficial effect.

Consider the case where one wants to get the same lift from the finite wing as predicted by the 2D aerodynamic characteristics, or namely, $C_L = c_L$. From [figure 56](#), this is achieved by raising the angle of attack of the finite wing by a small amount over that of the 2D wing, that is,

$$\alpha_{3D} = \alpha_{2D} + \Delta\alpha \quad (C_L = c_L) \quad (31)$$

This increase in angle of attack to obtain the same lift is due to the effect of tip vortices on the downwash in changing the relative flow seen by the wing where for small angles

$$\Delta\alpha \approx \frac{w}{V_\infty} \quad (32)$$

It may be stated that the drag coefficient for the finite 3D wing is the infinite wing 2D drag coefficient plus the induced drag coefficient or

$$C_D = c_d + (C_D)_{\text{induced}} \quad (33)$$

where c_d here is the parasitic drag coefficient (skin-friction drag plus pressure drag coefficient) of the 2D wing operating at the higher angle of attack α_{3D} necessary to get C_L . This is greater than the original value of c_d operating at α_{2D} . $(C_D)_{\text{induced}}$ is inversely proportional to the aspect ratio AR and an "efficiency factor" e relating how close one comes to achieving an ideal elliptic spanwise lift

distribution shown by theory to give minimum induced drag ($e = 1$). Also, $(C_D)_{\text{induced}}$ is proportional to C_L^2 . Thus

$$(C_D)_{\text{induced}} = KC_L^2 \quad (34)$$

where K is related to the aspect ratio and the efficiency factor.

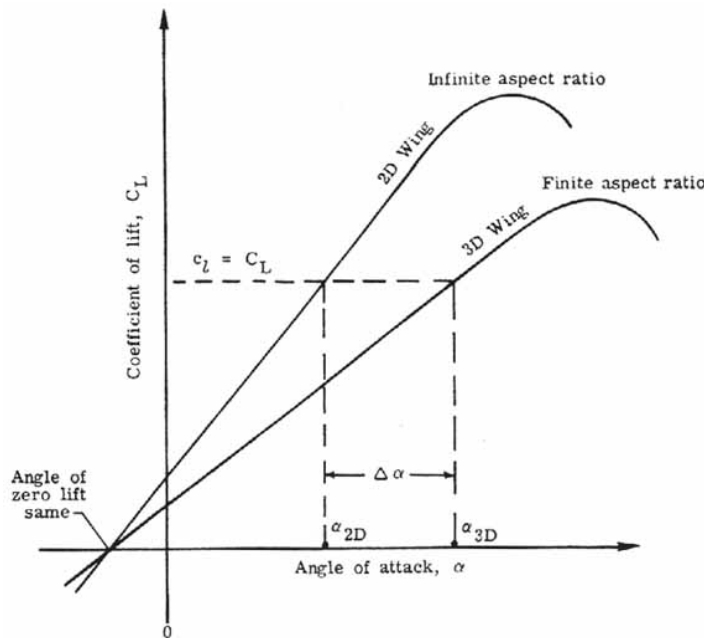


Figure 56.- Effect of aspect ratio on coefficient of lift.

To summarize to this point, a finite-span version of a 2D wing will give the same lift coefficient ($C_L = c_l$) only if its angle of attack is raised slightly. This increase in angle of attack causes an increase in the parasitic drag coefficient and, in addition, yields an induced drag coefficient. In this way, the 2D wind-tunnel data are modified.

It is important not to confuse the drag coefficient with the actual drag force it represents. If one converts the coefficient to actual induced drag, one finds that it is inversely proportional to (1) the span efficiency factor e, (2) the wing span squared b^2 , and (3) the free-stream velocity squared (V_∞)².

Methods of reducing induced drag - From the stated results it can be seen that NACA 2D wind-tunnel data may be used to obtain the lift and drag acting on the entire 3D wing if proper corrections for the tip vortices are included. One would like these corrections to be as small as possible to get the most lift with the least drag. How may the induced drag be reduced? From the previous discussion one may (1) increase the span efficiency factor to as close to $e = 1$ as possible, (2) increase the wing span b (or aspect ratio AR), and (3) increase the free-stream velocity V_∞ . This last fact points up that induced drag is a small component at high speeds (cruising flight) and relatively unimportant since it constitutes only about 5 to 15 percent of the total drag at those speeds. At low speeds (take-off or landing) it is a considerable component since it accounts for up to 70 percent of the total drag.

The efficiency factor e and wing span are physical factors that may be controlled by proper design. [Figure 57](#) shows two airplanes with rectangular wings. Both wings are at the same lift coefficient and

they have the same wing area. The only difference is that the wing span of the second wing is twice that of the first wing. Ideally, both wings should produce the same lift and drag. But the longer span wing (higher aspect ratio) has one-fourth the induced drag, and therefore, a greater efficiency.

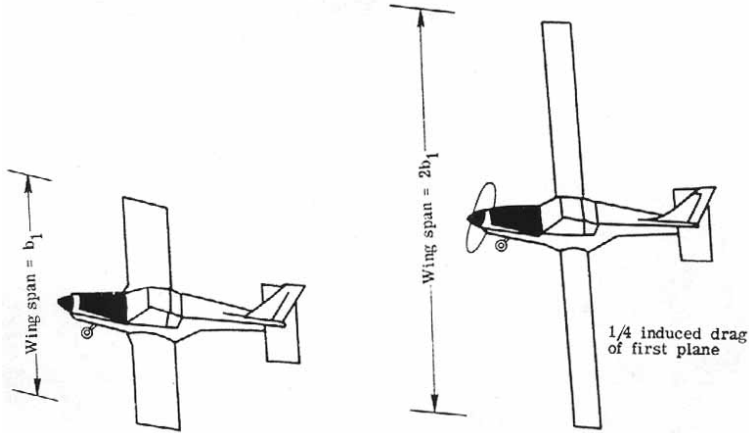


Figure 57.- Wing-span effect on induced drag for airplanes having same wing area, same lift coefficient, and same dynamic pressure.

The thought arises that with less induced drag with longer wing spans, why not make a wing with an extremely long wing span (high AR). This would give nearly idealized flow, the tip vortex effects being very small. In fact, as [figure 58](#) illustrates, sailplanes that must rely on high efficiencies, do have very long slender wings. But structural considerations become a dominant factor. A very thin long wing requires a large structural weight to support it.

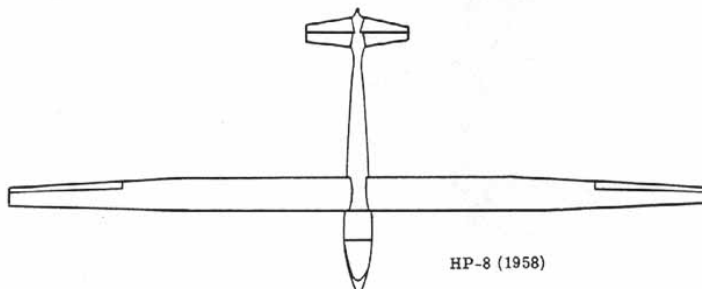


Figure 58.- High-aspect-ratio wing. $AR \approx 24$.

There comes a point where the disadvantage of increasing structural weight necessary to support increased wing span counteracts the advantage of decreased drag due to smaller vortex effects. A compromise aspect ratio would give the optimum performance. This is necessarily also dependent on factors such as fuel capacity, control characteristics, size allowances, and numerous other factors. A survey of airplane categories show sailplanes with an aspect ratio of 15 or more, single-engine light airplanes with an aspect ratio of about 6, and supersonic fighter airplanes with an aspect ratio of ≈ 2 .

Another interesting way of reducing induced drag is by the use of tip plates or tip tanks as shown in [figure 59](#). This arrangement tends to promote a 2D flow by inhibiting the formation of tip vortices. They have the same physical effect as an increase in wing span (or aspect ratio). Normally, these are not used since there are other more valuable drag reduction methods.

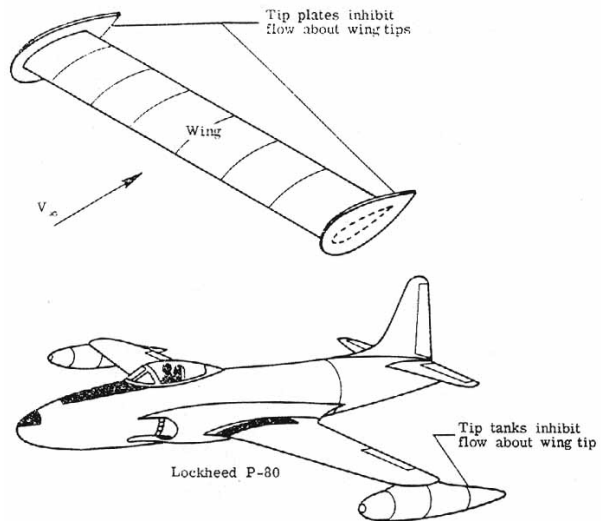


Figure 59.- Tip plates and tip tanks.

Before looking further at methods of reducing induced drag, it is necessary to define taper and twist for a wing. For a general wing, the airfoil sections may vary in three distinct ways along the wing. First, the size or chord length may change; second, the shape of the airfoil section may change as one moves along the wing, and lastly, the angles of attack of the airfoil sections may change along the wing. These variations give the wing taper and twist- terms that are now considered.

Planform taper is the reduction of the chord length and thickness as one proceeds from the root section (near the fuselage) to the tip section (at the wing tip) so that the airfoil sections also remain geometrically similar. (See [fig. 60\(a\)](#).)

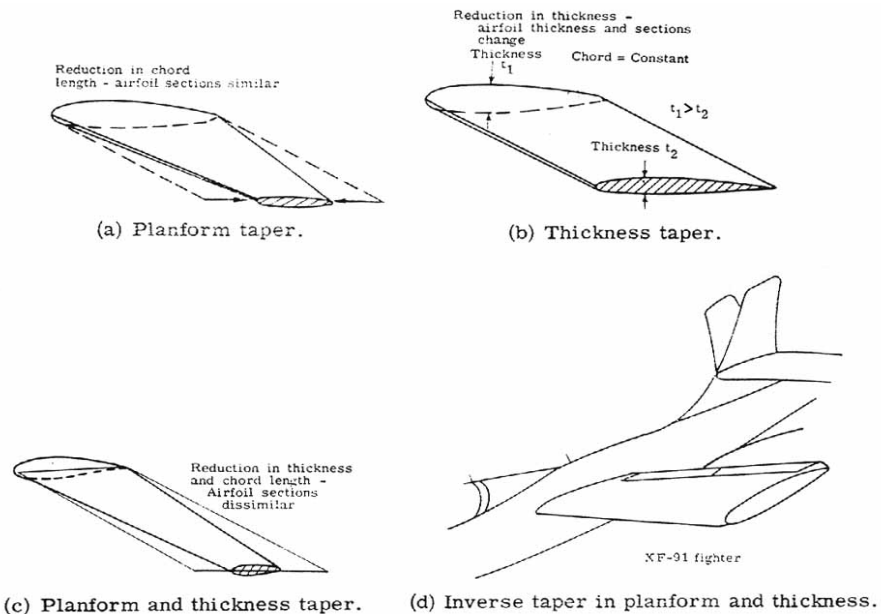
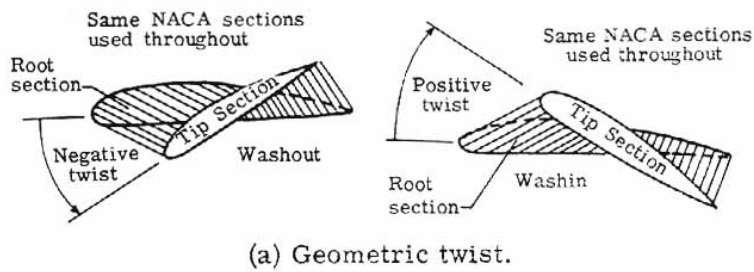


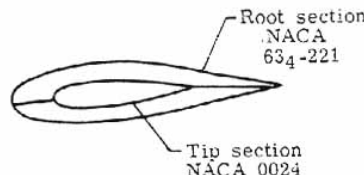
Figure 60.- Planform and thickness taper.

Thickness taper is the reduction of only the airfoil's thickness as one proceeds from the root section to the tip section-this reduction results in thinner airfoil sections at the wing tip. (See [fig. 60\(b\)](#).) The chord remains constant. [Figure 60\(c\)](#) shows a typical wing with both planform and thickness taper. One notable exception to this normal taper was the XF-91 fighter which has inverse taper in planform and thickness so that the wing tips were thicker and wider than the inboard stations. (See [fig. 60\(d\)](#).)

Wings are given twist so that the angle of attack varies along the span. A decrease in angle of attack toward the wing tip is called washout whereas an increase in angle of attack toward the wing tip is called washin. Geometric twist ([fig. 61\(a\)](#)) represents a geometric method of changing the lift distribution, whereas aerodynamic twist, by using different airfoil sections along the span represents an aerodynamic method of changing the lift distribution in a spanwise manner ([fig. 61\(b\)](#)). To give minimum induced drag it was demonstrated that the spanwise efficiency factor ϵ should be as close to 1 as possible. This is the case of an elliptic spanwise lift distribution. A number of methods are available to modify the spanwise distribution of lift.



(a) Geometric twist.



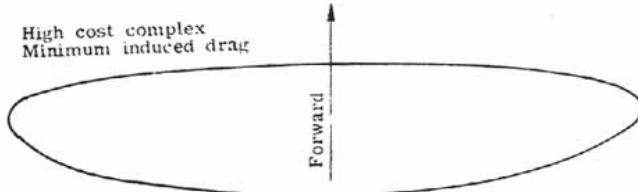
(b) Aerodynamic twist.

Figure 61.- Geometric and aerodynamic twist.

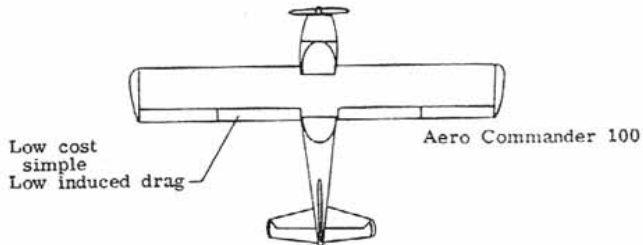
These methods include (1) planform taper to obtain an elliptic planform as shown in [figure 62\(a\)](#) for the Spitfire wing which is remarkably elliptic; (2) a geometric twist and/or aerodynamic twist to obtain elliptic lift distribution; or (3) a combination of all of these methods.

An elliptical planform is hard to manufacture and is costly. Of course, from the point of view of construction, the best type of wing is the untapered, untwisted wing. This is used considerably by light plane manufacturers. (See [fig. 62\(b\)](#).) Surprisingly, there are data that indicate that a square-tipped rectangular wing is very nearly as efficient as the elliptic wing so that the gains in reduced induced drag may be insignificant. This result may be traced to the fact that for a real wing the lift distribution does fall off to zero at the wing tips and approximates an elliptical distribution.

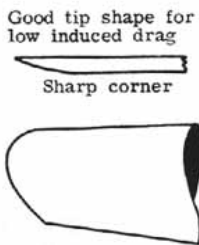
The wing-tip shape, being at the point of production of the tip vortices, appears to be of more importance in minimizing tip vortex formation and thus minimizing induced drag. [Figure 62\(c\)](#) presents a good wing-tip shape, whereas [figure 62\(d\)](#) indicates a less favorable one.



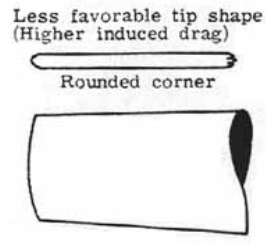
(a) Elliptic wing – Supermarine Spitfire Mk. I.



(b) Untapered, untwisted wing.



(c) Good tip shape.



(d) Poor tip shape.

Figure 62.- Reduction of induced drag.

Taper and twist are perhaps of greater importance when the problem of stalling is discussed later.

Aerodynamic Devices

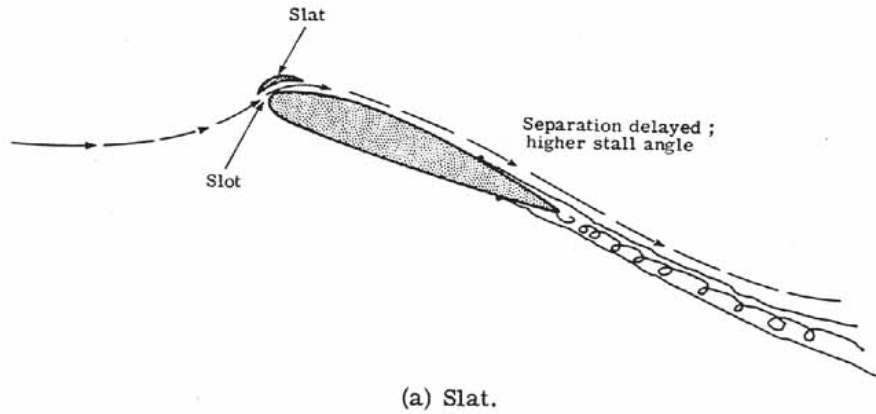
One of the most fascinating subjects of aerodynamics of flight is the vast number of, for want of a better term, "aerodynamic devices" affixed to a simple wing to achieve increases or decreases in lift and drag such as slats, slots, flaps, spoilers, and dive brakes. With all these devices hanging on a wing, the unsuspecting air traveler might well think that the wing is a piece of modern art. The sound of flaps and slats opening as one approaches for a landing combined with a visual inspection of the wing "coming apart at the seams" may unnerve the unknowledgeable. But a purpose exists for all of these devices and the safety and economy of air travel is dependent on them.

It is in the interest of safety to perform take-off and landing maneuvers at as low a speed as possible. But also, one does not want the normal flying characteristics to be affected. Consider a near-level flight condition in which the airplane weight is equal to the lift ($L = W$). For minimum flying speed (take-off or landing) the wing would be operating at maximum lift or $C_{L,max}$. From equation (25) after some manipulation, solving for the minimum flight velocity, V_{min} yields

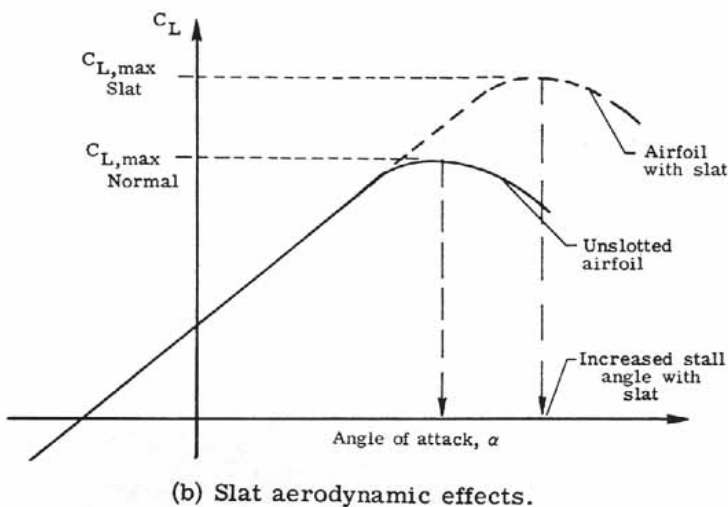
$$V_{\min} = \sqrt{\frac{2W}{\rho_{\infty} C_{L,\max} S}} \quad (35)$$

The density ρ_{∞} is considered to be constant and if the weight is considered a fixed characteristic of the airplane, then it is obvious that the only way to reduce V_{\min} is to increase $C_{L,\max}$ and/or the wing area S . Slots and flaps are used for this purpose.

Slots - The maximum coefficient of lift may be increased through the use of a slot formed by a leading-edge auxiliary airfoil called a slat. [Figure 63\(a\)](#) illustrates the operating principle. When the slot is open, the air flows through the slot and over the airfoil. The slot is a boundary-layer control device and the air thus channeled energizes the boundary layer about the wing and retards the separation. The airfoil can then be flown at a higher angle of attack before stall occurs and thus get a higher $C_{L,\max}$ value. A curve showing C_L as a function of α [Greek letter alpha] for the normal and the slotted airfoil is given in [figure 63\(b\)](#). Notice particularly that for angles of attack less than the stall angle, the airfoil lift curve is relatively unaffected whether the slot is opened or closed.



(a) Slat.



(b) Slat aerodynamic effects.

Figure 63.- Slat-slot operation.

There are two types of slots -fixed and automatic. The fixed slot is self explanatory; the leading-edge slat is mounted a fixed distance from the airfoil. Its main disadvantage is that it creates excessive drag

at high speeds. [Figure 64](#) shows a German World War II designed rocket fighter - the Me-163 with fixed slots in the wing. The automatic slot depends on air pressure lifting the slat away from the wing at high angles of attack to open the slot. At low angles of attack the slat is flush against the wing leading edge and reduces drag at high speeds compared with the fixed slot. Its main disadvantages are its added weight, complexity, and cost.

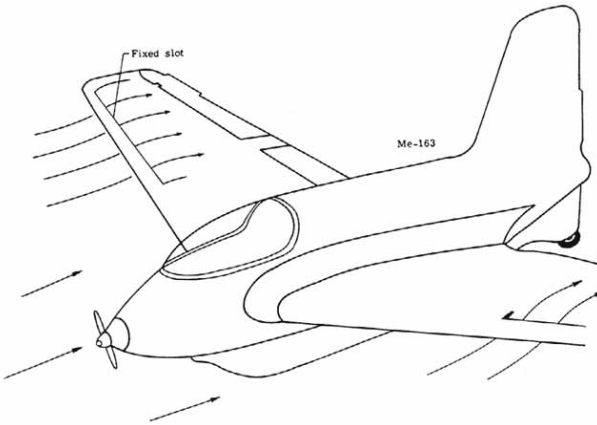
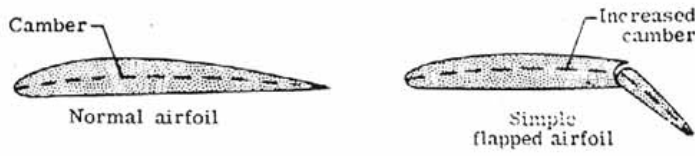


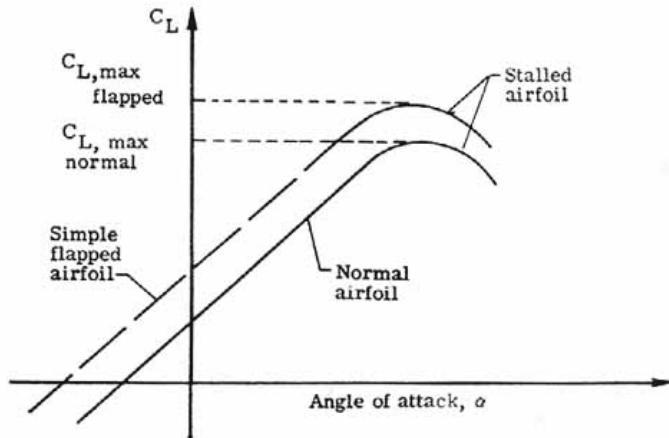
Figure 64.- Fixed slots.

One main disadvantage of both types of slots is the high stall angle created. The airplane must approach for a landing in an extreme nose-up attitude which promotes reduced visibility.

Flaps - Flaps may be used to increase the maximum lift coefficient, increase the wing area, or both. A change in the maximum lift coefficient may be realized by a change in the shape of the airfoil section or by increased camber. The trailing-edge flap is one method of accomplishing this. [Figure 65\(a\)](#) shows a normal airfoil and the same shaped airfoil with a simple flap in the down position for increased camber. The maximum lift coefficient for the airfoil with the simple flap is greater than that for the unflapped airfoil. Also, the coefficients of lift are increased over the entire angle-of-attack range. This is shown in [figure 65\(b\)](#). Note also that the stall angle is essentially unchanged from that of the unflapped airfoil. This is opposed to the slot operation where a higher stall angle was obtained. The flapped airfoil reduces the disadvantage that the slot has in high landing angles.



(a) Flap.

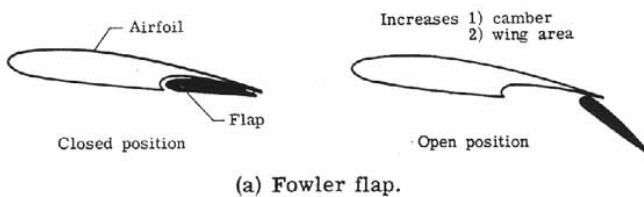


(b) Flap aerodynamic effects.

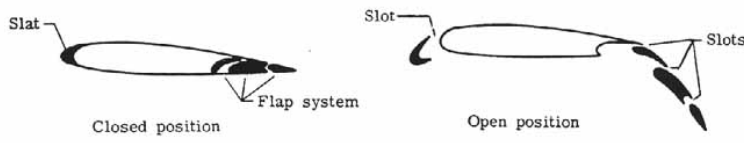
Figure 65.- Simple flap operation.

[Figure 66\(a\)](#) shows a Fowler flap which is hinged such that it can move back and increase the airplane wing area. Also, it may be rotated down to increase the camber. A very large increase in maximum lift coefficient is realized.

There are many combinations of slots and flaps available for use on airplanes. [Figure 66\(b\)](#) shows the arrangement on a Boeing 737 airplane which utilizes a leading-edge slat and a triple-slotted trailing-edge flap. This combination is a highly efficient lift-increasing arrangement. The slots in the flaps help retard separation over the flap segments and thus enhance lift.



(a) Fowler flap.



(b) Complex slotted flap of Boeing 737.

Figure 66.- Types of flaps.

It may also be noted that flaps in an extreme down position (50° to 90°) act as a high-drag device and can retard the speed of an airplane before and after landing.

Boundary-layer control - Another method of increasing $C_{L,\max}$ is by boundary-layer control. The idea is to either remove the low-energy segment of the boundary layer and let it be replaced by high-energy flow from above or by adding kinetic energy to the boundary layer directly. Both of these methods maintain a laminar flow for a longer distance over the airfoil, delay separation, and allow one to get a larger angle of attack before stall occurs, and thus a higher $C_{L,\max}$. The slot was shown to be one means of passing high-energy flow over the top surface of a wing.

The low-energy boundary layer may be sucked through slots or holes in the wing as shown in [figure 67\(a\)](#) or high-energy air may be blown into the boundary layer through backward facing holes or slots as shown in [figure 67\(b\)](#).

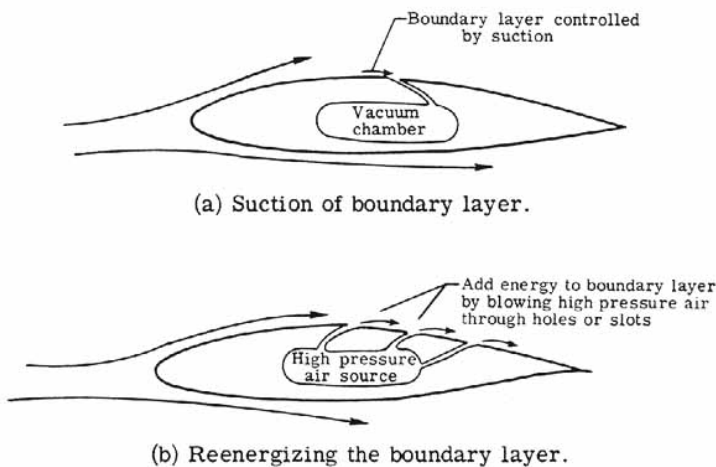


Figure 67.- Forms of boundary-layer control.

Spoilers - Spoilers are devices used to reduce the lift on the airplane wing. They may serve the purpose as on gliders to vary the total lift and control the glide angle. Or on large commercial jets they may be used to help the aileron control by "dumping" lift on one wing and thus help to roll the airplane. Also, on landing, with spoilers up, the lift is quickly destroyed and the airplane may quickly settle on its landing gear without bouncing. [Figure 68](#) shows the spoiler arrangement on a Boeing 707 wing.

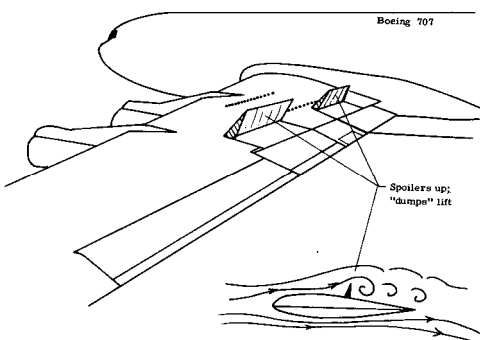


Figure 68.- Use of spoilers.

Dive brakes - Dive (or speed) brakes are used in airplanes to control descent speed. Whether slowing down quickly when approaching for a landing, after landing, or in a dive, these aerodynamic brakes are helpful. Essentially, they promote a large separation wake and increase the pressure drag. [Figure 69](#) shows a civilian aircraft speed-brake arrangement and two military aircraft dive brake arrangements.

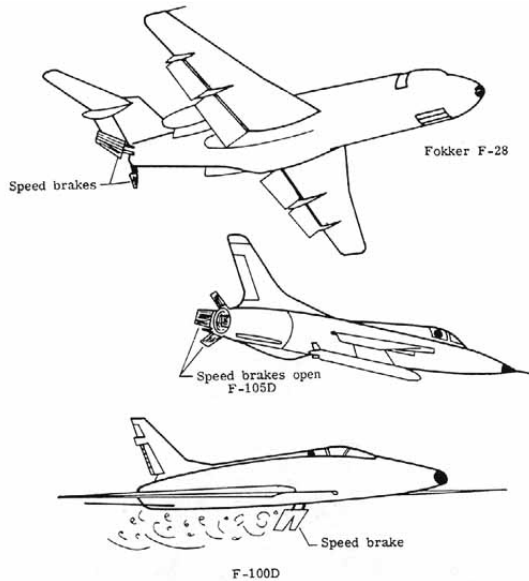
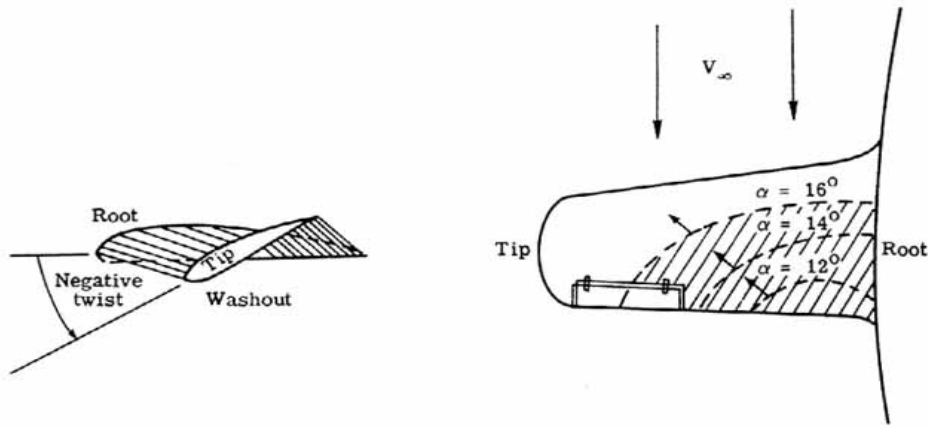


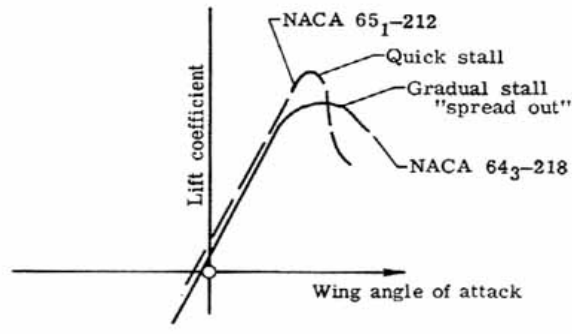
Figure 69.- Dive (speed) brake arrangements.

Stall characteristics - The present discussion has concentrated considerably on operating near or at the stall condition $C_{L,\max}$. A further word about stalling is in order. A wing should possess favorable stall characteristics so that (1) the pilot has adequate warning of the stall, (2) the stall is gradual, and (3) there is little tendency to spin after a stall. This may be achieved by "forcing" the stall to occur at the wingroot section first and let it progress toward the wing tips. The outboard, wing-tip stations should be the last to stall so that the ailerons remain effective (are not immersed in a turbulent "dead air" wake). Use of twist, namely washout, is often employed so that the wing-root section reaches the stall angle first. (See [fig. 70\(a\)](#).) Also, airfoil sections with gradual stall characteristics are more favorable than ones with quick stall characteristics. (See [fig. 70\(b\)](#).)

As the inboard root stations stall, turbulent flow from the wing strikes the tailplane and buffets the pilot's controls. This condition is an adequate stall warning device. With a gradual stall on both wings, the plane should maintain a level attitude with few spin tendencies.



(a) Twist and stall. Note that stalled region moves toward wing tip as wing angle of attack increases.



(b) Gradual stall.

Figure 70.- Stall characteristics.

Total Drag of Airplane

Up to now the drag acting on a finite wing has been considered. It has been shown that three components are present: (1) skin-friction drag, (2) pressure drag, and (3) induced drag. Of course, an airplane is composed of many other components and each will introduce a total drag of its own. Possible airplane component drags include (1) drag of wing, wing flaps, (2) drag of fuselage, (3) drag of tail surfaces, (4) drag of nacelles, (5) drag of landing gear, (6) drag of wing tanks and external stores, (7) drag of engines, and (8) drag of miscellaneous parts. The net drag of an aircraft is not simply the sum of the drag of the components. When the components are combined into a complete aircraft, one component can affect the flow field, and hence, the drag of another. These effects are called interference effects, and the change in the sum of the component drags is called interference drag. Thus,

$$(\text{Drag})_{I+2} = (\text{Drag})_1 + (\text{Drag})_2 + (\text{Drag})_{\text{interference}}$$

Generally, interference drag will add to the component drags but in a few cases, for example, adding tip tanks to a wing, total drag will be less than the sum of the two component drags because of reduced induced drag.

Interference drag can be minimized by proper fairing and filleting which induces smooth mixing of air past the components. [Figure 71](#) shows a Grumman F9F Panther Jet with a large degree of filleting. No adequate theoretical method will predict interference drag; thus, wind-tunnel or flight-test measurements are required. For rough computational purposes a figure of 5 percent to 10 percent can be attributed to interference drag on a total aircraft.

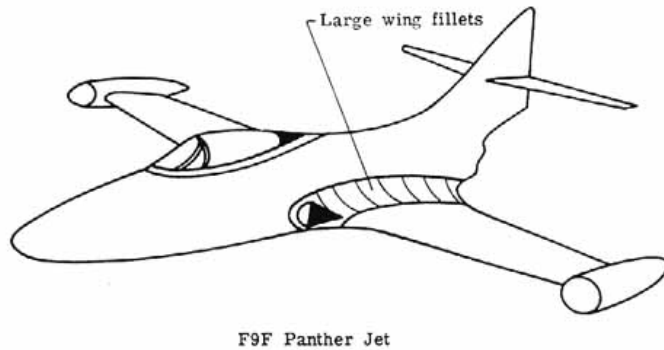
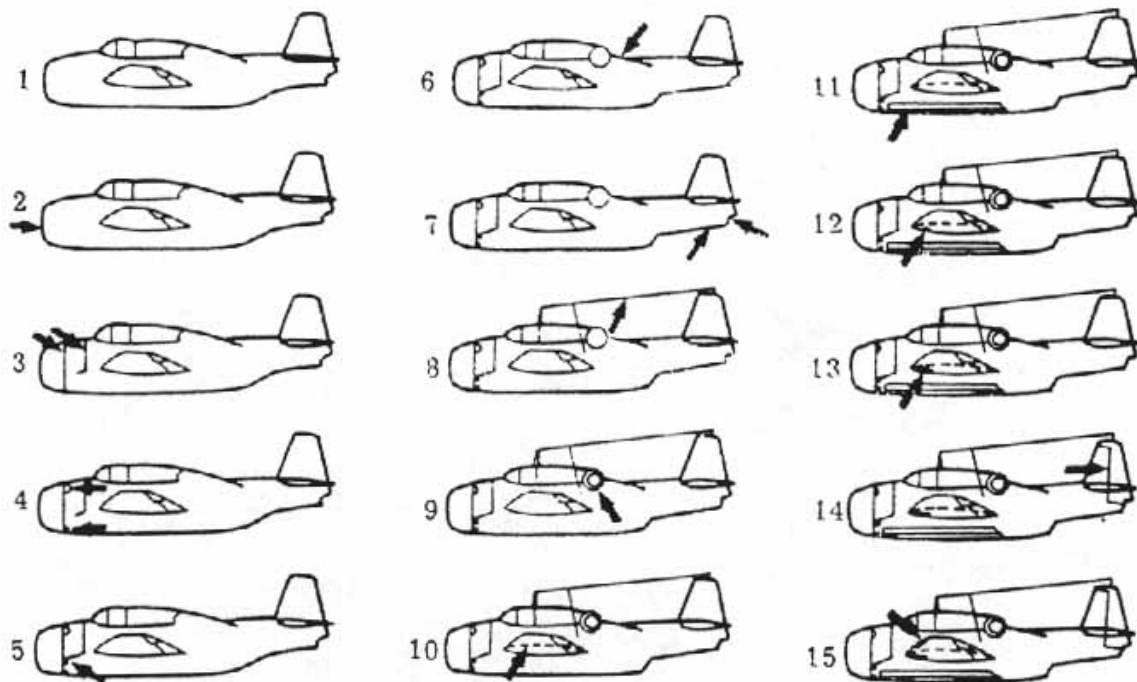


Figure 71.- Wing fillets.

Small items also add to the total aircraft drag and although seemingly trivial, they can greatly reduce the aircraft's top speed. [Figure 72](#) shows a TBF Avenger aircraft from World War II and shows the increase in drag coefficient as these small changes and components are accounted for.

[Figure 73](#) shows a Me-109G German fighter from World War II. Shown is the percentage breakdown of the drag (includes interference drag) of the components.

[Figure 74](#) presents a graph of how the total airplane drag coefficient has decreased over the years. Doing away with bracing wires, shielding engines behind streamline cowls, use of flush-riveting techniques, and use of polished surfaces have all aided in the reduction of drag. It is beyond the scope of this discussion to expand upon what has been introduced about total airplane drag at subsonic speeds. Although prediction of drag and wind-tunnel drag measurements of models does yield good results, final drag evaluation must be obtained by flight tests. Even here, however, the accuracy of the measurements is dependent on flight-test equipment, pilot technique, and subsequent proper evaluation of test data.



(National Advisory Committee for Aeronautics.)

Condition	Airplane configuration	C_D at $C_L = 0.245$	Reference condition (see column 1)	C_D
1	Airplane completely sealed and faired	0.0183	-	-
2	Flat plate removed from nose	0.0189	1	0.0006
3	Seals removed from flapped-cowling air exits	0.0199	2	0.0010
4	Seals removed from cowling-flap hinge-line gaps	0.0203	3	0.0004
5	Exhaust stacks replaced	0.0211	4	0.0008
6	Canopy flaring removed, turret leaks sealed	0.0222	5	0.0011
7	Tail wheel and arresting-hook openings uncovered	0.0223	6	0.0001
8	Aerial, mast, and trailing antenna tube installed	0.0227	7	0.0004
9	Canopy and turret leak seals removed	0.0230	8	0.0003
10	Leak seals removed from shock strut, cover plate, and wing-fold axis	0.0234	9	0.0004
11	Leak seals removed from bomb-bay doors and miscellaneous leak seals removed	0.0236	10	0.0002
12	Fairings over catapult hooks removed	0.0237	11	0.0001
13	Wheel-well cover plates removed	0.0251	12	0.0014
14	Seals removed from tail-surface gaps	0.0260	13	0.0009
15	Plates over wing-tip slot openings removed. Airplane in service condition.	0.0264	14	0.0004
Total drag change				0.0081

Figure 72. Small item influence on total airplane drag.

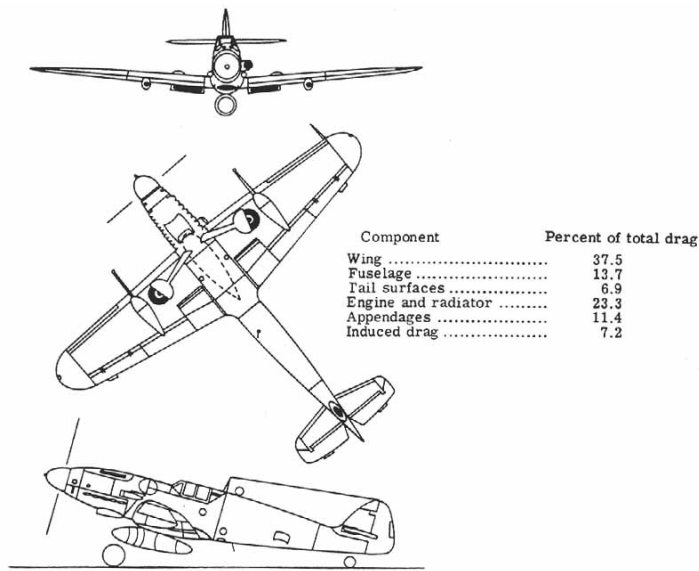


Figure 73.- Typical fighter-drag breakdown.

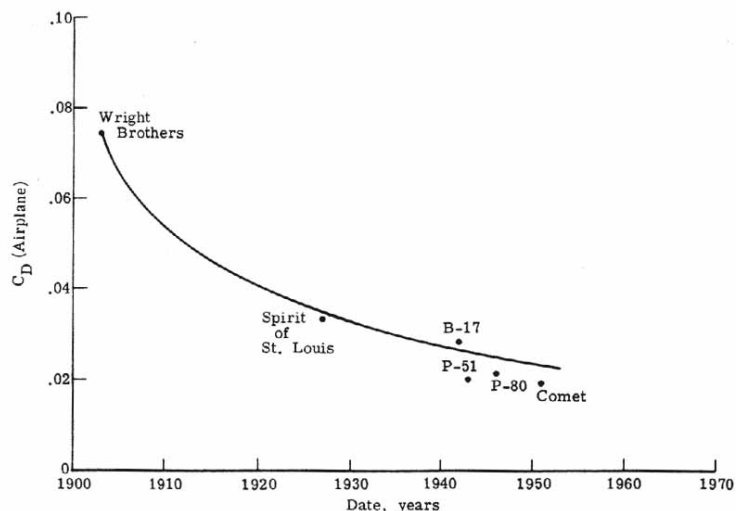


Figure 74.- Decrease in airplane drag coefficient with time.

Propellers and Rotors

Propellers - The propeller converts the turning power of an engine's crankshaft into the thrust force. This thrust is equal to the mass of air forced backward by the propeller per second times the added velocity imparted to this air. If one has ever stood behind a spinning propeller while the airplane was at rest on the ground, this backward moving air, the slipstream, is very noticeable.

Figure 75 shows a variety of propeller configurations used on military and civilian airplanes. Basically, a propeller blade is a small wing producing a resultant aerodynamic force which for the purposes of this discussion, may be resolved into a force pointing along the axis of the airplane (thrust), and a force in the plane of the propeller blades (the torque force). (See fig. 76.) The torque force opposes the rotary motion of the engine by acting as a "drag" on it. In equilibrium, the propeller rotates at a constant rate determined by the engine torque equal and opposite to the propeller torque.

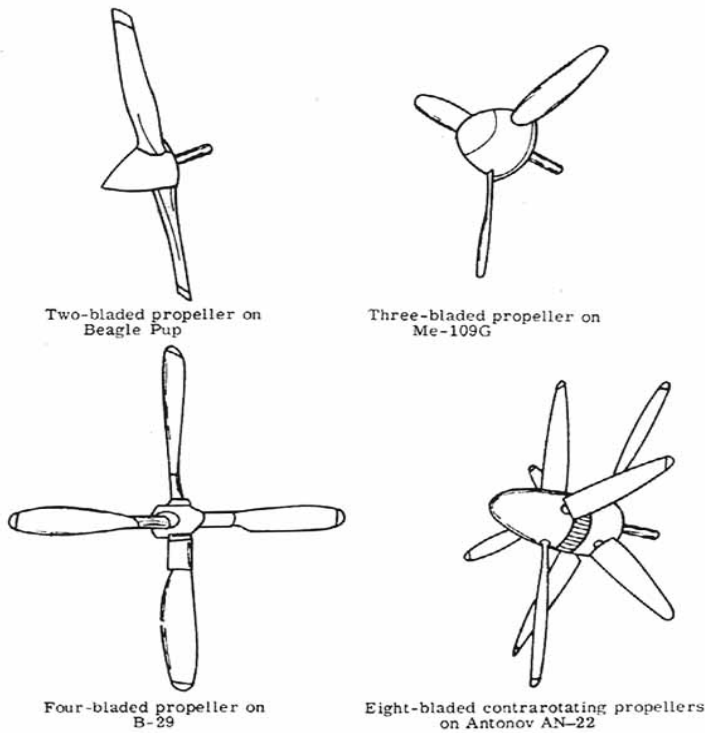


Figure 75.- Various propeller configurations.

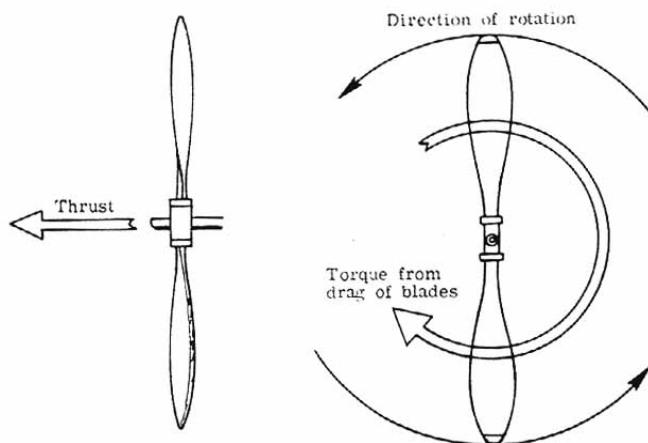


Figure 76.- Thrust and torque of a propeller.

As [figure 77](#) shows, the propeller blade consists of a set of airfoil-shaped sections which may vary in shape from the tip to the root of the blade. Although a wing is fixed with respect to the airplane and sees only the relative free-stream flow of air ([fig. 78\(a\)](#)), the propeller is also rotating with respect to the airplane, and it sees an oncoming relative flow of air which is the vector sum of the airplane free-stream velocity and the propeller rotational velocity. (See [fig. 78\(b\)](#).) The angle between this relative velocity and the plane of the propeller rotation is called the helix angle or angle of advance. For a particular airplane velocity this helix angle varies from the root to the tip since the tip sections of the propeller are revolving faster than the root sections. As one approaches the root, the

relative velocity vector comes inclined closer to the oncoming free-stream velocity of the aircraft, that is, the helix angle approaches 90° .

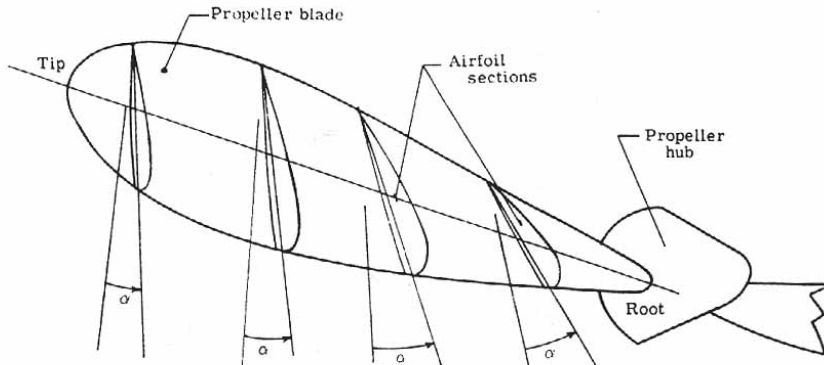


Figure 77.- Propeller blade sections. α , denotes angle of attack of airfoil sections.

Figure 77.- Propeller blade sections

To obtain an aerodynamic force, the airfoil blade section is placed at an angle of attack to the relative velocity vector. Thus, the total angle from the plane of the propeller rotation to the chord line of the blade section is the sum of the helix angle and angle of attack for that section as shown in [figure 78\(c\)](#). This is known as the blade angle. A propeller blade appears to be twisted with the tip sections with small blade angles and the root sections with large blade angles due in main to the increase in helix angle.

The blade angle is also called the pitch angle. This pitch angle may be fixed for a propeller blade, hence a fixed-pitch propeller, or may be adjustable by hand on the ground (adjustable pitch propeller) or controlled automatically in the air (controllable pitch propeller). The efficiency of a propeller is power output divided by power input and would desirably be as close to a value of one (or 100 percent) as possible. The efficiency is proportional to the free-stream velocity and for maximum efficiency requires a different pitch-angle setting. For take-off, an airplane uses a fine or low pitch (flat blade angle or small angle of attack) to provide high revolutions per minute. A coarse or high pitch is used for cruising and gives low revolutions per minute. This effect is illustrated in [figure 79\(a\)](#).

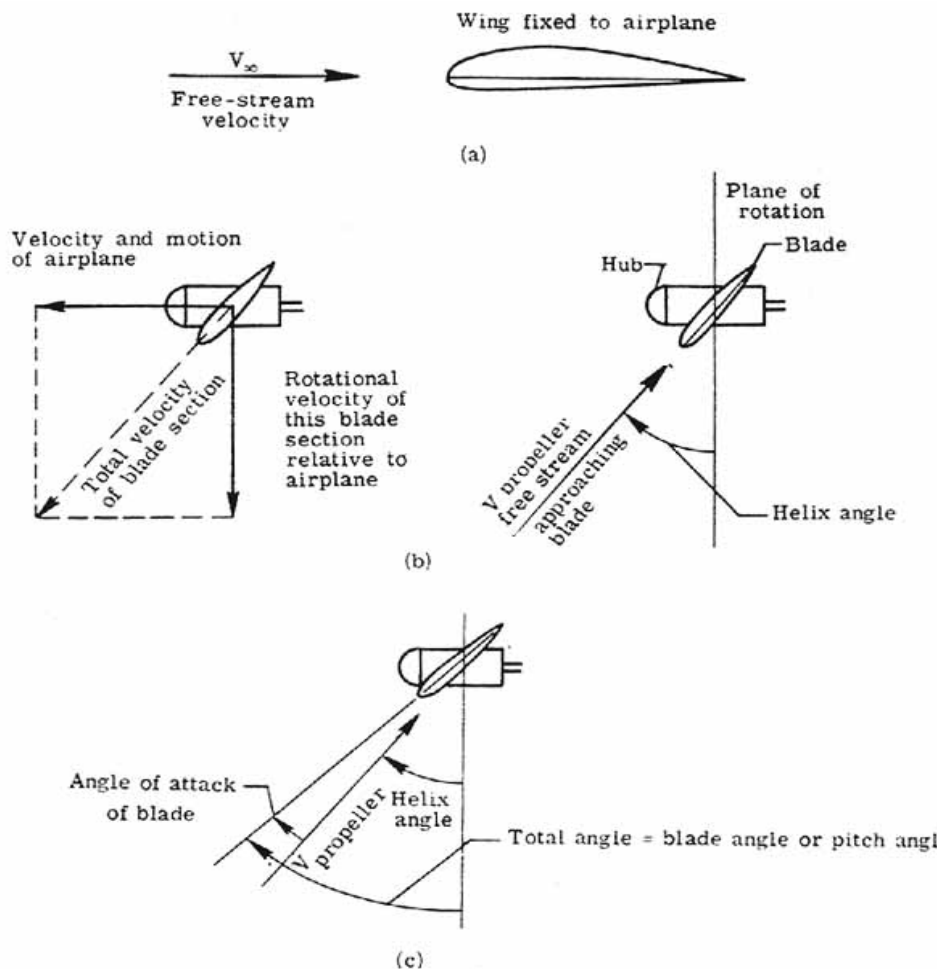


Figure 78.- Propeller terminology.

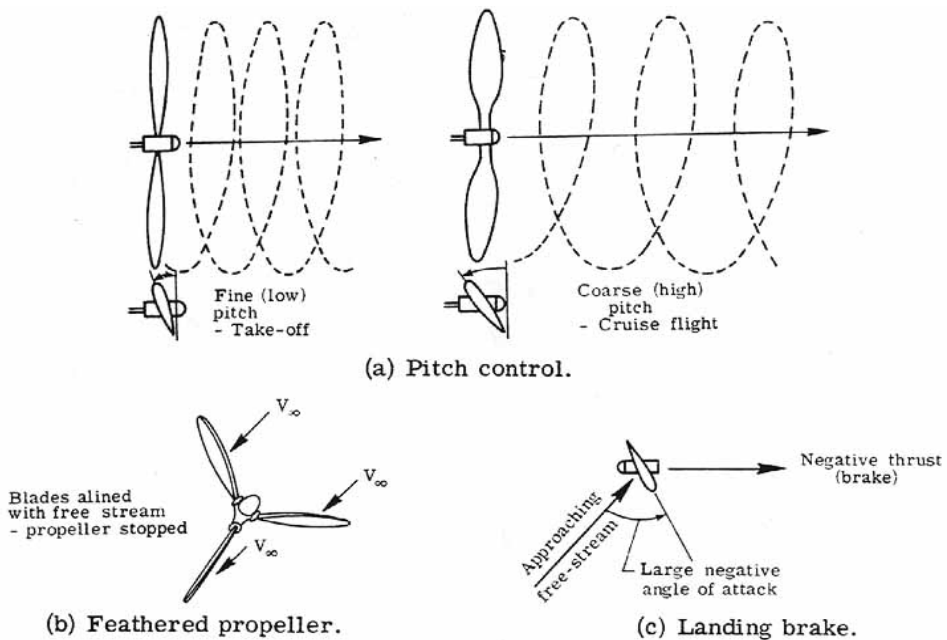


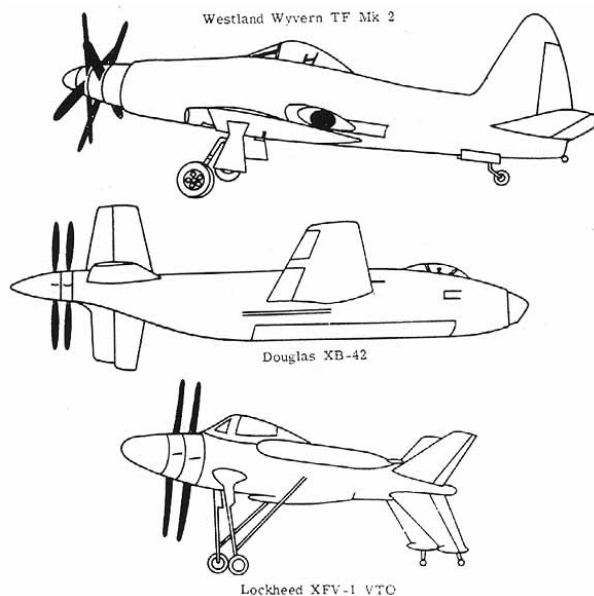
Figure 79.- Use of pitch control.

Some propellers may be feathered in flight. This means that the blades are turned so that the leading edges of the airfoil sections are aligned to the free-stream velocity. Feathering is used on a stopped propeller to avoid damaging an engine and to decrease the propeller drag. (See [fig. 79\(b\)](#).) Some propellers have reversible pitch for use as a landing brake. (See [fig. 79\(c\)](#).) In this case, negative thrust is obtained by turning the blade to a large negative angle of attack.

The design of a propeller, like an airplane, is influenced by many factors, some of which cause contradictions in design. The overall shape is determined by compromise and is largely dependent on the mission to be performed. For low speeds the propeller blade is usually slender with rounded tips. For high speeds larger paddleshaped blades are used or more propeller blades are used.

The slipstream is produced by a propeller producing thrust by forcing air backwards. It is a cylindrical core of spiraling air that flows back over the fuselage and sailplane. The fact that it strikes the sailplane has important effects - some detrimental and some beneficial. The slipstream flow is faster than the free-stream flow; this means that the drag of the fuselage, sailplane, and other parts exposed to it is larger. The slipstream moves over the sailplane and is beneficial in providing for effective control by the tail surfaces since the aerodynamic forces produced by these surfaces are dependent on the square of the velocity of the air moving over them. This is important in the cases of taxiing or false-off when the free-stream velocities may be low.

The rotary motion of the slipstream, however, causes the air to strike the tailplane at an angle and not head on. This may have an effect on the stability and control of the airplane (considered in a later discussion). The effects of the rotary motion of the propeller may be counteracted by using contrarotating propellers (spinning in "opposite directions"). [Figure 80](#) shows three aircraft that used this form of a thrust-producing device.



(a) Westland Wyvern TF Mk 2, (b) Douglas XB-42.
(c) Lockheed XFV-1 VTO.

Figure 80.- Contrarotating propellers.

Lifting rotors - For a helicopter the rotor is the lift-producing device. The blades of the rotor are airfoil shaped and are long and slender (large aspect ratio). The number of blades varies with the design. [Figure 81](#) shows three helicopters, each employing a different number of blades. Generally, for the heavier helicopter, more blades are used to reduce the load that each must carry.



(a) Bell AH-1G Huey Cobra. Two-bladed.
 (b) Hughes OH-6A. Four-bladed.



(c) Sikorsky CH-3C. Six-bladed.

Figure 81.- Helicopters with varying blade numbers.

As for the airplane propeller, the helicopter rotor blades have a pitch angle defined as the angle between the plane of rotation of the blades and the chord line of the blades. The pitch of the blades may be controlled collectively (collective pitch) or controlled individually (cyclic pitch).

Collective pitch changes the pitch of all blades together and with changes in engine power settings, produces the lift necessary for the helicopter to take-off, hover, climb, and descend.

Cyclic pitch is controlled by the swashplate of the rotor head which allows the pitch of individual blades to vary as they rotate about the hub. When a pilot wishes to fly forward, the swashplate is tilted forward. As each rotor blade approaches the forward position (toward the direction of flight) of its cycle, its pitch decreases, the blade lift is reduced, and its flight path descends. As the blade rotates to the rear, the pitch is increased, the blade lift is increased, and the flight path ascends. The net effect is to tilt the whole rotor disk forward to the desired angle, the total lift vector is rotated (see [fig. 82](#)) and a forward thrust component is given to the helicopter.

The rotation of the main rotor blades produces a reactive torque which tends to rotate the helicopter body in the opposite direction. Directional control is accomplished by a tail rotor. It

provides sufficient thrust to counteract this rotational tendency. Additionally, by controlling the thrust of the tail rotor, the heading of the helicopter may be controlled.

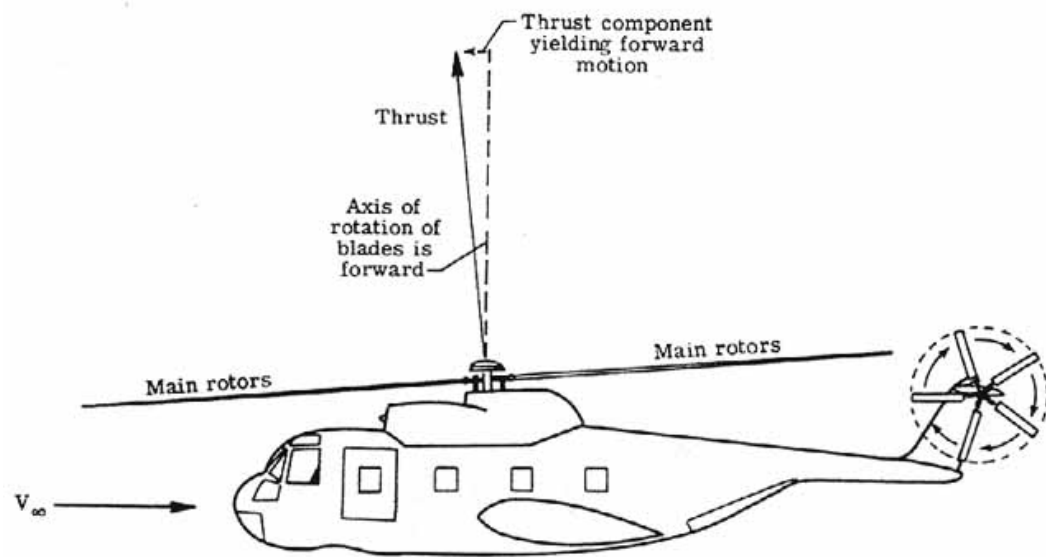


Figure 82.- Helicopter forward motion.

V. TRANSONIC FLOW

Up to this point the airplane was considered to be in motion at subsonic speeds. The air was treated as though it was incompressible and a study of the aerodynamics involved using this simplifying assumption was made. As the airplane speed increases, however, the air loses its assumed incompressibility and the error in estimating, for example drag, becomes greater and greater.

The question arises as to how test an airplane must be moving before one must take into account compressibility. One important quantity which is an indicator is the speed of sound of the air through which the airplane is flying.

A disturbance in the air will send pressure pulses or waves out into the air at the speed of sound. Consider the instance of a cannon fired at sea level. An observer situated some distance from the cannon will see the flash almost instantaneously but the sound wave is heard (or the pressure wave is felt) some time later. The observer can easily compute the speed of sound by dividing the distance between him and the cannon by the time it takes the sound to reach him. The disturbance propagates out away from the cannon in an expanding hemispherical shell as shown in [figure 83](#).

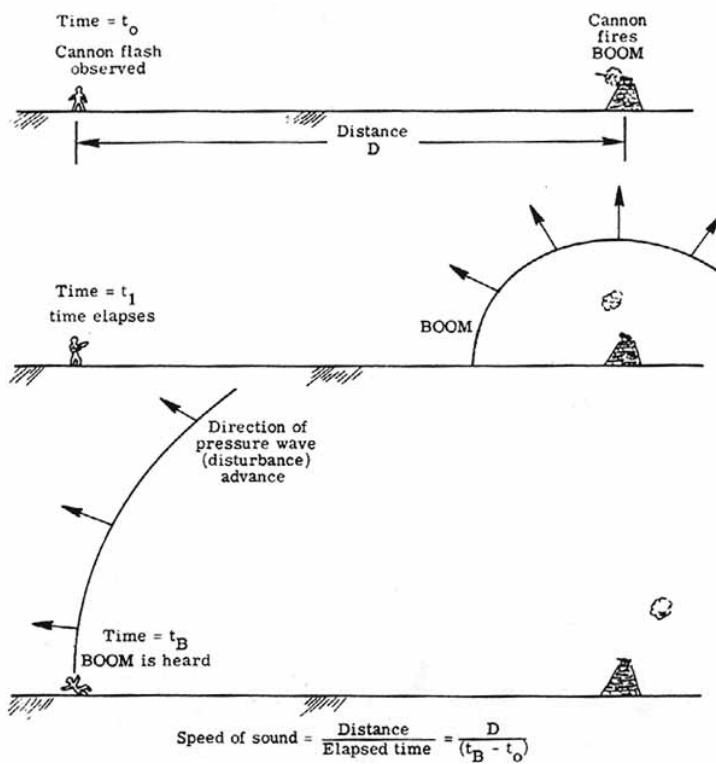
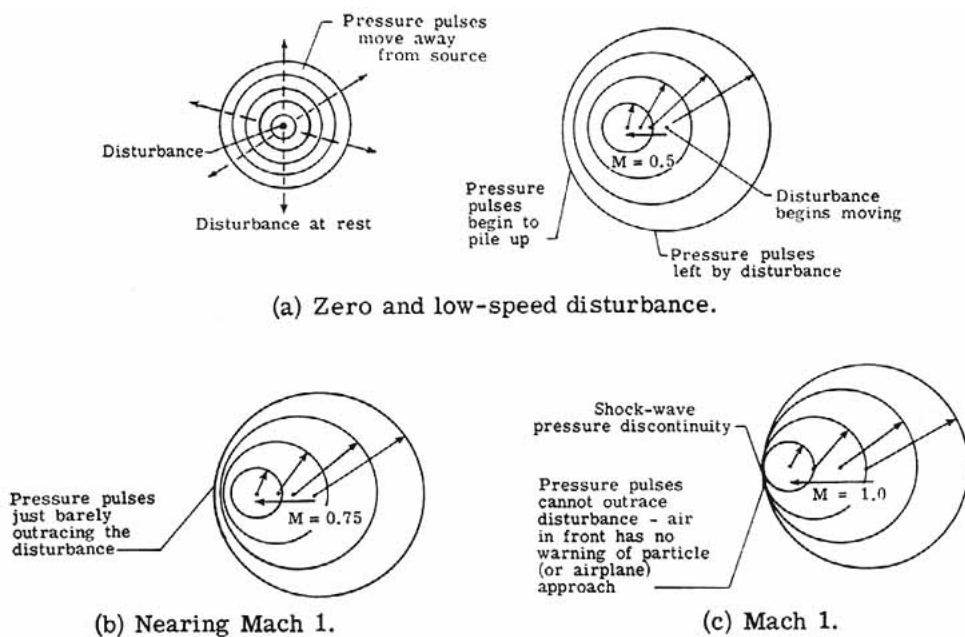


Figure 83.- Speed of sound of a disturbance.

As was shown in [figure 7](#), the speed of sound varies with altitude. To be more precise, it depends upon the square root of the absolute temperature. At sea level under standard conditions ($T_0 = 288.15$ K) the speed of sound is 340.3 m/sec but at an altitude of 15 kilometers where the temperature is down to 216.7 K the speed of sound is only 295.1 m/sec. This difference indicates that an airplane flying at this altitude encounters the speed of sound at a slower speed, and, therefore, comes up against compressibility effects sooner.

An airplane flying well below the speed of sound creates a disturbance in the air and sends out pressure pulses in all directions as shown in [figure 84\(a\)](#). Air ahead of the airplane receives these "messages" before the airplane arrives and the flow separates around the airplane. But as the airplane approaches the speed of sound, the pressure pulses merge closer and closer together ([fig. 84\(b\)](#)) in front of the airplane and little time elapses between the time the air gets a warning of the airplane approach and the airplane's actual arrival time At the speed of sound ([fig. 84\(c\)](#)) the pressure pulses move at the same speed as the airplane. They merge together ahead of the airplane into a "shock wave" which is an almost instantaneous line of change in pressure, temperature, and density. The air has no warning of the impending approach of the airplane and abruptly passes through the shock system. There is a tendency for the air to break away from the airplane and not flow smoothly about it; as a result, there is a change in the aerodynamic forces from those experienced at low incompressible flow speeds.



[Figure 84.- Shock-wave formation.](#)

The Mach number is a measure of the ratio of the airplane speed to the speed of sound. In other words, it is a number that may relate the degree of warning that air may have to an airplane approach. The Mach number is named after Ernst Mach, an Austrian professor (1838 to 1916). [Figure 85](#) shows the names given to various flight regimes. For Mach numbers less than one, one has subsonic flow, for Mach numbers greater than one, supersonic flow, and for Mach numbers greater than 5 the name used is hypersonic flow. Additionally, transonic flow pertains to the range of speeds in which flow patterns change from subsonic to supersonic or vice versa, about Mach 0.8 to 1.2. Transonic flow presents a special problem area as neither equations describing subsonic flow nor those describing supersonic flow may be accurately applied to the regime.

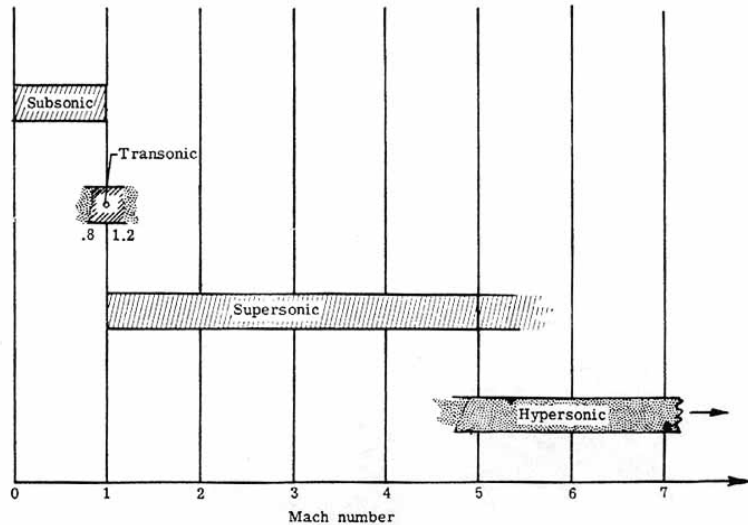


Figure 85.- Flight regime terminology.

With these definitions in mind, one may now examine in a little more detail the flow at high speeds. Up to now, the airplane was considered to be in motion at subsonic speeds. Drag was composed of three main components- skin-friction drag, pressure drag, and induced drag (or drag due to lift). At transonic and supersonic speeds there is a substantial increase in the total drag of the airplane due to fundamental changes in the pressure distribution.

This drag increase encountered at these high speeds is called wave drag. The drag of the airplane wing, or for that matter, any part of the airplane, rises sharply and large increases in thrust are necessary to obtain further increases in speed. This wave drag is due to the unstable formation of shock waves which transforms a considerable part of the available propulsive energy into heat, and to the induced separation of the flow from the airplane surfaces. Throughout the transonic range, the drag coefficient of the airplane is greater than in the supersonic range because of the erratic shock formation and general flow instabilities. Once a supersonic flow has been established, however, the flow stabilizes and the drag coefficient is reduced. [Figure 86](#) shows the variation of an airplane wing drag coefficient with Mach number. The total drag at transonic and supersonic speeds can be divided into two categories: (1) zerolift drag composed of skin-friction drag and wave (or pressure-related) drag of zero lift and (2) lift-dependent drag composed of induced drag (drag due to lift) and wave (or pressure-related) drag due to lift. The infamous "sound barrier" shows up rather clearly in [figure 86](#) since to fly supersonically the airplane must provide enough thrust to exceed the maximum transonic drag that is encountered. In the early days of transonic flight, the sound barrier represented a real barrier to higher speeds. Once past the transonic regime, the drag coefficient and the drag decreases, and less thrust is required to fly supersonically. However, as it proceeds toward higher supersonic speeds, the drag increases (even though the drag coefficient may show a decrease).

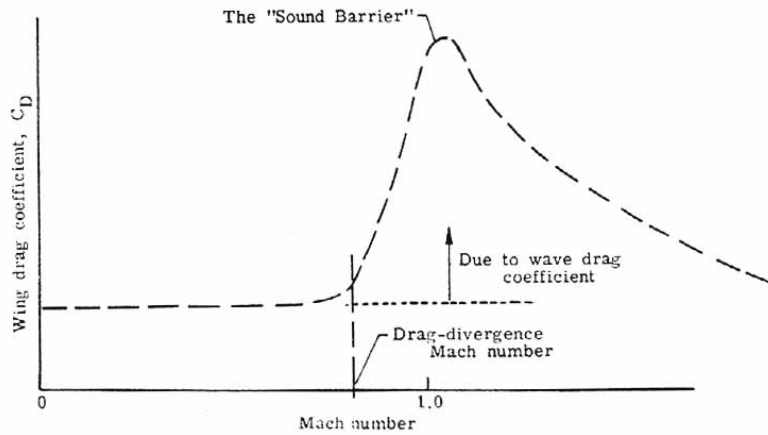


Figure 86.- Variation of wing drag coefficient with Mach number.

There is a famous little story, untrue of course, of the pilot who flew his plane beyond the sound barrier and then got trapped there because of insufficient reverse thrust to get back below the speed of sound. Another case of perpetual motion.

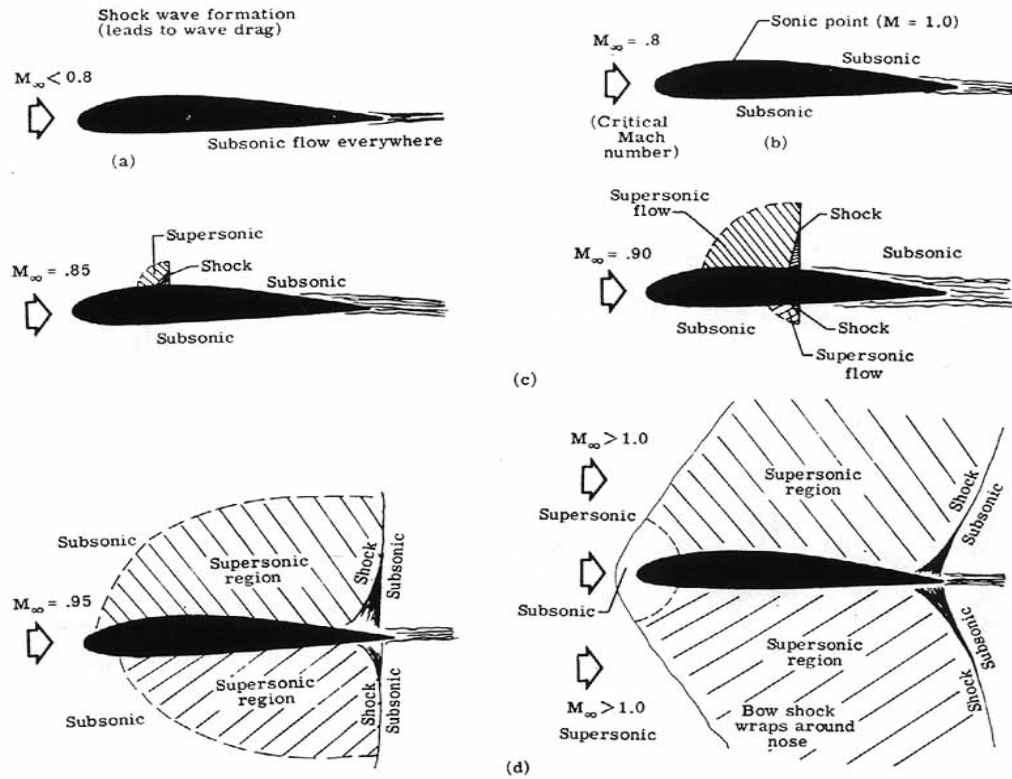


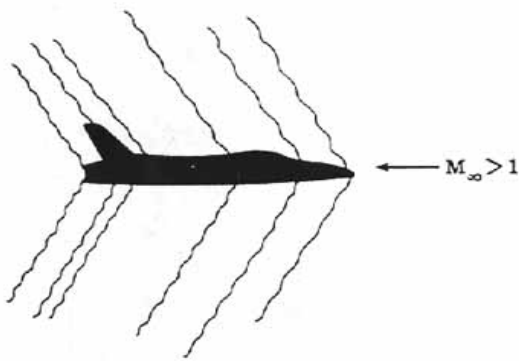
Figure 87.- Shock formation.

It is a large loss in propulsive energy due to the formation of shocks that causes wave drag; [figure 87](#) shows this shock formation about an airfoil. Up to a free-stream Mach number of about 0.7 to 0.8, compressibility effects have only minor effects on the flow pattern and drag. The flow is subsonic everywhere ([fig. 87\(a\)](#)). As the flow must speed up as it proceeds about the airfoil, the local Mach number at the airfoil surface will be higher than the free-stream Mach number. There eventually occurs a freestream Mach number called the critical Mach number at which a sonic point appears

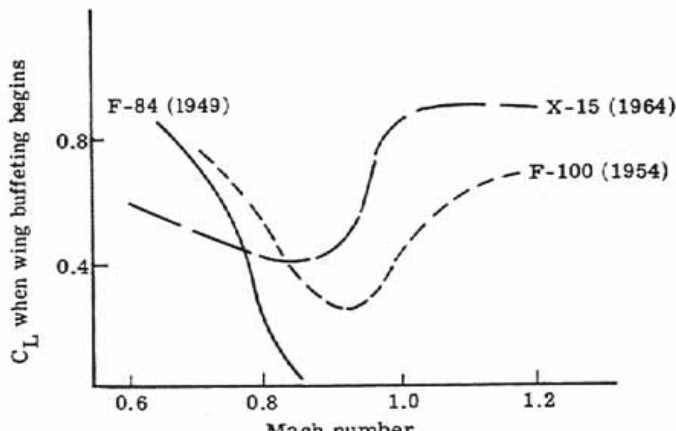
somewhere on the airfoil surface, usually near the point of maximum thickness and indicates that the flow at that point has reached Mach 1 ([fig. 87\(b\)](#)). As the freestream Mach number is increased beyond the critical Mach number and closer to Mach 1, larger and larger regions of supersonic flow appear on the airfoil surface ([fig. 87\(c\)](#)). In order for this supersonic flow to return to subsonic flow, it must pass through a shock (pressure discontinuity). This loss of velocity is accompanied by an increase in temperature, that is, a production of heat. This heat represents an expenditure of propulsive energy which may be presented as wave drag. These shocks appear anywhere on the airplane (wing, fuselage, engine nacelles, etc.) where, due to curvature and thickness, the localized Mach number exceeds 1.0 and the airflow must decelerate below the speed of sound ([fig. 88\(a\)](#)). For transonic flow the wave drag increase is greater than would be estimated from a loss of energy through the shock. In fact, the shock wave interacts with the boundary layer so that a separation of the boundary layer occurs immediately behind the shock. This condition accounts for a large increase in drag which is known as shock-induced (boundary-layer) separation.

The free-stream Mach number at which the drag coefficient of the airplane increases markedly is called the drag-divergence Mach number. Large increases in thrust are required to produce any further increases in airplane speed. If an airplane has an engine of insufficient thrust, its speed will be limited by the drag-divergence Mach number. The prototype Convair F-102A was originally designed as a supersonic interceptor but early flight tests indicated that because of high drag, it would never achieve this goal. It will be explained later how success was achieved for this airplane through proper redesigning.

[Figure 87\(d\)](#) shows the character of the flow at a free-stream Mach number close to one where large regions are in supersonic flow and the shocks are very strong. At a free-stream Mach number greater than 1, a bow shock appears around the airfoil nose. Most of the airfoil is in supersonic flow. The flow begins to realign itself parallel to the body surface and stabilize, and the shock-induced separation is reduced. This condition results in lower drag coefficients. Supersonic flow is more well behaved than transonic flow and there are adequate theories that can predict the aerodynamic forces and moments present. Often, in transonic flow, the flow is unsteady and the shock waves on the body surface may jump back and forth along the surface, thus disrupting and separating the flow over the wing surface. This sends pulsing unsteady flow back to the tail surfaces of the airplane. The result is that the pilot feels a buffeting and vibration of both wing and tail controls. This condition occurred especially in the first airplane types to probe the sound barrier. With proper design, however, airplane configurations gradually evolved to the point where flying through the transonic region posed little or no difficulty in terms of wing buffeting or loss of lift ([fig. 88\(b\)](#)).



(a) Total aircraft shocks.



(b) Improving transonic flight.

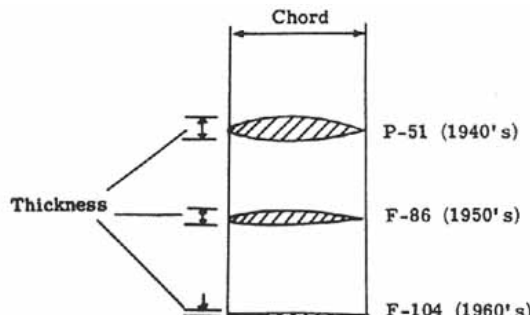
Figure 88.- Supersonic characteristics.

The question as to whether one may delay the drag-divergence Mach number to a value closer to 1 is a fascinating subject of novel aerodynamic designs. What this really suggests is the ability to fly at near-sonic velocities with the same available engine thrust before encountering large wave drag. There are a number of ways of delaying the transonic wave drag rise (or equivalently, increasing the drag-divergence Mach number closer to 1). These include

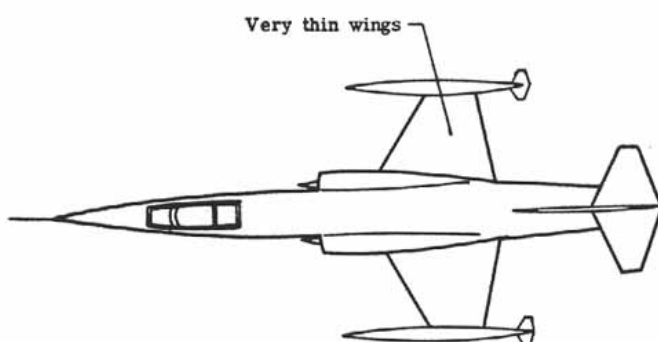
- (1) Use of thin airfoils
- (2) Use of sweep of the wing forward or back
- (3) Low-aspect-ratio wing
- (4) Removal of boundary layer and vortex generators
- (5) Supercritical and area-rule technology

These methods are now discussed individually.

Thin airfoils: The wave drag rise associated with transonic flow is roughly proportional to the square of the thickness-chord ratio (t/c). If a thinner airfoil section is used, the flow speeds around the airfoil will be less than those for the thicker airfoil. Thus, one may fly at a higher free-stream Mach number before a sonic point appears and before one reaches the drag-divergence Mach number. The disadvantages of using thin wings are that they are less effective (in terms of lift produced) in the subsonic speed range and they can accommodate less structure (wing fuel tanks, structural support members, armament stations, etc.) than a thicker wing. [Figure 89\(a\)](#) shows the airfoil sections used by three U.S. fighters over the past three decades. As the speeds have increased, the thickness-chord ratios have decreased. The F-104 ([fig. 89\(b\)](#)) was designed to achieve the minimum possible wave drag but was penalized with low subsonic lift. As a result, the landing speed of this airplane was particularly high and landing mishaps were common among untrained pilots.



(a) Changes in airfoil sections.



(b) F-104G airplane.

Figure 89.- Thin airfoils.

[Figure 90](#) illustrates the effect of using a thinner section on the transonic drag. Notice, in particular, that the drag divergence Mach number is delayed to a greater value.

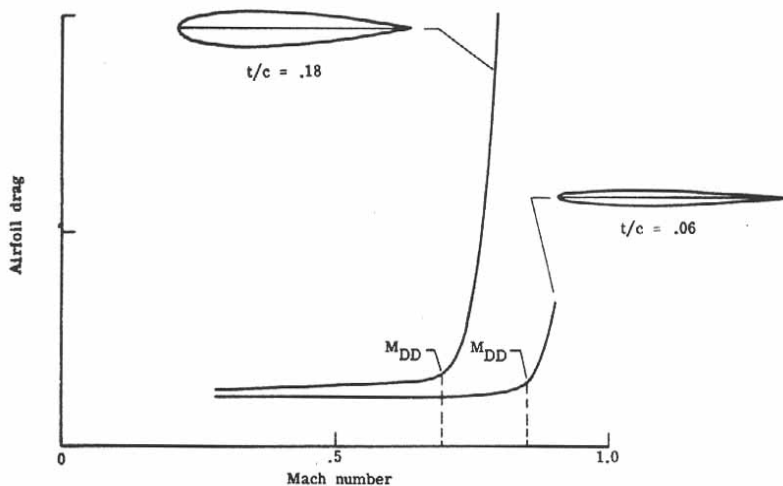


Figure 90.- Effect of airfoil thickness on transonic drag. Lift = 0;
 $q = \text{Constant}$; M_{DD} , drag divergence Mach number.

Sweep: It was Adolf Busemann in 1935 who proposed that sweep may delay and reduce the effects of compressibility. A swept wing will delay the formation of the shock waves encountered in transonic flow to a higher Mach number. Additionally, it reduces the wave drag over all Mach numbers. [Figure 91](#) shows experimental data confirming this result as a wing is swept from no sweep to a high degree of sweep.

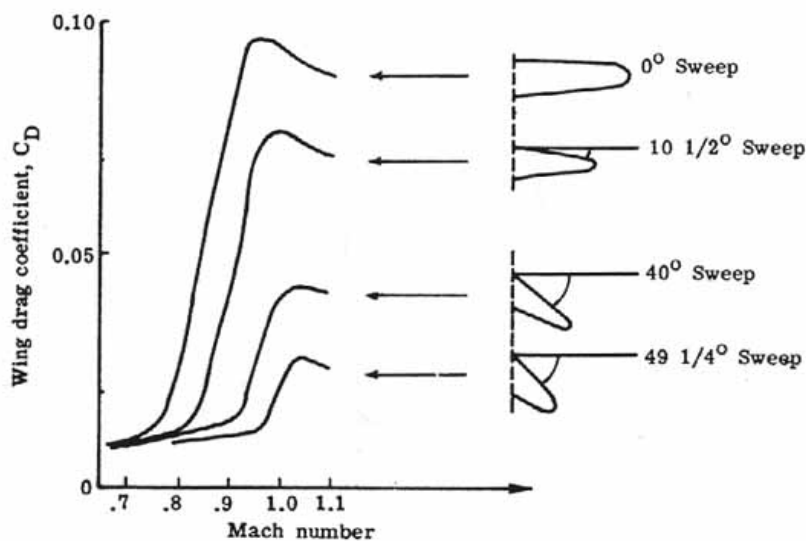


Figure 91.- Effects of sweep on wing transonic drag coefficient.

One may view the effect of sweep of a wing as effectively using a thinner airfoil section (t/c reduced). In [figure 92\(a\)](#) a straight wing is shown with the airflow approaching perpendicularly to the wing. Notice a typical airfoil section. If the wing is now swept to some angle of sweep Λ , the same flow over the wing encounters new airfoil sections that are longer than previously. The maximum ratio of thickness to chord has been reduced. (See [fig. 92\(b\)](#).) One is effectively using a thinner airfoil section as the flow has more time in which to adjust to the situation. The critical Mach number (at which a sonic point appears) and the drag-divergence Mach number are delayed to higher values; Sweepforward or sweepback will accomplish these desired results.

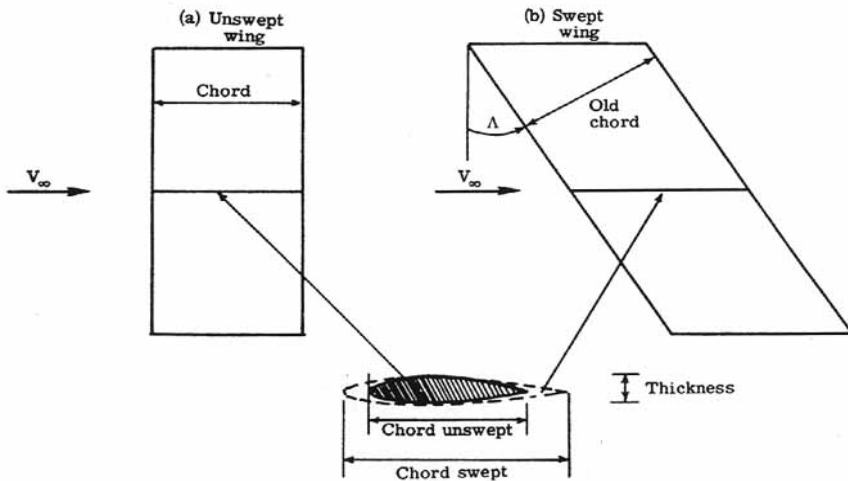


Figure 92.- Sweep reduces effective thickness-chord ratio.

[Figure 93](#) shows a modern jet airplane employing forward sweep. Forward sweep has disadvantages, however, in the stability and handling characteristics at low speeds.

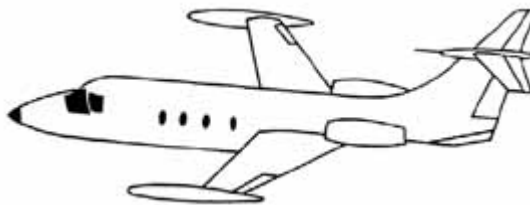


Figure 93.- HFB 320 Hansa-Jet with forward sweep.

A major disadvantage of swept wings is that there is a spanwise flow along the wing, and the boundary layer will thicken toward the tips for sweepback and toward the roots for sweepforward. In the case of sweepback, there is an, early separation and stall of the wing-tip sections and the ailerons lose their roll control effectiveness. The spanwise flow may be reduced by the use of stall fences, which are thin plates parallel to the axis of symmetry of the airplane. In this manner a strong boundary layer buildup over the ailerons is prevented. (See [fig. 94\(a\)](#).) Wing twist is another possible solution to this spanwise flow condition.

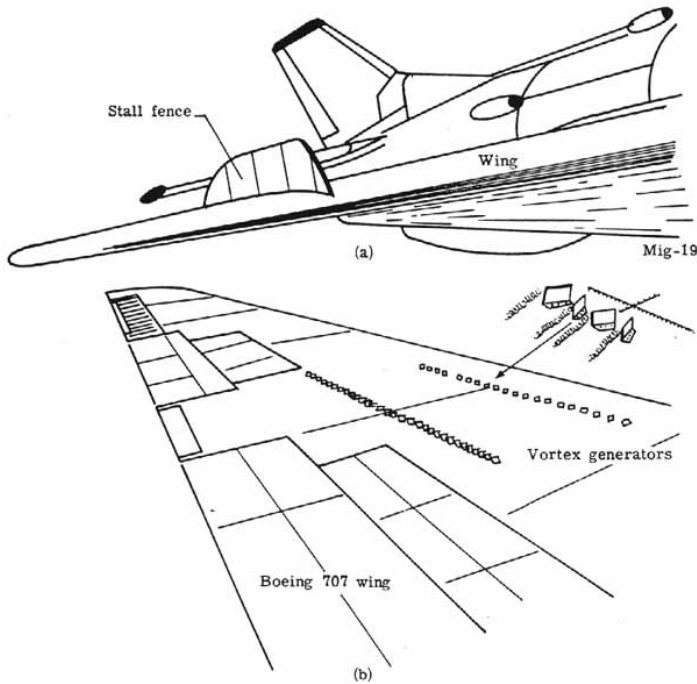


Figure 94.- Stall fences and vortex generators.

Low aspect ratio: The wing's aspect ratio is another parameter that influences the critical Mach number and the transonic drag rise. Substantial increases in the critical Mach number occur when using an aspect ratio less than about four. However from previous discussions, low-aspect-ratio wings are at a disadvantage at subsonic speeds because of the higher induced drag.

Removal or reenergizing the boundary layer: By bleeding off some of the boundary layer along an airfoil's surface, the drag-divergence Mach number can be increased. This increase results from the reduction or elimination of shock interactions between the subsonic boundary layer and the supersonic flow outside of it.

Vortex generators are small plates, mounted along the surface of a wing and protruding perpendicularly to the surface as shown in [figure 94\(b\)](#). They are small wings, and by creating a strong tip vortex, the generators feed high-energy air from outside the boundary layer into the slow moving air inside the boundary layer. This condition reduces the adverse pressure gradients and prevents the boundary layer from stalling. A small increase in the drag-divergence Mach number can be achieved. This method is economically beneficial to airplanes designed for cruise at the highest possible drag-divergence Mach number.

Supercritical and area-rule technology: One of the more recent developments in transonic technology and destined to be an important influence on future wing design is the NASA supercritical wing developed by Dr. Richard T. Whitcomb of the NASA Langley Research Center. A substantial rise in the drag-divergence Mach number is realized. [Figure 95\(a\)](#) shows a classical airfoil operating near the Mach 1 region (supercritical- beyond the critical Mach number) with its associated shocks and separated boundary layer. [Figure 95\(b\)](#) shows the supercritical airfoil operating at the same Mach number. The airfoil has a flattened upper surface which delays the formation and strength of the shocks to a point closer to the trailing edge. Additionally, the shock- induced separation is greatly

decreased. The critical Mach number is delayed even up to 0.99. This delay represents a major increase in commercial airplane performance.

The curvature of a wing gives the wing its lift. Because of the flattened upper surface of the supercritical airfoil, lift is reduced. However, to counteract this the new supercritical wing has increased camber at the trailing edge.

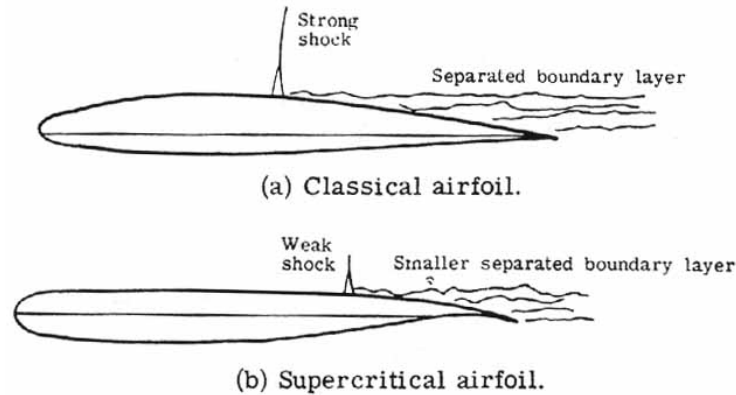


Figure 95.- Classical and supercritical airfoils.

There are two main advantages of the supercritical airfoil as shown in [figure 96](#). First, by using the same thickness-chord ratio, the supercritical airfoil permits high subsonic cruise near Mach 1 before the transonic drag rise. Alternatively, at lower drag divergence Mach numbers, the supercritical airfoil permits a thicker wing section to be used without a drag penalty. This airfoil reduces structural weight and permits higher lift at lower speeds.

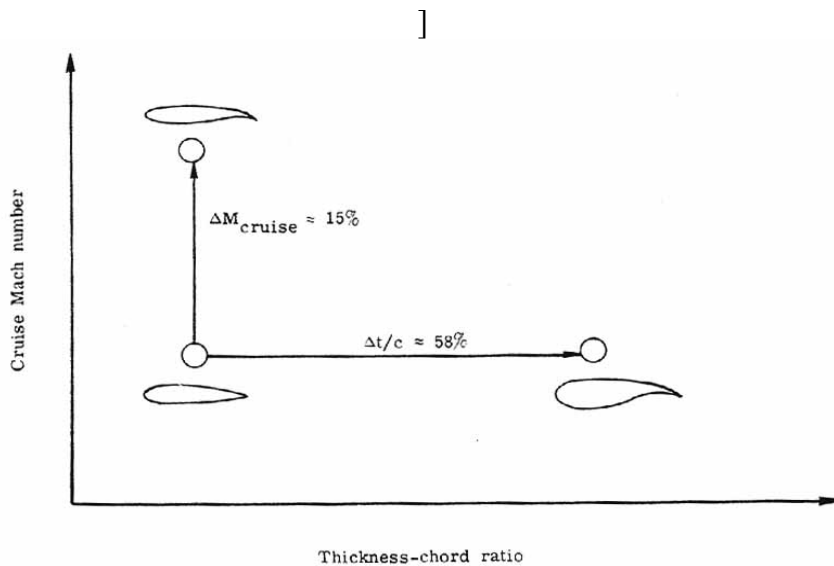


Figure 96.- Two uses of supercritical wing.

Coupled to supercritical technology is the "area-rule" concept also developed by Dr. Richard T. Whitcomb of NASA Langley Research Center in the early 1950's for transonic airplanes and later applied to supersonic flight in general.

Basically, area ruling states that minimum transonic and supersonic drag is obtained when the cross-sectional area distribution of the airplane along the longitudinal axis can be projected into a body of revolution which is smooth and shows no abrupt changes in cross section along its length. Or, if a graph is made of the cross-sectional area against body position, the resulting curve is smooth. If it is not a smooth curve, [116] then the cross section is changed accordingly. [Figure 97](#) presents the classic example of the application of this concept-the Convair F-102A.

The original Convair F-102A was simply a scaled-up version of the XF-92A with a pure delta wing. But early tests indicated that supersonic flight was beyond its capability because of excessive transonic drag and the project was about to be canceled. Area ruling, however, saved the airplane from this fate. [Figure 97\(a\)](#) shows the original form of the F-102A and the cross-sectional area plotted against body station. Notice that the curve is not very smooth as there is a large increase in cross-sectional area when the wings are encountered. [Figure 97\(b\)](#) shows the F-102A with a coke-bottle-waist-shaped fuselage and bulges added aft of the wing on each side of the tail to give a better area-rule distribution, as shown in the plot. The F-102A was then able to reach supersonic speeds because of the greatly reduced drag and entered military service in great numbers.

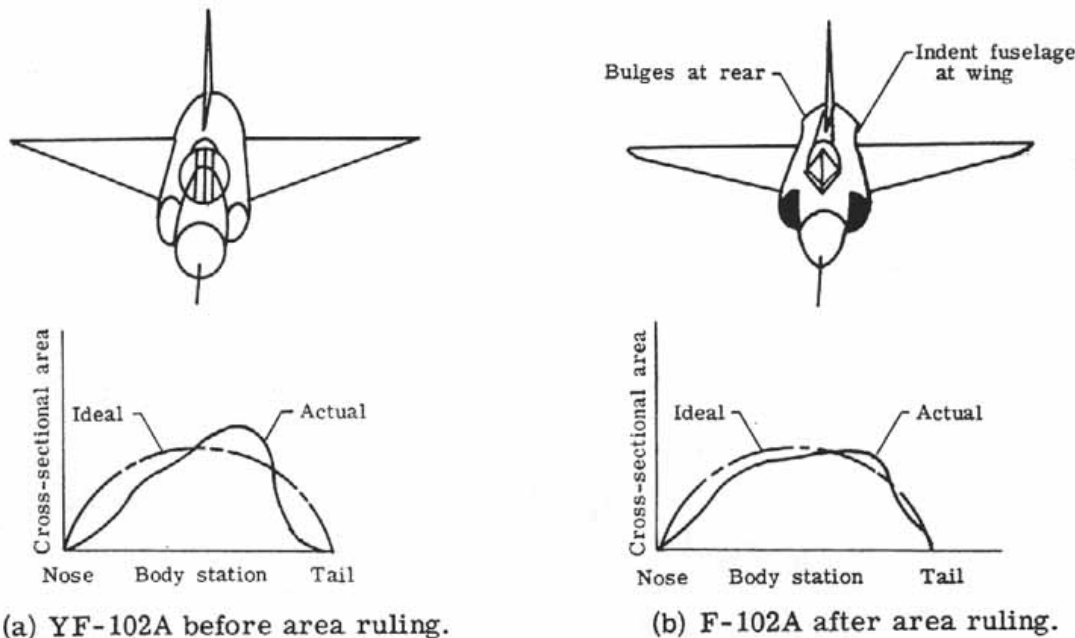


Figure 97.- Area ruling of F-102A airplane.

Recently, the area-rule concept has been applied to design a near-sonic transport capable of cruising at Mach numbers around 0.99. In addition to area ruling, a supercritical wing is used. [Figure 98](#) shows the configuration obtained and the resulting cross-sectional area plot. Notice this curve now is completely smooth and indicates that the shape is near optimum. The shocks and drag divergence are delayed to a near-sonic Mach number.

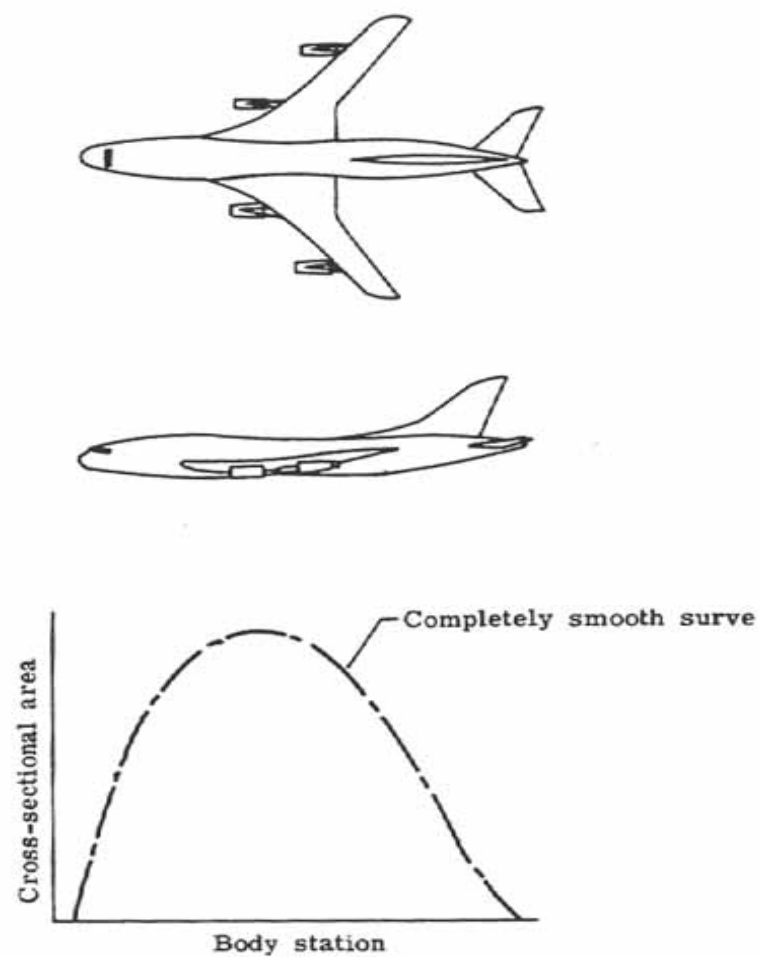


Figure 98.- Near-sonic transport area ruling.

VI. SUPERSONIC FLOW

The previous discussion has centered mainly on the transonic drag rise and how, through proper design, it may be delayed. Many of the techniques used also are directly applicable in designing the airplane to fly with minimum wave drag in the supersonic regime.

If one returns to the discussion of shock formation, it was shown that a bow shock wave will exist for free-stream Mach numbers above 1.0. (See [fig. 88](#).) In three dimensions, the bow shock is in reality a cone in shape (a Mach cone) as it extends back from the nose of the airplane. [Figure 99](#) demonstrates that the Mach cone becomes increasingly swept back with increasing Mach numbers. As long as the wing is swept back behind the Mach cone, there is subsonic flow over most of the wing and relatively low drag.

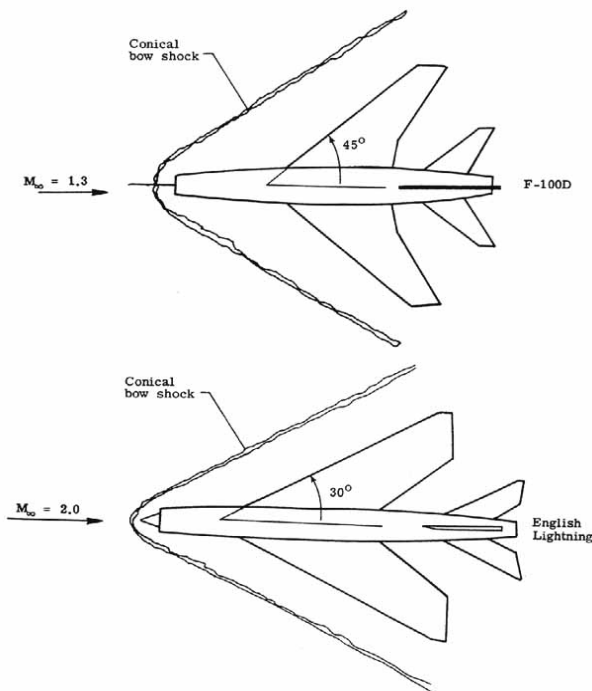


Figure 99.- Mach cone and use of sweep.

A delta wing ([fig. 100](#)) has the advantage of a large sweep angle but also greater wing area than a simple swept wing to compensate for the loss of lift usually experienced in sweepback. But, at still higher supersonic Mach numbers, the Mach cone may approach the leading edge of even a highly swept delta wing. This condition causes the total drag to increase rapidly and, in fact, a straight wing (no sweep) becomes preferable.

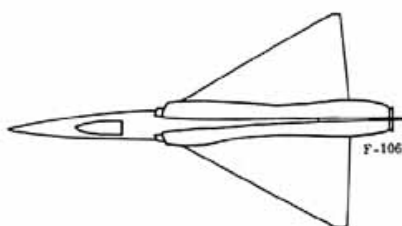


Figure 100.- Delta-wing airplane (F-106).

[Figure 101](#) shows qualitatively the drag advantage that a straight wing has over a swept or delta wing at higher Mach numbers.

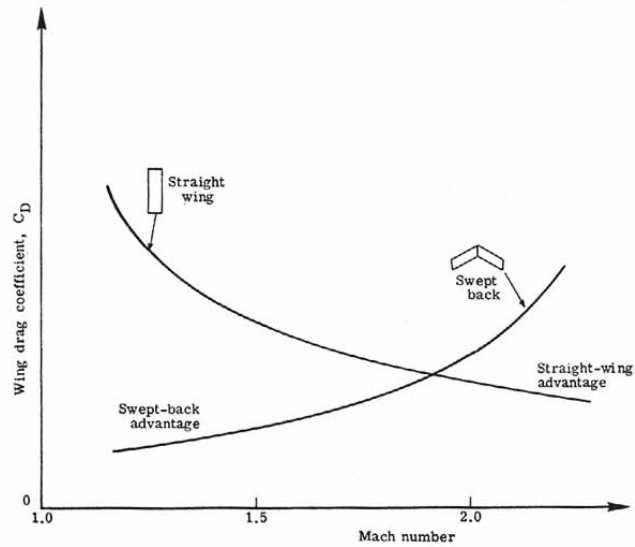


Figure 101. - Wing design drag coefficients as functions of Mach number.

Sweepback has been used primarily in the interest of minimizing transonic and supersonic wave drag. At subsonic Mach numbers, however, the disadvantages are dominant. They include high induced drag (due to small wing span or low aspect ratio), high angles of attack for maximum lift, and reduced effectiveness of trailing-edge flaps. The straight-wing airplane does not have these disadvantages. For an airplane which is designed to be multi-mission, for example, subsonic cruise and supersonic cruise, it would be advantageous to combine a straight wing and swept wing design. This is the logic for the variable sweep or swing-wing. [Figure 102](#) shows $(L/D)_{\max}$, a measure of aerodynamic efficiency, plotted against Mach number for an optimum straight-wing and swept-wing airplane.

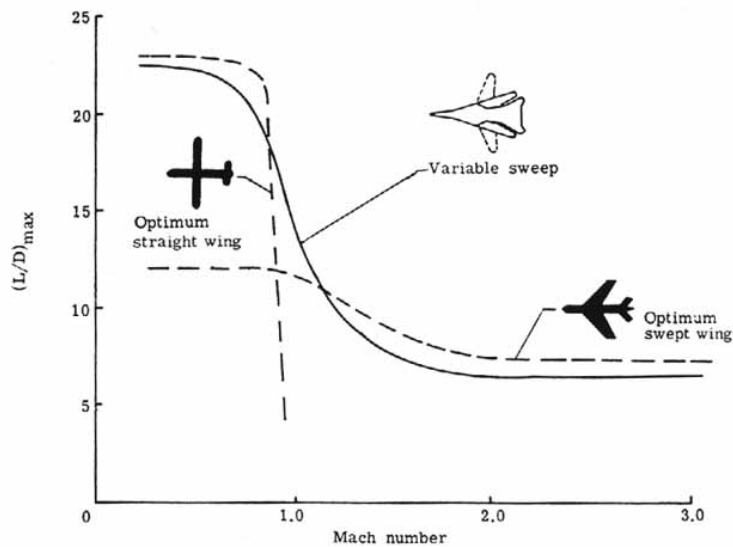


Figure 102. Variation of $(L/D)_{\max}$ with Mach number. Variable sweep airplane.

Although not necessarily equal to the optimum configurations in their respective speed regimes, it is evident that an airplane with a swing-wing capability can in a multi-mission role, over the total speed regime, be better than the other airplanes individually. One major drawback of the swing-wing airplane is the added weight and complexity of the sweep mechanisms. But technological advances are solving these problems also. [Figure 103](#) shows a variety of modern airplanes employing a swing-wing.

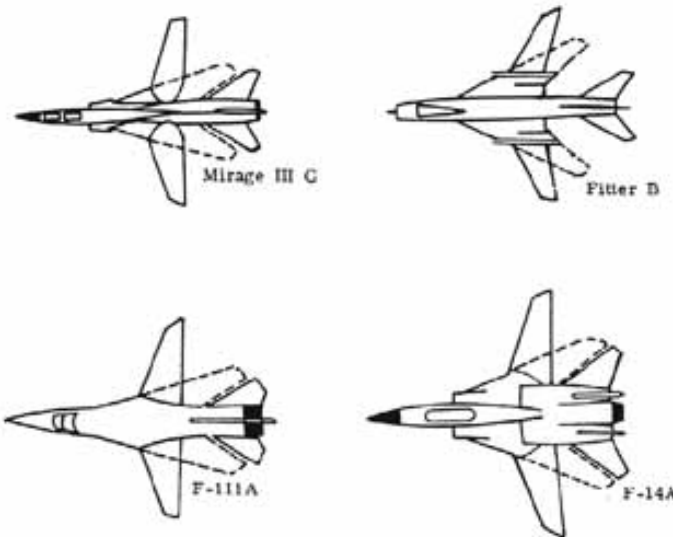


Figure 103.- Modern variable-sweep airplanes.

In addition to low-aspect-ratio wings at supersonic speeds, supersonic wave drag may also be minimized by employing thin wings and using area ruling. Also long, slender, cambered fuselages minimize drag and also improve the spanwise lift distribution.

The SST

On June 5, 1963 in a speech before the graduating class of the United States Air Force Academy, President Kennedy committed this nation to "develop at the earliest practical date the prototype of a commercially successful supersonic transport superior to that being built in any other country in the world" What lay ahead was years of development, competition, controversy, and ultimately rejection of the supersonic transport (SST) by the United States, and it remains to be seen whether the British-French Concorde or Russian TU-144 designs will prove to be economically feasible and acceptable to the public.

NASA did considerable work, starting in 1959, on basic configurations for the SST. There evolved four basic types of layout which were studied further by private industry. Lockheed chose to go with a fixed-wing delta design; whereas, Boeing initially chose a swing-wing design.

One problem associated with the SST is the tendency of the nose to pitch down as it flies from subsonic to supersonic flight. The swing-wing can maintain the airplane balance and counteract the pitch-down motion. Lockheed needed to install canards (small wings placed toward the airplane nose ([fig. 104\(a\)](#)) to counteract pitch down. Eventually, the Lockheed design used a double-delta configuration ([fig. 104\(b\)](#)) and the canards were no longer needed. This design proved to have many

exciting aerodynamic advantages. The forward delta begins to generate lift supersonically (negating pitch down). At low speeds, the vortices trailing from the leading edge of the double delta ([fig. 105\(a\)](#)) increase lift as shown in [figure 105\(b\)](#). This means that many flaps and slats could be reduced or done away with entirely and a simpler wing design was provided. In landing, the double delta experiences a ground-cushion effect which allows for lower landing speeds. This is important since three-quarters of the airplane accidents occur in take-off and landing.

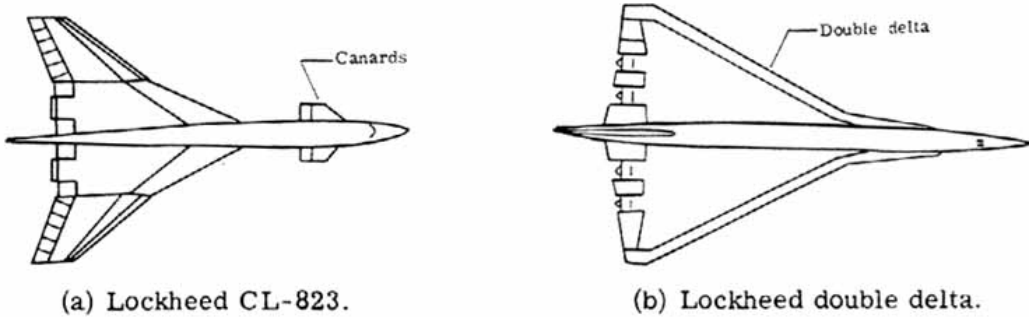
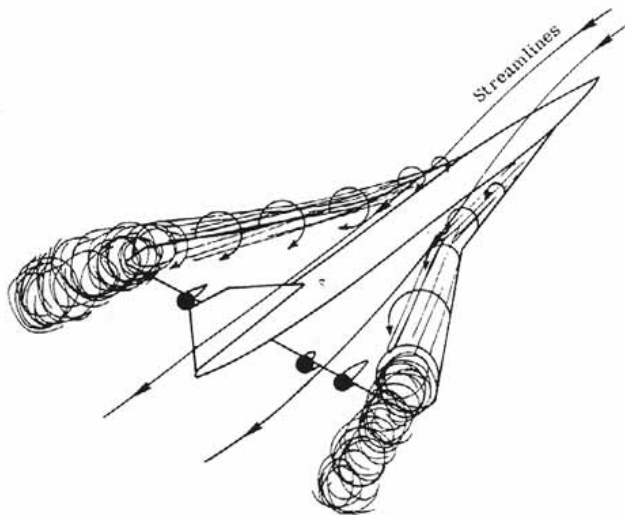
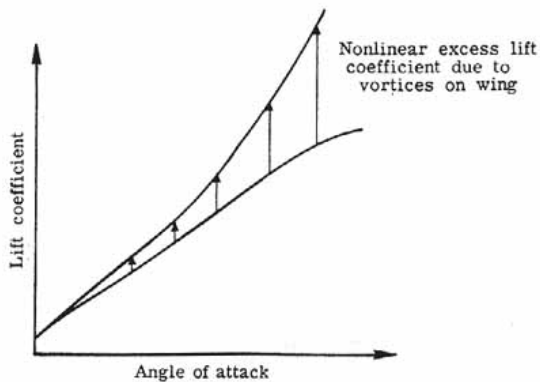


Figure 104.- Lockheed SST configurations.



(a) Vortices on double delta wing.



(b) Lift coefficient increase due to vortices.

Figure 105.- Lifting vortices of double delta wing.

[Figure 106](#) shows the British-French Concorde and the Russian TU-144 prototypes. They use a variation of the double delta wing called the ogee wing. It, too, uses the vortex-lift concept for improvement in low-speed subsonic flight.

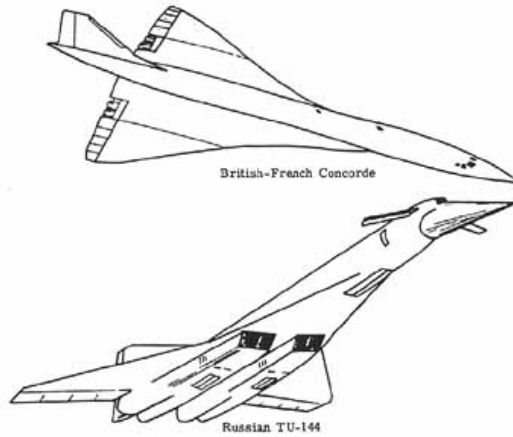


Figure 106. British-French, and Russian SST airplanes.

Ultimately, Boeing with a swing-wing design was selected as the winner of the U.S. SST competition. [Figure 107](#) shows the evolution of this design originally derived from one of the NASA designs. The size of the airplane grew to meet airline payload requirements. Major design changes were incorporated into the Boeing 2707-100 design. The supersonic cruise lift-drag ratio increased from 6.75 to 8.2 and the engines were moved further aft to alleviate the exhaust impinging on the rear tail surfaces. Despite the advantages previously quoted for a swing-wing concept, technological advances in construction did not appear in time. Because of the swing-wing mechanisms and beefed-up structure due to engine placement, incurable problems in reduction of payload resulted. Boeing had no recourse but to adopt a fixed-wing concept. [Figure 107](#) shows the final configuration adopted—the B2707-300. Political, economic, and environmental factors led the United States to cancel the project in 1972.

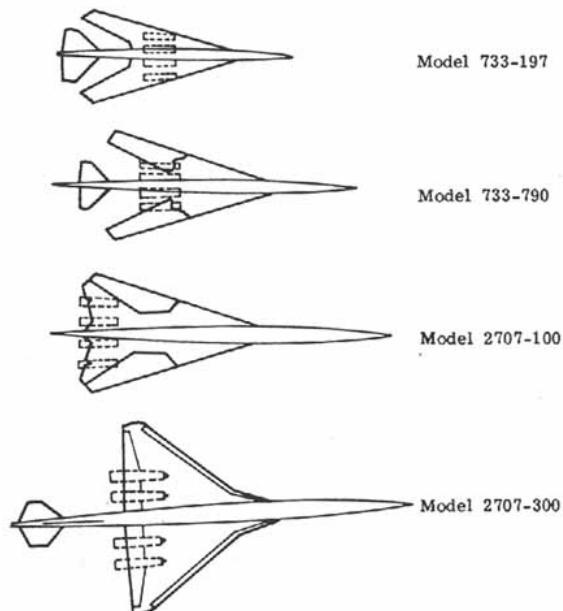


Figure 107.- Evolution of Boeing SST design.

While the British-French Concorde and Russian TU-144 fly, research is still continuing into advanced supersonic transports in the United States. Whereas, the Concorde and TU-144 cruise at $M = 2.2$ to 2.4 , and the Boeing design cruised at $M = 2.7$, configurations with a cruise speed of $M = 3.2$ are being analyzed. One such design tested at the NASA Langley Research Center is shown in [figure 108](#).

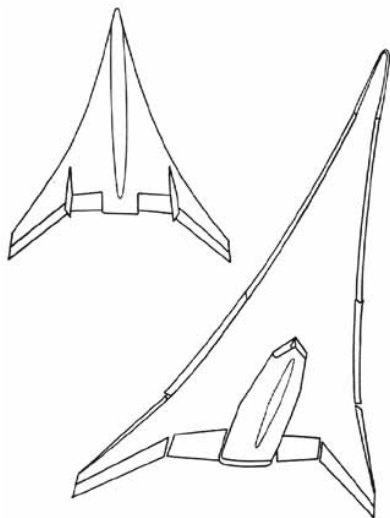


Figure 108.- Langley advanced SST design.

Sonic Boom

One of the more objectionable of the problems facing any supersonic transport is commonly referred to as the "sonic boom." To explain sonic boom, one must return to a description of the shock-wave formation about an airplane flying supersonically. A typical airplane generates two main shock waves, one at the nose (bow shock) and one off the tail (tail shock). Shock waves coming off the canopy, wing leading edges, engine nacelles, etc. tend to merge with the main shocks some distance from the airplane. (See [fig. 109.](#)) The resulting pressure pulse changes appear to be "N" shaped as shown.

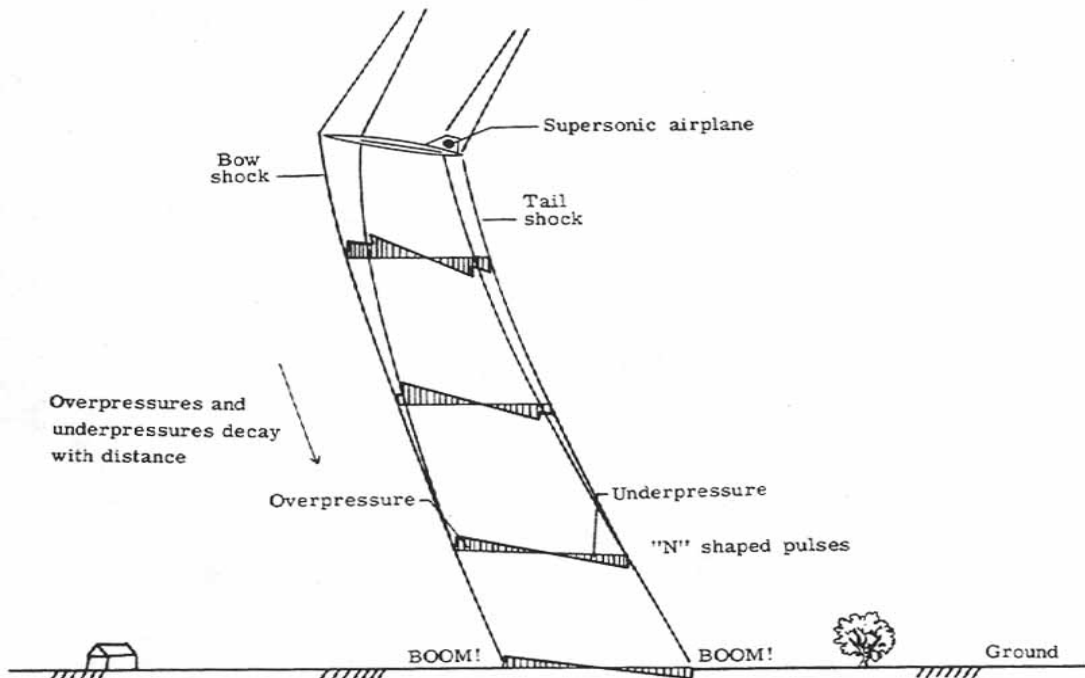


Figure 109.- Sonic-boom generation.

To an observer on the ground, this pulse is felt as an abrupt compression above atmospheric pressure followed by a rapid decompression below atmospheric pressure and a final recompression to atmospheric pressure. The total change takes place in one-tenth of a second or less and is felt and heard as a double jolt or boom.

The sonic boom, or the overpressures that cause them, are controlled by factors such as airplane angle of attack, altitude, cross-sectional area, Mach number, atmospheric turbulence, atmospheric conditions, and terrain. As shown in [figure 110](#), the overpressures will increase with increasing airplane angle of attack and cross-sectional area, will decrease with increasing altitude, and first increase and then decrease with increasing Mach number.

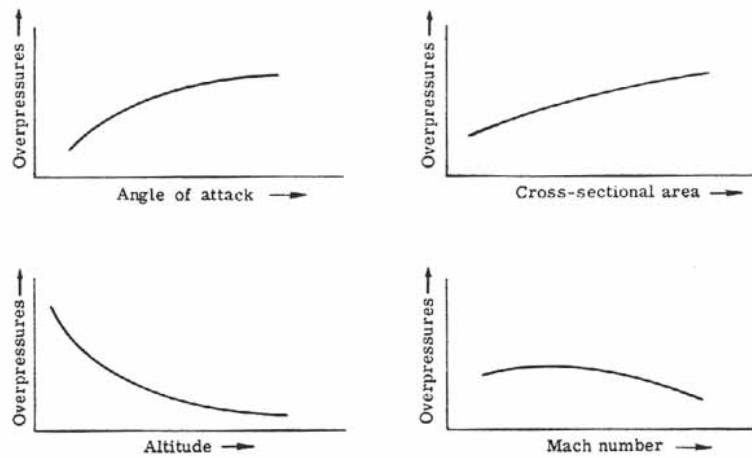


Figure 110.- Factors affecting sonic-boom overpressures.

Turbulence in the atmosphere may smooth the "N" wave profile and thus lessen the impact of the boom or, on the other hand, may in fact amplify the overpressures. Reflections of the overpressures by terrain and buildings may cause multiple booms or post-boom aftershocks. In a normal atmospheric profile, the speed of sound increases with decreasing altitude. [Figure 111](#) shows that the directions in which the overpressures travel are refracted in this normal case and that they will at some point curve away from the Earth. The strongest sonic boom is felt directly beneath the airplane and decreases to nothing on either side of the flight path. It is interesting to note that a turning supersonic airplane may concentrate the set of shock waves locally where they intersect the ground and produce a superboom.

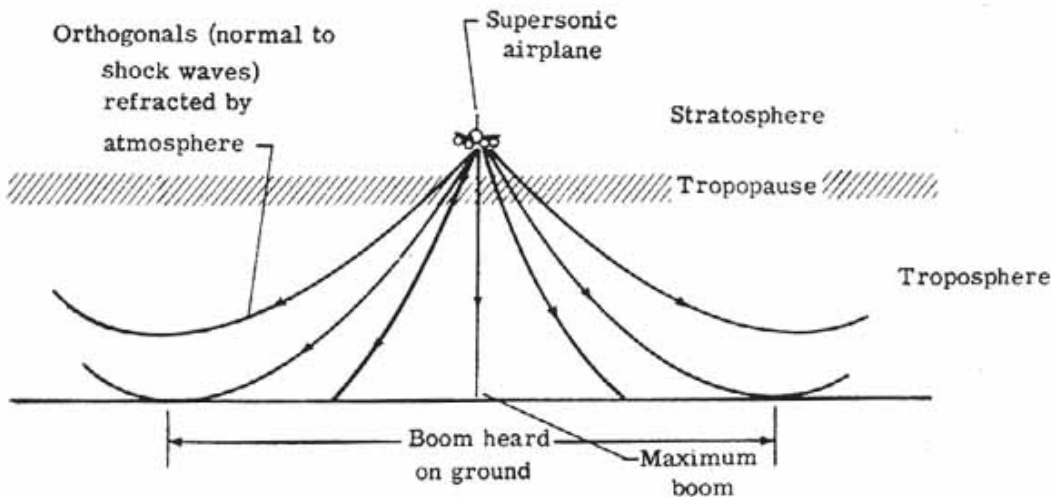


Figure 111.- Refraction of shock waves.

Perhaps the greatest concern expressed about the sonic boom is its effect on the public. The effects run from structural damage (cracked building plaster and broken windows) down to heightened tensions and annoyance of the citizenry. For this reason, the world's airlines have been forbidden to operate supersonically over the continental United States. This necessitates, for SST operation, that supersonic flight be limited to over-water operations. Research for ways in which to reduce the sonic boom continues.

VII. BEYOND THE SUPERSONIC

Hypersonic Flight

Hypersonic flight is arbitrarily defined as flight at speeds beyond Mach 5 although no drastic flow changes are evident to define this. To date, speeds of this magnitude have been achieved only by rockets and spacecraft and the NASA X-15 research airplane. Several formidable problems are encountered at these speeds. First, the shock waves generated by a body trail back at such a high angle that they may seriously interact with the boundary layers about the body. For the most part, these boundary layers are highly turbulent in nature. Secondly, across the strong shocks, the air undergoes a drastic temperature increase. Aerodynamic heating of the body is a major problem. For sustained hypersonic flight most normal metals used in today's airplanes would quickly melt; therefore new materials or methods that can withstand the high-temperature effects are required. The temperature of the leading edge of the airplane wing may be reduced by using a high degree of sweepback. Additionally, to obtain a good lift-drag ratio, a flat-plate design wing is used.

Control surfaces for hypersonic flight must be strategically placed so that they encounter sufficient dynamic pressure about them to operate. Otherwise, if shielded from the approaching flow by the fuselage, for example, they will be ineffective.

[Figure 112](#) shows two proposed hypersonic airplanes that exhibited much of this design philosophy. The modified NASA X-15 research airplane shows the highly swept delta wing and the X-20 Dynasoar reentry craft has control surfaces out on the wing tips for effective control.

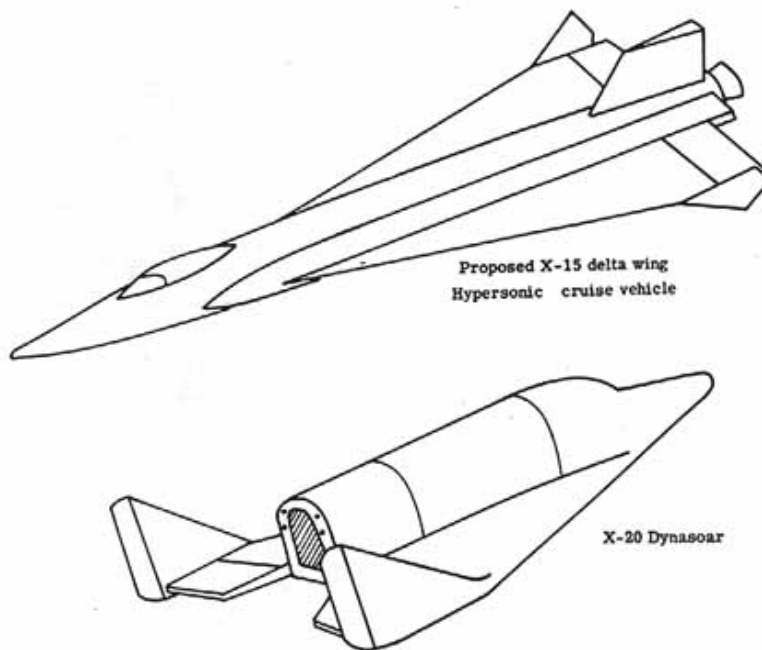


Figure 112.- Examples of hypersonic designs.

Although commercial hypersonic flight is a long way from being realized, studies are being conducted by NASA to obtain the basic knowledge necessary for design. [Figure 113](#) shows a proposed hypersonic transport (HST).

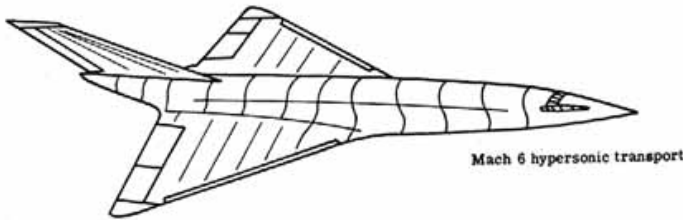


Figure 113.- Proposed hypersonic transport (HST).

Propulsion is another major problem at hypersonic speeds. Economically, the most promising prospect is the ramjet engine. The ramjet engine works on the principle that at high Mach numbers the shock waves compress the air for combustion in the engine. This does away with many moving parts and represents an efficient propulsion method. NASA research is also continuing in this field.

Lifting Bodies

Because of the cost and safety, it has long been recognized that designs of reentering spacecraft must be found that would enable the crew to maneuver the craft to a landing from a great distance. Up to now spacecraft have reentered and followed near ballistic entries with little control over the landing site. Large recovery forces and operations were usually necessary. Starting in the late 1950's, however, NASA has been involved in designing aircraft that produce more lift than drag and yet resemble spacecraft. They are called lifting bodies, for they have no wings but obtain lift because of their body shapes.

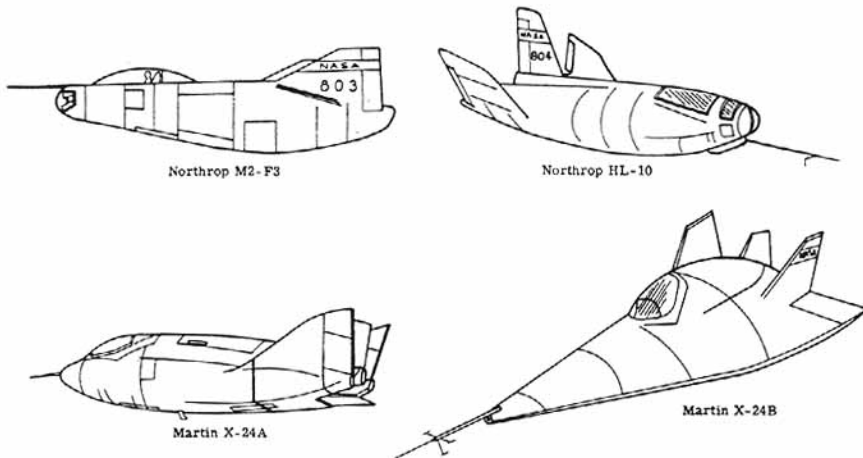


Figure 114.- Lifting bodies.

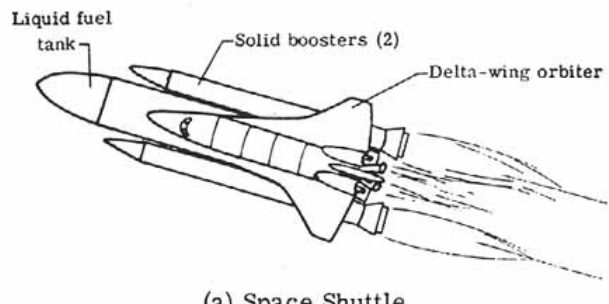
[Figure 114](#) shows four of the shapes being tested to evaluate the handling characteristics and flight qualities of this unusual concept. The M2 vehicle type developed at the NASA Ames Research Center is flat topped with a rounded belly and combines the advantages of stability at hypersonic speeds with high lift-drag ratios at subsonic speeds. The HL-10 lifting body developed by the NASA

Langley Research Center is shaped to provide optimum trim at Mach 10+ and, in contrast to the M2 vehicle, it possesses a rounded top and a flat belly. The Martin Marietta X- 24A is very different in shape from the previous two since it is more rounded although it, like the HL- 10, has a flat bottom. Rebuilt as the X-24B, it now has a double-delta planform and a more pointed nose.

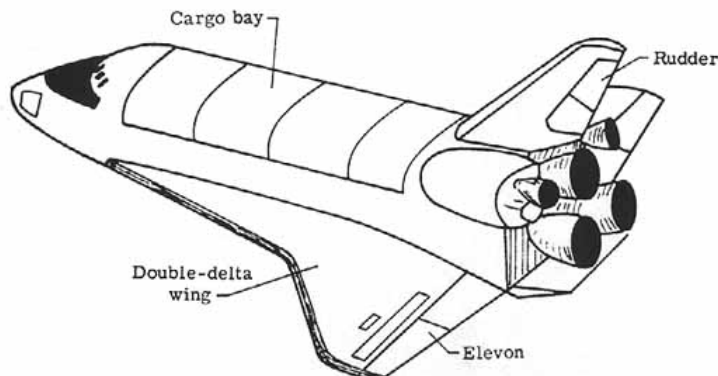
The lifting bodies being flight-tested are exploring the subsonic and low supersonic speed ranges to show how control over the lift-drag ratio may aid in the landing of more advanced vehicles. Representative of a new generation of vehicles primarily benefiting from this research is the Space Shuttle.

Space Shuttle

The Space Shuttle represents the United States' commitment to developing a low-cost method of delivering and returning payloads to and from orbit. The basic design settled upon is shown in [figure 115\(a\)](#). The booster stage consists of two recoverable solid-fuel rockets and a large nonrecoverable external fuel tank used by the orbiter stage engines to complete the boost into orbit. The orbiter stage shown in [figure 115\(b\)](#) is the actual part of the total vehicle to go into orbit and return to Earth to a controlled landing. Aerodynamic interest is centered about the boost and landing stages of the mission when dynamic pressures are evident. The entire range of Mach numbers from subsonic to supersonic is covered. There are some unique problems associated with the boost phase such as the range of dynamic pressures acting on the vehicle, staging aerodynamics, the recovery of the solid-fuel boosters by parachutes, as well as stability and control considerations both at low and high Mach numbers.



(a) Space Shuttle.



(b) Orbiter.

Figure 115.- Space Shuttle designs.

The landing phase of the mission is an area of great concern. The orbiter vehicle must be able to deorbit and land like a conventional airplane. There are numerous aerodynamic research problems associated with this part of the mission.

The orbiter ([fig. 115\(b\)](#)) uses a double-delta wing configuration to optimize the hypersonic flight characteristics and still provide for a good lift-drag ratio in the landing phase. With this lift-drag capability, the orbiter has a side-to-side range capability of about 2000 km. The orbiter reenters the atmosphere at a high angle of attack-about 30°. This high angle of attack is used to concentrate the maximum aerodynamic heating on the underside of the vehicle where the greatest thermal protection is provided. In the upper reaches of the atmosphere, attitude is controlled by a reaction control system, but as the dynamic pressure builds, the vertical tail (to control yaw) and elevons (combined elevators and ailerons to control pitch and roll) become effective. On landing, the rudder splits open to act as a speed brake and a parachute is deployed to slow the orbiter to a stop. The Space Shuttle represents a challenge to aerodynamic research for years to come and is a stimulus for probing further into the unknowns of high-speed flight.

VIII. PERFORMANCE

In the earlier discussions, the concepts of lift and drag were explored extensively to discover how these forces arise. With these basic ideas in mind, it is relatively easy to follow the results of the application of the fundamental forces on a complete airplane.

As indicated earlier, there are four basic forces that act on an airplane - these include lift, drag, weight, and thrust. Additionally, in curved flight another force, the centrifugal force, appears. Performance, to be considered first, is basically the effects that the application of these forces have on the flight path of the airplane. Stability and control, considered later, is the effect that these forces have over a short term on the attitude of the airplane itself. For performance purposes the airplane is assumed to possess stability and a workable control system.

Motions of an Airplane

Figure 116 illustrates the various flight conditions encountered by an airplane. All the motions may be grouped into one of three classes: (1) unaccelerated linear flight, (2) accelerated and/or curved flight, and (3) hovering flight.

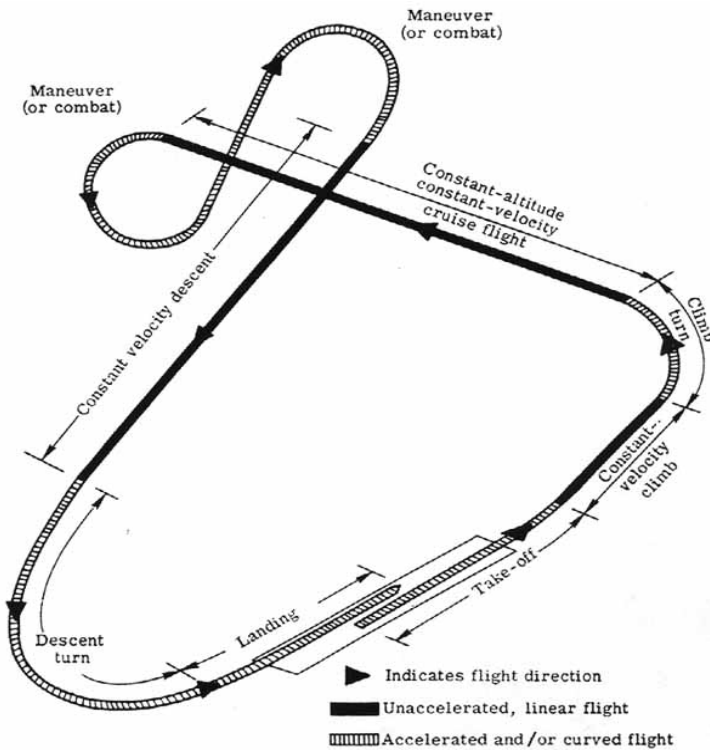


Figure 116.- Airplane flight conditions.

Performance of an airplane is a very broad subject and much could be written on it alone. In the interest of brevity, therefore, only the simplest, but probably the most important, aspects of airplane flight are considered.

Class 1 Motion

Straight and level unaccelerated flight (cruise flight) - Although straight and level flight may occur only over a small section of the total flight, it is very important since it is usually considered the standard condition in the design of an airplane. This condition has been touched on before but some additional comments will be made.

[Figure 117](#) shows the force system for straight and level flight. The flight path is horizontal to the Earth's surface and for simplicity it is assumed that the thrust always acts along this horizontal plane. For the flight to be horizontal, or constant altitude, it is easily seen that lift must equal weight. To fly at constant velocity (unaccelerated) the thrust must equal the drag.

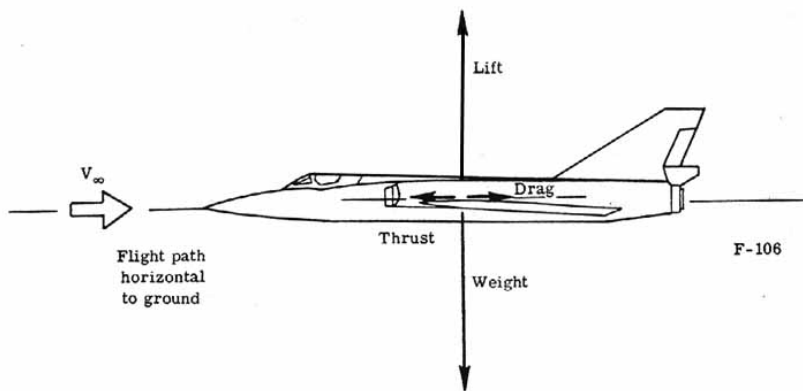


Figure 117.- Straight and level flight. Lift = Weight and Thrust = Drag.

The velocity of the airplane must be sufficient to produce a lift equivalent to the weight. If one examines this statement closely, it says that there is a range of velocities over which the plane may fly straight and level. Expanding equation (25) and combining it with the condition that Lift = Weight, one obtains:

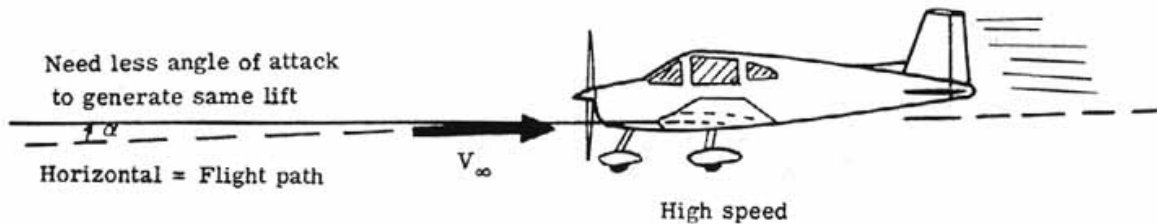
$$\text{Weight} = \frac{1}{2} \rho_{\infty} V_{\infty}^2 C_L S \quad (36)$$

If it is assumed that the weight, air density ρ_{∞} and wing area S are constant, one easily observes that as the velocity V_{∞} increases, the wing lift coefficient C_L decreases, which may be accomplished by a decrease in the wing angle of attack. Minimum flying speed for straight and level flight occurs when the wing is operating at $C_{L,\max}$, that is, near the stall angle. The maximum flying speed for straight and level flight is limited by the thrust available from the engine. This condition also requires a small value of C_L and hence a small angle of attack.

In conclusion, at low speeds to fly straight and level the airplane angle of attack is large (fig. 118(a)) whereas for high speeds the airplane angle of attack is small (fig. 118(b)).



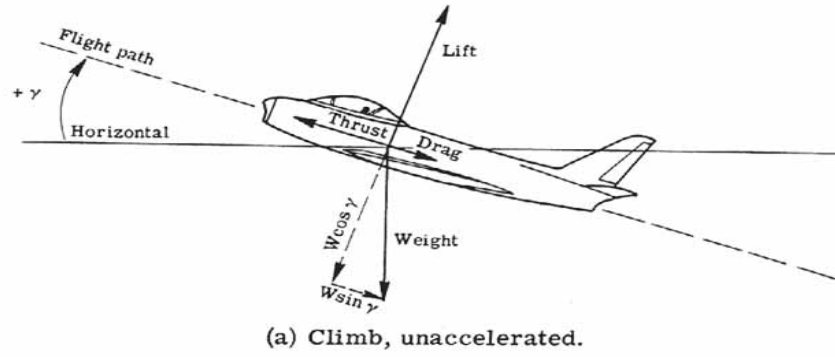
(a) Straight and level – low speed.



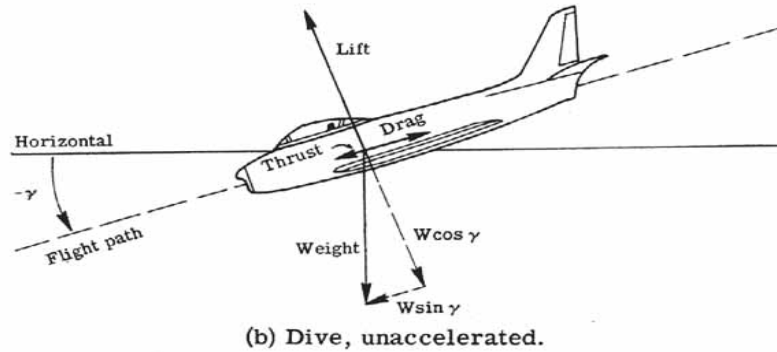
(b) Straight and level – high speed.

Figure 118.- Speed effects on straight and level flight.

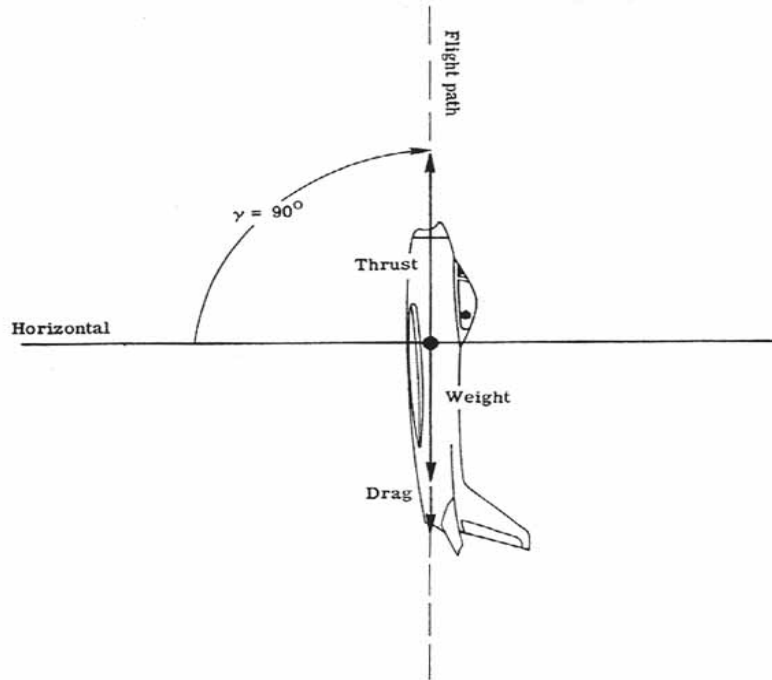
Straight, unaccelerated ascent (climb) or descent (dive) - [Figure 119](#) illustrates the force systems for the cases of an airplane in a straight, constant-velocity climb or dive. It has been assumed that the thrust line lies along the free-stream direction or flight path. The climb or descent angle is given by $+\gamma$ or $-\gamma$ [Greek letter gamma], respectively.



(a) Climb, unaccelerated.



(b) Dive, unaccelerated.



(c) Unaccelerated vertical climb.

Figure 119.- Unaccelerated ascent and descent.

If the forces are summed parallel and perpendicular to the flight path, it is seen that the weight force is resolved into two components. One obtains

$$L = W \cos \gamma = W \cos (-\gamma) \quad (\text{Climb or dive}) \quad (37)$$

$$T = D + W \sin \gamma \quad (\text{Climb}) \quad (38)$$

$$T = D + W \sin (-\gamma) = D - W \sin \gamma \quad (\text{Dive}) \quad (39)$$

To maintain a straight climbing (or diving) flight path, the lift equals the component of weight perpendicular to the flight path (eq. (37)). In the case of the climb condition to maintain a constant velocity the thrust must equal the drag plus a weight component retarding the forward motion of the airplane. In the case of the dive condition the weight component along the flight path helps the thrust by reducing the drag component for constant velocity.

The conclusion is that one must use an increased thrust to climb at constant velocity and use less thrust to dive at constant velocity. This is analogous to the situation of a car where one must "give it the gas" (apply more thrust) to prevent the car from slowing down in going up a hill and "let up on the gas" (use less thrust) to prevent the car from speeding up when going down a hill.

It is interesting also to examine three special cases of the use of equations (37), (38), and (39). First, in straight and level flight, the climb angle γ is zero, hence $\sin \gamma = 0$ and $\cos \gamma = 1$. This yields the previously derived conditions that Lift = Weight ($L = W$) and Thrust = Drag ($T = D$). Secondly in a vertical climb $\gamma = 90^\circ$, and hence $\sin \gamma = 1$ and $\cos \gamma = 0$. Thus, the thrust necessary to climb vertically is equal to the drag plus the airplane weight ($T = D + W$). Also, for a vertical climb, the lift equals zero ($L = 0$). This condition is shown in [figure 119\(c\)](#).

The final condition to be discussed is gliding flight. In gliding flight the thrust equals zero. It is therefore necessary to balance the aerodynamic reaction forces of lift and drag with the weight. Equation (37) remains unchanged but equation (39) is simplified. In a glide,

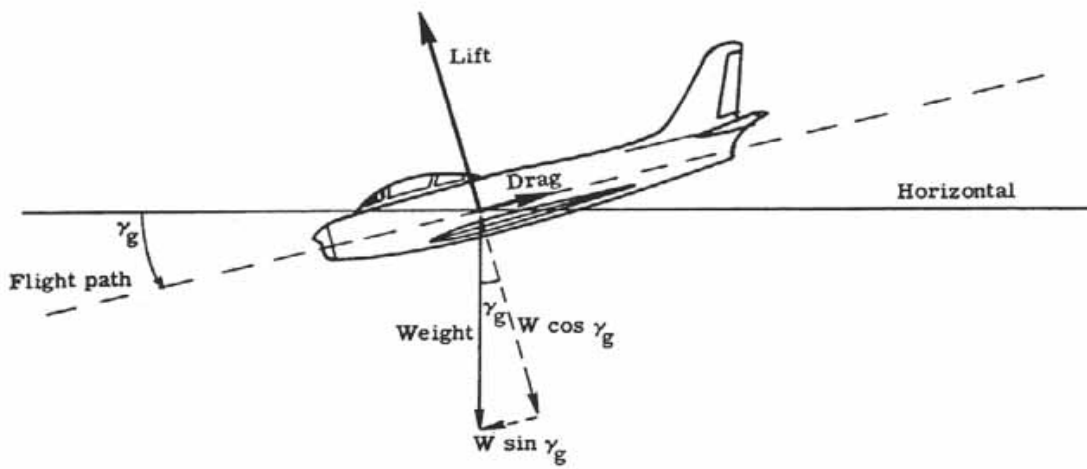
$$L = W \cos \gamma_g \quad (40)$$

$$D = W \sin \gamma_g \quad (41)$$

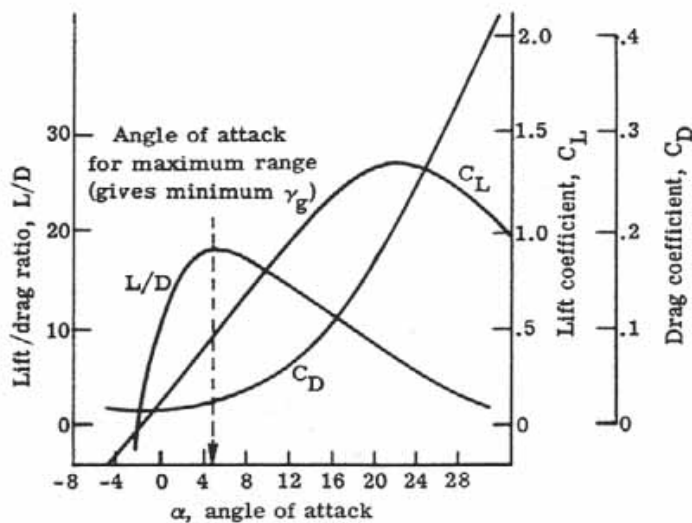
as shown in [figure 120\(a\)](#). If one divides equation (40) by equation (41), the result is:

$$L/D = 1/\tan \gamma_g \quad (42)$$

In nonmathematical language this means that the smallest glide angle, and hence maximum gliding range, is obtained when the lift-drag ratio is the maximum. The lift-drag ratio is a measure of the aerodynamic efficiency of the airplane. Sailplanes possess the greatest lift-drag ratios with excellent aerodynamic design since they rely on air currents to keep them aloft. For a particular airplane, as shown in [figure 120\(b\)](#), the lift-drag ratio varies with the angle of attack of the airplane (not to be confused with the glide angle of the flight path). There is a particular angle of attack for which this ratio is a maximum. This is then the angle of attack for minimum glide angle and maximum range. For any other angle of attack, the lift-drag ratio is less and the glide angle is increased; hence, a steeper glide results. It is a natural tendency for a pilot to raise the airplane nose (increase the angle of attack) to try to get maximum range but unless this gives the maximum lift-drag ratio, the descent will be steeper instead.



(a) Unaccelerated glide conditions.



(b) Glide aerodynamic characteristics.

Figure 120. Glide characteristics.

Class 2 Motion

Class 2 accelerated motion and curved flight is considered, specifically for the cases of take-off, landing, and the constant-altitude banked turn.

Take-off - The take-off of an airplane is a case of accelerated motion. From the instant the airplane begins its take-off roll to the time it begins its climb out after leaving the ground, it is under continuous acceleration. (See [fig. 121](#).) The total takeoff distance needed may be considered to consist of three parts: (1) the ground-roll distance, (2) the transition distance, and (3) the climb out distance over, say, a 15.25-m (50-ft) obstacle.

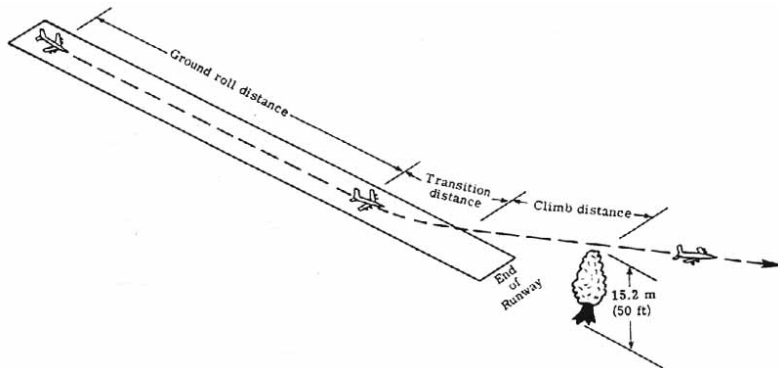


Figure 121.- Total take-off distance.

[Figure 122](#) shows the forces acting during the ground roll. In addition to thrust, weight, drag, and lift, there is a rolling frictional force due to the landing gear. The sum of the forces in a horizontal direction is equal to the net force acting to accelerate the airplane down the runway. At the beginning of the ground roll, lift and drag are zero as dynamic pressure is still zero (assuming no winds). Acting under the net acceleration (thrust exceeding the total retarding force), the velocity increases and lift and drag build. The airplane remains in a horizontal attitude until some velocity (about 10 percent above the airplane stall velocity for safety) is reached at which point the airplane is "rotated" or pitched up. The pitch increases the airplane angle of attack, the lift quickly exceeds the weight, and the airplane leaves the ground. Rolling friction forces drop to zero at liftoff, and the airplane's total drag decreases greatly as the landing gear is retracted. At the end of transition, about 20 percent above the stall velocity, the airplane begins its climb-out usually at constant velocity. The ordinary equations for climb (eqs. (37) and (38)) apply in this case.

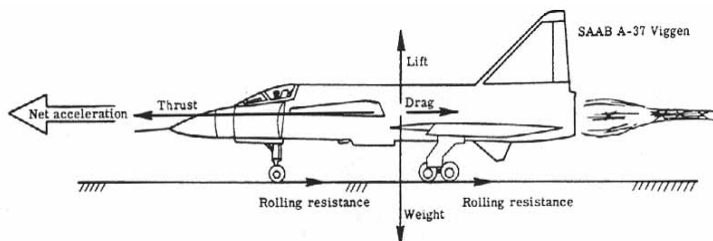


Figure 122.- Forces acting during take-off ground roll.

The total distance for the airplane to clear 15.25 m (50 ft) from the start of its roll is important and determines the amount of runway required for design purposes. Additionally, the pilot should know

the maximum speed from which the take-off may be aborted so that sufficient runway exists for deceleration to a stop.

The take-off distance may be reduced by the use of flaps and other high lift devices. However, there is a limit to their use since they also contribute to increased drag and retard the airplane's acceleration. There is usually an optimum flap setting for an airplane which will minimize the take-off distance. Some airplanes may also use rocket-assisted units to take off in the minimum distance. These units represent a transitory increase in thrust and provide a means of high acceleration for short periods. On board an aircraft carrier, this method takes the form of a catapult, where flying speed is achieved in a matter of a second or two.

Landing - Landing an airplane consists of touching down at the lowest possible vertical and horizontal velocities. The approach phase and its associated techniques to a landing will not be considered, but only the two terminal phases, namely, the touchdown and ground rollout.

Under touchdown conditions it is assumed that the vertical velocity is near zero and that the lift equals the weight. The previous discussion about flaps indicates that they are used advantageously to decrease the landing velocity. Indeed, they increase the maximum lift coefficient and decrease the landing velocity as indicated by equation (35).

[Figure 123](#) presents the forces acting on an airplane during the landing rollout. They are the same as during the take-off except for their magnitude and direction. The rolling friction is greater as the brakes are applied. For safe operation this condition occurs near the end of the rollout. Spoilers on the wings are used to "dump" the airplane lift to prevent the airplane from rebounding into the air after touchdown. This condition increases the rolling friction as the normal force is increased. The engine thrust is zero or, more usually for large commercial and military airplanes, is negative. This condition is accomplished by using reversible pitch propellers or thrust reversers. For ground roll during landing the thrust force is retarding. The airplane drag may be increased by setting the flaps for maximum drag. From [figure 123](#), therefore, there is a net deceleration acting on the airplane to slow it to a stop. Another favorite braking device used by military airplanes is the parachute which is opened at touchdown. On board aircraft carriers, the usual landing brake is mechanical in the form of the arresting hook on the airplane engaging a cable laid across the flight deck. Deceleration is exceedingly swift and the airplane is subjected to large structural forces.

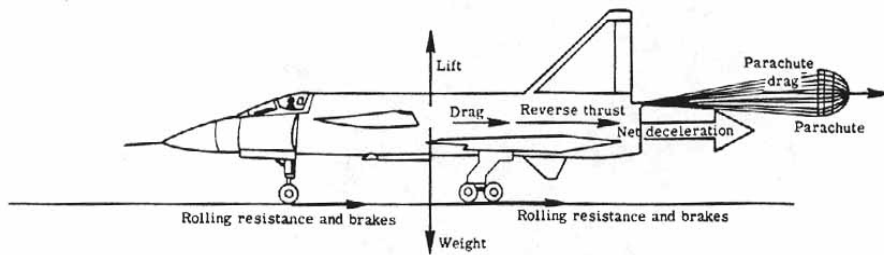


Figure 123.- Forces acting after landing.

Constant-altitude banked turn - As shown in [figure 116](#), not all motions of an airplane are in a straight line. There are ample cases of curved flight paths. These cases include the climbing and descending turns, maneuvers in combat and aerobatics. One of the basic maneuvers required to change the flight-path heading is the constant altitude banked turn.

In the previous discussions of motions of an airplane, accelerations due to a change of direction of flight were insignificant. But in a turn they acquire added significance. By Newton's first law, a body in motion in a straight line will continue in motion in that same line unless acted upon by an external force. To maintain an airplane in a curved path requires that an acceleration be supplied toward the center of the curve. By Newton's second law the force required to perform this, called centripetal force, is proportional to the acceleration required to maintain the curved flight. By Newton's third law there is a reactive force by the body, opposite the centripetal force, called the centrifugal force. The centrifugal force is given by

$$F_C = \frac{mV_\infty^2}{R} \quad (43)$$

where m is the mass of the airplane, V_∞ is the velocity of the airplane in the curve, and R is the radius of the turn or curved flight path. From this equation one sees that the highest centrifugal forces occur for massive airplanes at high speeds in tight turns.

[Figure 124](#) shows the disposition of forces in a properly executed turn. Notice particularly that the wings are banked at an angle θ [Greek letter theta] to the horizontal. This angle causes the resultant lift on the wings to bank also. When resolved into vertical and horizontal components, it is seen that it is the horizontal component of lift that is the centripetal force needed to maintain the curved flight path. This force is balanced by the reaction centrifugal force. For a constant-altitude turn the vertical component of lift must equal the weight. Thus, the total lift must be increased to maintain constant altitude when entering a banked turn.

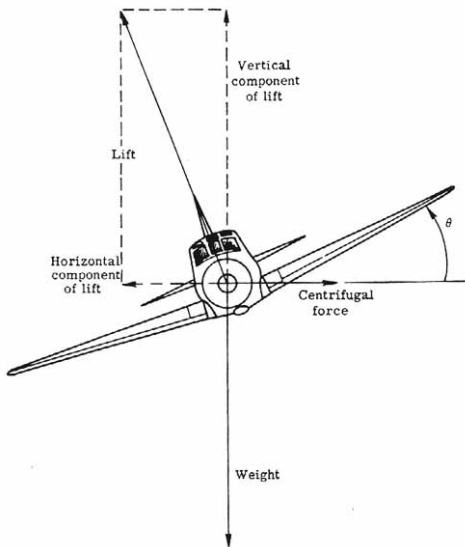


Figure 124.- Forces in a properly banked turn. Vertical lift = Weight;
Horizontal lift = Centrifugal force.

The smaller the turning radius is or the greater the velocity in a turn, the larger the banking angle must be. This is required to produce a large enough horizontal lift component to hold the airplane in the turn.

Class 3 Motion-Hovering Flight

Class 3 motion has been assigned to a special flight condition; that of hovering flight. In hovering flight there is no motion of the aircraft with respect to the atmosphere. As such, this results in no aerodynamic reaction forces of the aircraft on the whole, that is, no lift and drag forces. In equilibrium, the remaining forces, thrust and weight, must be balanced as shown in [figure 125](#). Hence, for hovering flight,

$$\text{Thrust} = \text{Weight} \quad (44)$$

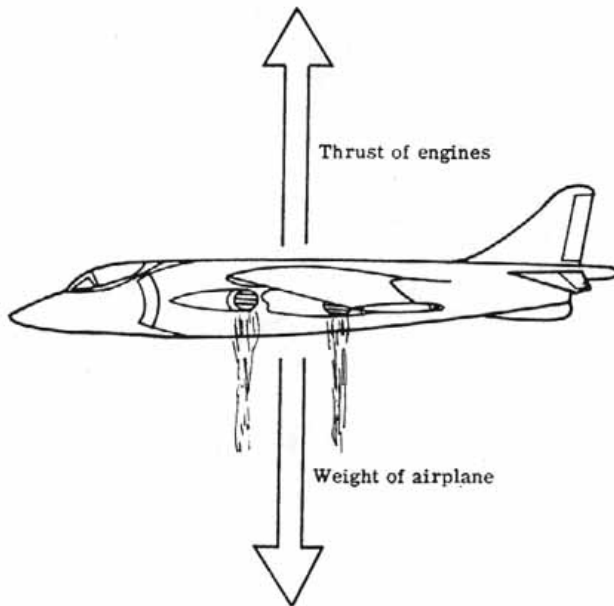


Figure 125.- Hovering flight. Thrust = Weight.

By properly controlling the thrust, the aircraft may be made to rise and descend vertically as shown in [figure 126](#). The chief advantage of such aircraft is their ability to land and take-off in small spaces without the use of long runways. Since they land and take-off vertically they are called VTOL aircraft. They have the added distinction of being able to perform at high speeds as a conventional airplane in flight. This is why helicopters, although capable of hovering flight, are usually not included in this grouping. They are, at present, incapable of the speeds and maneuvers of conventional airplanes.

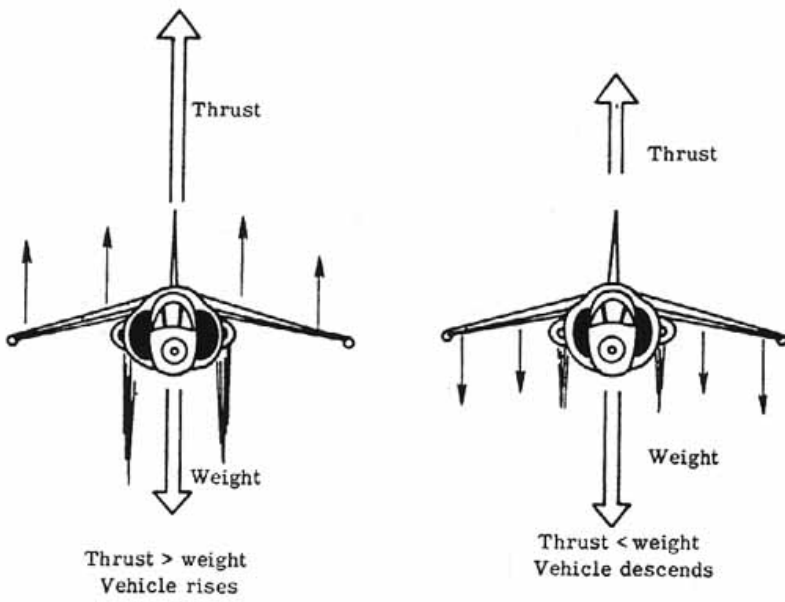


Figure 126.- VTOL ascent and descent.

The first concepts to be tried were three "tail sitting" airplanes, the Lockheed XFY-1, the Convair XFY-1, and the Ryan X-13 Vertijet as shown in [figure 127](#). The first two used turboprop-powered contrarotating propellers to supply the vertical thrust needed whereas the X-13 was jet powered. The main problems with these VTOL airplanes were the tricky piloting maneuvering required in the take-off and landing and the need to tilt the entire aircraft over into conventional flight.

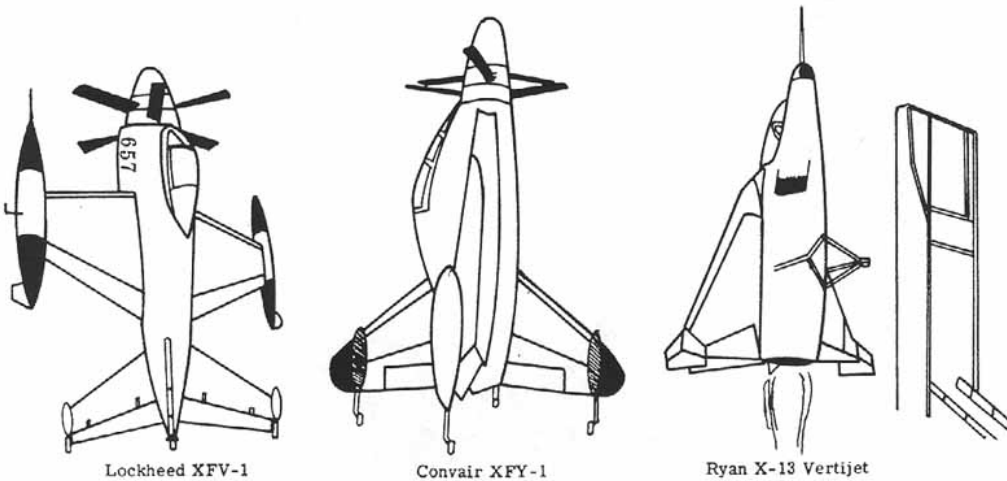
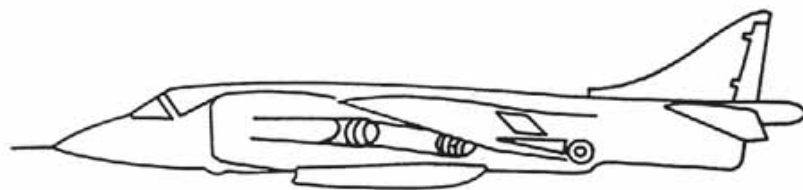


Figure 127.- Figure 127. Early VTOL airplanes.

The next concept tried was to keep the main body of the aircraft in a conventional sense but tilt the wing and engines from the vertical to the horizontal. The LTV-Hiller-Ryan XC-142A in [figure 128\(a\)](#) was such an aircraft.

Another concept was to use separate powerplants for vertical take-off and landing and conventional level flight. But this added dead weight to each flight regime. For simplicity and efficiency, the Hawker Siddeley Harrier ([fig. 128\(b\)\)](#) is one of the best present-day VTOL aircraft. This plane uses the concept of "vectored thrust" where four rotating exhaust nozzles are used to deflect the exhaust from vertically down to directly behind as shown in [figure 128\(c\)](#). Control at low flight velocities and in hovering flight is supplied by reaction jets in the wing tips, nose, and tail.



(b) Harrier GR MKI.



(c) Example flight.

Figure 128. VTOL concepts.

IX. STABILITY AND CONTROL

The subject of stability and control of an airplane has throughout the previous chapters been kept in the background so as not to complicate the study of the forces acting on an airplane and the related performance considerations. It remains now to consider this subject in view of the presented material.

Stability

Simply defined, stability is the tendency, or lack of it, of an airplane to fly a prescribed flight condition. Control is the ability of a pilot to change the airplane's flight conditions. The subject of stability is considered first.

For an airplane to be in equilibrium for a particular flight condition, the sum of all the forces and moments on it must be zero. For example, consider an airplane flying straight and level as in [figure 129\(a\)](#). Then the lift equals the weight, the thrust equals the drag, and there are no net rotating moments acting on it. It is in equilibrium.

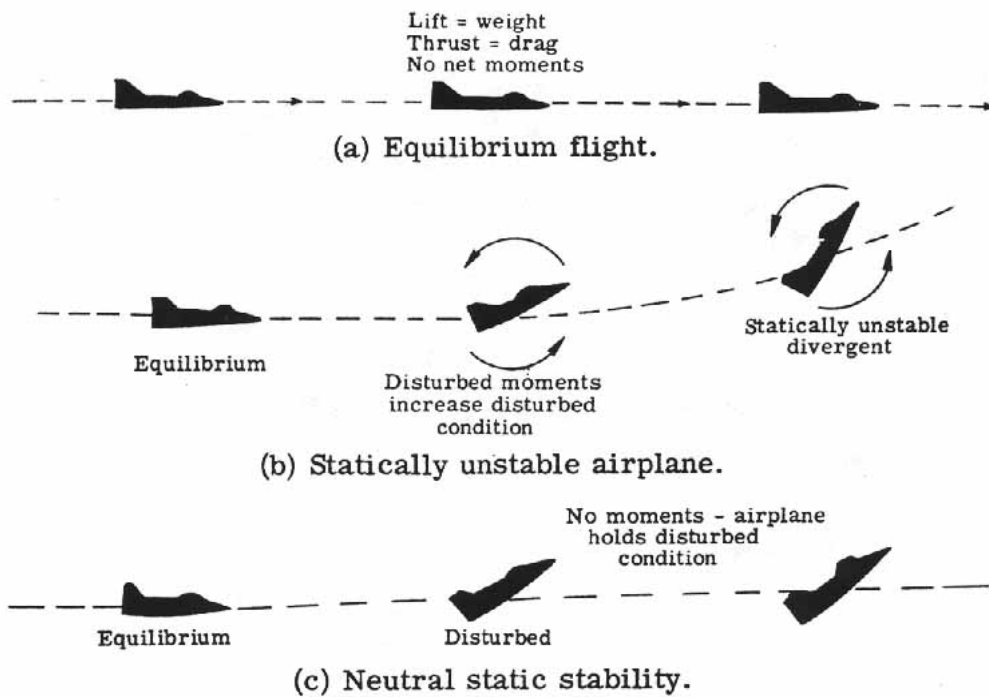


Figure 129.- Static stability.

Now, if the airplane is disturbed, for example, by atmospheric turbulence, and noses up slightly (angle of attack increases), the airplane is no longer in equilibrium. If the new forces and moments, caused by the angle-of-attack increase, produce a tendency to nose up still further, the airplane is statically unstable and its motion will diverge from equilibrium. (See [fig. 129\(b\)](#).) If the initial tendency of the airplane is to hold the disturbed position, the airplane has neutral static stability. (See [fig. 129\(c\)](#).) On the other hand, if restoring forces and moments are generated by the airplane that tend initially to bring it back to its equilibrium straight and level condition, it is statically stable.

If it is assumed that the airplane is statically stable, it may undergo three forms of motion with time. It may nose down, overshoot, nose up, overshoot to a smaller degree, and eventually return to its former equilibrium condition of straight and level flight. (See [fig. 130\(a\)](#).) This type of decaying oscillatory motion indicates that the airplane is dynamically stable. Or it may continue to nose up and down thereafter at a constant amplitude. The airplane is said to have neutral dynamic stability ([fig. 130\(b\)](#)) or, in the worst case, it may nose up and down with increasing magnitude and be dynamically unstable ([fig. 130\(c\)](#)).

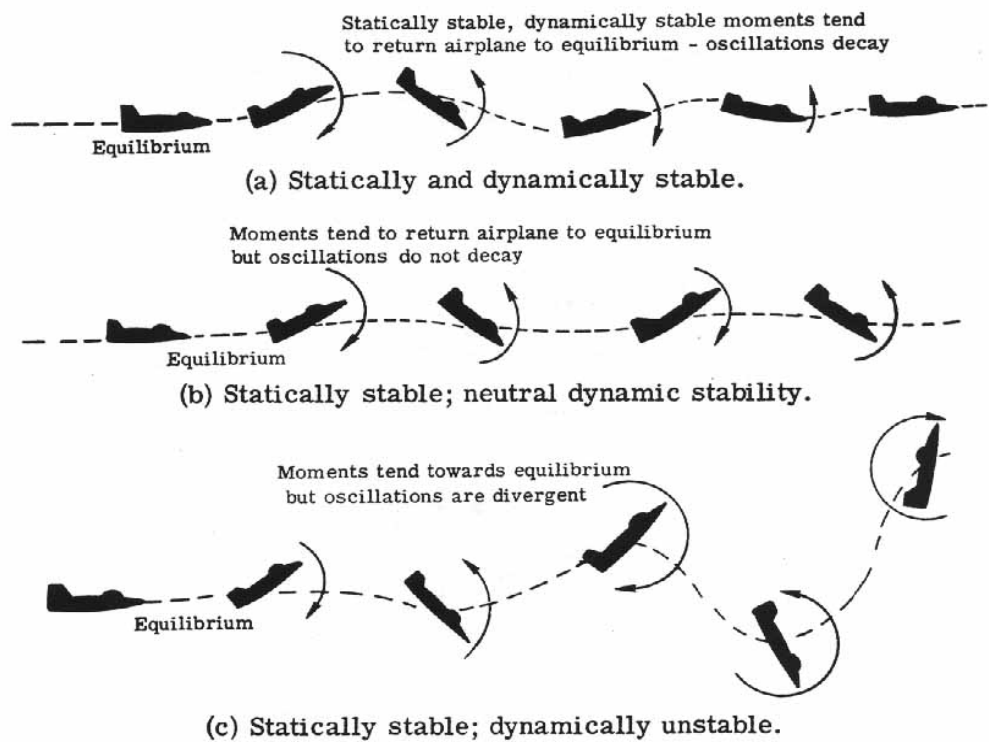


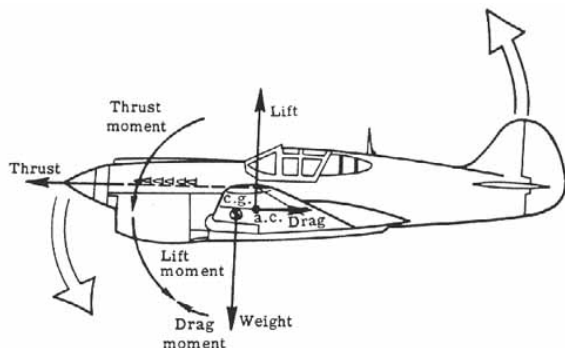
Figure 130.- Dynamic stability.

An airplane may be dynamically unstable and still be flyable if the pilot uses control by working the elevators in this last instance. But, ideally, he should not need to do this. An airplane of this design has poor flying qualities. An airplane which is statically and dynamically stable can be flown "hands off" by a pilot with no control necessary except to change the equilibrium flight condition.

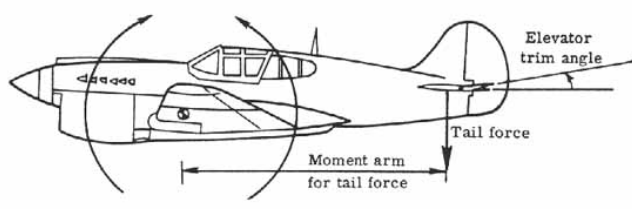
Longitudinal stability and control is concerned with an airplane's pitching motion, lateral stability and control relates to an airplane's rolling motion, and directional stability and control relates to an airplane's yawing motion. Lateral and directional stability are closely interrelated and, therefore, the two are sometimes simply referred to as lateral stability.

Longitudinal stability - Since longitudinal stability can be considered independent of lateral and directional stability, it is discussed first. Consider an airplane "trimmed" to fly at some angle of attack, α_{trim} [Greek letter alpha]. This statement says that the airplane is in equilibrium and there are no moments tending to pitch the airplane about its center of gravity.

[Figure 131\(a\)](#) shows how pitch equilibrium is achieved for an airplane. The forces acting are the weight through the center of gravity, the lift and drag at the aerodynamic center, and the thrust along the thrust line. The aerodynamic center of the airplane usually is very close to the aerodynamic center of the wing alone. In this example it lies in back of and above the center of gravity. The thrust line may lie above or below the center of gravity; in this case, above. The moments about the center of gravity are the forces times the distance between them and the center of gravity. It is seen in this case that the lift and thrust both contribute nose-down moments whereas the drag contributes a nose-up moment. If these do not cancel each other out, the airplane will not be in equilibrium. It is evident that another moment source is needed—the horizontal tail. The horizontal tail acts as a small wing and the pilot can achieve lift or negative lift by elevator control. Because of the long moment arm from the center of gravity to the aerodynamic center of the horizontal tail, only relatively small forces are needed. Thus, the horizontal tail supplies the balancing moment as shown in [figure 131\(b\)](#). To fly in a particular equilibrium condition, the elevator is "trimmed" to a particular angle. The total moment about the airplane center of gravity is zero.



(a) Net moment pitches airplane down.



(b) Equilibrium condition.

Figure 131.- Pitch equilibrium.

If the airplane is statically stable in a longitudinal sense, then if disturbed away from the trim angle of attack, moments are generated that tend to return the airplane to the equilibrium α_{trim} [Greek letter alpha]. It is customary to express the moment nondimensionally as a coefficient of moment about the center of gravity, or $(C_m)_{\text{cg}}$. (See eq. (27).) [Figure 132](#) shows the longitudinal statically stable case of the moments plotted against the angle of attack. Of course, there is no moment at the trim angle of attack; negative moments rotate the nose down for angles of attack above α_{trim} [Greek letter alpha], and positive moments rotate the nose up for angles below α_{trim} [Greek letter alpha].

Now the curve of [figure 132](#) is a composite of all the moment curves caused by the different components of the airplane, for example, the wing, fuselage, tail, and thrust. [Figure 133](#) shows this qualitatively.

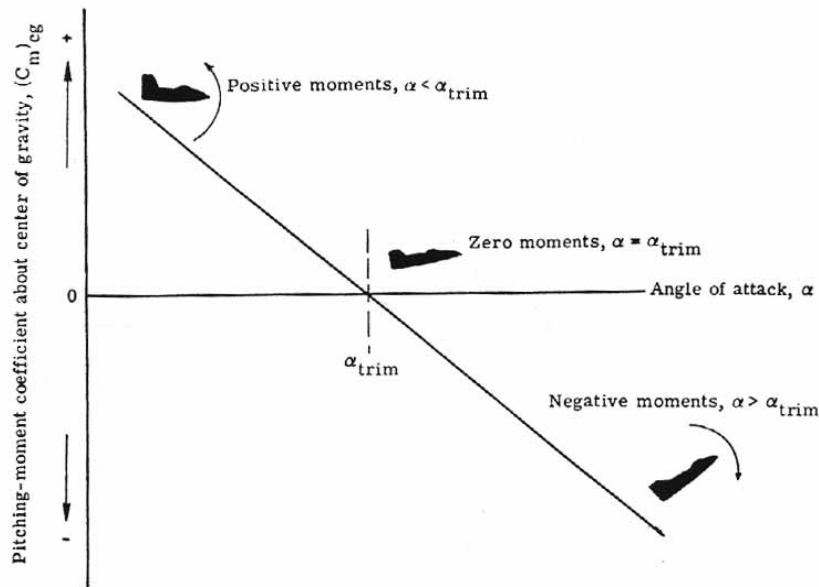


Figure 132.- Longitudinal static stability moments
as a function of angle of attack.

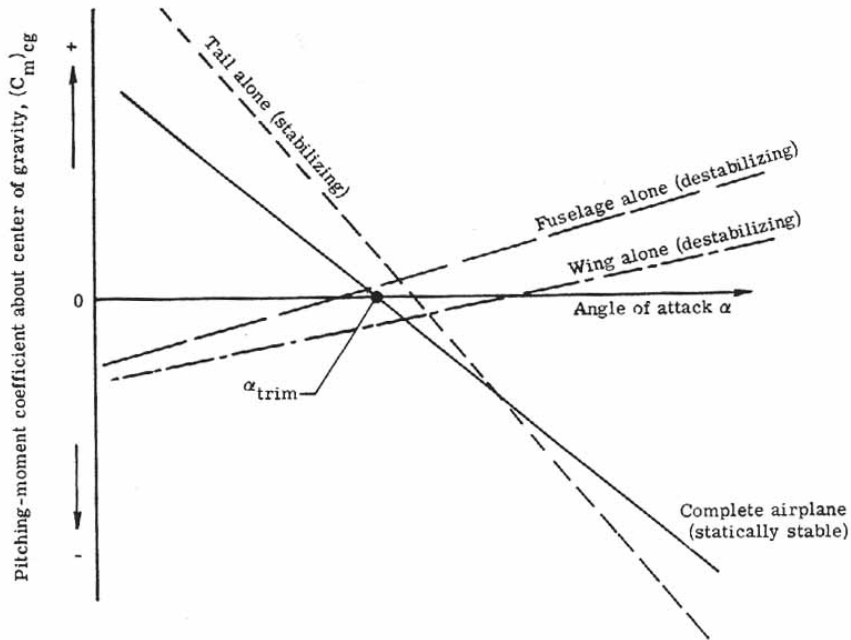


Figure 133.- Longitudinal static stability components.

Some fundamental facts are important. First, the horizontal position of the center of gravity has a great effect on the static stability of the wing, and hence, the entire airplane static stability. As shown in [figure 134](#), if the center of gravity is sufficiently forward of the aerodynamic center (points A or B), then the airplane is statically stable. If the center of gravity of the airplane is moved toward the tail sufficiently, there is a point, the neutral point (point C in [fig. 134](#)), where the moment curve becomes horizontal; this airplane is neutrally stable. If the center of gravity is moved further back (point D in [fig. 134](#)) the moment curve has positive slope, and the airplane is longitudinally unstable. Likewise, if the center of gravity is moved forward toward the nose too far (forward of point A), the pilot will not be able to generate enough force on the tail to raise the angle of attack to achieve the maximum lift coefficient.

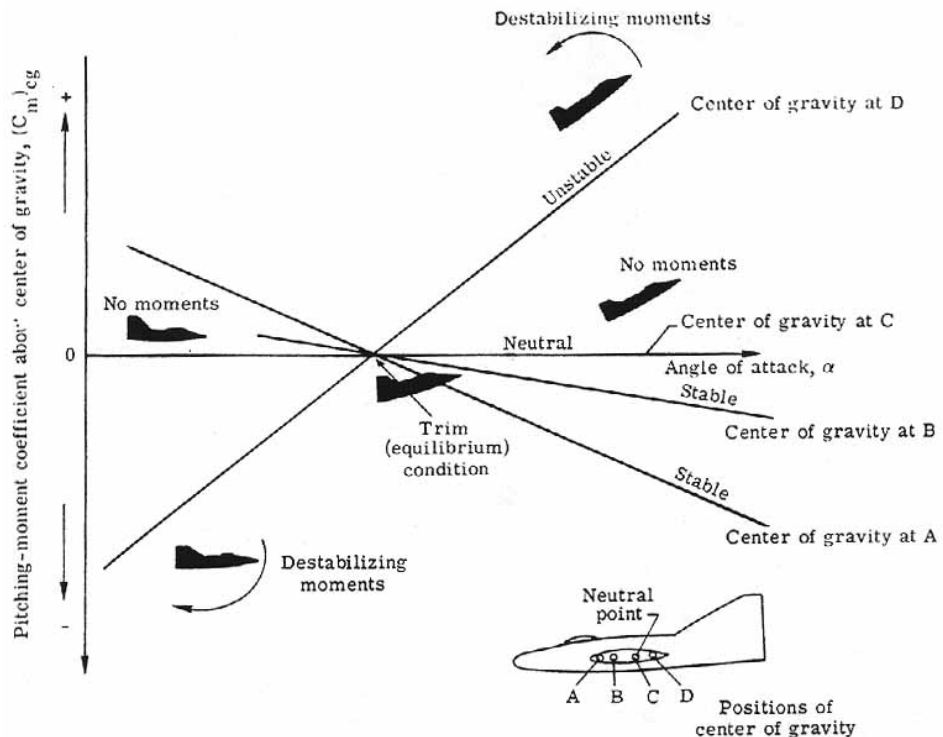


Figure 134.- Stable, neutral, and unstable static stability.

With power off the usable center-of-gravity range is relatively large ([fig. 135\(a\)](#)). There are, however, additional factors which reduce the usable center-of-gravity range. These include engine-on thrust effects and ground effects (including landing gear, flaps, and other considerations) as shown in [figure 135\(b\)](#). To insure that the actual center of gravity of the airplane falls within the usable range, an airplane is carefully designed and loaded. For example, there are cases of transport airplanes crashing because the airplane was loaded or the cargo shifted in flight so that the center of gravity fell outside the range of usable limits. The airplane then became unstable. The location of the center of gravity is an important factor in a stable airplane.

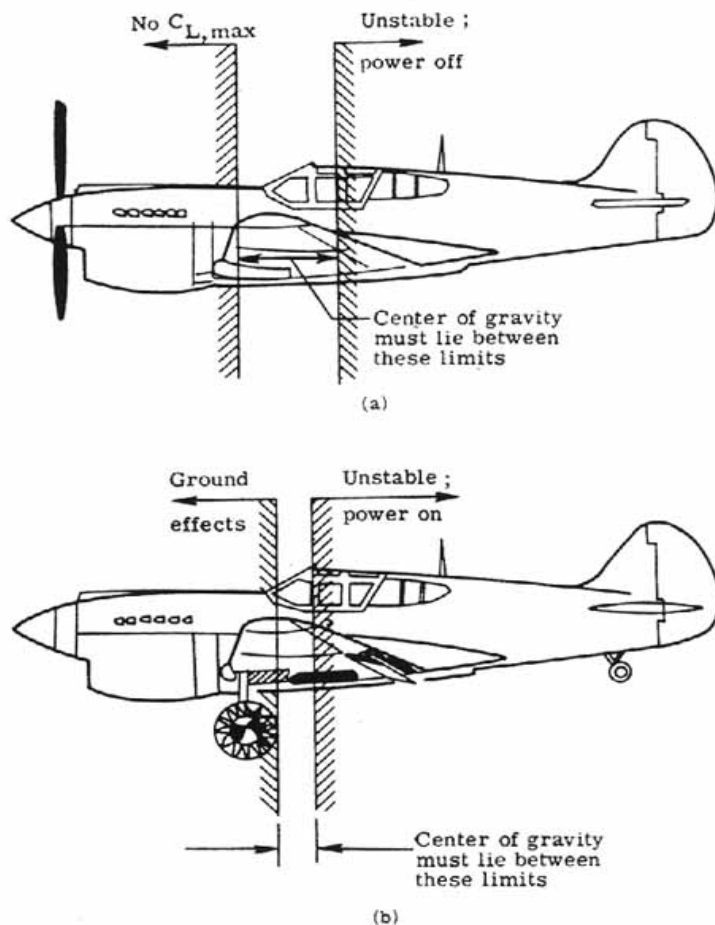


Figure 135.- Usable center-of-gravity range.

The horizontal tail is the main controllable moment contributor to the complete airplane moment curve. A larger horizontal tail will give a more statically stable airplane than a smaller tail (assuming, as is the normal case, that the horizontal tail lies aft of the center of gravity of the airplane). Of course, its distance from the center of gravity is important. The further away from the center of gravity it is, the more it enhances the static stability of the airplane. The tail efficiency factor depends on the tail location with respect to the airplane wake and slipstream of the engine, and power effects. By design it is made as close to 100 percent efficiency as possible for most static stability.

Finally, with respect to the tail, the downwash from the wing is of considerable importance. [Figure 136\(a\)](#) shows how the air is deflected downward when it leaves a wing. This deflection of air results in the wing reaction force or lift. This deflected air flows rearward and hits the horizontal-tail plane. If the airplane is disturbed, it will change its angle of attack and the downwash angle also changes. The degree to which it changes directly affects the tail effectiveness. Hence, it will reduce the stability of the airplane. For this reason, the horizontal tail is often located in a vertical location such that it is exposed to as little downwash as possible, as shown in [figure 136\(b\)](#).

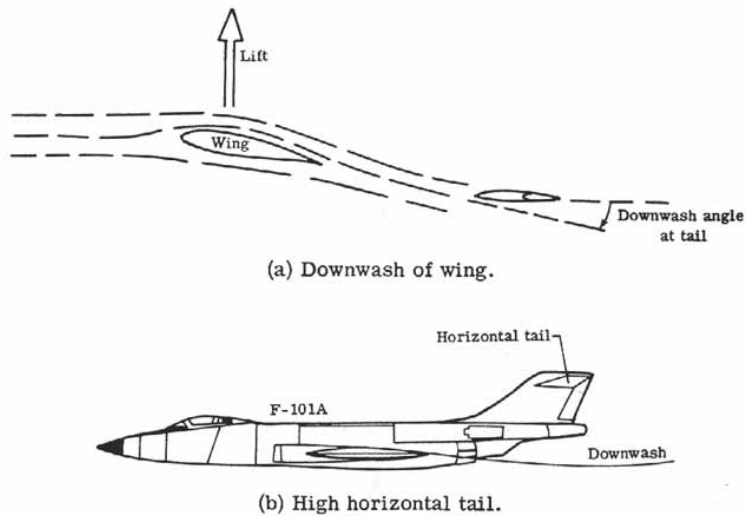


Figure 136.- Downwash effects on tail.

Dynamic longitudinal stability is concerned with the motion of a statically stable airplane. Again, this is a very broad subject and no attempt is made to treat this subject in detail. Basically, there are two primary forms of longitudinal oscillations of interest with regard to an airplane attempting to return to an equilibrium trimmed flight condition after being disturbed. The first form is the phugoid mode of oscillation which is a long period, slow oscillation of the airplane's flight path. (See [fig. 137\(a\).](#)) Often, it is poorly damped and can be an annoyance. The pilot generally can control this oscillation himself although the more highly damped it is, the greater the drag is. The second oscillation is a short- period variation of the angle of attack as shown in [figure 137\(b\)](#). Usually, this oscillation damps out very quickly with no pilot effort. However, with its natural short period, the oscillation may worsen if a pilot attempts to damp it out by use of a control because of the pilot's slow reaction time where he may get "out of phase" with the oscillation, and thus, induce dynamical instability that may eventually lead to destructive forces. A second type of short term oscillation occurs if the elevators are left free. This is called the "porpoising" mode, and is influenced by the elevator balance. The main effect is vertical accelerations of the airplane that may get out of hand if a coupling between the free elevator and airplane occur. Proper design is essential here.

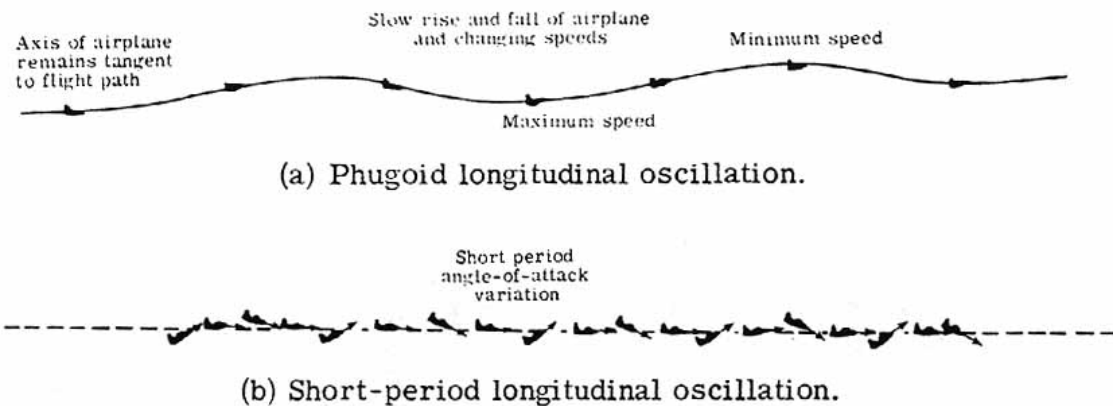


Figure 137.- Two types of dynamic longitudinal oscillations.

Insofar as compressibility effects are concerned, the rearward movement of the aerodynamic center of the wing as the airplane goes supersonic is most evident. This condition increases the static stability to such an extent that the airplane may "tuck under" and be extremely stable in a steep dive.

This condition has been discussed previously with regard to the SST. One answer to this problem is to move the center of gravity rearward by a transfer of fuel as the airplane goes supersonic. Other solutions include the double-delta wing configuration or canards placed at the nose of the airplane to develop an additional nose-up moment due to lift in the transonic and supersonic range. This arrangement has an added advantage of contributing to the airplane lift.

The use of a canard for trim and a rear sailplane for control is beneficial. The canard would trim the rearward shift of the aerodynamic center at supersonic speeds, and the strong nose-down moments from high lift devices (flaps) at low speeds by providing uplift. When not used, the canard can be allowed to trail in the free stream at zero lift and also generate minimum drag.

[Figure 138](#) shows the North American XB-70. It has a pair of canards for stability at supersonic speeds to prevent "tuck under." Additionally, the wing tips are turned downward to keep the aerodynamic center forward.

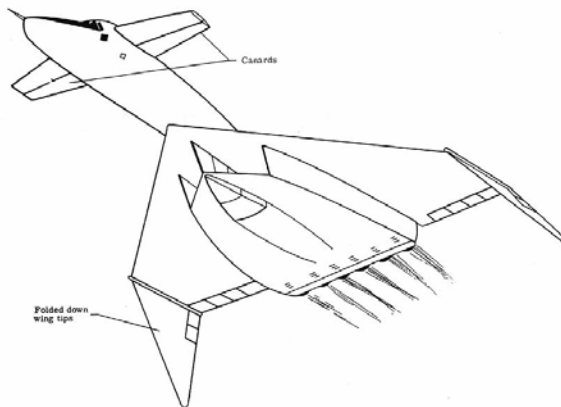
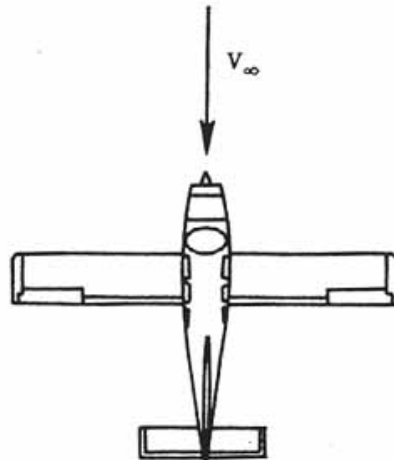
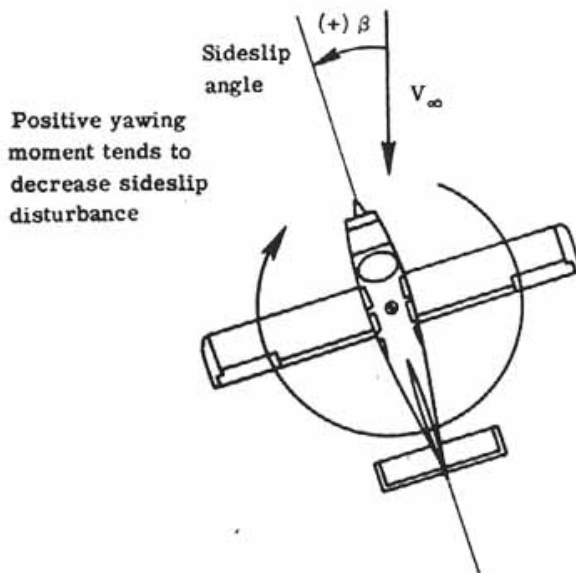


Figure 138.- XB-70 airplane.

Directional stability - Many of the basic ideas involving longitudinal stability also apply to directional stability. In the usual equilibrium condition, an airplane flies so that the yaw angle is zero as shown in [figure 139\(a\)](#). To have static directional stability, a positive yawing moment should be generated if the airplane is disturbed to a negative yaw angle or alternatively by convention, a positive sideslip angle β and a negative yawing moment generated for a negative sideslip angle excursion. The previous condition is shown in [figure 139\(b\)](#). If the airplane holds its disturbed position, it has neutral directional stability. If the tendency is to increase the disturbed position, further away from equilibrium, the airplane is directionally unstable.



(a) Equilibrium condition of zero yaw.



(b) Sideslip disturbance.

Figure 139.- Static directional stability.

[Figure 140](#) shows the variation of yawing-moment coefficient with sideslip angle. Here, one observes a positively sloping line as a directionally stable case.

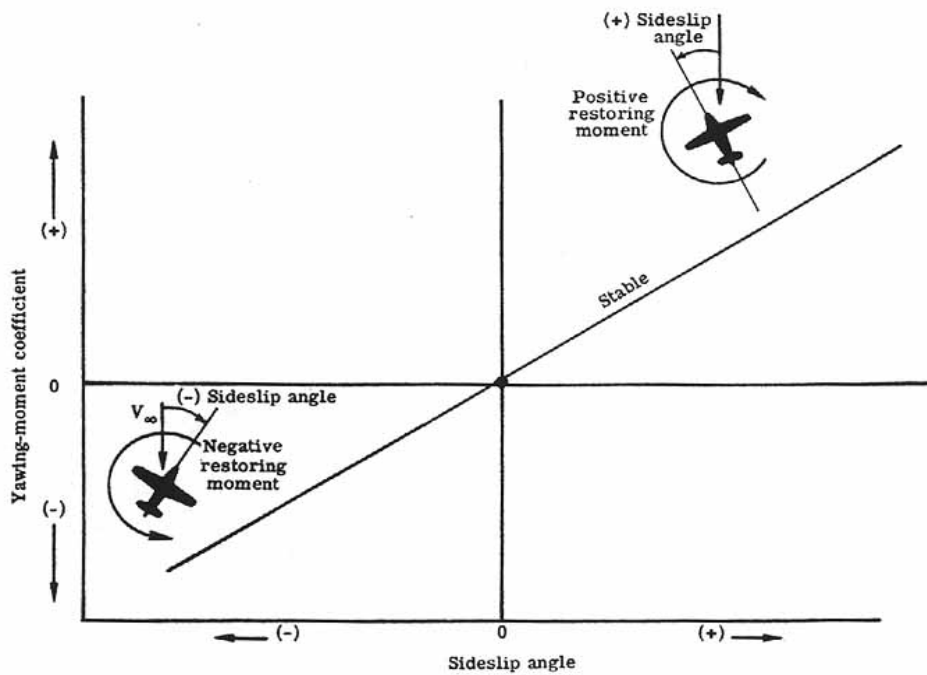


Figure 140.- Directional stability curve.

The fuselage and the vertical tail are the two most influential components in directional stability. As [figure 141](#) shows, when an airplane is in a disturbed condition at a sideslip angle β , in general the fuselage alone will generate a moment that tends to increase the disturbance; that is, it is unstable. The vertical tail is the main component of static directional stability. When placed at an angle of attack due to the sideslip disturbance, it generates a side force which when multiplied by the moment arm (center of gravity of airplane to aerodynamic center of vertical tail) produces a stabilizing moment that tends to move the airplane back to a zero sideslip or yaw condition. The size of the vertical tail is dependent on many factors that cannot be adequately covered here. Some observations are useful, however. The vertical tail usually has a low aspect ratio to prevent stalling. If a stall should occur, instability results and a catastrophic sideslip divergence may result.

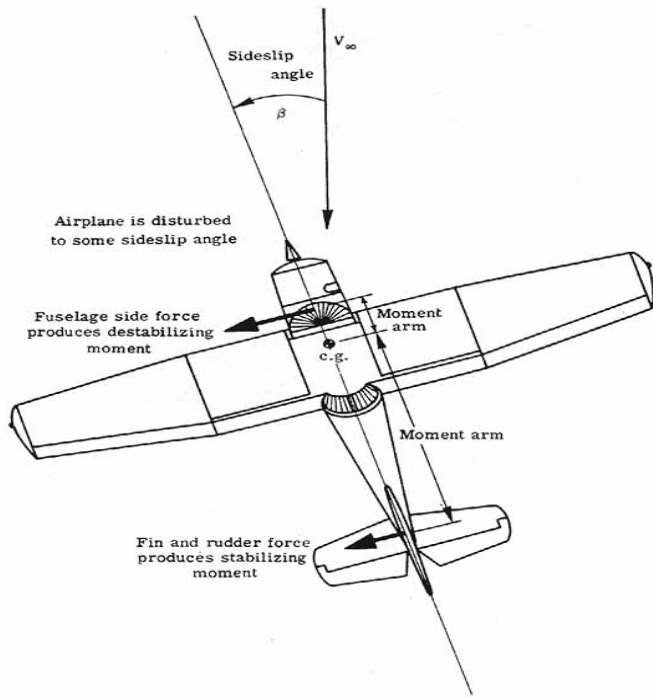


Figure 141.- Directional stability moments.

Adding more vertical tail by use of a dorsal fin extension or ventral tail area provides a stable yawing moment at large sideslip angles. [Figure 142](#) shows a B-17 bomber before and after addition of a dorsal fin extension.

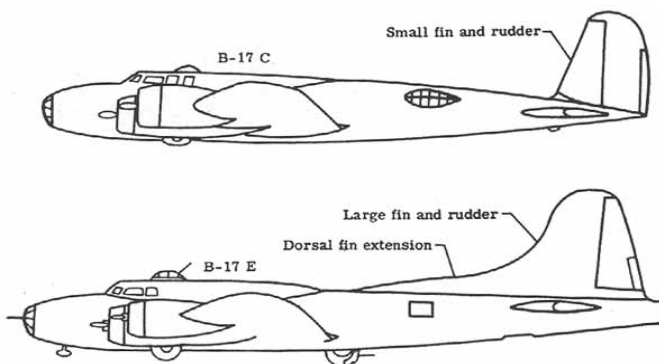


Figure 142.- Improving directional stability.

A tractor propeller of a typical airplane is a destabilizing influence on the directional stability, and it also imparts a rotational velocity to the slipstream. As shown in [figure 143](#) it produces a sidewash angle at the tail that reduces the static stability effectiveness of the tail. This effect can be very pronounced in aircraft with large engines. The Grumman F8F Bearcat, a carrier plane, would require a certain degree of rudder offset by the pilot to counteract the yaw induced by the sidewash during high powered take-offs. Contrarotating propellers are a solution to this problem.

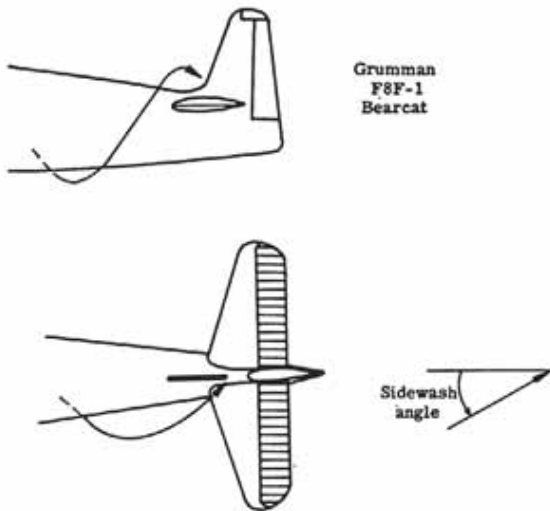


Figure 143.- Slipstream effect at tail.

The wing's degree of sweep influences the yawing moments. A sweepback wing will add to the directional stability whereas, a swept forward wing will detract from the total directional stability since it is by itself a destabilizing influence. This is a contributing reason for choosing sweepback wings over swept-forward wings.

Lateral stability - An airplane is said to possess lateral static stability if after undergoing a disturbance that rolls it to some bank angle θ [Greek letter theta], it generates forces and moments that tend to reduce the bank angle and restore the equilibrium flight condition.

Dihedral is often used as a means to improve lateral stability. [Figure 144\(a\)](#) shows a headon view of an airplane that has dihedral where the wings are turned up at some dihedral angle to the horizontal. Under the condition shown, in straight and level flight, the lift produced by both wings just equals the weight. Now, assume that a disturbance causes one wing to drop relative to the other as shown in [figure 144\(b\)](#). The lift vector rotates and there is a component of the weight acting inward which causes the airplane to move sideways in this direction. The airplane is said to sideslip and the relative free-stream direction is now in a direction toward which the airplane is sideslipping. If the airplane is laterally stable, moments arise that tend to reduce the bank angle. From geometric considerations, when wings have dihedral, the wing closer to the sideslip (that is, toward the free-stream velocity), hence the lower wing, will experience a greater angle of attack than the raised wing and hence greater lift. There results a net force and moment tending to reduce the bank angle as shown in [figure 144\(c\)](#).

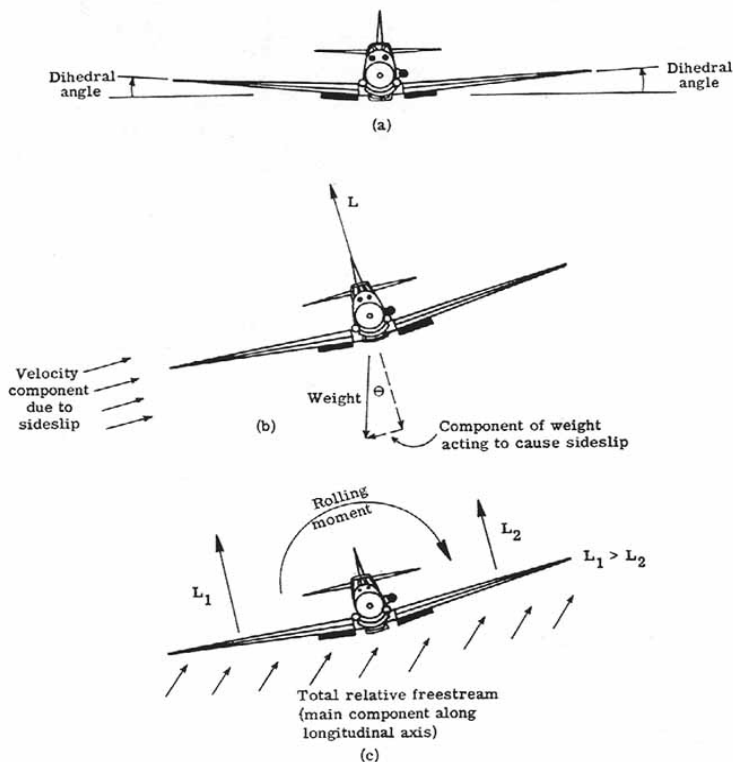


Figure 144.- Dihedral effect on lateral stability.

The position of the wing also has an impact on the lateral stability. A high-wing airplane design, as shown in [figure 145](#), contributes to the lateral stability, whereas a low wing placement has a destabilizing effect in roll. However, this effect may be counteracted by including more dihedral to improve the overall lateral stability.

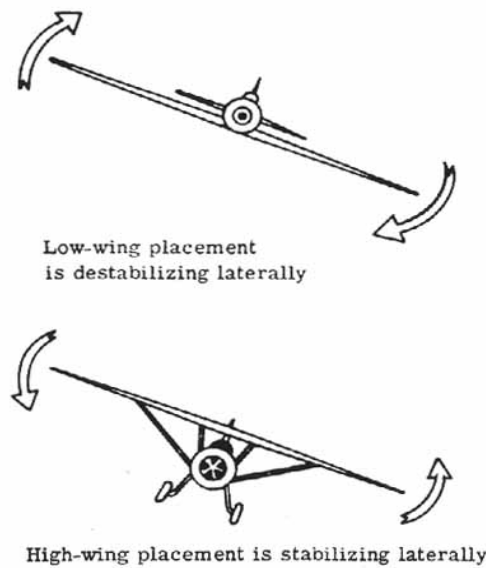


Figure 145.- Effect of wing placement on lateral stability.

Wing sweep will help promote lateral stability as [figure 146](#) shows. When a swept-wing airplane is sideslipping, the wing toward the sideslip will experience a higher velocity normal to the wing's leading edge than the wing away from the sideslip. More lift is generated on the wing toward the sideslip and a roll moment arises that tends to diminish the bank angle and return the airplane to equilibrium. It may be noted that the combination of dihedral and sweep may produce too much lateral stability and some airplanes will use a small amount of anhedral (wings turned down slightly) to lessen the lateral stability.

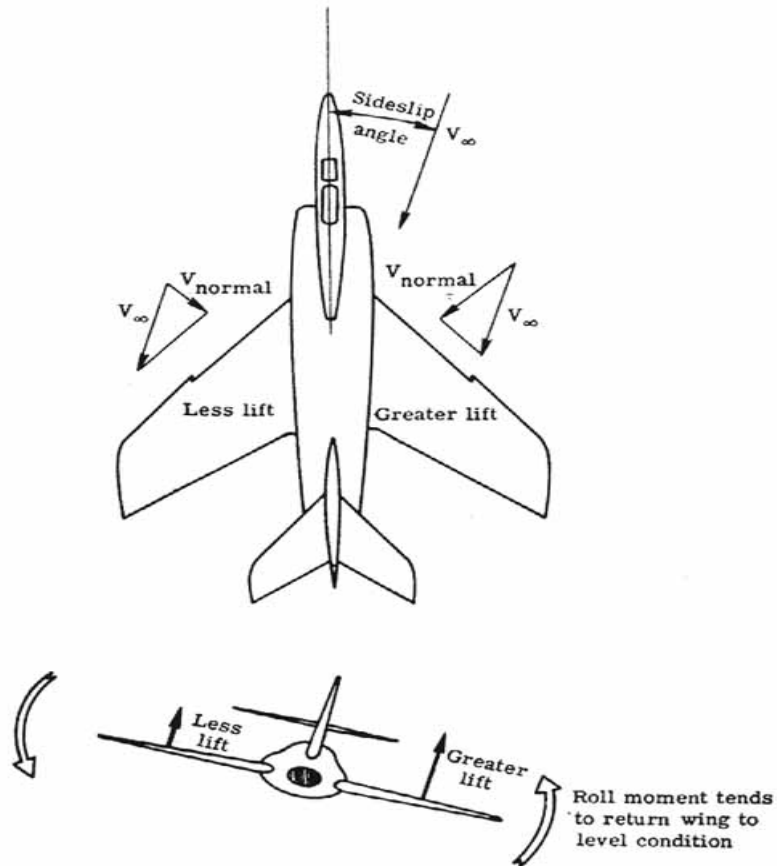


Figure 146.- Wing sweep aids lateral stability.

The effects of the fuselage and vertical tail may contribute to or detract from the airplane lateral stability. In a sideslip, there will be a side force caused by the area presented by the fuselage and vertical tail. If the side force acts above the center of gravity, as shown in [figure 147](#), there is a roll moment generated that tends to diminish the bank angle. If the side force is below the center of gravity, there is a destabilizing moment set up that will further increase the bank angle.

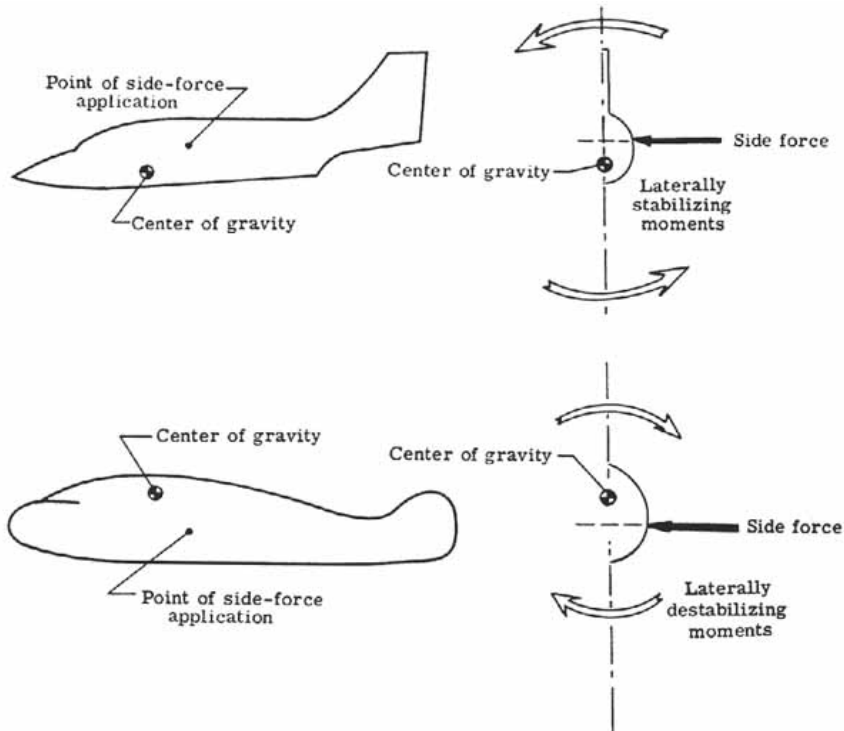


Figure 147.- Effects of fuselage and tail on lateral stability.

Destabilizing moments that also tend to increase the bank angle of an airplane in a sideslip arise because of the direction of the slipstream for a propeller-driven airplane and the use of partial span flaps. Added dihedral or sweep again may be used to decrease these detrimental effects.

Cross effects and dynamic effects - As mentioned earlier, lateral and directional stability are interrelated. Briefly stated, the motions of an airplane are such that a roll motion causes a yaw motion and a yaw motion causes a roll motion. Thus, cross-coupling exists between the directional static stability and lateral static stability and gives rise to the three important dynamic motions observed: directional divergence, spiral divergence, and Dutch roll.

Directional divergence is a result of a directionally unstable airplane. When the airplane yaws or rolls into a sideslip so that side forces on the airplane are generated, the yawing moments that arise continue to increase the sideslip. This condition may continue until the airplane is broadside to the relative wind. (See [fig. 148\(a\)](#).)

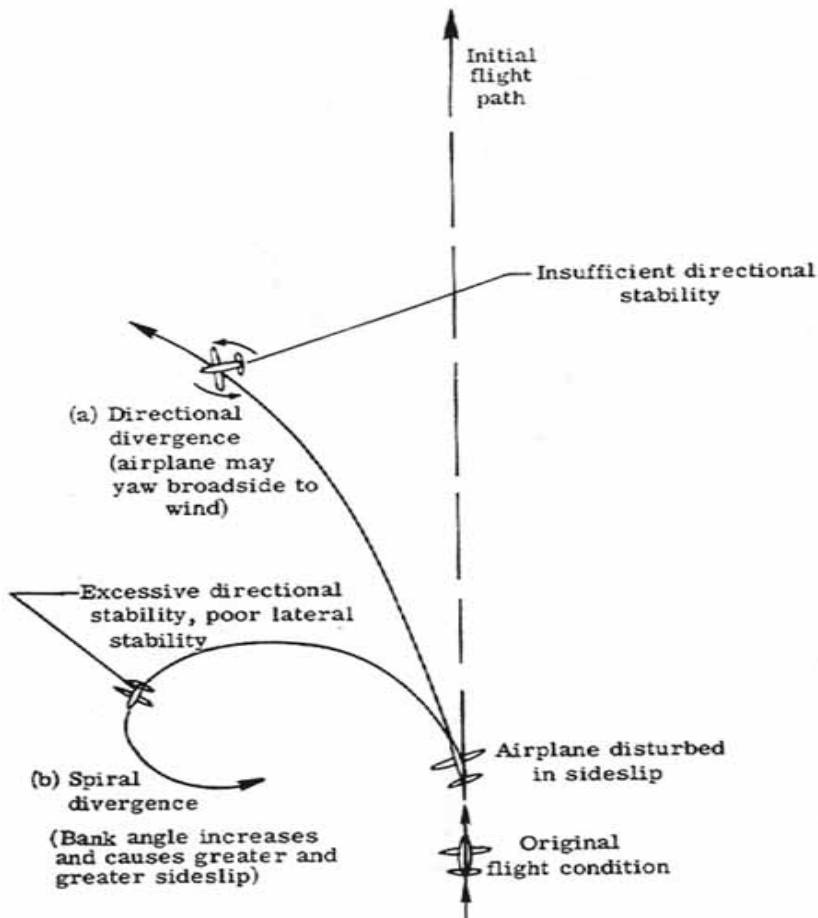


Figure 148.- Directional and spiral divergence.

Spiral divergence is characterized by an airplane that is very stable directionally but not very stable laterally; for example, a large finned airplane with no dihedral. In this case when the airplane is in a bank and sideslipping, the side force tends to turn the plane into the relative wind. The outer wing travels faster, generates more lift, and the airplane will roll to still a higher bank angle. No lateral stability is present to negate this roll. The bank angle increases and the airplane continues to turn into the sideslip in an ever-tightening spiral. (See [fig. 148\(b\)](#).)

Dutch roll is a motion exhibiting characteristics of both directional divergence and spiral divergence. The lateral stability is strong, whereas the directional stability is weak. If a sideslip disturbance occurs, as the airplane yaws in one direction, the airplane rolls away in a countermotion. The airplane wags its tail from side to side. [Figure 149\(a\)](#) illustrates this effect.

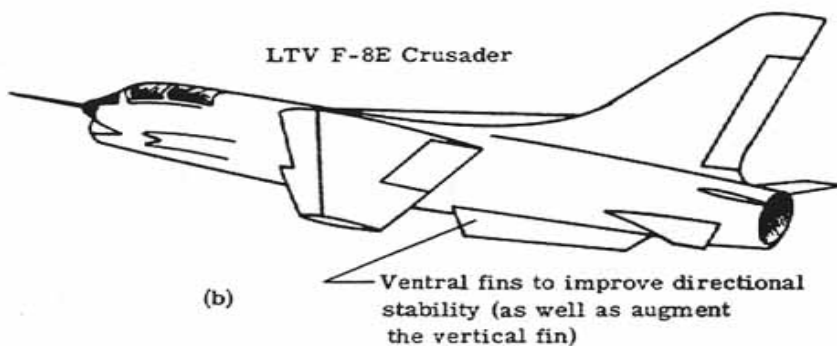
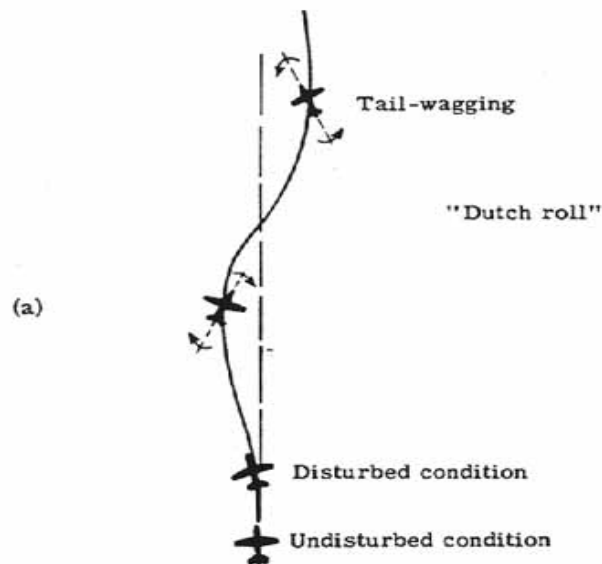


Figure 149.- Dutch roll.

Ventral fins, although primarily used to augment the vertical fin which may be in the wake of the wing at high angles of attack, are also beneficial in decreasing the lateral stability and increasing the directional stability to reduce the effects of Dutch roll.

Control

Control, whether an airplane is stable or unstable, is the ability of a pilot to change the airplane's flight conditions. It is brought about by the use of devices that alter the lift force on the surface to which they are attached.

The familiar controls are shown in [figure 15](#). They include the elevator to provide longitudinal control (in pitch), the ailerons to provide lateral control (in roll), and the rudder to provide directional control (in yaw). Some other control devices are discussed later.

[Figure 150](#) shows a simple basic control system as operated by a pilot. His link to the control surfaces is by use of the control stick and rudder pedals.

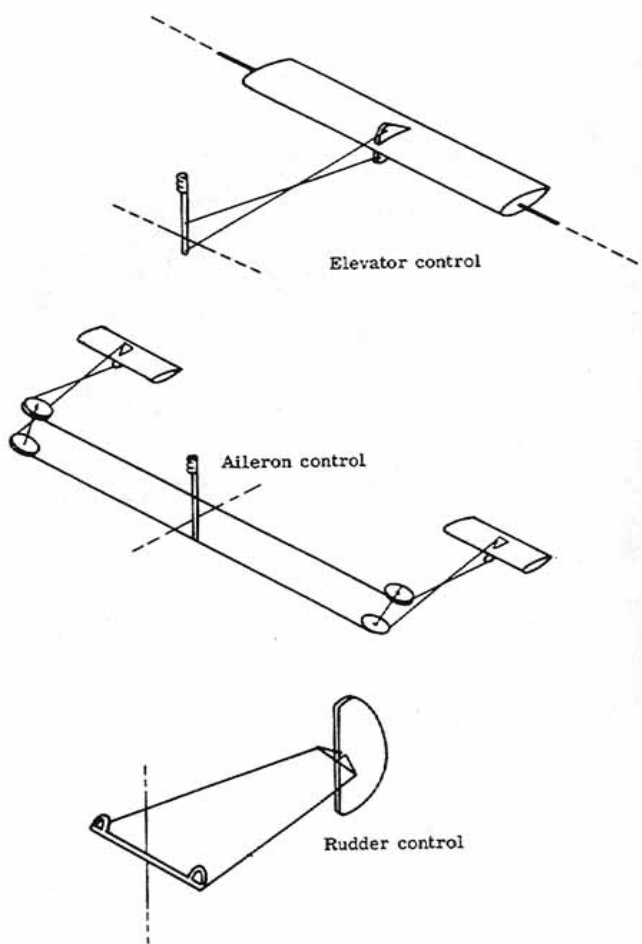
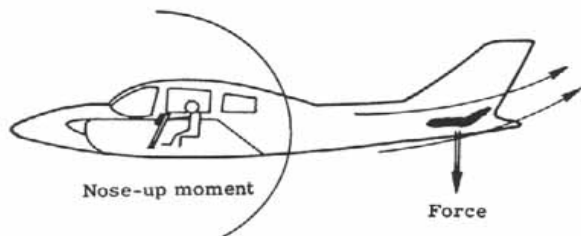


Figure 150.- Basic control system.

From the pilot's point of view, if he pulls the control stick back, the elevator turns upward ([fig. 151\(a\)](#)). This movement gives a negative camber to the entire horizontal-tail surface and a downward lift is produced. This, in turn, produces a nose-up moment about the airplane center of gravity and the airplane pitches upwards. A side motion of the control stick results in the movement of one aileron up and the other down as shown in [figure 151\(b\)](#). This reduces the camber of one wing while it increases the camber of the other wing. One wing then produces more lift than the other and a rolling moment results. This condition causes the airplane to roll about its longitudinal axis in the direction toward which the control stick was pushed.

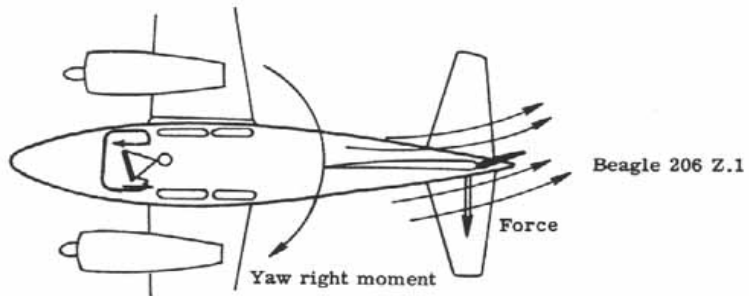
Applying pressure to the rudder pedals will deflect the rudder. If the pilot pushes the right pedal forward (the left pedal comes back), the rudder deflects to the right. As shown in [figure 151\(c\)](#), this movement increases the vertical tail camber and a tail force to the left results. A moment arises that yaws the nose to the right and hence, the airplane turns right.



(a) Elevator control.



(b) Aileron control.



(c) Rudder control.

Figure 151.- Control surface operations.

Control effectiveness is a measure of how well a control surface does its job. In general, the larger the control surface is with respect to the entire surface to which it is fitted, the greater the control effectiveness. Also, high-aspect-ratio control surfaces possess greater control effectiveness than low-aspect-ratio surfaces. (See [fig. 152](#).)

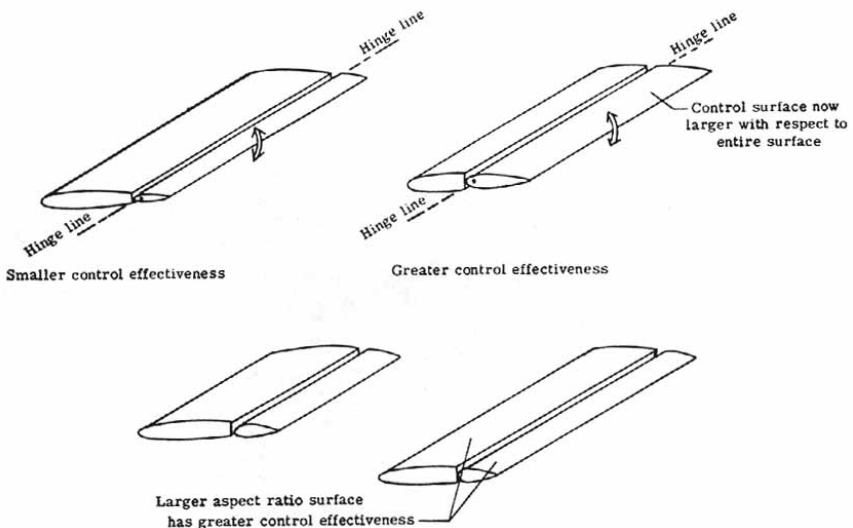
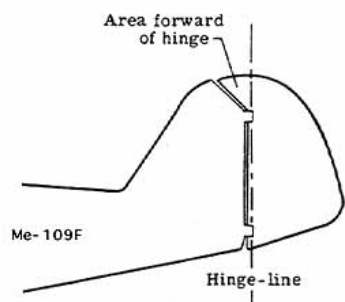


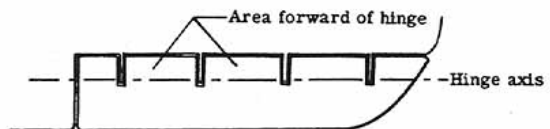
Figure 152.- Control effectiveness.

Balanced controls - Whenever a pilot deflects a control surface into the fluid flow, a pressure distribution will be set up that tends to force the control surface back to its original position. The force necessary to hold a particular control surface deflection may or may not be small depending upon the control surface design. Not only must the pilot be able to deflect the surface at will, but the forces should be small enough to insure that the pilot does not tire. Balance is used to reduce the deflection forces required. In [figure 153\(a\)](#) two forms of aerodynamic balance are shown. The hinge of the surface is set so that when the surface is deflected, the air that strikes the surface forward of the hinge creates a pressure distribution, hence force, that helps turn the surface even further. This counteracts the force aft of the control surface tending to reduce the control surface deflection. By careful design, the pilot-supplied effort is considerably reduced. However, care must be exercised so that the controls are not "too light" (little effort needed to move them) lest the pilot unwittingly over control the airplane to its destruction. The control systems of today's airplanes are power-operated and, whether aerodynamic balance is used or not, the pilot-felt control forces are small. In fact, artificial feel is incorporated into the controls so that the pilot has a sense of feel in the controls.

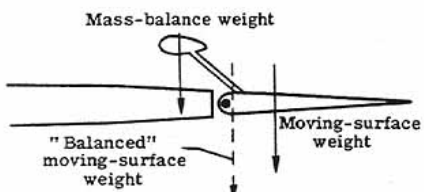
Mass balance is employed in front of the hinge line of a control surface to prevent flutter of the surface which may occur due to accelerations on the airplane. It is a dynamic effect and a control surface that deflects about on its own may lead to dynamic instability of the airplane. The solution is to move the control surface center of gravity near or forward of the hinge line. This may be accomplished by adding lead forward of the hinge line or as shown in [figure 153\(b\)](#), by using small mass balances.



(a) Horn balance.



(a) Inset hinge balance.



(b) Mass-balanced weight.

Figure 153.- Aerodynamic and mass balance.

Tabs - Tabs are auxiliary control surfaces placed at the trailing edges of the primary control surfaces. Tabs serve two purposes: (1) to balance and (2) to trim.

As shown in [figure 154\(a\)](#), balance tabs are set up to move opposite and proportional to the primary control surface movement. They are used to assist the pilot in moving the control surface and in reducing stick forces. If the pilot wishes, for example, to move the elevator down, the balance tab will deflect upward as the elevator deflects downward and the pressure distribution set up will create a force, hence moment, to move the control surface down. Because they are placed at the trailing edge, balance tabs possess long moment arms and are very powerful in action.

Trim tabs are used to reduce pilot stick forces to zero for particular chosen flight conditions. They are very important since they insure that the pilot will not tire in holding steady flight. Trim tabs may be set when the airplane is on the ground or manually operated and set by the pilot. [Figure 154\(b\)](#) shows a deflected control surface with the trim tab set to reduce moments about the hinge line to zero. The airplane will continue to fly in this condition and no pilot effort is required to hold the control surface deflection. When a new control deflection is needed, the trim tab must be readjusted for the new setting (if adjustable).

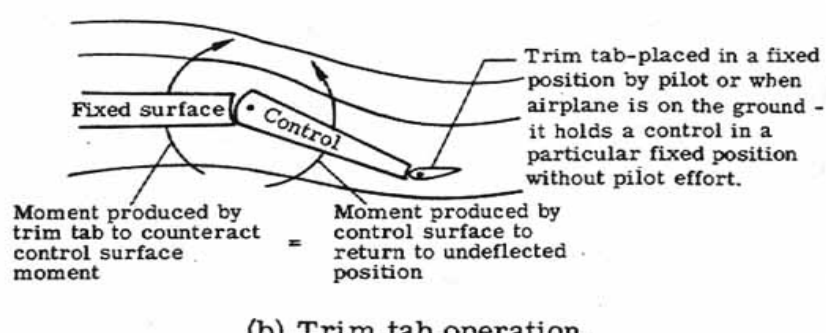
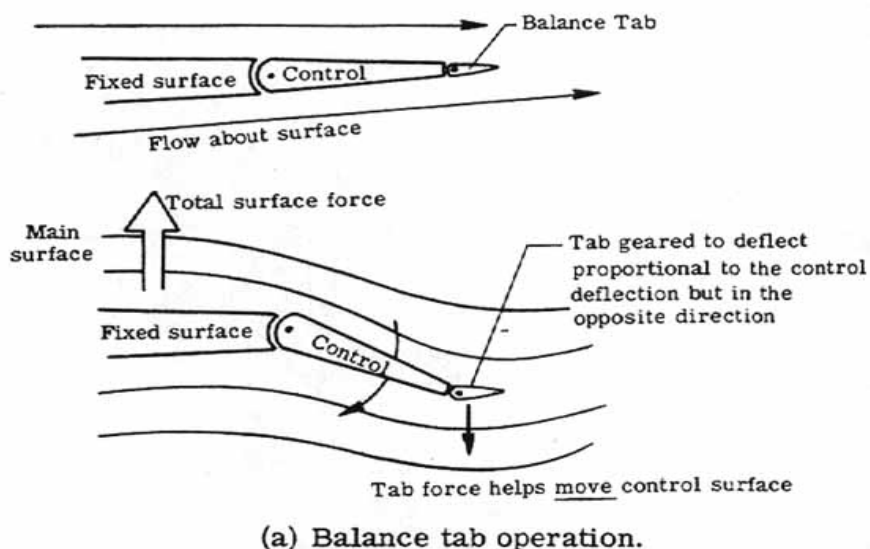


Figure 154.- Balance and trim tabs.

Other control devices - Some control devices do not fall into the conventional categories outlined above. They are used in unusual flight circumstances or for added control advantages. Included are spoilers, all-moving surfaces, reaction controls, and the butterfly tail.

Spoilers, previously discussed with respect to subsonic flow, are used to reduce or "dump" the lift on a wing by altering the pressure distribution. They are useful on gliders to vary the lift- drag ratio for altitude control and on airliners on landing to reduce lift quickly to prevent the airplane from bouncing into the air. But, they are also useful in lateral (roll) control. At low speeds, ailerons are the primary lateral control devices. At high speeds, however, they may cause bending moments on the wing that distort the wing structure. At transonic speeds compressibility effects may limit their effectiveness. Spoilers may be used to avoid these disadvantages. As shown in [figure 155](#) by reducing the lift on one wing, the spoiler will cause a net rolling moment to roll the airplane about its longitudinal axis.

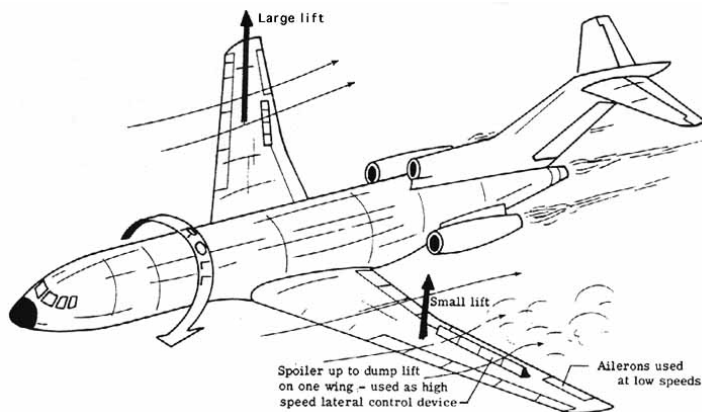


Figure 155.- Lateral control with spoilers.

Control effectiveness may be increased by increasing the chord length of the control surface relative to the entire surface to which it is fitted. The limiting case is the all-moving control surface. Whereas the conventional control surface changed lift by a change in camber, the all-moving control surface controls lift by angle-of-attack variations. Examples are to be seen on the horizontal-tail surfaces of the F-4 Phantom and the F-14A airplanes ([fig. 156](#)). By being able to change its angle of attack, the all-moving surfaces can remain out of a stalled condition. The conventional control surfaces are considerably less effective at high speeds where compressibility effects are dominant. The all-moving horizontal tails may be moved independently as well to provide lateral control.

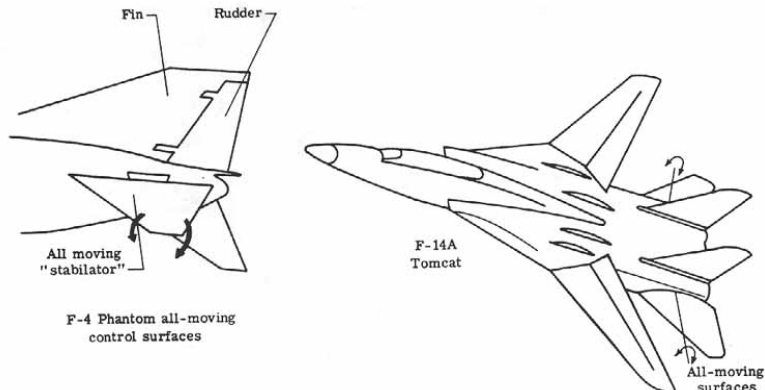


Figure 156.- Examples of all-moving surfaces.

At low dynamic pressures aerodynamic control surfaces become largely ineffective because only small forces and moments are present. Under these conditions, reaction control devices may be used. These are small rockets placed at the extremities of the aircraft to produce the required moments necessary to turn the airplane about each of its axes. At zero or low speeds, the Hawker Harrier VTOL airplane uses reaction rockets placed in the nose, wing tips, and tail as shown in [figure 157](#).

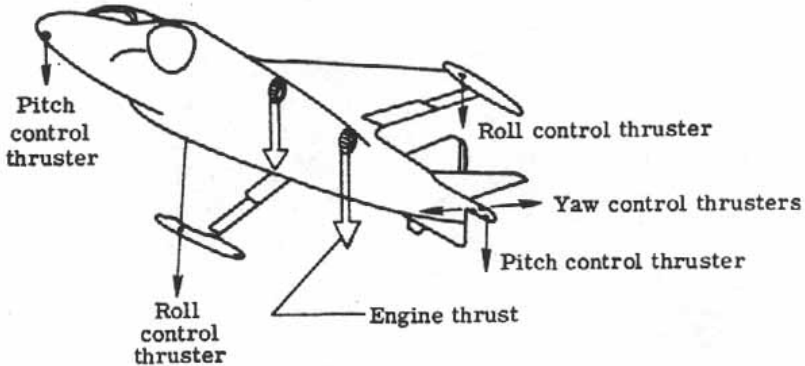
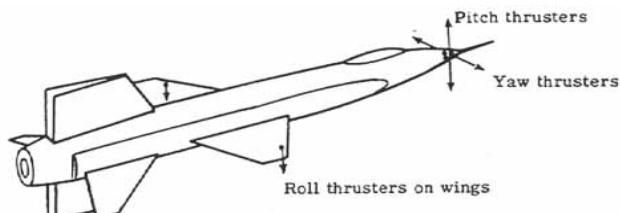
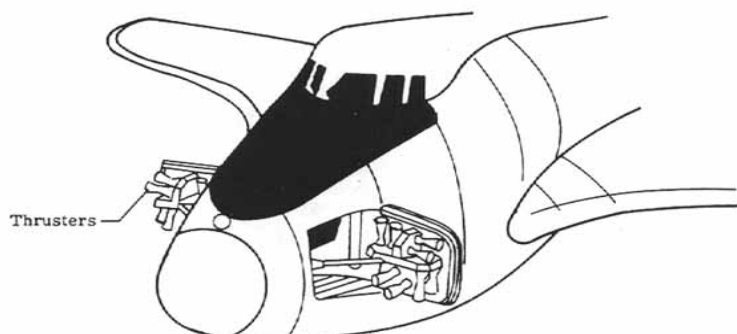


Figure 157.- Hawker Harrier reaction control system.

The North American X-15 rocket plane used reaction controls when it flew at altitudes of such low air density that the aerodynamic surfaces were useless ([fig. 158\(a\)](#)). In the same manner, the Space Shuttle will use reaction controls ([fig. 158\(b\)](#)) for the same reason to change its pitch, yaw, and roll attitudes.



(a) X-15 reaction controls.



(b) Space Shuttle reaction controls.

Figure 158.- Reaction controls.

The butterfly tail ([fig. 159\(a\)](#)) is an interesting variation of the conventional control system since it combines the functions of the vertical and horizontal tail. The advantages claimed are reduced weight and drag. However, there are increased problems in cross-coupling of the pitch, yaw, and roll motions and reduced directional dynamic stability. To pitch up or down, both control surfaces are moved up or down [[178](#)] together ([fig. 159\(b\)](#)). To yaw right or left the "ruddervators" as they are called are moved in opposite directions through equal deflections as shown in [figure 159\(c\)](#).

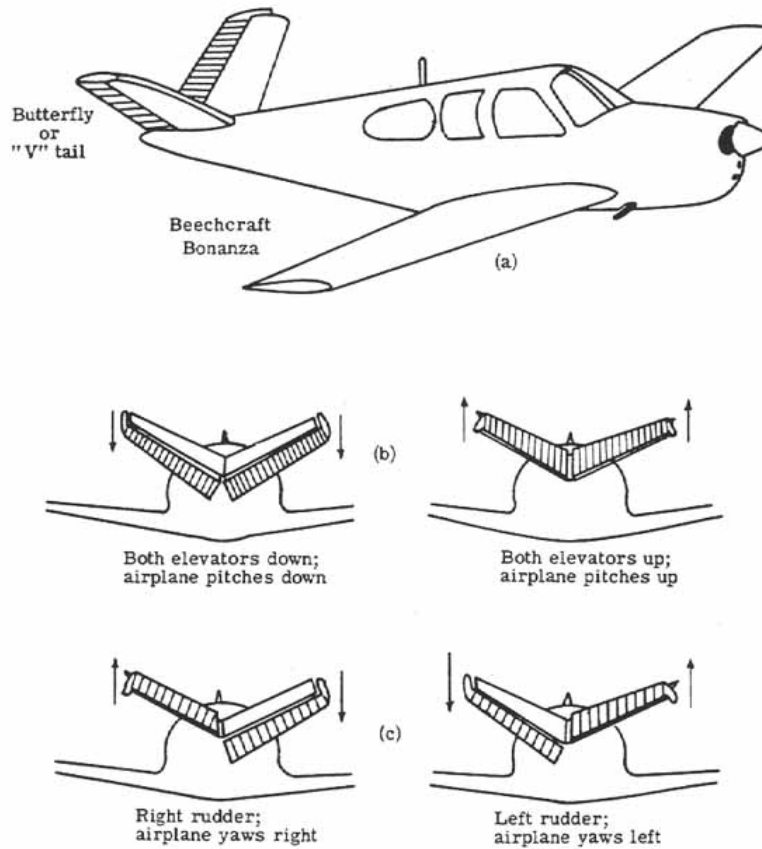


Figure 159.- Butterfly tail operation.

This brief introduction to stability and control has shown many factors that influence the design of an airplane. It must be stressed that the final design is at best a compromise to often conflicting parameters. As one moves towards multi-mission airplanes, the compromises become more frequent. Cost and competition are the final arbiters of design.

Appendix A

AERONAUTICAL NOMENCLATURE

General Definitions	
aircraft	any machine or weight-carrying device (whether lighter or heavier than air) designed to be supported by the air, either by buoyancy or by dynamic action
aerodyne	that class of aircraft being heavier than air and deriving its lift in flight chiefly from aerodynamic forces
airplane (aeroplane)	a subset of aerodynamics, specifically, a mechanically driven fixed-wing aircraft, heavier than air, which is supported by the dynamic reaction of the air against its wings
aerodynamics	the science that deals with the motion of air and other gaseous fluids, and of the forces acting on bodies when the bodies are in relative motion with respect to such fluids
aerostat	that class of aircraft being lighter than air and deriving its support chiefly from buoyancy derived from aerostatic forces
airship	a subset of aerostats, specifically, an aerostat provided with a propelling system and with a means of controlling the direction of motion
aerostatics	the science that deals with the equilibrium of gaseous fluid and of bodies immersed in them
aeronautics	the science and art of designing, constructing, and operating aircraft

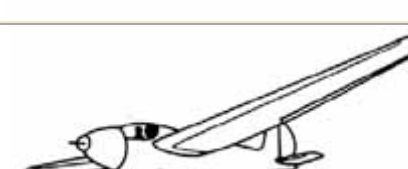
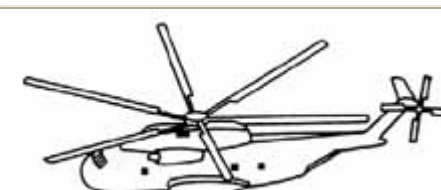
Aircraft Types

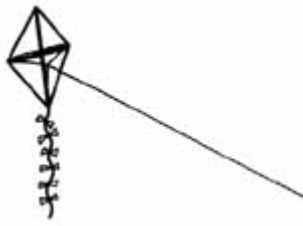
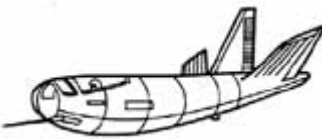
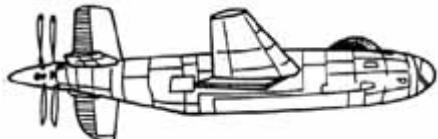
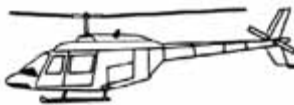
Figure 160 presents sketches of the aircraft types defined herein.

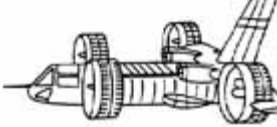
airships (dirigibles)	nonrigid (blimp): a lighter-than-air craft having a gas bag, envelope, or skin that is not supported by any framework or reinforced by stiffening. Its shape is maintained by the internal pressure of the gas with which it is filled. semirigid (sometimes blimp): a dirigible having its main envelope reinforced by a keel but not having a completely rigid framework. rigid: a dirigible having several gas bags or cells enclosed in an envelope supported by an interior rigid framework structure.
amphibian	an airplane designed to rise from and alight on either water or land
autogyro	a rotary-wing aerodyne whose rotor is turned throughout its flight by air forces resulting from the motion of the craft through the air
balloon	a bag, usually spherical, made of silk or other light, tough, nonporous material filled with some gas which is lighter-than-air. It is an aerostat without a propelling system.
biplane	an airplane having two wings or supporting surfaces, one located above the other
boat, flying	type of airplane in which the fuselage (hull) is especially designed to provide flotation on water
glider	an engineless airplane flown by being manipulated into air currents that

	keep it aloft
helicopter	a type of rotary-wing aerodyne whose lift and forward thrust are derived from airfoils mechanically rotated about an approximately vertical axis
kite	a light frame, usually of wood, covered with paper or cloth and designed to be flown in the wind at the end of a string
lifting body	an aerodyne which derives most or all of its lift in flight from the shape of its fuselage, the wings being essentially nonexistent
monoplane	an airplane having but one wing or supporting surface
ornithopter	a type of aircraft achieving its chief support and propulsion from the bird-like flapping of its wings
parachute	cloth device, consisting of a canopy and suspension lines, which basically produces a drag force to retard the descent of a falling body
paraglider	a flexible-winged, kite-like vehicle designed for use in a recovery system for launch vehicles
pusher airplane	an airplane with the propeller or propellers aft of the main supporting surfaces
rotary-wing aircraft	a type of aerodyne which is supported in the air wholly or in part by wings or blades rotating about a substantially vertical axis
tailless airplane	an airplane in which the devices used to obtain stability and control are incorporated in the wing
tractor airplane	an airplane with the propeller or propellers forward of the main supporting surfaces
STOL	short take-off and landing airplane
VTOL	vertical take-off and landing airplane
V/STOL	an airplane which has both STOL and VTOL capabilities

Figure 160.- Examples of aircraft types.

Nonrigid airship	
Rigid airship	
Balloon	
Amphibian (Grumman SA-16A Albatross)	
Autogyro	
Biplane (Bristol F2B)	
Flying boat (Shin Meiwa PX-S)	
Glider (Schweizer 1-23)	
Helicopter (Sikorsky CH-3C)	

Kite	
Lifting body (HL-10)	
Monoplane (Piper Arrow)	
Flapping wing ornithopter	
Parachutes	 <p>Cross or plus</p>  <p>Modified ring-sail</p>  <p>Disk-Gap-Band</p>
Paraglider	
Pusher airplane (XB-42)	
Rotary-wing aircraft (Bell Jet Ranger)	

Tailless airplane (Avro 707B)	
Tailless airplane (YB-49)	
Tractor airplane (Boeing 377 Stratocruiser)	
STOL- Short Take-off and landing airplane (DHC-6 Twin Otter)	
VTOL - Vertical take-off and landing airplane (P1227 Harrier)	
V/STOL airplane (X-22A)	

Appendix B

DIMENSIONS AND UNITS

There is a fundamental difference between dimensions and units. A dimension represents the definition of an inherent physical property which remains independent of the particular scheme used to denote its measure. For example, the quantity of matter present in a lump of metal has the dimension of mass and the physical size of the edge of a book has the dimension of length.

A unit represents the particular, arbitrary scheme used to denote the magnitude of a physical property. Thus, the mass of matter in the lump of metal may be expressed in kilograms or slugs and the length of the book expressed in meters or feet depending on the system of units selected. Usually the quantity to be measured influences the choice of units to be employed, that is, meters or feet to measure the length of the book rather than kilometers or miles.

Basic Dimensions

There are four basic dimensions of general interest to aerodynamicists. These are called the basic or primary dimensions and are length, mass, time, and temperature. They may be abbreviated by using, respectively, L, M, T, and θ [Greek letter theta].

Derived Dimensions

The dimensions of all other quantities may be found to be combinations of quantities expressible in terms of the basic or primary dimensions. These are known as derived or secondary dimensions. For example, area may be represented as a length times a length or L^2 . A list of the more common quantities encountered in aerodynamics and their dimensions are included in table II.

Angular Measurement

The measure of the central angle of a circle is defined as the ratio of the subtended arc of the circle divided by the radius, that is, a ratio of two lengths. Thus, this measure is dimensionless but is assigned a special name of radians. Additionally one may express the angle in degrees by noting that an angle of 1 radian equals about 57.3° . The fact that both radian measure and degree measure are dimensionless means that the numerical value of an angle does not change from one system of units to another.

Systems of Units

There are two basic engineering systems of units in use in aerodynamics. They are the International System of Units (SI) and the British Engineering System of Units (B.E.S.). In 1964 the United States National Bureau of Standards officially adopted the International System of Units to be used in all of its publications. The National Aeronautics and Space Administration has adopted a similar policy and this is the system of units used in this report. Table II lists the SI and B.E.S. units for both the basic dimensions and some of the more common aerodynamic quantities.

Vectors and Scalars

Vectors are quantities that have both a magnitude and a direction. Examples of physical quantities that are vectors are force, velocity, and acceleration. Thus, when one states that a car is moving north at 100 kilometers per hour, with respect to a coordinate system attached to the Earth, one is specifying the vector quantity velocity with a magnitude (100 kilometers per hour) and a direction (north).

Scalars are quantities that have a magnitude only. Examples of physical quantities that are scalars are mass, distance, speed, and density. Thus, when one states only the fact that a car is moving at 100 kilometers per hour one has specified a scalar, speed, since only a magnitude (100 kilometers per hour) is given (that is, no direction is specified).

To represent a vector on a diagram, an arrow is drawn. The length of the arrow is proportional to the magnitude of the vector and the direction of the arrow corresponds to the direction of the vector. [Figure 161](#) shows the side view of a wing called the airfoil cross section (or simply airfoil section). Two aerodynamic forces are known to act on the section: lift and drag. They are vectors and may be drawn to act through a special point called the center of pressure discussed in the text. In the first step a scale is chosen and the force magnitudes are scaled. The second step is to place the vectors at the center-of-pressure point in the directions specified from the physical definition that lift always acts perpendicularly to the incoming velocity of the air V_∞ and drag always acts parallel to and away from the incoming velocity of the air.

Vectors may be added together (composition) to form one vector (the resultant) or one vector may be broken down (resolution) into several components. In [figure 161](#) the lift and drag have been composed into the resultant shown. The resultant can be resolved back into the lift and drag components.

TABLE II.- SYSTEMS OF UNITS

Quantity	Basic dimensions	Units	
		SI	B.E.S
Length	L	meter	foot
Mass	M	kilogram	slug
Time	T	second	second
Temperature	θ [Greek letter theta]	$^{\circ}\text{C}$ (relative)	$^{\circ}\text{F}$ (relative)
		K (absolute)	$^{\circ}\text{R}$ (absolute)
Quantity	Derived dimensions	Units	
		SI	B.E.S
Area	L^2	meters^2	feet^2
Volume	L^3	meters^3	feet^3
Velocity	LT^{-1}	meters/second	feet/second
Acceleration	LT^{-2}	meters/second 2	feet/second 2
Force	MLT^{-2}	newton	pound

Pressure	$ML^{-1}T^{-2}$	newtons/meter ²	pounds/foot ²
Density	ML^{-3}	kilogram/meter ³	slugs/foot ³
Kinematic viscosity	L^2T^{-1}	meters ² /second	feet ² /second
Momentum	MLT^{-1}	newton-second	pound-second
Energy	ML^2T^{-2}	joule	foot-pound
Power	ML^2T^{-3}	watt	foot-pound/second
Angle	-	radian or degree	radian or degree
Angular velocity	T^{-1}	radians/second	radians/second
Angular acceleration	T^{-2}	radians/second ²	radians/second ²
Moment of inertia	ML^2	kilogram-meter ²	slug-ft ²

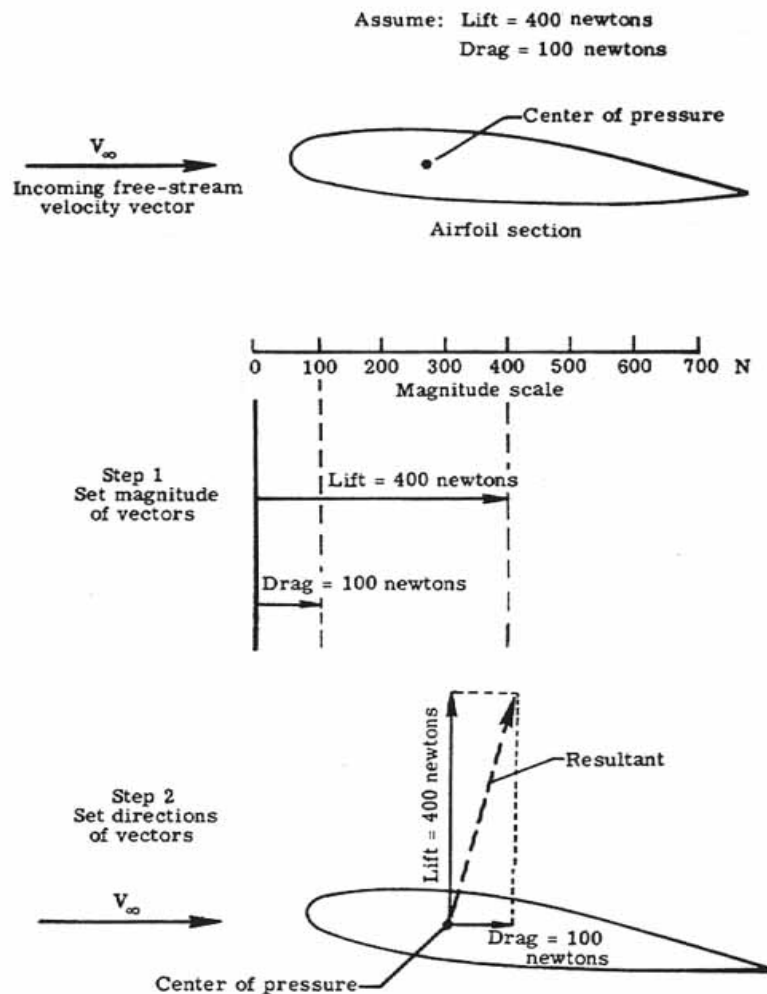
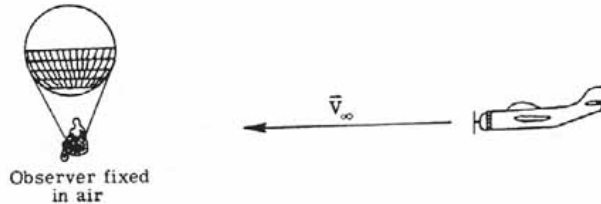


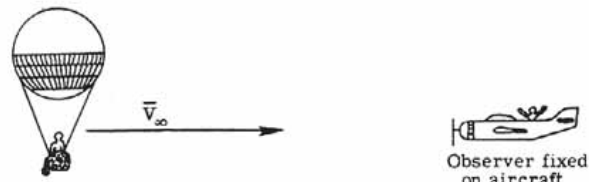
Figure 161.- Vector representation.

Motion

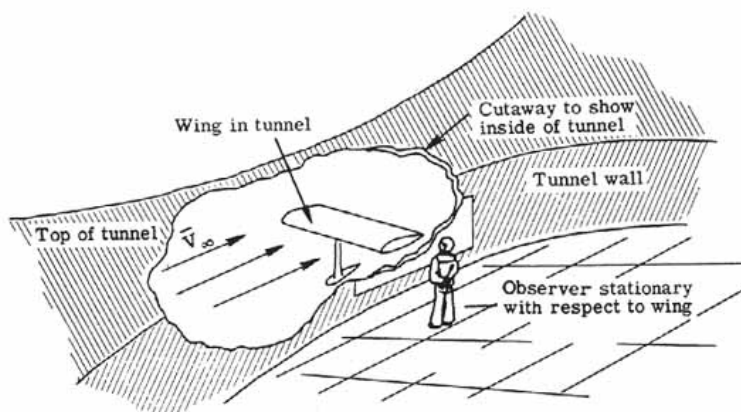
Motion is the movement or change in position of a body. Motion is always with respect to a particular observer. Consider the flight of an aircraft through the air. One may adopt two points of view. First an observer fixed in the air sees the aircraft approach at velocity V_∞ (See [fig. 162\(a\)](#).) On the other hand an observer fixed on the aircraft sees the air (or observer fixed in air) approach him at velocity V_∞ from the opposite direction. (See [fig. 162\(b\)](#).) The two observers read the same magnitude of velocity (that is, speed) but indicate opposite directions. In many cases, for example, in the use of a wind tunnel, the second point of view is adopted where the aircraft or airfoil is fixed in the tunnel and air is forced to flow past it. (See [fig. 162\(c\)](#).)



(a) Observer fixed in air.



(b) Observer fixed on aircraft.



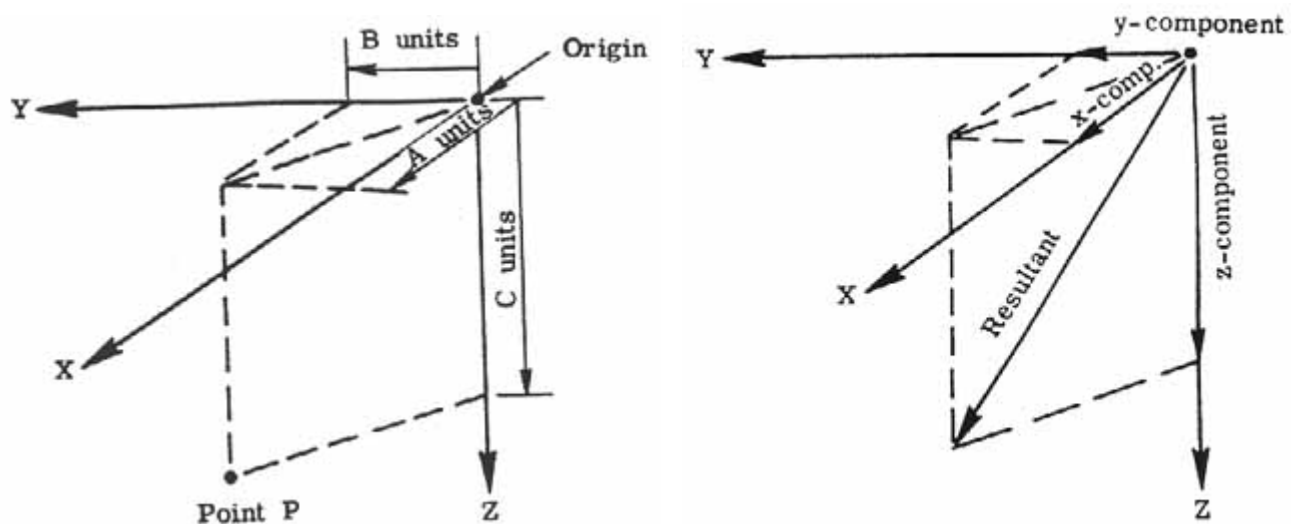
(c) Wind-tunnel operation – wing fixed in place and air placed in motion over wing with velocity \bar{V}_∞ .

Figure 162.- Relative motion.

Appendix C

COORDINATE SYSTEMS

A point in space may be located by referencing it to a known point. The known point is considered to be the origin of three mutually perpendicular lines which constitute what is known as a rectangular Cartesian coordinate system. The unknown point is then located by specifying the number of units along each of the three axes as measured from the origin. This system is shown in [figure 163\(a\)](#). Additionally, a vector oriented at random in space whose tail is set at the origin may be resolved into its three components along the X, Y, and Z axes. (See [fig. 163\(b\)](#).) Three coordinate systems, employing right-handed rectangular Cartesian axes, are generally used. They are the Earth-axis system, the body-axis system, and the wind-axis system.



(a) Location of a point in a right-hand rectangular coordinate system. Right-hand system-X, Y, Z axes point along thumb, first and second fingers of right hand, respectively.

(b) Location of a vector in a right-hand rectangular Cartesian coordinate system. Resolution into components.

Figure 163.- Rectangular Cartesian coordinate system.

Earth-Axis System

In the Earth-axis system the Earth is considered to be flat and nonrotating. The X and Y axes lie in the geometric plane of the Earth, X pointing north and Y pointing east. The Z-axis points down toward the center of the Earth as shown in [figure 164](#).

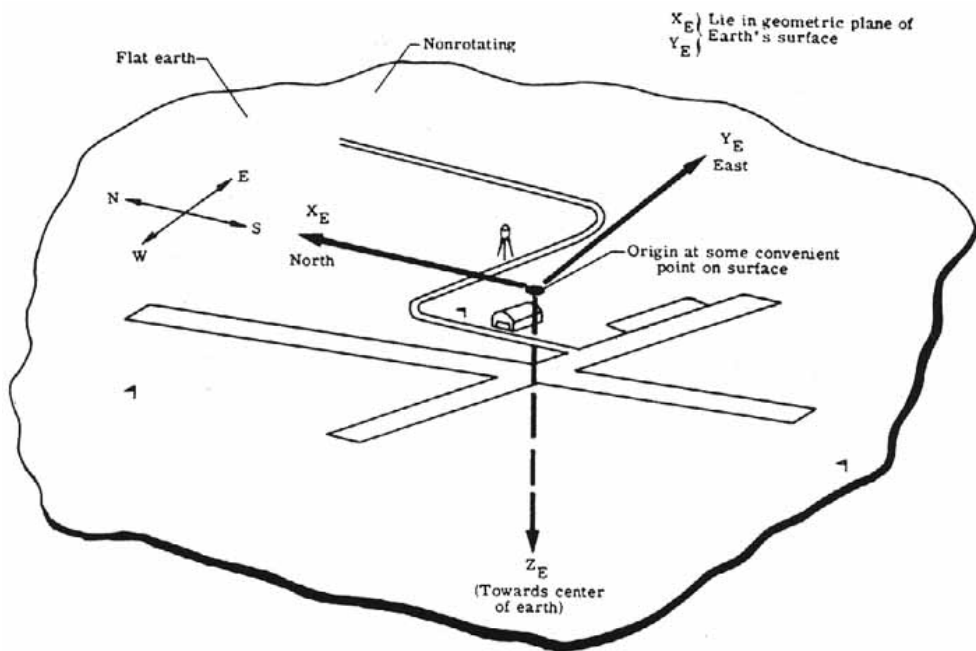


Figure 164.- Earth-axis system.

Body-Axis System

In the body-axis system the rectangular Cartesian axis system is oriented such that the X-axis points out of the nose of the aircraft and is coincident with the longitudinal axis of the aircraft. The Y- axis is directed out of the right wing of the aircraft and the Z-axis is perpendicular to both the X and Y axes and is directed downward. The origin of the entire system is taken to be the center of gravity of the aircraft. At this point it is useful to define the important angular displacement terms roll, pitch, and yaw.

- Roll: the airplane rotates about its longitudinal axis (that is, X-axis). A positive roll is defined as the Y-axis turning toward the Z-axis, that is, the right wing drops.
- Pitch: the airplane rotates about the Y-axis. A positive pitch is defined as the Z-axis turning toward the X-axis, that is, the nose of the airplane rises.
- Yaw: the airplane rotates about the Z-axis. A positive yaw is defined as the X-axis turning towards the Y-axis, that is, the nose moves to the right ("Clockwise when viewed from above").

The body-axis system and the concepts of roll, pitch, and yaw are illustrated in [figure 165](#).

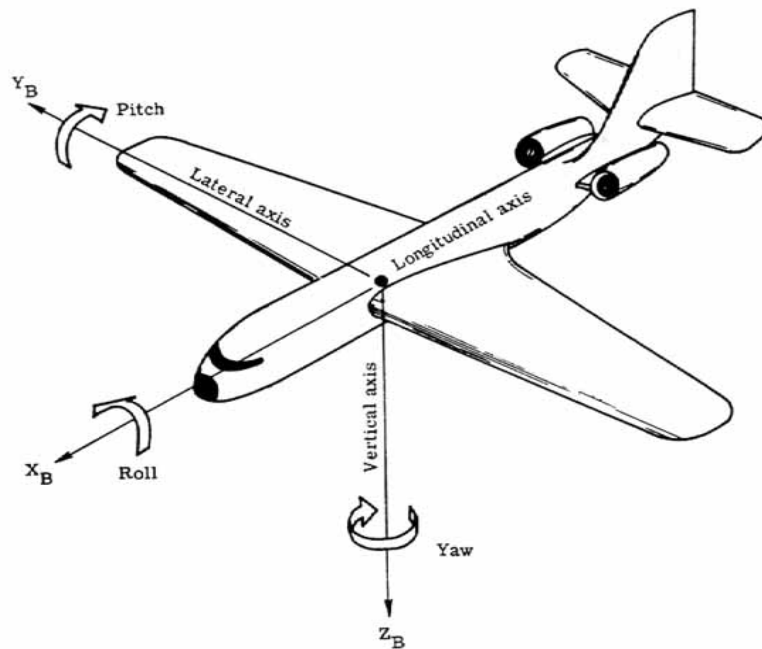


Figure 165.- Body-axis system.

Wind-Axis System

In the general wind-axis system, the origin of the rectangular Cartesian system is at the center of gravity of the aircraft. The X-axis points into the direction of the oncoming free-stream velocity vector. The Z-axis lies in the plane of symmetry of the airplane and is perpendicular to the X-axis and is directed generally downward. The Y-axis is perpendicular to both the X and Z axes ([fig. 166\(a\)](#)). In many problems of interest airplane motion is in the geometric plane of symmetry (no yawing motion) so that the X-axis also lies in the plane of symmetry. This means that the Y-axis points out of the right wing. The Z-axis again is in the plane of symmetry. The system then is termed the simplified wind-axis system and is illustrated in [figure 166\(b\)](#)).

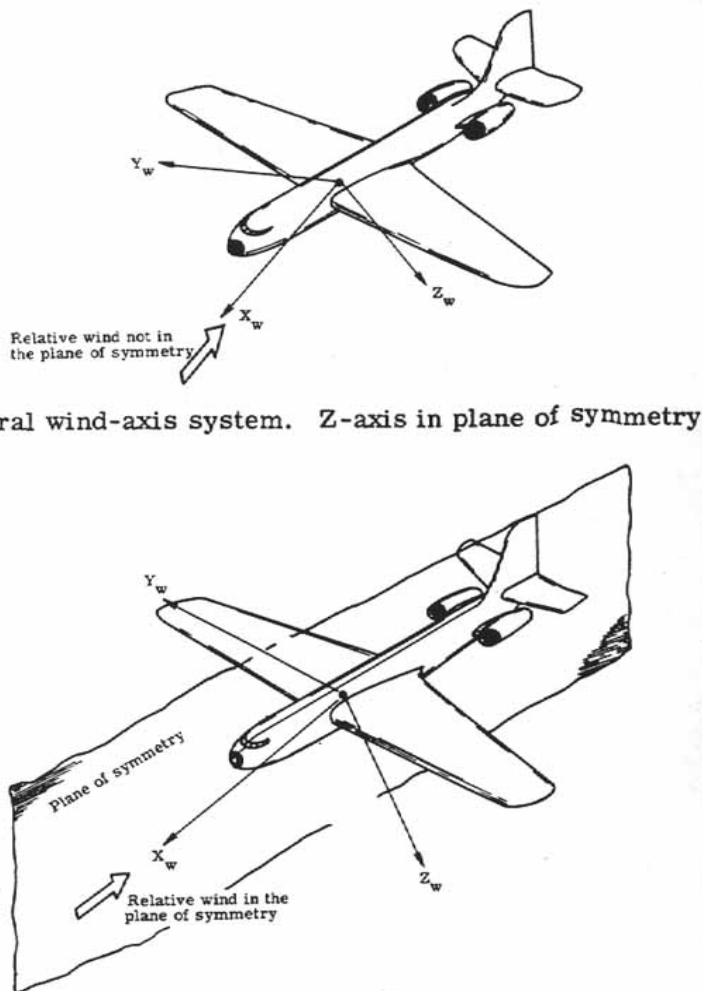


Figure 166.- Wind-axis system.

Bibliography

- Abbott, Ira H.; and Von Doenhoff, Albert E.: Theory of Wing Sections. Dover Publ., Inc., c.1959.
- Alelyunas, Paul: L > D Spacecraft. Space/Aeronaut., vol. 47, no. 2, Feb. 1967, pp. 52-65.
- Anderton, David A.: Aeronautics: Space in the Seventies. NASA EP-85, 1971.
- Anon.: The Lore of Flight. Tre Tryckare Cagner & Co. (Gothenburg), c.1970.
- Anon.: U.S. Standard Atmosphere Supplements, 1966. Environ. Sci. Serv. Admin., NASA, and U.S. Air Force, 1966.
- Applegate, L. Burnell; Benn, Omer; et al.: Fundamentals of Aviation and Space Technology. Inst. Aviat., Univ. of Illinois, c.1971.
- Archer, Robert D.: Evolution of the Supersonic Shape. Space/Aeronaut., vol. 48, no. 1, July 1967, pp. 89-104.
- Ayers, Theodore G.: Supercritical Aerodynamics: Worthwhile Over a Range of Speeds. Astronaut. & Aeronaut., vol. 10, no. 8, Aug. 1972, pp. 32-36.
- Butler, S. F. J.: Aircraft Drag Prediction for Project Appraisal and Performance Estimation. Aerodynamic Drag, AGARD CP No. 124, 1973.
- Caswell, Charles H.: Basic Science for the Aviation Maintenance Technician. McCutchan Pub. Corp. c.1970.
- Collis, R. T. H.: Treating the Sonic Boom. Astronaut. & Aeronaut., vol. 8, no. 6, June 1970, pp. 42-43.
- Corning, Gerald: Aerospace Vehicle Design. Published by author (College Park, Md.), c.1964.
- Dommasch, Daniel O.; Sherby, Sydney S.; and Connolly, Thomas F.: Airplane Aerodynamics. Pitman Pub. Corp., 1951.
- Duke, Neville; and Lanchberry, Edward: "Sound Barrier"- The Story of High-Speed Flight. Philosophical Library, Inc., 1955.
- Dwiggins, Don: The SST: Here It Comes Ready or Not. Doubleday & Co., Inc., 1968.
- Eggers, A. J., Jr.; Petersen, R. H.; and Cohen, N. B.: Hypersonic Aircraft Technology and Applications. Astronaut. & Aeronaut., vol. 8, no. 6, June 1970, pp. 30-41.
- Etkin, Bernard: Dynamics of Flight. John Wiley & Sons, Inc., c.1959.
- Goodmanson, Lloyd T.; and Gratzer, Louis B.: Recent Advances in Aerodynamics for Transport Aircraft. Astronaut. & Aeronaut., vol. 11, no. 12, Dec. 1973, pp. 30-45.

Hoerner, Sighard F.: Fluid-Dynamic Drag. Published by the author (148 Busteed Drive, Midland Park, N.J. 07432), 1965.

Kermode, A. C.: An Introduction to Aeronautical Engineering. Vol. I- Mechanics of Flight. Sixth ea., Sir Isaac Pittman & Sons, Ltd. (London), 1950.

Kuethe, A. M.; and Schetzer, J. D.: Foundations of Aerodynamics. Second ea., John Wiley & Sons, Inc., c.1959.

Lamar, William E.: Military Aircraft: Technology for the Next Generation. Astronaut. & Aeronaut., vol. 7, no. 9, Sept. 1969, pp. 68-78.

Levin, Stuart M.: Why the Swing-Wing? Space/Aeronaut., vol. 50, no. 6, Nov. 1968, pp. 69-75.

Levin, Stuart M.: The SST-How Good? Space/Aeronaut., vol. 48, no. 1, July 1967, pp. 74-88.

Malkin, M. S.: The Space Shuttle/The New Baseline. Astronaut. & Aeronaut., vol. 12, no. 1, Jan. 1974, pp. 62-78.

McKinley, James L.; and Bent, Ralph D.: Basic Science for Aerospace Vehicles. Third ea., McGraw-Hill Book, Co., Inc., c.1963.

Perkins, Courtland D.; and Hage, Robert E.: Airplane Performance Stability and Control. John Wiley & Sons, Inc., c.1949.

Pope, Alan: Wind Tunnel Testing. Second ea., John Wiley & Sons, Inc., c.1954.

Prandtl, Ludwig: Essentials of Fluid Dynamics. Hafner Pub. Co., Inc., 1952.

Stinton, Darrol: The Anatomy of the Aeroplane. American Elsevier Pub. Co., Inc., c.1966.

Shapiro, Ascher H.: Shape and Flow. The Fluid Dynamics of Drag. Doubleday & Co., Inc., 1961.

Swihart, John M.: Our SST and Its Economics. Astronaut. & Aeronaut., vol. 8, no. 4, Apr. 1970, pp. 30-51.

Von Mises, Richard: Theory of Flight. McGraw-Hill Book Co., Inc., 1945.

Whitaker, Stephen: Introduction to Fluid Mechanics. Prentice-Hall, Inc., c.1968.